UNIVERSITÀ
DEGLI STUDI
DI PADOVA

Sede Amministrativa: Università degli Studi di Padova

Dipartimento di GEOSCIENZE

CORSO DI DOTTORATO DI RICERCA IN: **SCIENZE DELLA TERRA**

CICLO: **XXIX**

GEOMORPHIC RESPONSE TO EXTREME FLOODS IN ALLUVIAL AND SEMI-ALLUVIAL RIVERS

Tesi redatta con il contributo finanziario della Fondazione CARIPARO

Coordinatore: Ch.mo Prof. FABRIZIO NESTOLA

Supervisore: Ch.mo Prof. NICOLA SURIAN

Co-Supervisore: Prof. FRANCESCO COMITI, Dr. LORENZO MARCHI, Prof. ELLEN WOHL

Dottorando : MARGHERITA RIGHINI

CONTENTS

ABSTRACT **2**

RIASSUNTO **5**

PART I – RESEARCH QUESTIONS AND METHODOLOGICAL ISSUES **7**

1. Introduction 8
2. Remote sensing as a tool for analysing channel dynamics and geomorphic effects of floods 18

PART II – CHANNEL RESPONSE TO EXTREME FLOODS: CASE STUDIES **52**

3. Channel response to extreme floods: Insights on controlling factors from six mountain rivers in northern Apennines, Italy 54
4. Channel widening during extreme floods: how to integrate it within river corridor planning? 87
5. Geomorphic response to an extreme flood in two Mediterranean rivers (northeastern Sardinia, Italy): analysis of controlling factors 98
6. The flash-flood of the Lierza Creek (northeastern Italy): analysis and interpretation of its limited geomorphic effects 134

PART III – CONCLUSIONS **150**

7. Final remarks 151

APPENDIX **159**

Appendix 1: An integrated approach for investigating geomorphic response to extreme events: methodological framework and application to the October 2011 flood in the Magra River catchment, Italy

ACKNOWLEDGEMENTS **186**

ABSTRACT

Extreme floods are one of the major natural hazards that affect Italian territory causing causalities, severe damages to human properties and infrastructures and major economic losses.

High intensity flood events can significantly affect channel morphology with extremely variable magnitude and pattern among river reaches, even within the same catchment, depending on the initial morphological conditions and being a function of the balance between flood driving and channel boundary resistant forces. This work addresses a better comprehension of morphodynamic processes during extreme flood events through the use of integrated and interlinked approaches.

The thesis addresses: i) the documentation and analysis of channel response and its variability during large floods through different morphological settings (i.e., alluvial/semi-alluvial and confined/unconfined rivers); ii) the development of a systematic approach to assess and quantify geomorphic changes; iii) the investigation of the main factors controlling such changes; iv) the development of empirical and conceptual models for the their prediction.

This research presents a quantitative assessment of the geomorphic effects of extreme hydrological events in three Italian catchments recently affected by large floods. The evaluation of channel response is based on an integrated approach that makes a synergic use of two main methodologies employed in the geomorphological study of rivers: remote sensing and GIS analyses, and field surveys. Flood effects detection was carried out by means of a stepwise approach mainly based on multi-temporal GIS analysis of remote sensing data (i.e., aerial photos and satellite images) in synergy with other topographic data (e.g., DEMs, DTMs) integrated by field surveys.

The research was conducted on alluvial and semi-alluvial rivers displaying typical characteristics of mountain streams and covering relatively wide ranges in terms of physiographic and geomorphological setting (e.g., channel width, channel gradient, lateral confinement, human impacts). The study rivers include six tributaries of the Magra River (northern Apennines) with basin areas ranging from 8 to 38 km^2, the Posada River and its main tributary (northeastern Sardinia) with a basin area of 680 km^2, and the Lierza Creek (Venetian Prealps) with a basin area of 7.5 km^2.

Planimetric changes are the main focus of the study. Channel widening was the most remarkable morphological response to the analysed extreme rainfall events, from alluvial unconfined channel reaches subjected to intense adjustments (i.e., very high effectiveness and magnitude) to lower or negligible adjustments in confined semi-alluvial channels. However, in the upstream reaches, generally characterized by high confinement and steep gradients, the flood power was high enough to erode the valley sides. A deeper analysis of channel width changes underlined two different behaviours depending on the initial channel width, showing larger variability in width changes in the narrower reaches than in the wider reaches.

The results of this study reflect the physical complexity of the river system and the complex nature of high-magnitude events, as they show that flood-driven geomorphic changes are controlled by several factors, both morphological and hydraulic ones, which lead to variable patterns of change. The flood peak stream power is often not sufficient to explain satisfactorily the channel response to floods, and inclusion of other factors turned out to be necessary to increase explanatory capability. In particular, a statistical analysis of controlling factors showed that channel widening magnitude depends – besides unit stream power calculated using the pre-flood channel width – on lateral confinement, especially in unconfined alluvial channels with erodible channel beds. Although the highest values in peak unit stream power were observed in confined and partly confined semi-alluvial reaches, the most intense channel widening did not occur in such reaches. Unit stream power – calculated based on the pre-flood channel width – has a major role in determining channel width changes in alluvial reaches, suggesting that most of width changes occurred after flood peak.

The results of this thesis confirm how predicting geomorphic effects of extreme floods in fluvial systems is challenging. However, a robust geomorphological approach as the one deployed here can contribute to i) the identification of the most probable reaches subject to dramatic morphological effects; ii) to define the minimum lateral extension that should be expected by flood erosion; iii) to provide a basis for the definition of sound river management strategies and interventions.

RIASSUNTO

Gli eventi idrologici estremi sono uno dei maggiori rischi naturali che affliggono il territorio italiano causando la perdita di vite umane, ingenti danni ai beni economici, ai beni privati e alle infrastrutture.

Eventi di piena estremi possono modificare significativamente la morfologia dell'alveo con un'elevata variabilità tra tratti dello stesso corso d'acqua, ma anche all'interno dello stesso bacino idrografico, ,in relazione alle condizioni morfologiche iniziali e in funzione dell'equilibrio tra le forze innescanti e le forze resistenti determinate dalle condizioni al contorno dell'alveo. Perciò, il lavoro è volto ad una migliore comprensione dei processi morfodinamici durante eventi di piena estremi attraverso l'impiego di approcci sinergici ed integrati.

Il lavoro di tesi è volto i) all'analisi e alla documentazione del comportamento e della variabilità della risposta morfologica in contesti morfologici differenti (in corsi d'acqua alluvionali e semi-alluvionali, confinati e non confinati); ii) allo sviluppo di un metodo sistematico indirizzato alla valutazione e quantificazione delle variazioni geomorfologiche; iii) allo studio dei principali fattori che controllano tali variazioni; iv) allo sviluppo di modelli empirici e concettuali per la loro possibile previsione.

Questa ricerca propone di valutare tramite un'analisi quantitativa gli effetti dei processi geomorfologici dovuti ad eventi idrologici estremi in tre differenti bacini idrografici italiani, recentemente colpiti da eventi ad elevata magnitudo. La valutazione della risposta geomorfologica è basata su un approccio integrato attraverso l'uso sinergico delle due principali metodologie impiegate nello studio geomorfologico dei corsi d'acqua, vale a dire l'impiego del telerilevamento e di analisi GIS e il rilevamento sul terreno. L'indagine degli effetti relativi agli eventi di piena considerati è stata effettuata attraverso un approccio *stepwise* grazie all'integrazione di analisi multitemporali in ambiente GIS di dati telerilevati (foto aeree ed immagini satellitari), in sinergia con altri dati topografici (ad esempio DEM o DTM), e rilievi sul terreno.

Lo studio è stato condotto in corsi d'acqua alluvionali e semi-alluvionali che presentano le tipiche caratteristiche di torrenti montani ma con caratteristiche fisiografiche e geomorfologiche differenti (come ad esempio la larghezza e la pendenza dell'alveo, il confinamento e l'impatto antropico) includendo sei affluenti del Fiume Magra (Appennini settentrionali) con bacini aventi aree comprese tra 8 e 38

km^2, il Fiume Posada ed il suo affluente principale (Sardegna nord orientale) avente un bacino di 680 km^2, e infine il torrente Lierza (Prealpi venete) con un bacino di 7.5 km^2.

Le variazioni planimetriche rappresentano l'aspetto maggiormente analizzato in questo studio. L'allargamento dell'alveo, la riattivazione della pianura alluvionale e l'erosione dei versanti risultano essere la risposta geomorfologica dominante agli eventi estremi analizzati, con intensità da molto elevata, negli alvei alluvionali non confinati, a bassa o praticamente trascurabile, negli alvei semi-alluvionali confinati. Tuttavia, nei tratti di studio situati più a monte, dove generalmente il fondovalle risulta più confinato, ovvero dove la pianura alluvionale è di limitata larghezza e la pendenza è elevata, il flusso è altamente concentrato tende a causare l'arretramento dei versanti che ne limitano la mobilità trasversale, coinvolgendo nel processo erosivo anche porzioni poste al di fuori dello stesso corridoio fluviale erodibile. Un'analisi più dettagliata delle variazioni di larghezza dell'alveo ha fatto emergere due comportamenti differenti a seconda della larghezza iniziale, mostrando un'elevata variabilità nelle variazioni di larghezza maggiore nei tratti più stretti rispetto ai tratti più larghi.

I risultati mostrano che le differenti variazioni morfologiche dovute a tali eventi sono controllate da molteplici fattori, sia morfologici che idraulici, riflettendo la complessità fisica sia del sistema fluviale che della natura di eventi a così elevata intensità. La potenza unitaria della corrente non è spesso sufficiente per l'interpretazione di una determinata risposta geomorfologica, perciò si rende necessario considerare altri fattori al fine di aumentare la capacità esplicativa di tali processi. L'analisi dei fattori di controllo ha evidenziato che la variazione di larghezza dell'alveo dipende essenzialmente da i) il confinamento laterale, specialmente nei tratti alluvionali a fondo mobile, dove il basso confinamento laterale controlla l'allargamento in un fondovalle in cui l'alveo è libero di modificarsi lateralmente, e ii) la potenza unitaria della corrente, calcolata utilizzando la larghezza dell'alveo iniziale (i.e., prima dell'evento). Nonostante nei tratti semi-alluvionali confinati e parzialmente confinati siano stati osservati i maggiori valori della potenza unitaria della corrente, non sono stati rilevati i processi di allargamento più significativi tra quelli osservati. La potenza unitaria della corrente, calcolata utilizzando la larghezza dell'alveo iniziale, risulta invece avere un ruolo maggiore nel determinare il processo di allargamento

nei tratti alluvionali, suggerendo altresì che la maggior parte delle variazioni di larghezza si siano verificate successivamente al picco dell'evento di piena.

I risultati di questa tesi confermano come la previsione degli impatti geomorfologici sul sistema fluviale rimanga un aspetto di non facile risoluzione. Ciò nonostante pongono l'attenzione sull'importanza di un'analisi geomorfologica quantitativa che può contribuire all'identificazione dei tratti più sensibili a variazioni morfologiche di elevata intensità e alla definizione di azioni di pianificazione volte alla mitigazione del rischio e alla scelta di strategie di gestione ed eventuali interventi.

PART I – RESEARCH QUESTIONS AND METHODOLOGICAL ISSUES

1. INTRODUCTION

Extreme floods and geomorphic effectiveness

The World Meteorological Organization (WMO) in 2015 defined '*extreme event' in general* as *'occurrence of a value of a weather or climate variable above or below a threshold value near the upper or lower ends (i.e., tails) of the array of observed values of the variable*'. Impacts from current climate-related extremes (i.e., heat waves, droughts, floods, cyclones and wildfires) disclose considerable vulnerability of some ecosystems and many human systems (IPCC, 2014). In the case of floods, extreme events are not triggered by variation in a single atmospheric weather and climate variable, but they are generally the result of specific conditions, such as precipitation extremes or surface conditions (WMO, 2015). The occurrence of heavy precipitation events is a major hazard that has often led to floods, causalities, severe damages to human properties and infrastructures and major economic losses. In many highly populated countries of the world, it is likely that there have been statistically significant increases in the frequency and intensity of heavy precipitation events and extreme rainfall in the last few decades (Brunetti et al., 2002; IPCC, 2014), although it is not uniform in all regions (U.S. EPA, 2016). On account of this, some basic parameters should be included in defining extreme precipitation, including magnitude (intensity), duration, severity and spatial extent (WMO, 2015). WMO defined noticeable precipitation event with a total precipitation exceeding a certain threshold defined for a given area occurring during a period of time of 1h, 3h, 6h, 12h, 24h or 48 hours.

In many countries variation in total precipitation is directly connected with change in the amount of precipitation during extreme events (Easterling et al., 2000). The recent increase (i.e., 1951-1995) of climate extremes is an important indicators of global warming. The resultant redistribution of the daily rainfall intensities over the Mediterranean (i.e., torrential/heavy against the moderate/light precipitation) might be a significant consequence inducing severe flash floods impacts (Alpert et al., 2002). Existing studies have shown a tendency toward a decrease in total precipitation together with an increase in precipitation events intensity and frequency over the last 120 years in Italy (i.e., for the period 1880–2002), more evident in the northern

regions during the last 50 years (Brunetti et al 2001; Alpert et al., 2002; Brunetti et al., 2002; Brunetti et al., 2004).

Differently, from the geomorphological point of view no singular definition for extreme flood event exits. A flood may be considered catastrophic if it implies significant geomorphic change by non-recurring natural flow events or multiple events, such as glacial-outburst floods, failure of landslide dams, or rapid drainage of glacial-meltwater lakes, or failure of artificial or natural jams (Baker, 1977; Costa 1987). Other authors considered major events those floods significant in conditioning channel forms and in determining channel capacity, comparing abruptness and intensity of phenomena to average annual flood (Erskine, 1994). Furthermore, exceeding in the average range of existing conditions (e.g., largest flood in a long discharge record) or considerably interrupting the 'typical' geomorphic sequences, or evidence of comparable magnitude of geomorphic changes to Holocene-aged impacts (Magilligan et al., 2015) may be considered as distinguishing extreme events characteristics. Costa and O'Connor (1995), and more recently, Magilligan et al. (2015) considered large floods those that generate high values of peak stream power per unit area and shear stress, from moderate to long duration. Thus, for the purpose of this study extreme floods are considered those events with high-magnitude and low-frequency, as result of extreme precipitation and peak discharge (i.e., extreme hydrological event), often flashy and commonly causing notable geomorphic effects.

The role of large floods and their role into landscape changes in a short period of time has long been debate and remains one of the major open questions (Hooke, 2016). Besides, magnitude may be treated both in terms of work and effectiveness, and effectiveness/frequency studies expect more detail approach, considering both the characteristics of the flood and the spatial elements of the affected catchment for identifying thresholds phenomena and relationships between effectiveness and work assessment of magnitude (Newson, 1980; Lisenby et al., 2016).

Indeed, major flood may have contrasting channel responses depending on the state of the system and being a function of the balance between flood driving forces and channel boundary resistant (Wohl 2010; Hooke, 2015; Magilligan et al., 2015; Lisenby et al., 2016). Channel response to large floods may range from negligible to catastrophic changes, even within the same catchment (Costa, 1974;

Wolman and Gerson, 1978; Nanson, 1986; Costa and O'Connor, 1995; Fuller, 2008; Croke et al., 2013).

Many works demonstrated that the frequency of a dominant discharge may be influenced by climatic and geomorphological characteristics other than the mean annual flood, especially in certain fluvial system such as in arid and semi-arid areas (Wolman and Gerson 1978; Osterkamp and Friedman, 2010) or in ephemeral (Hooke and Mant, 2000), and bedrock system (Tinkler and Wohl, 1998). Some studies have considered proximity to a moisture source, mesoscale circulation patterns, and orographic effects as potential causes in determine effective flood in both semi-arid and humid regions (Maddox et al., 1980; Smith et al., 1996). Milan (2012) argued that rare large events appear to be the effective geomorphic agents, although the degree to which a system is sensitive to change depends on the proximity of the system to the extrinsic threshold. Thus, systems prone to changes tend to react to events with a greater magnitude and frequency in comparison to less responsive systems to changes. Some authors have assumed that areas close to a source of warm moist air and that have high relief, and characterized by thin or impermeable soils, sparse vegetation, high land-surface slopes, flashy hydrograph, at catchment scales <1000–2000 km^2, are more prone to extreme flooding occurrence that lead to major geomorphic response (Osterkamp and Friedman, 2010; Wohl, 2010; Marchi et al., 2016).

Motivation of this work

Italy is one of the countries with largest number of casualties due to flood events in Europe, and it is particularly susceptible to the negative effects of high intensity precipitation events (Brunetti et al., 2004).

Motivation for this thesis arose from the need for increasing our understanding of floods processes and capability of forecasting the trajectories of change in the short term in mountain river systems. Prediction of the morphological response of a stream channel to an extreme event is very challenging and the comprehension of the fluvial system adjustment during short-time events should improve the connotation of 'flood hazard'. Besides hydraulic hazard (i.e., probability of inundation of a given area), geomorphological hazard owing to channel dynamics (e.g., channel

lateral mobility, changes in bed elevation, intense sediment and wood transport) should be considered as a crucial aspect, especially in small-sized mountain streams which may experience intense channel adjustment. Forecasting the occurrence of extreme floods and predicting their impacts on the fluvial system remain challenging and many limitations exist. However, a robust geomorphological analysis can contribute to the identification of the most prone reaches to drastic effects (Rinaldi et al., 2016).

Specifically, this work deals with the quantitative analysis of geomorphic response to recent extreme floods in alluvial and semi-alluvial systems through the application of an integrated approach on real cases of study, in order to provide an insight into the driving forces of morphodynamic processes. Besides focusing on hydraulic forces, the study considered geomorphic channel pre-conditions as crucial key factor for understanding channel behavior. The thesis addresses i) the analysis and documentation of behavior of channel response and its variability through different morphological settings (i.e., alluvial/semi-alluvial and confined/unconfined rivers), ii) the development of a systematic approach to assess and quantify geomorphic changes, iii) the investigation of the main controlling factors, iv) the development of conceptual and empirical models.

A practical implication of this research will be supporting implementation of the Floods European Directive (2007/60/CE) that aims to reduce and manage the risks that floods pose to human health, environment, cultural heritage and economic activity (European Commission, 2007).

Integrated approach to investigate geomorphic response to extreme events

The complex pattern of an extreme meteorological event and the high spatial variability of the morphological responses necessitate integrated and interlinked approaches involving different disciplines and skills operating at different spatial scales (Rinaldi et al., 2016) (Fig. 1).

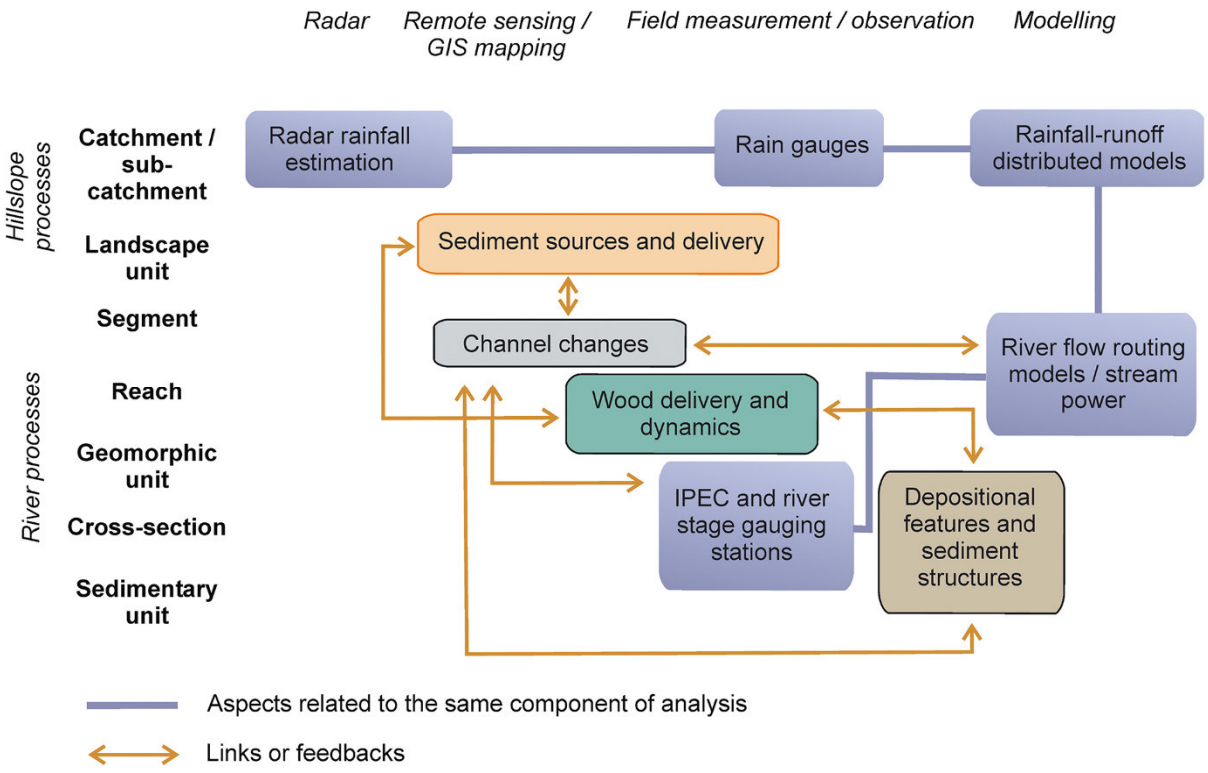

Figure 1. Schematic diagram of spatial scales, approaches, and coupling of process controls on the flood timescale (Rinaldi et al., 2016).

For this reason, the study arose from fundamental collaborations that involved many research groups, as a key for a better understanding of such events. Thus, Appendix 1 would be a guideline describing and discussing an overall methodological framework for using interlinked observations to investigate geomorphic impacts of an extreme event (e.g., hydrological analysis, sediment sources and delivery, wood transport and deposition, morphological and sedimentological processes and features, morphological channel response).

This work has been performed in parallel to William Amponsah PhD project (Department of Land, Environment, Agriculture and Forestry, University of Padova; CNR IRPI, Padova, Italy), although examining the same cases of study from different, strictly correlated point of views: hydrological and hydraulic analysis (i.e., reconstruction of the hydrological event and analysis of flood hydraulic variables) and morphodynamic analysis of extreme floods event (i.e., quantification and detailing analysis of magnitude and patterns of channel geomorphic changes by field and remotely-sensed data), that allowed a better understanding and prediction of such events.

Specifically, my contribution on this work mainly regards the second aspect concerning the analysis of geomorphic response to studied floods, the insight on controlling factors and the develop of investigated case of study and data analysis.

Finally, results of the study provide the delineation of a stepwise approach protocol for an analytical framework for channel change detection analysis in response to extreme flood events, applicable to a wide array of cases of study and likely transposed elsewhere (Fig. 2).

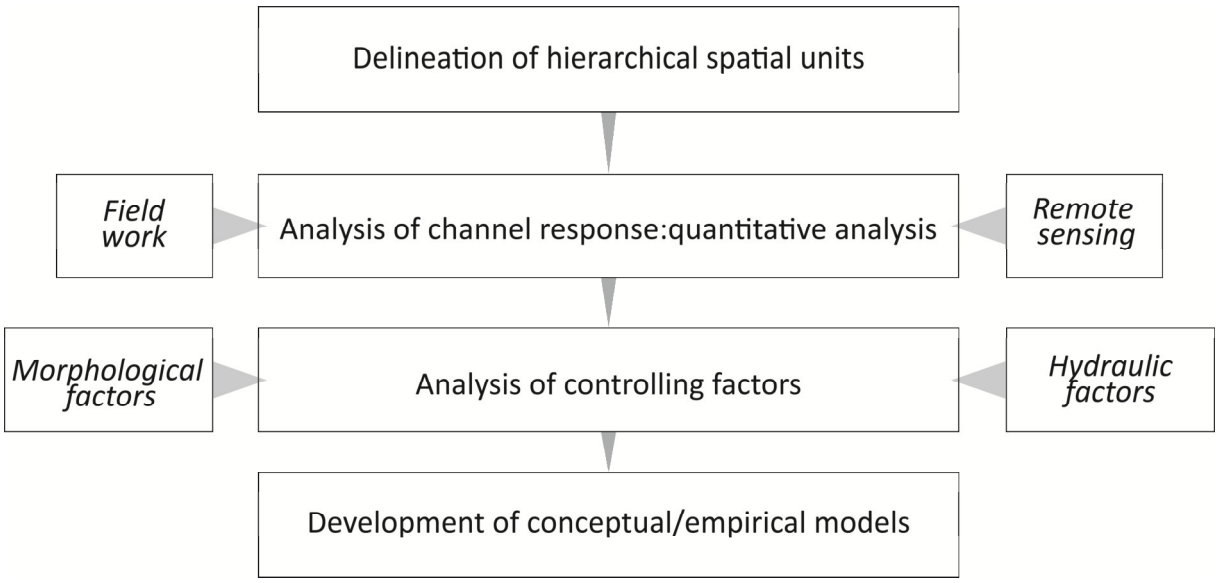

Figure 2. Stepwise approach for channel response analysis to extreme flood event.

Thesis structure

The thesis deals with the analysis of geomorphic response to three recent extreme floods that affected alluvial and semi-alluvial rivers, representative of different physiographic, climatic and morphological conditions in Italian upland catchments.

As a basis for this study, the second chapter regards a methodological and literature review section dedicated to illustrate remote sensing approach as a tool for detection of channel dynamics and geomorphic response to floods. This first part underlies the increasing availability and use of high resolution topographic data, space and airborne remote sensing imagery and GIS platforms in enhancing more rapid and spatially extensive assessment of flood-related geomorphic change with a focus on optical data. This chapter includes i) a literature overview about advance in

channel change-detection analysis over time in parallel to the progressive advance in technology and detection techniques, ii) a focus on the use of optical remote sensing in quantifying channel changes reporting many examples of applications of remote sensing to river change detection analysis in response to floods, and iii) an analytic framework describing the feasibility of detecting geomorphic changes considering assumptions, advantages and limitation.

Chapters three and four deal with the analysis of channel response to a flood event occurred in the Magra River catchment (northern Apennines, Italy), with insights on potential controlling factors and on a new methodological framework (IDRAIM) developed to guide river corridor planning and management in the long-term and during extreme events. My contributions in this two works regarded the definition of the morphological characteristics and the delineation of spatial units, and the quantitative analysis of morphological changes through remote sensing analysis on high-resolution data. I have also conducted the analysis of the potential controlling factors and the development of the empirical models.

Chapter five documented the geomorphic response to an extreme flood occurred in two Mediterranean rivers (northeastern Sardinia, Italy). In this work the investigation of the behaviour of low human impact reaches characterized by different morphological settings and the analysis of the role of a range of both geomorphic and hydraulic driving forces are the focus, with regards to sensitivity to geomorphic adjustment and to the role of the valley-bottom vegetation during the flood.

In Chapter six geomorphic effectiveness related to the flood duration is the focus, rather than the controlling factors considered in previous chapters. In investigating a Venetian Prealps catchment hit by an extreme flood, the study expanded the analysis to provide a context of the role of flow duration in explaining the type of geomorphic impacts examining combined influence of flow duration and available amount of cumulate energy expenditure.

The last chapter proposes a brief statement of the main remarks that came up from the results obtained by the study. Analysis and documentation of behaviour of channel response and its variability through different morphological settings and spatial scales was crucial to provide a basis for developing conceptual models to

improve our capability of predicting channel dynamics and related geomorphological hazard during extreme events.

The appendix outlines the spatial scales and methods related to the various components of an overall analysis of geomorphic response to flood events concerning with a range of different approaches and methods through the application on a real case of study. Regarding this work, my contribution concerned with the pre and post-flood GIS analysis of two analysed rivers and the quantitative assessment of the geomorphic changes to the flood.

References

Alpert, P., Ben-Gai, T., Baharad, A., Benjamini, Y., Yekutieli, D., Colacino, M., Diodato, L., Ramis, C., Homar, V., Romero, R., Michaelides, S., Manes, A., 2002. The paradoxical increase of Mediterranean extreme daily rainfall in spite of decrease in total values. Geophysical Research Letters **29** (11): 31-1–31-4.

Baker, V.R., 1977. Stream channel response to floods with examples from central Texas. Geological Society of America Bulletin **88**: 1057–1071.

Brunetti, M., Colacino, M., Maugeri, M., Nanni, T., 2001. Trends in the daily intensity of precipitation in Italy from 1951 to 1996: Int. J. Climatol., **21**: 299-316.

Brunetti, M., Maugeri, M., and Nanni, T., 2002. Droughts and extreme events in regional daily italian precipitation series, Int. J. Clim., **22**: 543– 558.

Brunetti, M., Maugeri, M., Monti, F., and Nanni T., 2004. Changes in daily precipitation frequency and distribution in Italy over the last 120 years, J. Geophys. Res., **109**, D05102. doi:10.1029/2003JD004296

Costa, J.E., 1987. A comparison of the largest rainfall-runoff floods in the United States with those of The People's Republic of China and the world. Journal of Geology **96**: 101–115.

Costa, J.E., 1974. Response and recovery of a Piedmont watershed from tropical storm Agnes, June 1972. Water Resour. Res. **101**: 106–112.

Costa, J.E, O'Connor, J.E. 1995. Geomorphically effective floods. In Natural and Anthropogenic Influences in Fluvial Geomorphology, Costa JE, Miller AJ, Potter KW, Wilcock PR (eds). Geophysical Monograph **89**, The Wolman Volume, American Geophysical Union: Washington, DC. 45–56.

Croke, J., Fryirs, K., Thompson, C., 2013. Channel–floodplain connectivity during an extreme flood event: implications for sediment erosion, deposition, and delivery. Earth Surf. Process. Landforms **38**: 1444–1456. DOI: 10.1002/esp.3430

Easterling, D.R., Meehl, G.A., Permesan, C., Changnon, S.A., Karl, T.R., Mearns, L.O., 2000. Climate extremes: observations, modeling, and impacts. Science **289**: 2068–2074.

Erskine, W.D., 1994. 'Sand slugs generated by catastrophic floods on the Goulburn River, NSW', International Association of Hydrological Sciences Publication No. **224**: 143–151.

EUROPEAN COMMISSION (2007). DIRECTIVE 2007/60/EC OF THE EUROPEAN PARLIAMENT AND OF THE COUNCIL of 23 October 2007 *on the assessment and management of flood risks.* Official Journal L 288, 06/11/2007, 27–34 pp.

Fuller, I.C., 2008. Geomorphic impacts of a 100-year flood: Kiwitea Stream, Manawatu catchment, New Zealand. Geomorphology **98**: 84–95.

Hooke, J.M., Mant, J.M., 2000. Geomorphological impacts of a flood event on ephemeral channels in SE Spain. Geomorphology **34**: 163–180.

Hooke, J.M., 2015. Variations in flood magnitude–effect relations and the implications for flood risk assessment and river management. Geomorphology **263**:19–38.

Hooke, J.M., 2016. Morphological impacts of flow events of varying magnitude on ephemeral channels in a semiarid region. Geomorphology **252**: 128–143.

IPCC, 2014: Climate Change 2014: Synthesis Report. Contribution of Working Groups I, II and III to the Fifth Assessment Report of the Intergovernmental Panel on Climate Change [Core Writing Team, R.K. Pachauri and L.A. Meyer (eds.)]. IPCC, Geneva, Switzerland, 151 pp.

Lisenby, P ., Croke, J., Fryirs, K., 2016. Geomorphic Effectiveness: A Linear Concept in a Non-linear World. Earth Surface Processes and Landforms, under review.

Maddox, R.A., Canova, F., Hoxit, L.R. 1980. Meteorological characteristics of flash flood events over the western United States. Monthly Weather Review **108**: 1866–1877.

Magilligan, F.J., Buraas, E.M., Renshaw, C.E., 2015. The efficacy of stream power and flow duration on geomorphic responses to catastrophic flooding. Geomorphology **228**: 175–188.

Marchi, L., Cavalli, M., Amponsah, W., Borga, M., Crema, S., 2016. Upper limits of flash flood stream power in Europe, Geomorphology **272**: 68-77. doi.org/10.1016/j.geomorph.2015.11.005

Milan, D.J., 2012. Geomorphic impact and system recovery following an extreme flood in an upland stream: Thinhope Burn, northern England, UK. Geomorphology **138**: 319–328.

Nanson, G.C., 1986. Episodes of vertical accretion and catastrophic stripping: a model of disequilibrium flood-plain development. Bulletin of the Geological Society of America **97**: 1467–1475.

Newson, M., 2006. The geomorphological effectiveness of floods — a contribution stimulated by two recent events in mid-wales. Earth Surf. Proc. **5**: 1–16.

Osterkamp, W. R., Friedman, J. M., 2000. The disparity between extreme rainfall events and rare floods-with emphasis on the semi-arid American West. Hydrol. Process. **14**, 2817–2829.

Rinaldi, M,. Surian, N., Comiti, F., Bussettini, M., 2015. A methodological framework for hydromorphological assessment, analysis and monitoring (IDRAIM) aimed at promoting integrated river management. Geomorphology **251**: 122-136.

Rinaldi, M., Amponsah, W., Benvenuti, M., Borga, M., Comiti, F., Lucìa, A., Marchi, L., Nardi, L., Righini, M., Surian, N., 2016. An integrated approach for investigating geomorphic response to extreme events: methodological framework and application to the October 2011 flood in the Magra River catchment, Italy. Earth Surface Processes and Landforms **41**: 835–846. doi: 10.1002/esp.3902.

Smith, J.A., Baeck, M.L., Steiner, M., 1996. Catastrophic rainfall from an upslope thunderstorm in the central Appalachians: the Rapidan storm of June 27, 1995. Water Resources Research **32**: 3099–3113.

Tinkler, K.J., Wohl, E.E., 1998. Rivers over rock: Fluvial processes in bedrock channels: American Geophysical Union Geophysical Monograph **107**.

U.S. Environmental Protection Agency, 2016. 'Climate Change Indicators in the United States, 2016 (Fourth Edition)'.

Wohl, E., 2010. Mountain rivers revisited. AGU, Water Resources Monograph **19**.

Wolman, M.G., Gerson, R., 1978. Relative scales of time and effectiveness of climate in watershed geomorphology. Earth Surface Processes and Landforms **3**: 189–208.

World Meteorological Organization, 2015: Guidelines on the definition and monitoring of extreme weather and climate events, draft version – First review by TT-Dewce.

2. REMOTE SENSING AS A TOOL FOR ANALYSING CHANNEL DYNAMICS AND GEOMORPHIC EFFECTS OF FLOODS

Margherita Righini [a], Nicola Surian [a,*]

[a] *Department of Geosciences, University of Padova, Italy;* [b]

in: Refice, A., D'Addabbo, A., Capolongo, D., Flood Monitoring through Remote Sensing, Springer, in revision.

Abstract

Over the past two decades the use of optical remote sensing in fluvial geomorphology has become widely employed for several applications, due to improvements in geospatial technologies and data availability. However, applications focused on change detection of channel dynamics and geomorphic response to individual flood events are still relatively rare. Insights into the complexity of interactions driving geomorphic changes might be obtained by application of diverse remote sensing approaches, depending on several factors (e.g., temporal and spatial resolution, magnitude of detected change). An overview about remote sensing as a tool for channel dynamics and geomorphic response to flood detection is illustrated, including discussion about advantages and limitations of optical remote sensing.

1. Introduction

Flood event studies require multidisciplinary approaches to enable the understanding of the phenomena (Tholey et al., 1997). Analysis of geomorphic responses to flood is a significant aspect of research, improving our capability of forecasting channel dynamics and related flood hazard (Wolman and Miller, 1960; Baker, 1977; Miller, 1990; Costa and O'Connor, 1995; Phillips, 2002; Krapesch et al., 2009; Nardi and Rinaldi, 2014; Magilligan et al., 2015; Rinaldi et al., 2016; Surian et al., 2016). Among the available tools, remotely sensed data have become a valuable source of information over the two past decades, and they are widely employed for several applications in fluvial geomorphology due to increasing of geospatial technologies and data availability (Piégay et al., 2015).

CHAPTER 2

This chapter aims to provide a review of the channel change detection analysis in response to flood events, with a specific focus on the use of optical remote sensing as a tool, often used in concert with other remotely sensed data. It specifically addresses river flood change-detection analysis in the context of passive optical remote sensing, with some references to the active one. The main focus is on channel dynamics and geomorphic effects of floods (e.g., bank erosion, channel aggradation, channel avulsion), while other processes related to floods, such as inundation processes, are not addressed in this work.

The chapter is organised into two main sections. The first section reports an overview about the advance in channel change detection analysis over time, strictly matching the progressive advance in technology and detection techniques. The second section describes the change detection analysis using optical remote sensing data by i) analysing the potential for observing river changes through the use of multi-resolution and multi-temporal data, ii) discussing assumptions, advantages and limitations of optical remote sensing data applied to channel change detection and iii) reviewing some studies on river response to flood event, with a focus on the observed and investigated river changes iv) finally, describing how optical remote sensing data have been employed to support channel change detection during a flood event by means of illustrative case of study.

2. Channel response to floods: detection and technology advancements over the last decades

Flood events may or may not affect channel morphology, shaping channels and floodplains. Since early 1950s, research begun to explore the effects of floods on riverine landscape and the comprehension of their role in determining the physical processes driving channel forms and their impacts on morphodynamics became a central theme of fluvial geomorphology. The examination of riverine landscape revealed also to be strictly linked to advances in technology, and consequently it drastically improved over the past decades (Marcus et al., 2008; Mertens et al., 2008).

Leopold and Maddock (1953) argued that channel-shape adjustment during individual floods occurred in response to a varying sediment load. In early 1960s, research explored physical effects induced on the natural landscape by floods

considering the relative importance of geomorphic processes of flood events with variable discharge (Wolman and Miller, 1960). In 1963 Schumm and Lichty investigated periods of channel widening related to floods of high peak discharge, and of floodplain construction related to floods of low peak discharge in a semi-arid region. Stewart and La Marche (1967) show that flood with recurrence interval >100 years largely determine valley morphology, channel pattern and location, and the character of alluvial deposits. They mapped erosional and depositional features on post-flood aerial photographs and determined the amount of destruction of land and forests by comparing pre- and post-flood aerial photographs as support to field surveys. However, prior to the 1970s, the sensors mainly consisted of black and white photographic film, and the platform was an airplane in the context of geomorphological mapping (Gilvear and Bryant, 2003). In the 1970s, researchers began to analyse channel changes related to flood magnitude, focusing on the effects of floods of extremely rare occurrence (Gupta and Fox, 1974; Baker, 1977) and their effects across several climate regions (Wolman and Gerson, 1978). However, most of these works were based on traditional field survey observations of river cross-sections and relied on mostly qualitative, and rarely quantitative, flood-related impact studies.

In 1972 the launch of Landsat I started the first continuously acquired collection of space-based remote sensing data of terrestrial environments (Wohl, 2014). Nevertheless, in the early phases of satellite remote sensing, the data available had 80 meter ground resolution and the pioneering investigations in the field of application of remote sensing to flood were predominantly focused on flood monitoring and mitigation, with particular regard to the recognition of flood prone regions of USA (Tamminga et al., 2015) and flood extents (Smith, 1997). Large pixel sizes, in many cases larger than the stream width, limited the use of satellite-based imagery in channel change detection and river features mapping. Subsequently, and until the late 1990s, researcher have long used air photos to document changes in channel parameters, based on visual interpretation or photogrammetric analysis (Hooke, 2004; Marcus and Fonstad, 2008). In the mid-1980s, imaging spectrometry became an earth observation tool, even if the increase of the spectral resolution required a lower spatial resolution, slacking space-borne hyperspectral development (Fonstad, 2012).

A significant shift in river research occurred during the mid-1990s, from field-based surveys of river cross-section, coupled with qualitative interpretation of aerial photography through new tools available to fluvial geomorphologists (Lane et al., 2001). The technical progress accomplished in the past two decades of research in remote sensing made a considerable contribution to river sciences (Carbonneau and Piégay, 2012) and, among these methods, optical remote sensing of rivers has experienced some of the more dramatic advances (Marcus and Fonstand, 2008). Remote sensing becomes a reasonable alternative and a good support to ground–based field survey when it can monitor or map the variable of interest (Marcus et al., 2012). In addition, Digital Elevation Models (DEMs) became available during the 1990s. Optical remote sensing and DEMs greatly improved the ability to create and manipulate detailed imagery of Earth's surface, resulting in opportunities to detect features not previously recognized (Wohl, 2014). Over recent years, additional advances in technology allowed to overcome some logistic and cost constrains in investigating changes in fluvial settings. The development of Unmanned Aerial Systems (UAS), able to fly in non-urban areas at very low altitudes and to deliver very high spatial and temporal resolution imagery, reveals a significant potential in river sciences, offering very interesting alternatives to traditional platforms (Carbonneau and Piégay, 2012; Tamminga et al., 2015; Woodget et al., 2015).

3. Channel change detection analysis in response to floods

Change detection is the process of identifying differences and quantifying temporal effects of an object or a phenomenon using a multi-temporal data set (Singh, 1989). Hence, the primary purpose of a change detection analysis is to characterize environmental change over time and space (Walsh et al., 1998). Information on river morphology and changes over time is commonly needed for water resources planning, river management (Ghoshal et al., 2010) and hazard assessment, and for a better understanding of the main causes of those processes (Marcus et al., 2012). Hence, the most efficient change detection techniques are able to quantify areal surface, direction and rate of change, and to estimate the accuracy of change detection results (Lu et al. 2004). Singh (1989) reviewed a series of feasible procedures for change detection using remotely-sensed data in

environmental fields, identifying the post-classification comparison (i.e., comparison of independently classified images) as the most common method. The following issues are addressed in this section: (i) potential of observing river changes in response to a flood through optical remote sensing data; (ii) the use of remotely sensed data for channel change detection across multi-resolution and multi-temporal data; (iii) common assumptions, advantages and limitations of remote sensing techniques for channel change detection analysis; (iv) the use of optical remote sensing data in concert with other remote sensing, topographic and geospatial data; (v) the application of optical data for channel change detection by means of a real case of study.

3.1 Potential of observing river changes using remote sensing data

An important prerequisite to assess a change detection related to a flood event is the identification, the qualitative or quantitative assessment of riverine landscape forms and structures before and after the flood event. Optical remote sensing data allow change detection through several methods, ranging from classic visual skill-based interpretation procedures, to semi-automated and automated methods based on imagery characteristics. Regardless of the used technique, the success of change detection from imagery will depend on both the nature of the change involved and the success of the image pre-processing and classification procedures (Bryant et al., 1999). Most of the works documenting spatial and temporal variations of channel response to flood are mainly focused on two components of potential observing changes, such as planimetric 2D changes and 3D changes. Other contributions came up from studies illustrating hydraulic or geomorphic derived variables or indicators, which should develop a better understanding of the mechanisms responsible for channel changes to floods and further predictive models. We reviewed a number of works which focused on a wide spectrum of channel responses and magnitudes of floods (e.g., from moderate to extreme flood events), investigating channel or floodplain changes at different spatial and temporal scales, in diverse climate and geomorphic settings, using different remote sensing data sources and approaches (Table 1). Depending on the detection purpose optical remote sensing data have been often used in concert with other topographic data integrating field surveys. Among the analysed works, some focused on channel

planimetric 2D, while others on 3D changes, according to the dominant changes occurred and to data availability.

River	Flood event	Recurrence interval (year)	Detection purpose	Method	Remote sensing data	Spatial scale detection analysis	Time scale detection analysis	Reference
Planimetric 2D changes								
River Dee, Welsh–English border, UK	n.a.	n.a.	Spatial and temporal trends in the channel planform	Pre- and post-flood aerial photographs comparison	Six sets of air photographs	Reach (18 km)	115 year period (1987–1992)	Gurnell, 1997
Eel River and its five tributaries, northern California, USA	1955; 1964; 1997	50 years 200 years 12-15 years	Variation in channel width and position	Pre- and post-flood aerial photographs comparison	Sets of aerial photographs at 3–7 year interval	Catchment	Three-flood events	Sloan et al., 2001
Sabie River, South Africa	February 2000	200 years	Changes in morphologic unit composition and spatial coverage	Aerial photographs comparison	Pre-and post-flood aerial photographs (1:10,000 scale)	Channel types (1-20 km); morphologic units (up to metre-scale)	One-flood event	Heritage et al., 2004
River Bollin, NW England	2000 2001	n.a.	Occurrence and causes of multiple cutoffs on a meandering river	Aerial photographs mapping	Aerial photographs	Reach (600 m)	2000-2001	Hooke, 2004
Guadiana River, Spain	5–6 November 1997	>500-year	Sedimentary and erosive features	Pre and post flood aerial photographs mapping	Aerial photographs	Reach (500 m-2 km)	One flood-event	Ortega et al., 2009
River Dane, NW England	> 25 years period	n.a.	Change in morphological characteristics of meander bends	Photogrammetric mapping	Sets of aerial photographs (from 1984 to 2007)	Meander bends	25 years	Hooke, 2010
Seven rivers along the Mediterranean coast, Israel	n.a.	n.a.	Geomorphic effect on river mouth	Pre- and post-flood aerial photographs comparison	Pre-and post-flood aerial photographs	River mouth	1918-2005	Lichter and Klein, 2011
Five Alpine gravel bed rivers, western Austria	28 August 2005	~500 years	Variation in channel width	Pre- and post-flood orthoimages comparison	Pre- and post-flood aerial photos; LiDAR data (1×1m).	Reach (range: 20–56km); sub-reach (500-5000m); cross section(200m spacing)	One-flood event	Krapesch et al., 2011
Rapti River, India	2011 Monsoon floods	>500 years	Channel migration	Aerial photographs comparison	SRTM DEM data (90m); satellite images (Landsat MSS 60m, TM 30m,ETM+ panchromatic-8 band, 15m)	Reach	Monsoon season-flood events	Kumar et al., 2013
White and Saxtons Rivers, Vermont, USA	Tropical Storm Irene 2011	>100 years	Channel geometry changes	Aerial photographs comparison	Pre and post-flood color aerial imagery (1m); WorldView 1 panchromatic Satellite Imagery (0.50m); DEMs	Reach	One-flood event	Buraas et. al. 2014; Magilligan et. al., 2015
Six mountain tributaries, Italy	October 25th 2011	>100 yaers	Variation in channel width	Pre- and post-flood aerial photos comparison	Aerial photos (0.50m)	Reach (1-6 km); Sub-reach (300-500 m)	One-flood event	Surian et al., 2016
3D changes								
River Tay, Scotland, UK	January 1993	40-65 years	Land cover change; bathymetric change	Classification comparison and bathymetric mapping	Airborne imagery-Daedalus 1268 (ATM); colour aerial photography of 1:12,000	Reach	1992-1994	Bryant and Gilvear , 1999
Lockyer Creek, southeast Queensland (SEQ), Australia	January 2011	~2000 years in the upper catchment to ~30 years downstream	River bank erosion	DoD	Multi-temporal LiDAR; high resolution pre and post flood aerial imagery	Catchment	One-flood event	Grove et al., 2013
Rio Puerco, New Mexico, USA	2006	n.a.	Topographic changes	DoD	Quickbird II panchromatic aimage (0.6m); Multiple airborne LiDAR (0.5m) derived DEMs	Segment (12 km)	One-flood event	Perignon, 2013
Elbow River, southwestern Alberta, USA	June 19 and 23 2013	500 years	Sediment erosion and deposition	DoD; geostatistical models (pre and post-flood variograms)	UAS survey: orthoimagery, DEMs (5 cm/pixel and 4 cm/pixel)	Reach	One- flood event	Tamminga et al., 2015
Planimetric and 3D changes								
Lower Yuba River, Sacramento Valley, California, USA	Eight major floods (1907, 1909, 1955, 1964, 1970,	n.a.	Planimetric changes; volumetric changes in sediment storage	Pre- and post-flood aerial photos comparison ;DoD	Pre and post-flood aerial photographs; DEMs (3x3m)	Reach	1906-1999	Ghoshal et al., 2010
River Dane, NW England	> 20 year period	From 9 to 57 years	Rates and occurrence of erosion, deposition, calibre of sediment and morphological changes	Photogrammetric Mapping to an accuracy of ± 0.5 m	Set of aerial photographs	Reach (10 km)	1981–2002	Hooke and Yorke, 2010
Thinhope Burn, northern England, UK	July 17 2007	n.a.	Spatial patterns of erosion and deposition; volumetric changes	Pre- and post-flood aerial photos comparison ;DoD	Pre and post- flood aerial imagery; DEMs	Catchment and Reach	One-flood event	Milan, 2012
Lockyer Creek, southeast Queensland (SEQ), Australia	January 2011	~2000 years in the upper catchment to ~30 years downstream	Areal changes extend of geomorphic features, variation in channel width	Pre- and post-flood aerial photos comparison ;DoD	Multi-temporal LiDAR-derived DEMs (5cm); pre- and post-flood aerial photos	Reach	One-flood event	Thompson and Crooke, 2013
Magra River, Italy	October 25th 2011	From 30 to 200 years	Variation in channel width; eroded volumes of sediment	Pre- and post flood aerial photos comparison ;DoD	Pre and post flood aerial photos (0.50m); LiDAR derived DEM	Reach (1.6 km) Sub-reach (300-500 m)	One-flood event	Nardi and Rinaldi, 2014

Table 1. Examples of application of remote sensing to river change detection analysis in response to floods. n.a.: not available data.

Planimetric 2D changes

Channel planform change has been the research focus of many fluvial geomorphologists (Gilvear and Fonstad, 2003). The main intent of planimetric change detection analysis is to characterize or quantify channel and floodplain planform changes (Richardson and Fuller, 2010). Airborne and satellite-based remote sensing data have long been used to map channel boundaries, bars, floodplain cover, in-stream islands and other features (Gilvear and Bryant, 2003). When a series of several images, or at least a set of two images is available, it is possible to observe changes on different timescales (Gilevar et al., 2000), related to one or to a series of flood events with diverse magnitude and recurrence intervals.

Most of the studies analysing planimetric changes in response to diverse event magnitude (i.e., from extreme to moderate floods) used airborne imagery across diverse spatial scales (i.e., from catchment to morphologic units metre-scale), and time scales (i.e., from one flood event to wide temporal intervals > 100 years). These studies mainly focused on (i) channel width changes (Gurnell, 1997; Sloan et al., 2011; Krapesch et al.,2011; Thompson and Crooke, 2013; Nardi and Rinaldi, 2014; Surian et al., 2016), (ii) channel and geomorphic features pattern changes (Hooke, 2004; Ortega et al., 2009; Hooke and Yorke, 2010; Lichter and Klein 2011; Milan, 2012; Thompson and Crooke, 2013), (iii) substrate type changes (Heritage et al., 2004) (Fig. 1), (iv) channel shifting (Sloan et al., 2011) (Fig. 2), (v) bank retreat (Grove et al., 2013; Nardi and Rinaldi, (2014) (Fig. 3) and (vi) land coverage changes (Bryant and Gilver, 1999).

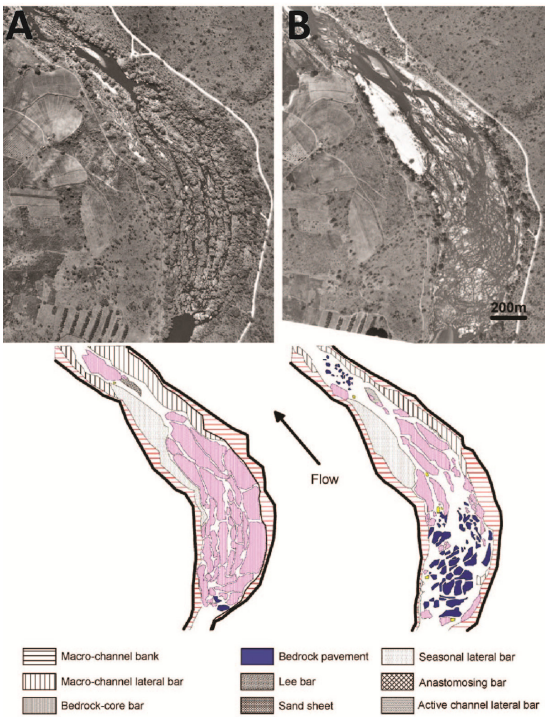

Figure 1. Example of cohesive mixed anastomosed channel type on the Sabie River, showing (A) pre-flood and (B) change in morphologic unit composition following the extreme flood of 2000 on aerial photographs (1:10,000 scale) (Heritage et al., 2004).

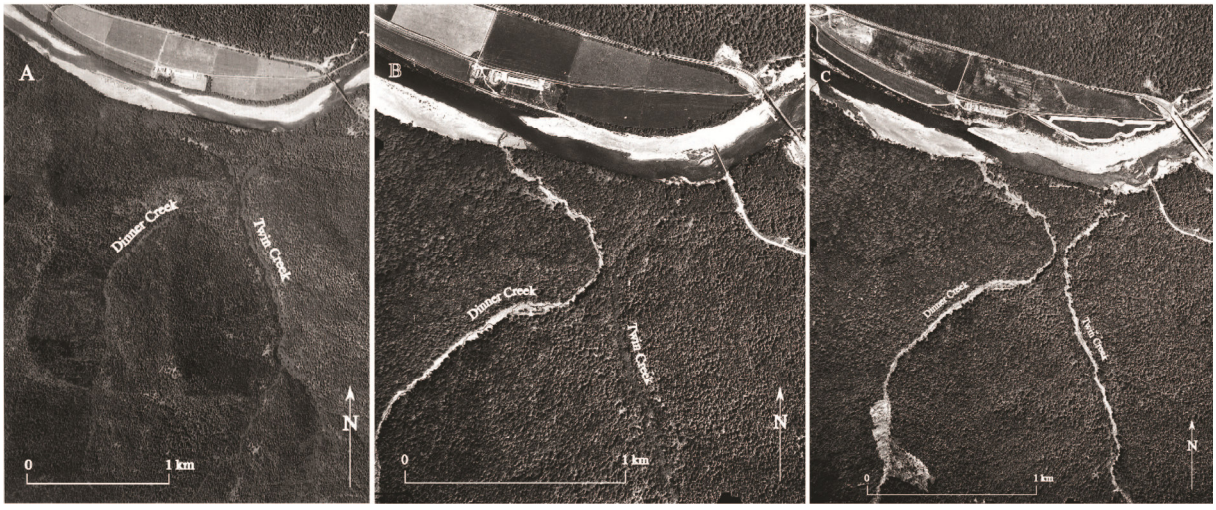

Figure 2. Variation in channel width and position on a set of aerial photos of Dinner and Twin Creeks: (A) before the 1955 flood (1954 photograph), (B) after the 1955 flood (1960 photograph), (C) after the 1964 flood (1966 photograph). Hillslope failures were also identified on the 1966 photos in both basins. (Sloan et al., 2011).

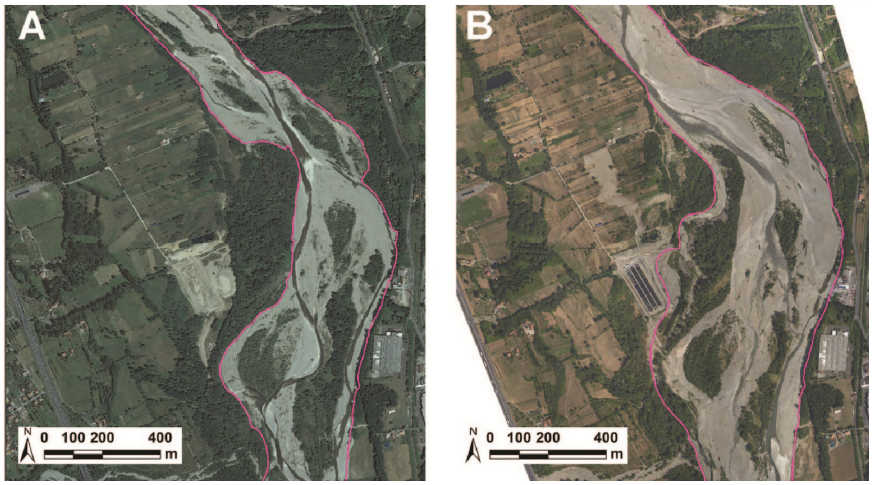

Figure 3. Digitalization of the active channel on color aerial photos (spatial resolution=0.50 m) to evaluate variation in channel width (A) before the flood and (B) after the flood (Nardi and Rinaldi, 2014).

Studies of large rivers are generally based on satellite imagery which provide spatially extensive images over large areas for low costs. Therefore, if the pixel size is suitable for the river size, the regular revisit frequency of orbital sensors allows easier multi-temporal approach analysis compared to airborne data.

Kumar et al. (2013) used multi-temporal satellite images to assess the impacts of 2011 monsoon flood in the alluvial Rapti River (India) quantifying both areal (i.e., channel area, channel belt area, bar area) and linear characteristics of channel belt before and after the flood (i.e., active channel and channel belt width, sinuosity, channel central line shifting). Authors used Landsat MSS, TM, ETM+ data, with spatial resolution of 60, 30 and 15 m respectively, in concert with SRTM elevation data to map geomorphological features, quantify geomorphic processes and resultant landforms at various spatial scales ranging from basin to reach level. In this case, employment of medium spatial resolution data turned out to be suitable for channel having an average initial channel width greater than 60 m at reach scale and notable magnitude of change in terms of channel lateral expansion and shifting, and channel belt area variations. Higher spatial resolution space-born imagery were used by Buraas et al. (2014) and Magilligan et al. (2015) to investigate channel widening occurred in the William, White and Saxtons Rivers, Vermont (USA) during the Tropical Storm Irene. Post-flood panchromatic satellite imagery from WorldView 1 (0.50 m of spatial resolution) were used to define major erosional features across floodplains, and channel width changes exceeding the natural ‘range of variability’ of

channel width observed in the absence of extreme floods (i.e., pre-Irene 20-year period) (Magilligan et al., 2015). The available imagery allowed to analyse large portions of affected channels (i.e., up to 40 km) at reach scale showing a channel widening up to 12 m of net change, from average pre-flood width of 18 and 48 m, respectively for the Saxtons and White Rivers (Fig. 4).

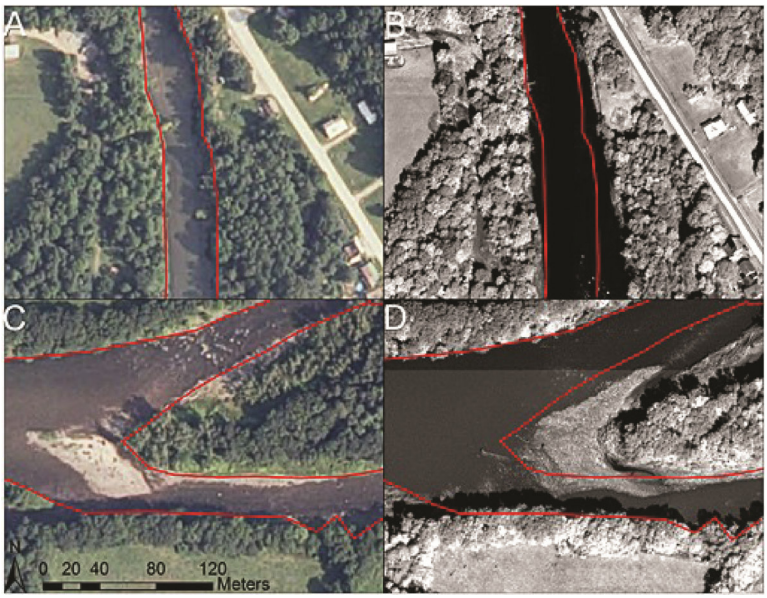

Figure 4. Width changes on the White River on color aerial photos (spatial resolution=1m): (A) pre-image with channel delineation, (B) post-image displaying bank erosion, (C) pre-image with island delineation, (D) post-image displaying erosion of the head on an island as cause for channel widening (Buraas et al, 2014).

Furthermore, Buraas et al. (2014) used satellite data as support for developing a method able to predict more susceptible reaches to major geomorphic change. Space-born data were also employed as support in assessing the distribution and the role of riparian vegetation (i.e., type and density) in influencing geomorphic effects during extreme flood affected the Rio Puerco, New Mexico (USA) in 2006 (Perignon et al., 2013). Principally Quickbird II panchromatic images (0.61 m of spatial resolution) were employed to map the distribution and pattern of plants in the landscape using unsupervised classification approach in order to categorize each pixel as either bare ground or vegetation (i.e., darkest areas). Satellite imagery turned out to be effective for identifying young plants and sandbar willow compared to airborne LiDAR which was not suitable for detecting thin vertical stems and branches, because of their difficulty in reflecting laser signals.

3D changes

Recent methodological advances, including Light Detection and Ranging (LiDAR), Structure from Motion (SfM) and Terrestrial Laser Scanning (TLS), allow investigation of other aspects of channel adjustment to floods, such as the investigation of the three-dimensional river structure and changes (e.g., scour and fill, bank erosion) (Tamminga et al., 2015). Bed-level change, lateral erosion, variation in sediment storage, floodplain scour, fill and associated volumes of erosion and sedimentation are the more common 3D channel changes detected as response to a flood. However, one of the main issues related to 3D channel changes detection analysis is the diverse approach needed for exposed (e.g., channel bars or exposed channel beds) and submerged areas. Aerial photogrammetry and laser altimetry are employed to detect and quantify channel changes for exposed areas, while optical and multi- and hyper-spectral imagery might detect variations in water depth in shallow non turbid and deeper and more turbid channels respectively (Gilvear and Bryant, 2003; Legleiter et al., 2009; Pan et al., 2015). The “DEM of Difference” (DoD) approach, derived by photogrammetry or LiDAR, is one of the most common methods to analyse 3D river changes (Table 1).

Hooke (2008) recorded the magnitude and conditions of process and morphological response of the channel (i.e., rates and occurrence of erosion, deposition, calibre of sediment and morphological changes) related to discharge characteristics variations for a sequence of more than 50 bends in a 10 km length reach in an active meandering river in NW England over a 20-year period. Measurements and monitoring of the study reach have consisted of detailed field mapping, bends ground photographs comparison and three sets of aerial photographs. Bank lines were mapped photogrametrically to an accuracy of ±0.5 m from air photos and the digitised courses compared in ArcGIS to produce calculations of erosional and depositional areas and rates.

Beside mapped riparian vegetation type and distribution, Perignon et al. (2013) presented the results of an airborne LiDAR differencing study (0.5 m of spatial resolution) of the topographic effects on the Lower Rio Puerco, New Mexico (USA). Authors analysed erosion and deposition volume changes along the channel and the floodplain, and removal of vegetation from river corridor.

Some works integrated the planimetric changes detection analysis with topographic analysis. Grove et al. (2013) and Thompson et al. (2013) carried out a multi-temporal LiDAR-derived DoD analysis to map and quantify the three-dimensional form or morphology, volume and rates of different of bank erosion processes before and after the flood (Fig. 5).

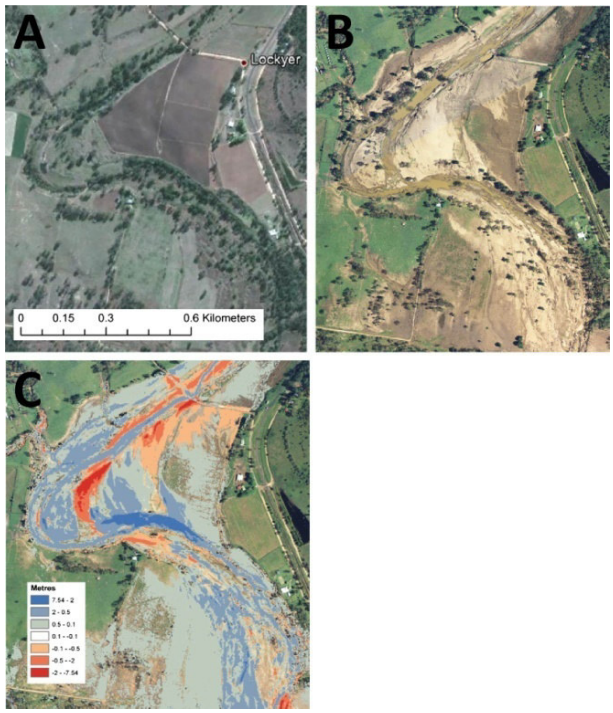

Figure 5. Change (i.e., erosion/deposition, variation in channel width and reorganisation of the channel morphology) along unconfined reach of Lockyer Creek showing (A) pre-flood aerial photos, (B) post-flood aerial photos, (C) elevation change from DoD (Thompson and Croke, 2013).

The DoD approach was also used to quantify the eroded volumes of sediment derived from riverbank retreat (Nardi and Rinaldi, 2014), the spatial patterns of erosion and deposition and volumetric changes (Milan, 2012), volumetric changes in sediment storage (Ghoshal et al., 2010). Tamminga et al. (2015) used the same approach employing digital elevation models produced from photogrammetry using pre and post-flood high-resolution (4–5 cm/pixel) imagery to detect reach-scale spatial patterns, volume and area of erosion and deposition acquired by an unmanned aircraft systems (UASs) in Elbow River, Alberta (USA). They also applied a different approach to investigate reach-scale morphology and changes applying variogram analysis to topographic data elevations in order to determine characteristic horizontal and vertical length scales and variance of elevations taking into account varying channel complexity and anisotropy in different directions.

Derived variables and parameters

Research is moving to use optical remote sensing data, usually in synergy with other remotely sensed (i.e., LiDAR or SAR) and topographic data (e.g., DEMs, DTMs), to extract other variables and parameters or indicators, potentially explanatory for understanding river response to flood and for developing predictive models. These approaches enable to extract and map the following variables or parameters: i) hydraulic variables, such as water surface slope, stream power (Jordan and Fonstand, 2005), or specific stream power and shear stress (Vocal Ferencevic and Ashmore, 2012; Bizzi and Lerner, 2013; Magiligan et al., 2015); ii) morphological parameters and indexes, such as confinement index or confinement degree, defining valley setting (Rinaldi et al., 2009; Rinaldi et al., 2016; Surian et al., 2016), the sinuosity index, the anabranching index (Surian et al., 2009), the braiding index (Allen et al., 2015), the alluviation index (Heritage, 2004), the width ratio (Krapesch et al., 2011); iii) channel instability or susceptibility parameters, such as the mobility index (Bledsoe and Watson, 2001) or the erosion and deposition index (Piégay et al., 2005; Hooke, 2008), and the bend stress parameter (Buraas et al., 2014); iv) sediment connectivity indicators, like the connectivity index (Cavalli et al., 2013).

3.2 Flood effects detection across spatial and time scale using optical remote sensing data

Natural processes frequently operate on larger spatial scale and longer time scales than traditional river sciences and management (Carbonneau and Piègay, 2012). In the past, understanding of environmental changes was constrained by inability to quantify spatial variation and change in fluvial landforms over long distance or long time periods. The result of using numerous local measurements, or sporadic, spatially widespread measurements, led to consider the channel as a discontinuous system (Marcus and Fonstad, 2008). The relevance of such small scale for developing mechanistic models of changing river channels and understanding larger systems might be problematic, and a generalization from discrete patches to an integrated whole might be questionable (Yang et al., 1999).

Then again, both the limited temporal scale of flooding and the transient effects of changes on the river channel and floodplain, or the low frequency of geomorphic effective flood events, constrained forecasting and prediction perspectives. Access to, and availability of remote sensing data, operating at a range of spatial and temporal scales, enhanced the ability to survey wider areas, particularly in large or inaccessible fluvial systems, and allowed change-over-time analysis (Fonstad and Marcus, 2010), overcoming the issue of channel response to floods as temporary phenomena, usually followed by a variable recovery period (Wolman and Gerson, 1978). Indeed, remotely sensed data and imagery is the only approach that could conceivably give continuous data over entire catchments (Mertes, 2002; Fonstad and Marcus, 2010) and provide synoptic information (Marcus and Fonstad, 2008), retrospective viewing and multi-temporal analysis.

Understanding of river processes and morphodynamics requires investigations at larger scales considering river catchment as a holistic system, involving both floodplain and hillslope dynamics, and land use and human impact aspects. Remote sensing approaches provide the possibility to investigate from catchment to local scale, and determine changes affecting the entire basin, such as disturbances on channel–hillslope coupling, in order to better understand process linkages between fluvial and hillslope systems (Sloan et al., 2001; Dethier et al., 2016; Rinaldi et al., 2016; Surian et al., 2016). Moreover, the increasing availability of meter- to centimetre-resolution imagery enables the exploration of smaller scales and in-channel morphological changes and in-stream parameters. Recent research indicates that optical imagery can provide fine resolution watershed coverage of in-stream features, representing rivers as continuous systems (Marcus and Fonstad, 2008). Hence, the necessity to investigate rivers and its changes across different spatial and time scales has become more challenging, and the data acquisition should depend on both the nature and the scale of the purposed investigation (Prienstall and Aplin, 2006).

Two interesting frameworks that link spatial scales, temporal scales and data sources have been proposed by Prienstall and Aplin (2006) and Rinaldi et al. (2016). Prienstall and Aplin (2006) have suggested suitable spatial scales and data sources for river environment representation in digital form, taking in consideration different study scales (i.e., from catchment to micro topography) (Fig. 6A). Rinaldi et al. (2016) have proposed an integrated approach for investigating geomorphic response to

extreme events, highlighting the complexity of interactions driving change variability in riverine landscape across several spatial scales. Such approach outlines a summary of the spatial scales and methods related to the various components of an overall analysis of the geomorphic response to a flood event (Fig. 6B).

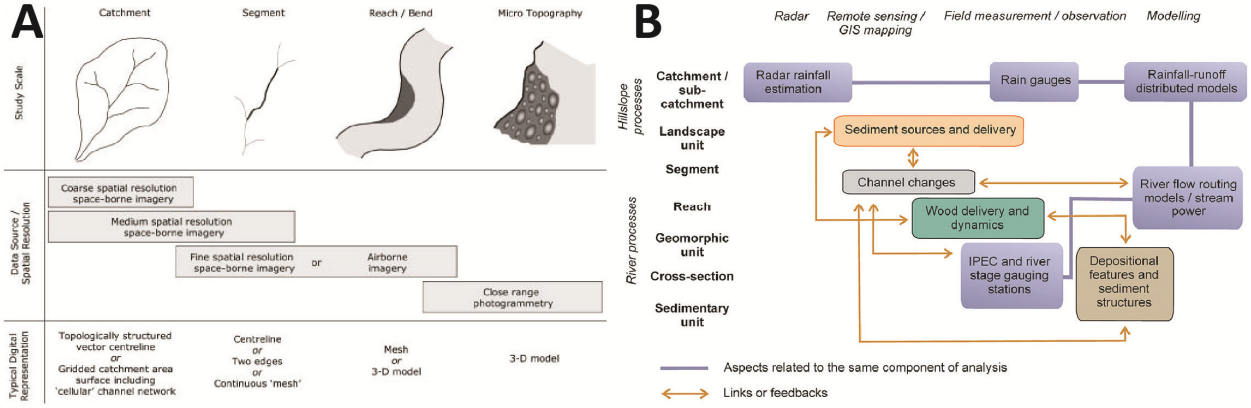

Figure 6. Spatial scales and approaches for analysing river environments and investigating geomorphic response to extreme events proposed by (A) Priestnall and Aplin (2006) and (B) Rinaldi et al. (2016) respectively.

3.3 Assumptions, advantages and limitations

In this section, we summarize some of the advantages and limitations of employing optical remote sense data in riverine landscape studies. Remote sensing compared to traditional data collection (i.e., cartographic and field-based data) reveals several advantages (Gilevar and Bryant, 2003), though it might encounter some issues and limitations and specific assumptions are needed to be correctly employed. First, remote sensing provides an approach for assessing the landscape as a function of the spatial, spectral, temporal, and radiometric resolutions at which sensor-platform systems operate. These four remote sensing resolutions combine to characterize the landscape from local to global spatial scale (Walsh et al., 1998). Spatial resolution, image extent and spectral characteristics play a large role in determining whether or not a particular sensor or data is capable of detecting individual features (Joyce et al., 2009). However, the most noticeable optical constraint is that the stream must be visible from above, and consequently optical remote sensing of streams cannot be done where trees, bridges, woods or other obstacles overhang the channels. The no-obstruction criterion is especially constraining in headwater streams, or along stream banks in dense forested environments (Marcus and Fonstad, 2008). Magilligan et al. (2015) for instance,

interpolated the channel boundary, at locations closest to the channel edge, to deal with the channel banks covered by shadows or overhanging vegetation.

Spatial coverage and temporal resolution: in the case of very large rivers, using aerial or space-borne remote systems is the only way to observe and quantify the overall morphology of the river (Gilvear and Bryant, 2003). According to the previous section, the use of remote sensing for tracking flow variability and flood effects is particularly important in areas without monitoring systems, or where access is limited. Indeed, one of the main recognized advantages of using remote sensing is the global view (Tholey et al., 1997; Maters, 2008; Carbonneau and Piégay, 2012). In addition, temporal resolution and coverage provided by remote sensing systems is crucial in change detection studies (Carbonneau and Piégay, 2012). Temporal resolution refers to the elapsed time between consecutive imagery. It turns out to be important in order to collect consecutive measurements and to carry out multi-temporal analysis and historical perspectives. Therefore, the temporal resolution has to be finer for acquisition of short-lived flood events (Mertes, 2008). Whereas, studies of large rivers based on satellite imagery have been able to exploit the regular revisit frequency of orbital sensors, airborne data is not acquired with the same regularity (Carbonneau and Piégay, 2012). However, commissioned flights are often necessary to attain suitable temporal resolution, particularly for a short-term change resulting from a single flood event (Gilvear and Fonstand, 2003). More recently, the acquisition of hyperspatial imagery (i.e., imagery with sub-decimetric spatial resolutions) (Rango et al., 2009; Carbonneau et al., 2012) at monthly or even daily temporal resolutions is now logistically and economically possible for river reaches of hectametric or kilometric scales. An essential assumption to apply the optical remote sensed approach in river change detection analysis is the temporal proximity of images to the flood event, that must be as much as possible representative of the pre- and post-flood geomorphic characteristics, avoiding the error of detecting changes not produced by the latest flood. Buraas et al. (2014) and Magilligan et al. (2015) deal with changes in channel width in the absence of extreme floods, determining thresholds of variations over the ~20 years preceding the Irene Storm, to avoid errors related to temporal resolution of data. In the study of Lichter and Klein (2011), the temporal resolution of the observations was limited to historical aerial photographs, which represent a specific moment in time. However, the database used in that study enabled an exceptional outlook into past flood events, covering an 85 years period.

Recent advance in technology allows the widespread availability of Unmanned Aerial System (UAS), existing in a very wide range of sizes and purposes, and available on the civilian commercial market (Carbonneau and Piégay, 2012).

Radiometric resolution: describes the sensor's ability to detect small changes in radiance and depends on the manner in which the continuous upwelling radiance signal is converted to discrete, digital image data. For example, an investigation of channel change might benefit from a highly sensitive detector with 12-bit radiometric resolution that enables very precise water depth estimates (Legleiter and Fonstad, 2012).

Spectral resolution: spectral resolution refers to the number of wavelength bands in which radiance measurements are made, as well as the location and width of these bands (Legleiter and Fonstad, 2012). The ability to accurately detect features from remote sensing therefore depends not only on increasing the number of bands beyond the visible spectrum, but also on an improvement of the spectral resolution. Indeed, the knowledge of spectral characteristics of the feature of interest and their response to environmental variables may enhance the use of remotely sensed data (Gilvear and Bryant, 2003). In image interpretation analysis, the human eye tends to assume contextual information for features identification and discrimination, whereas remotely sensed data allow distinguishing spectral discontinuities (Priestnall and Aplin, 2006). Panchromatic images, having a single, wide band and very high resolution, are generally used for details rendering, while multi-spectral images having several bands and lower resolution may have different reflective properties at different wavelengths. The grey-scale data of panchromatic images can be used to map channel planform, lateral migration, and, to a lesser extent, variations in water depth. However, incorporating spectral information allows channel morphology to be measured with greater confidence, and the possibility of examining other river attributes (Legleiter and Fonstad, 2012). Spectral resolution can be crucial in identifying certain materials, such as chlorophyll, based on their reflection of light as a function of the wavelength of the incident light. Therefore, in the case of limited spatial resolution, the availability of spectral bands achieving a greatest contrast between land and water is most suitable for channel planform detection (Gilvear and Bryant, 2003). Many airborne sensors and commercial satellites provide multispectral data, most often consisting of blue, green, red, and near-infrared bands, and more advanced hyperspectral instruments measure

radiance in a larger spectrum. For instance, the recently launched WorldView-3 satellite proposes a marked improvement in spectral terms with 8 bands in the visible and near infrared range and 8 bands in the short wave infrared (SWIR). Classification of imagery into surface categories based on their spectral properties may be carried out by several methods, allowing to support or speed up visual interpretation. Human features and structure, or riparian vegetation, might influence or limit significantly the behaviour of channel response to flood events. These features often stand out clearly on remotely sensed images, because of their shape and texture, and their different composition relative to surrounding materials, which enables their detection through automated, spectrally-based techniques (Marcus et al., 2012). Bryant and Gilvear (1999) illustrated the potential of multi-spectral and hyper-spectral airborne remote sensing (i.e., ATM) for detecting and quantifying changes in both fluvial sub-merged and exposed landforms (e.g., bar head accretion, bar tail formation and extension, bar dissection, localised bank erosion) and riparian land cover in a wandering gravel bed river before and after a flood. A maximum likelihood classifier was used on each image, and change detection analysis was carried out using a classification comparison approach. While bathymetric mapping was undertaken by applying a specific algorithm to ATM data.

Spatial resolution: spatial resolution defines the size of the smallest object which can be resolved on the ground (Carbonneau and Piégay, 2012), and it is just one of many variables that influence the extraction of pattern and the study of processes using remotely sensed imagery (Priestnall and Aplin, 2006). The difficulties in extracting rivers forms from imagery relate in part to the ‘precision’ with which one can identify and map a river feature, as determined by the spatial resolution offered by the instrument (Priestnall and Aplin, 2006). The identification of a feature might be difficult because of pixel size larger than the object, which may imply the possibility of mixed pixels containing a number of several objects (e.g., bed material, water, vegetation) and hence potentially misinterpretation (Gilvear and Bryant, 2003). Carbonneau and Piégay (2012) argued that there is no absolute rule for the number of pixels required to define a simple object, and identified a minimum of 5X5 pixels required to get an approximation of the object shape, whilst 3X3, or even 2X2 pixels are required to establish the presence of an object of undefined shape in the image. However, users should balance the potential inaccuracies of remote sensing based mapping techniques with the pixel resolution, and the

selection of an appropriate spatial resolution should require knowledge of the stream of interest and a thoughtful evaluation of the purpose of the study (Legleiter et al., 2004). Therefore, a pixel size that is adequate for one reach might not be suitable for other reaches. For instance, Ortega et al. (2009) mapped morpho-sedimentary features in each reach on a 1:4500 scale topographic map, showing only features large enough to be mappable at that scale. Hyperspectral data also create opportunities to apply more sophisticated approaches such as spectral mixture analysis, which could be especially helpful along the banks. Therefore, the purpose of an investigation may determine whether imageries are appropriate for the extraction of distinct objects or features (Priestnall and Aplin, 2006).

River size: one of the main critical factor in channel change or feature detection analysis is the relationship between the width of the river and the spatial resolution of the image (Priestnall and Aplin, 2006). The size of the stream relative to the sensor's ground instantaneous field of view can largely determine the utility of remote sensing for mapping channel morphology and in-stream features. For systems with coarser spatial resolution, pixels might be contaminated by radiance from the stream banks, and a pixel size of one half the mean channel width is a basic minimum requirement (Legleiter et al., 2004). Certain river settings do not work well for optical remote sensing, in particular high energy and small headwater streams. Investigation of relatively small channels may be also complicated by atmospheric conditions, vegetation cover and associated shadows along banks, making more complex feature digitization or extraction (Legleiter et al., 2004; Priestnall and Aplin, 2006).

Magnitude of change and accuracy: many authors recognized that estimates of channel changes are often affected by several errors (Rinaldi et al., 2016). Positional inaccuracy in digitized features considering channel or floodplain changes may often originate a spatial error being similar or greater than the magnitude of geomorphic changes (Priestnall and Aplin, 2006). Some works seemed to rely on inappropriate assumptions, where the magnitude of the error estimated using the most conservative methods is close to the magnitude of the measured change (Mount and Louis, 2005). Mount and Louis (2005) argued that rates of river channel migration or widening are only valid if it can be demonstrated that the amount of change in the measured parameters from images exceeds the measurement errors. They concluded that estimation and propagation of error in measurements of river

channel movement from aerial imagery requires knowledge of both the systematic error components and the random error components associated with the precision of feature identification, and that it is necessary to consider the following issues: i) a number of possible assumptions relating to the homogeneity/heterogeneity of error components, directional and temporal independence of errors and ii) the magnitude of systematic error compared to random error components. Recent advances in combining the output of global positioning system with image capture has increased the potential for accurate identification of an absolute location and allowed ground records to be matched to individual pixels on imagery, permitting more accurate image calibration and validation (Gilvear and Bryant, 2003). Changes may be the result of cumulative errors. Scale distortions in the original imagery, poor selection of ground control points used for georectification, and the algorithms used to transform the image to a specific coordinate system are possible sources of errors. These errors can be considerable and may sum up when attempting to detect change over time (Hughes et al., 2006). Hence, analyses of channel changes should include error assessment.

The majority of digital change detection techniques depend upon the precise accuracy of geometric registration of two images, which is very difficult to achieve due to the lack of accurate ground control points (Singh, 1989) and on the different scale between the pixel dimension and the object to be analysed (Mertes, 2008). Although the need to distinguish true geomorphic change from errors associated with image registration, no widely accepted framework for defining positional errors in image time series has been established (Lea and Legleiter, 2016). Standard methods of characterising accuracy in remote sensing assume that the ground data are correct (Marcus et al., 2012). Users should also consider the potential inaccuracy of supervised and unsupervised imagery classification techniques, though standard methods of accuracy assessment are normally included (Mertes, 2008). However, spatial errors and uncertainties related to geomorphological changes digitization and quantification, and the definition of a rigorous protocol for error assessment remain a controversial issue for many authors. Marcus and Fonstad (2008) highlighted the lack in bibliography about what levels of accuracy and precision are required to answer specific research questions, preventing a wider use of remote sensing techniques in fluvial geomorphology. In response to this lack of error quantification, Mount and Louis (2005) provided methods for estimating and propagating error in bankfull width

measurements made from aerial photographs in a GIS. The first issue, which came up from this latter study, is given by the multiple possible definitions of bankfull. They assumed that it is appropriate to locate bakfull from aerial photos according to the location of boundary features and the water-sediment interface, where overhanging vegetation does not obscure banks. Sloan et al. (2001) determined the minimum size of detected features based on the resolution of the aerial photographs and accuracy of measurements collected in the field, obtaining a 7% of error and determining a conservative estimation of change in channel width. Gurnell (1997) adopted several strategies in order to minimize errors in extracting information on channel change from air photographs such as (i) a standard definition of river bank location using channel bank vegetation limit, (ii) a standard set of spatial locations from which multi-temporal comparisons are made (i.e., cross-sections), (iii) a definition of a set of standard control points (i.e., from 15 to 25 points for individual photographs), (iv) the employment of air photograph coverage of similar scale, (v) the visual interpretation provided by the same operator, (vi) the use of standard non-linear least-squares transformation to minimize horizontal distortions. Buraas et al. (2014) and Magilligan et al. (2015) have considered several thresholds for defining a significant change in width, including 1–4 times the standard deviation in width changes in the absence of extreme floods. These thresholds are used to provide natural changes in width (i.e., not due to extreme flooding) and to account for the apparent variation due to different sources of error (e.g., shading, resolution of the imagery, overhanging vegetation covering the edge of the channel and operator error). Ghoshal et al. (2010) pointed out that different flow stages at dates of aerial photograph acquisitions might introduce erroneous planimetric indications of bar erosion or deposition because high flows on a later date may give a false measure of bar erosion, while low flows on a later date may misleadingly suggest bar deposition. However, in the case of high-magnitude channel changes, some authors considered negligible errors related to georectification and digitizing (Surian et al., 2016). More recently, Lea and Legleiter (2016) introduced a framework based on a leave-one-out cross-validation (LOOCV) approach to characterise the spatial distribution of image registration errors in the analysis of channel change for five sequential 1-m pixels aerial photographs pairs of Savery Creek, Wyoming, USA (i.e., from 1980 to 2012). Their findings revealed that spatially distributed estimates of registration error enabled detection of a greater number of statistically significant lateral migration vectors rather than the standard

metrics, such as spatially uniform RMSE or 90th percentile of GCP (i.e., ground control point) error (Lea and Legleiter, 2016).

The assessment of the error for 3D channel change detection approaches appears to be clearer. For instance, the uncertainty related to the DEM of Difference approach required the assessment of the minimum level of detection (LoD) that is detectable above the noise of the data (Brasington et al., 2000; Tamminga et al., 2015). Therefore, the uncertainty might be either spatially uniform, constant within zones of similar characteristics or variable for every cell of the raster (Lane et al., 2003; Perignon et al., 2013). However, the uncertainties related to this approach might be related to several sources of error, such as systematic error affecting the accuracy of the measurements, random error affecting the precision of the data (Grove et al., 2013; Thompson et al., 2013), interpolation errors arising during the creation of DTMs from point data, or filtering errors referred to discarding all off-terrain points in order to reconstruct the bare-earth only (Milan et al., 2011; Milan, 2012; Crosilla et al., 2013; Perignon et al., 2013; Tamminga et al.,2015).

Field validation and data matching: as argued in the previous sections, satellites offer to landscape studies a vantage point of Earth observation, computer compatibility of sensed data, historical perspectives, and near-global coverage. Nevertheless, spatial- and temporal-scale limitations of remotely sensed data imply that in-depth fieldwork, using both traditional and technologically advanced data-collection techniques, will continue to be an integral part of the science of geomorphology (Walsh et al., 1998). Many researchers have found remotely sensed data a valuable tool for quantifying and detecting channel features and changes, however few of them have addressed the problems of quantification and validation of change within the river and floodplain system from multi-date airborne or space-borne imagery (Bryant and Gilvear, 1999). The comparison between manifold field measurements and remote sensing techniques reveals a lower accuracy of remotely sensed data (Marcus and Fonstad, 2008). The dissimilarity between remote sensing data and field information is a general problem because of the mismatch between the scale of the objects and the spatial resolution of the data (Mertes, 2008). Often a direct comparison with field records is employed, however advanced error analysis typically lacks due to sparse distribution of field data (Mertes, 2008). Ghoshal et al. (2010), in their study involving aerial photographs rectification processes for planimetric analysis of lateral channel migration, used ground control points collected

in the field near river channels, to ensure greatest accuracy in rectification where most channel-change measurements were taken. On the other hand, the change detection algorithm employed by Bryant and Gilver (1999) to ATM data revealed subtle changes not noticed in the field. A remaining challenge is to achieve an exact match between the categories of landscape classification from the remote sensing analysis and data from the field survey or model outputs (Mertes, 2008). For Marcus and Fonstand (2008), logistical obstacles concern ground validation procedures on time of imagery acquisition, which is difficult to accomplish at watershed extents, particularly in large and difficult to access river basins.

Costs and data availability: the spatial extent of the study and the number of measurements needed over time are factors strictly driving costs (Marcus et al., 2012). Remote sensing becomes a reasonable alternative to ground-based field surveys when it can monitor or map the variables of interest and when it can do so on a cost effective or safer basis than ground-based techniques. One advantage of optical imagery for remote sensing of rivers is that these data are widely available through government mapping agencies and commercial vendors that usually collect and archive airborne and satellite optical imagery also providing historical records. Aerial surveys are not cheap to commission and repeat coverage at short time intervals is usually limited or impossible (Chandler et al., 2002). On the other hand, imagery from satellites is relatively cheap or freely available and the scale of the events roughly matches the resolution of the satellite imagery (Joyce et al., 2009).

3.4 Combination of optical techniques and other geospatial data in channel response to flood detection

In many studies, the use of combining diverse data sources and processing made the channel change detection analysis more robust and accurate (Table 1). The widespread availability of Geographic Information Systems (GIS) has allowed the wide use of optical imagery for channel change mapping, because it made easier the digitization of river features from aerial or satellite imagery and the assessment of a wide variety of spatial and change-over-time analyses (Marcus et al., 2012). The two technologies might be joined for a better examination of the landscape, investigating the interrelationships of scale, pattern and process (Walsh et al., 1998; Rinaldi et al., 2016). Specifically, GIS technology offers an analytical framework for

data synthesis, capture, storage, management, integration, analysis, display and forecast (Tholey et al., 1997; Walsh et al., 1998; Yang et al., 1999; Sanyal and Lu, 2004). In the case of geomorphic changes in flood detection analysis, GIS techniques allow to make several operations (e.g., overlay, intersect, merging) enhancing a multi-spatial and temporal analysis and to characterize and quantify channel changes (Dewan et al., 2007). Particularly, the possibility of digitizing channel features allows the assessment of the pre-flood morphological state of the channel and the definition of the post-flood channel morphological state in a qualitative and quantitative way.

The merging of optical remotely sensed data with other spatial information within a GIS offers the possibility of measurement and quantification of channel changes by using different data sources and different approaches to characterize also the nature of landscape changes, to assess GIS-derived geomorphic indices and variables as described in section 3.1, and to model the location and response of phenomena through interfaces (Tholey et al., 1997; Walsh et al., 1998). For instance, the use of digital elevation models derived by optical or radar remote sensing data within a GIS might provide the extraction of several morphological and hydrological parameters (e.g., altitude, slopes, orientation, basins and sub-basins, channel network, terraces, floodplain, curvature, aspect, flow direction, flow accumulation) as useful support for a change detection analysis. However, the consideration of an automated feature extraction approach remains controversial, because different variables could influence the reliability of this process (Priestnall and Aplin, 2006). Many authors described limits of automatic approaches to channel mapping including, for example, water level (Puech and Raclot, 2002), vegetation cover, shadows and soil moisture (Yang et al. 1999; Priestnall and Aplin, 2006).

3.5 Application: geomorphic effects of the November 2013 flood in the Posada catchment, Italy

An example of application of optical remote sensing as a tool in channel change detection is illustrated in this section. The study referred to one single high-magnitude and low frequency flood event that produced notable geomorphic response in two ungauged Mediterranean rivers in November 2013 (northeastern Sardinia, Italy) (Righini, 2017). The study area is located in the Posada River basin

which covers a total area of 685 km2, and the analysis specifically focused on 22-km-long and 18-km-long semi-alluvial single-thread channels of the Posada and Mannu di Bitti Rivers respectively.

The definition of channel morphological characteristics and features, and the quantification of channel planimetric 2D changes (i.e., channel widening, floodplain planform change and islands erosion/formation) through the use of high resolution space-born data within a geographic information system (GIS) are the main purposes of this remote sensing analysis. The choice of the study reaches is based on the fundamental assumption concerning the visibility of the channel and the feasibility of the assessment of geomorphic changes from above.

The evaluation of the initial morphological conditions deals with i) the spatial units definition (i.e., from catchment scale to sub-reach scale), and ii) the quantitative measurements of the areal and linear geomorphic features (i.e., channel width, channel slope, alluvial plain and island extension, valley confinement and channel sinuosity). The analysis on the pre flood high-resolution (1 m or higher) satellite images taken in April 2011 was carried out on data stored in the Basemap gallery available in ArcGIS Explorer Desktop by the World Imagery service (Fig. 7A). The planimetric 2D changes detection was carried out by means of multi-temporal analysis approach by visual skills-based interpretation procedure applied to a set of high resolution pre and post-flood satellite images and handled by the same operator. The post flood image analysis was conducted on WorldView-2 pan-sharped 4 band imageries with a spatial resolution of 50 cm taken in April 2014 (Fig. 7B).

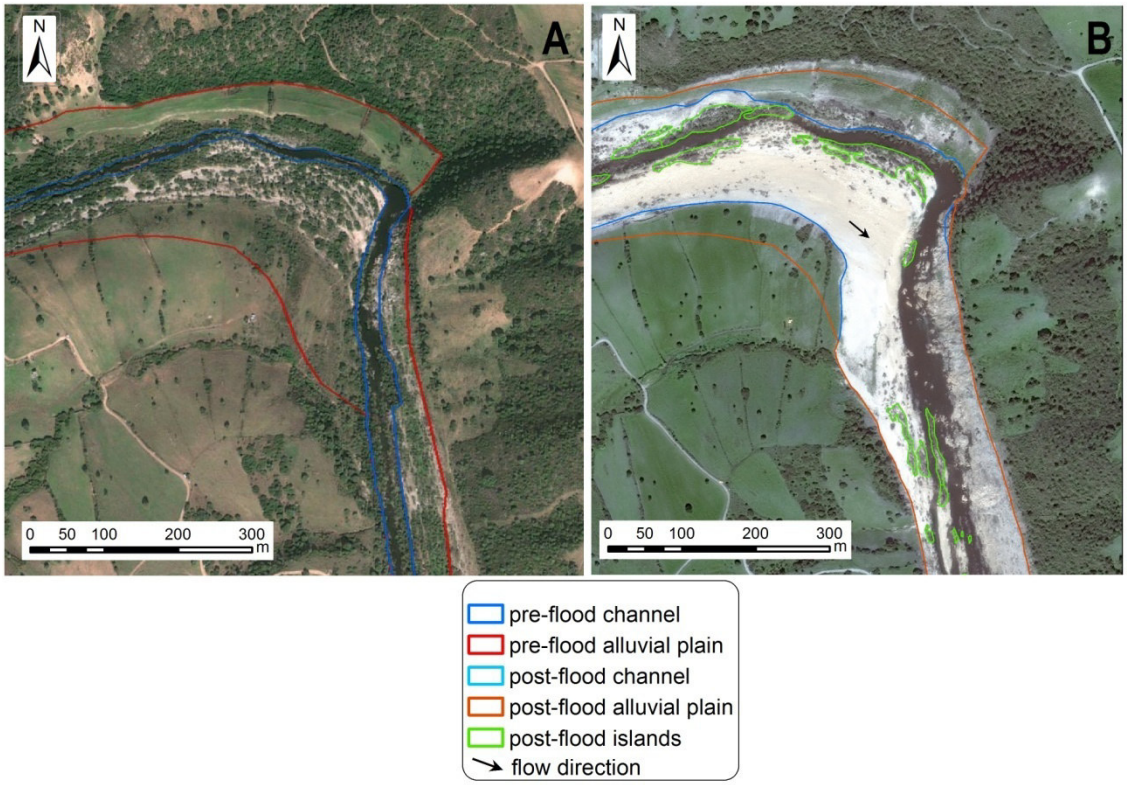

Figure 7. Planimetric 2D changes (i.e., channel widening, floodplain planform change and reactivation and island formation) on the Posada River (northeastern Sardegna, Italy) at sub-reach scale: (A) 2011 pre-flood satellite image from Basemap gallery available in ArcGIS Explorer Desktop by the World Imagery service (spatial resolution= 1m or higher); (B) 2014 post-flood WorldView-2 pan-sharped 4 band imagery (spatial resolution= 0.5 m).

The channel was digitized on pre and post satellite images, referring to the active-channel area, defined as the part of the river corridor relatively free of vegetation (unvegetated or sparsely vegetated bars), that conveys most of the water and sediment during high flow with an initial average width ranging from 9 to 141 m. Alluvial plain area encompassed present floodplain and low terraces, i.e. surfaces that can be some meters higher than the floodplain and can be infrequently flooded (Surian et al., 2016). Islands were recognized and outlined as in-channel landforms that persists sufficiently long to establish permanent vegetation (i.e., shrub or woody vegetation).

Analysis findings revealed channel widening as the dominant geomorphic response observed. Channel width increased from 1.1 (i.e., from a pre-flood channel width of 141 to 156.5 m) to 6.2 (from a pre-flood channel width of 12.2 to 76 m) times the pre-flood width. In Figure 7 an example of pre and post- flood satellite imagery comparison at sub-reach scale (i.e., 800 m) is reported. In that sub-reach the channel widened 5.5 times in comparison to the initial channel width (i.e., from 24 to 133 m).

Morphodynamic processes led to island formation and variation of large portion of floodplain planform. Specifically, in the sub-reach showed in Figure 7, floodplain enlarged from an initial average width of 158 m to an average post-flood width of 196 m (i.e., 38 m of net change), while the formation of islands reached an areal extension of 10346 km2.

The spatial resolution of satellite imagery was suitable for the study purpose because pixel size was much smaller than river size and appropriate for fluvial features identification and assessment of channel change. The approach allowed continuous measurements and data supply over long distance in a large but limited access basin area. However, the analysis might be affected by errors, in particular related to imagery interpretation and digitization. Besides, different coordinate systems of pre (i.e., WGS 1984 Web Mercator Auxiliary Sphere) and post-flood (i.e., UTM WGS 1984) satellite data originated small image shifting. The estimated error ranged from ±0% to ±16% of changes overestimation/underestimation, and it was obtained by calculating the difference between the maximum and the minimum shift values measured for each sub-reach. Errors were negligible considering that (i) images with high spatial resolution were used, (ii) magnitude of changes was very high (i.e., the amount of changes in measured parameters largely exceeded errors) and (iii) absolute values of pre and post-flood geomorphic features allowed to overcome shifting errors and to obtain net change values. Furthermore, additional information were collected from digital elevation model (10 m spatial resolution), topographic maps at 1:10000 scale, and field survey on representative reaches for minimizing errors, improving visual interpretation and obtaining a more robust analysis. Besides, the proximity of available data to the event allowed to minimize errors in considering possible natural geomorphic changes before or after the 2013 flood. Finally, the described remote sensing analysis allowed (i) a better understanding of channel dynamics and processes during high-magnitude flood event,(ii) defining the potential controlling factors of channel widening (i.e., both morphological and hydraulic variables) and (iii) developing predictive models describing magnitude and patterns of channel planimetric changes (Righini, 2017).

4. Discussion

As illustrated in the previous section, several approaches may be adopted to detect geomorphic changes in response to floods, depending on the object of investigation. The feasibility of a certain approach depends on several aspects (e.g., systematic, random, georectification and digitization errors; the relationship between the size of the detecting feature and the spatial data resolution; magnitude of changes) which have different importance in relation to the focus of the geomorphic analysis. The most common approaches to change detection in response to floods, and their related data and feasibility, are summarised in Table 2.

Change detection	Data	Method	Feasibility		
			Size of detected feature/data resolution	Change magnitude	Errors
Channel width	Aerial and satellite imagery	Multi-temporal and spatial analysis	+++	+++	+
Channel pattern	Aerial and satellite imagery	Multi-temporal and spatial analysis	+++	++	+
Channel shifting	Aerial and satellite imagery	Multi-temporal and spatial analysis	+++	++	+++
Bank retreat	Aerial and satellite imagery	Multi-temporal and spatial analysis	+++	+++	+++
Substrate type	Aerial and multi-spectral satellite imagery	Multi-temporal and spatial analysis; imagery comparison; field survey	+++	++	+
Grain size	Aerial, multi-spectral satellite and UAS imagery	Image analysis; field survey	+++	+	++
Sub-merged geomorphic feature	Airborne/spaceborne hyperspectral imagery	Imagery classification comparison; field survey	++	++	+
Topography	Airborne/spaceborne hyperspectral imagery	Bathymetric mapping	+	+++	+++
Erosion/deposition	LiDAR or photogrammetry derived DEMs/DTMs	DEM of Difference (DoD)	++	+++	+++
Land coverage	Aerial and multi-spectral satellite imagery	Multi-temporal and spatial analysis; imagery classification comparison	+	+	++

Table 2. Channel change detection analysis in response to floods: remotely sensed data, methods, and main aspects to be taken into account for detecting changes. Feasibility of detecting geomorphic changes considering three aspects: the relationship (i.e. ratio) between size of the detected feature and spatial resolution of imagery; magnitude of geomorphic change; errors due georectification, digitization, etc. The importance of each aspect is assessed as follows: +: negligible or little importance; ++: moderate importance; +++; high or very high importance

The best approach for channel width change analysis is a multi-temporal ad spatial analysis using high resolution airborne or space-borne imagery, whose applicability might be mostly affected by the magnitude of changes and by the channel width related to image spatial resolution. For changes in channel width, georectification and digitisation errors can be considered of negligible or little importance in case of high-magnitude changes. Conversely, the two latter aspects are very relevant in the applicability of pre- and post-flood comparison approach for channel shift or migration and banks retreat detection. Besides, these analyses do not necessarily require field survey validations. Channel pattern and substrate type change detection is usually conducted through qualitative multi-temporal and spatial

analyses to support field survey, hence the error assessment becomes less important, while the size of the detected object and the magnitude of the channel change remain necessary to reach a good matching between remotely sensed and field data. Analysis of exposed or submerged geomorphic features requires high-resolution multi- and hyperspectral imagery respectively to carry out a multi-temporal and spatial analysis. For exposed geomorphic features detection, suitability of imagery comparison approaches might be highly affected by the minimum size of the detected features based on data resolution, magnitude of change, but also by georeferencing and digitization errors. A fair submerged feature detection, instead, depends mostly on spectral resolution (see section 3.3). The grain size analysis necessitates the use of high-resolution airborne, space-borne or UAS imagery: in this case availability of very high spatial resolution can be crucial for an effective analysis. Land cover change analysis is usually performed by classified imagery comparison, which does not really need georeferencing and digitization error minimization for a qualitative analysis. Nevertheless, this aspect might be subtle if accomplish quantitative analysis. The definition of erosional or depositional process are mostly performed by the use of topographic data and by DoD approach. As described above, this kind of approach might be affected by several sources of error, however determining the minimum level of detection (LoD) is fundamental, as well as the magnitude of change related to data spatial resolution.

5. Final remarks

The present availability of data with high spatial resolution and short revisit time offers great opportunities and new challenges in the analysis of geomorphic response to floods: i) the possibility of time-sequential satellite image comparison; ii) a broad areal coverage and a synoptic view of channel dynamics of individual flood event across different scales (i.e. from in-stream units to the entire catchment); iii) continuous measurements and data supply of channel response to flood of the whole river corridor over long distances, particularly in large fluvial systems and where accessibility is more difficult; iv) insights into the complexity of interactions driving changes in riverine landscape during flood events; v) deeper understanding of stream morphodynamics and potential to develop more accurate models of

geomorphic response to floods to assess the magnitude of the flood event and areas of channel instability.

There are some key assumptions to be taken into account when optical remote sensing approach is used: (i) the temporal proximity of images to the flood event, for accurate analysis of the pre- and post-flood geomorphic characteristics; (ii) the size of watershed and stream channels; (iii) relationships between channel width, and other fluvial features, and the spatial resolution of the image; (iv) magnitude of channel changes that must be well identifiable to capture in-stream variations; (v) reduction of factors that may alter the quality of image interpretation or classification, such as seasonal stage, weather conditions and vegetation canopy. Furthermore, accuracy of optical remote sensing results is a still long debated aspect due to several sources of error.

References

Allen GH, and Pavelsky TM (2015) Patterns of river width and surface area revealed by the satellite-derived North American River Width data set. Geophys. Res. Lett., **42**: 395–402. doi:10.1002/2014GL062764

Baker VR (1977) Stream-channel response to floods, with examples from central Texas. Geological Society of America Bulletin **88**(8)

Bizzi S and Lerner DN (2015) The Use of Stream Power as an Indicator of Channel Sensitivity to Erosion and Deposition Processes. River Res. Applic., **31**: 16–27. doi: 10.1002/rra.2717

Bledsoe BP, Watson CC (2001) Logistic analysis of channel pattern thresholds: meandering, braiding, and incising. Geomorphology **38**: 281–300

Brasington J, Rumsby BT, and McVey RA (2000) Monitoring and modelling morphological change in a braided gravel-bed river using high-resolution GPS-based survey. Earth Surface Processes and Landforms **25**: 973–990

Bryant RG, Gilvear DJ (1999) Quantifying geomorphic and riparian land cover changes either side of a large flood event using airborne remote sensing: River Tay, Scotland. Geomorphology **29**: 307–321

Buraas EM, Renshaw CE, Magilligan FJ, Dade WB (2014) Impact of reach geometry on stream channel sensitivity to extreme floods. Earth Surface Processes and Landforms **39**: 1778–1789

Carbonneau PE and Piégay H (2012) Introduction: The Growing Use of Imagery in Fundamental and Applied River Sciences. In: Carbonneau P and Piégay H (ed) Fluvial Remote Sensing for Science and Management. Wiley-Blackwell, p 1-18

Carbonneau PE, Piégay H, Lejot J, Dunford R, Michel K (2012) Hyperspatial imagery in riverine environments. Fluvial Remote Sens. Sci. Manag. p 163–191

Cavalli M, Trevisani S, Comiti F, Marchi L (2013) Geomorphometric assessment of spatial sediment connectivity in small Alpine catchments. Geomorphology **188**: 31–41. doi:10.1016/j.geomorph.2012.05.007

Chandler J, Ashmore P, Paola C, Gooch M, Varkaris F (2002) Monitoring River-Channel Change Using Terrestrial Oblique Digital Imagery and Automated Digital Photogrammetry. Annals of the Association of American Geographers, **92**:4, 631-644. doi: 10.1111/1467-8306.00308

Costa JE, O'Connor JE (1995) Geomorphically effective floods. In: Costa, JE, Miller, AJ, Potter, KW, Wilcock, P (ed) Natural and Anthropogenic Influences in Fluvial Geomorphology Monograph, vol 89 American Geophysical Union, Washington, DC, p 45–56

Dethier E, Magilligan FJ, Renshaw CE, Nislow KH (2016) The role of chronic and episodic disturbances on channel–hillslope coupling: the persistence and legacy of extreme floods Earth Surf Process Landforms **41**:1437–1447. doi: 101002/esp3958

Dewan AM, Islam MM, Kumamoto T, Nishigaki M (2007) Evaluating Flood Hazard for Land-Use Planning in Greater Dhaka of Bangladesh Using Remote Sensing and GIS Techniques Water Resource Manage **21**: 1601–1612. doi:101007/s11269-006-9116-1

Ferencevic MV, Ashmore P (2012) Creating and evaluating digital elevation model-based stream-power map as a stream assessment tool River Research and Applications **28**: 1394–1416

Fonstad MA, Marcus WA (2010) High resolution, basin extent observations and implications for understanding river form and process Earth Surface Processes and Landforms, **35**(6): 680–698

Gilvear D J, Davids C and Tyler AN (2004) The use of remotely sensed data on channel hydromorphology; River Tummel, Scotland River Res. Applic. **20**: 1–17. doi: 101002/rra792

Gilvear DJ and Bryant R (2003) Analysis of aerial photography and other remotely sensed data. In: Kondolf GM and Piégay, H (ed) Tools in Fluvial Geomorphology, Wiley: London, p 133–168

Gilvear D, Winterbottom S, and Sichingabula H (2000) Character of channel planform change and meander development: Luangwa River, Zambia. Earth Surf Process Landforms, **25**: 421–436

Ghoshal S, James LA, Singer MB and Aalto R (2010) Channel and Floodplain Change Analysis over a 100-Year Period: Lower Yuba River, California. Remote Sensing **2**: 1797-1825. doi:103390/rs2071797

Grove JR, Croke J and Thompson C (2013) Quantifying different riverbank erosion processes during an extreme flood event. Earth Surf Process Landforms **38**: 1393–1406. doi: 101002/esp3386

Gupta A, Fox H (1974) Effects of high magnitude floods on channel form: a case study in the Maryland Piedmont. Water Resour Res **10**: 499–509

Gurnell AM (1997) Channel change of the river Dee meanders, 1946–1992, from the analysis of air photographs Regulated Rivers. Research and Management **13**: 13–26

Heritage GL, Large ARG, Moon BP, Jewitt G (2004) Channel hydraulics and geomorphic effects of an extreme flood event on the Sabie River, South Africa. Catena **58**: 151–181

Hooke JM (2004) Cutoffs galore!: occurrence and causes of multiple cutoffs on a meandering river. Geomorphology **61** (3–4): 225–238

Hooke JM (2008) Temporal variations in fluvial processes on an active meandering river over a 20-year period. Geomorphology **100**: 3–13

Hooke JM and Yorke L (2010) Rates, distributions and mechanisms of change in meander morphology over decadal timescales, River Dane, UK. Earth Surf. Process. Landforms **35**: 1601–1614

Hughes ML, McDowell PF, and Marcus WA (2006) Accuracy assessment of georectified aerial photographs: Implications for measuring lateral channel movement in a GIS. Geomorphology **74**: 1–16

Joyce KE, Belliss SE, Samsonov SV, McNeill SJ and Glassey PJ (2009) A review of the status of satellite remote sensing and image processing techniques for mapping natural hazards and disasters. Progress in Physical Geography **33**(2): 1–25. doi :101177/0309133309339563

Krapesch G, Hauer C, Habersack H (2011) Scale orientated analysis of river width changes due to extreme flood hazard. Natural Hazards and Earth System Sciences **11**: 2137–2147

Kumar R, Kamal V and Singh RK (2013) Geomorphic Effects of 2011 Floods on Channel Belt Parameters of Rapti River: A Remote Sensing and GIS Approach. Corona Journal of Science and Technology, vol 2, No II, p 4-12

Lane SN, Widdison PE, Thomas RE, Ashworth PJ, Best JL, Lunt IA, Sambrook Smith GH, and Simpson CJ (2010) Quantification of braided river channel change using archival digital image analysis. Earth Surf Process Landforms **35**: 971–985

Lane SN, Westaway RM, and Hicks DM (2003) Estimation of erosion and deposition volumes in a large, gravel bed, braided river using synoptic remote sensing. Earth Surface Processes and Landforms **28**(3): 249–271

Lane SN, Chandler JH, and Porfiri K (2001) Monitoring river channel and flume surfaces with digital photogrammetry. J. Hydraul. Eng. 127: 871

Lane S, Richards K, and Chandler J (1993) Developments in photogrammetry - The geomorphological potential. Progress in Physical Geography, **17**(3): 306–328

Lea DM , Legleiter CJ (2016) Refining measurements of lateral channel movement from image time series by quantifying spatial variations in registration error. Geomorphology **258**: 11–20

Legleiter CJ, Roberts DA, Marcus WA, Fonstad MA (2004) Passive optical remote sensing of river channel morphology and in-stream habitat: Physical basis and feasibility. Remote Sensing of Environment **93**: 493–510

Legleiter CJ, Roberts DA, and Lawrence RL (2009) Spectrally based remote sensing of river bathymetry. Earth Surface Processes and Landforms **34**: 1039–1059.

Legleiter CJ and Fonstad MA (2012) An Introduction to the Physical Basis for Deriving River Information by Optical Remote Sensing. In: Carbonneau P and Piégay H (ed) Fluvial Remote Sensing for Science and Management. Wiley-Blackwell, p 43-69

Leopold LB, and Maddock TJ (1953) Hydraulic geometry of stream channels and some physiographic implications. U.S. Geological Survey Professional Paper **252**: 55

Lichter M and Klein M (2011) The effect of river floods on the morphology of small river mouths in the southeastern Mediterranean Zeitschriftfür. Geomorphology vol **55**(3): 317–340

Magilligan FJ, Buraas EM, Renshaw CE (2015) The efficacy of stream power and flow duration on geomorphic responses to catastrophic flooding. Geomorphology **228**: 175-188

Magilligan FJ, Gomez B, Mertes LAK, Smith LC, Smith ND, Finnegan D, Garvin JB (2002) Geomorphic effectiveness, sandur development, and the pattern of landscape response during jökulhlaups: Skeiðarársandur, southeastern Iceland. Geomorphology **44**: 95–113

Magilligan FJ (1992) Thresholds and the spatial variability of flood power during extreme floods. Geomorphology **5**: 373–390

Marcus WA, Fonstad MA and Legleiter CJ (2012) Management Applications of Optical Remote Sensing in the Active River Channel. In: Carbonneau P and Piégay H (ed) Fluvial Remote Sensing for Science and Management. Wiley-Blackwell, p 19-41

Marcus WA and Fonstad MA (2008) Optical remote mapping of rivers at sub-meter resolutions and watershed extents. Earth Surface Process Landforms **33**: 4–24. doi: 101002/esp1637

Mertes LAK (2008) Remote sensing of riverine landscapes. Freshwater Biology **47**: 799–816

Milan DJ (2012) Geomorphic impact and system recovery following an extreme flood in an upland stream: Thinhope Burn, northern England, UK. Geomorphology **138**: 319-328

Miller AJ (1990) Flood hydrology and geomorphic effectiveness in the central Appalachians. Earth Surface Processes and Landforms **15**: 119–13

Milton JA, Gilvear DJ, Hooper ID (1995) Investigating river channel changes using remote sensed data. In: Gurnell A, Petts GE (ed) Changing River Channels. Chichester: Wiley, p277-301

Mount NJ and Louis J (2005) Estimation and propagation of error in measurements of river channel movement from aerial imagery Earth Surface Processes and Landforms, **30**: 635–643

Nardi L, Rinaldi M (2014) Spatio-temporal patterns of channel changes in response to a major flood event: the case of the Magra River (central-northern Italy). Earth Surface Processes and Landforms **40**: 326-339

Ortega JA, Guillermina GH (2009) Geomorphological and sedimentological analysis of flash-flood deposits The case of the 1997 Rivillas flood (Spain). Geomorphology **112**: 1–14

Pan Z, Glennie C, Legleiter C, and Overstreet B (2015) Estimation of water depths and turbidity from hyperspectral imagery using support vector regression, IEEE Geosci. Remote Sens. Lett., vol. **12**, no. 10, pp. 2165–2169,

Peixoto JMA, Nelson BW, Wittmann F (2009) Spatial and temporal dynamics of river channel migration and vegetation in central Amazonian white-water floodplains by remote-sensing techniques. Remote Sensing of Environment **113**: 2258–2266

Piégay H, Darby SE, Mosselman E, Surian N (2005) A review of techniques available for delimiting the erodible river corridor: a sustainable approach to managing bank erosion. River Research and Applications **21**: 773–789

Piégay H, Kondolf GM, Minearc JT, Vaudora L (2015) Trends in publications in fluvial geomorphology over two decades: A truly new era in the discipline owing to recent technological revolution?. Geomorphology **248**: 489-500

Phillips JD (2002) Geomorphic impacts of flash flooding in a forested 828 headwater basin. Journal of Hydrology **269**: 236–250

Pradhan B (2010) Flood susceptible mapping and risk area delineation using logistic regression, GIS and remote sensing. Journal of Spatial Hydrology vol **9**(2), p 1-18

Priestnall G and Aplin P (2006) Spatial and temporal remote sensing requirements for river monitoring International. Journal of Remote Sensing vol **27**(11): 2111–2120

Puech C and Raclot D (2002) Using geographical information systems and aerial photographs to determine water levels during floods. Hydrological processes **16** (8): 1593-1602

Rango A, Laliberte A, Herrick JE, Winters C, Havstad K, Steele C, and Browning D (2009) Unmanned aerial vehicle based remote sensing for rangeland assessment, monitoring, and management. Journal of Applied Remote Sensing, 3.10.1117/1.3216822

Richardson JM and Fuller IC (2010) Quantification of channel planform change on the lower Rangitikei River, New Zealand, 1949-2007: response to management? Palmestron North NZ: Massey University School of People, Environment and Planning

Rinaldi M, Simoncini C, Piégay H (2009) Scientific strategy design for promoting a sustainable sediment management: the case of the Magra River (Central – Northern Italy). River Research and Applications **25**: 607–625 doi: 101002/rra1243

Rinaldi M, Surian N, Comiti F, Bussettini M (2013) A method for the assessment and analysis of the hydromorphological condition of Italian streams: the Morphological Quality Index (MQI). Geomorphology **180-181**: 96–108. doi: 101016/jgeomorph201209009

Rinaldi M, Amponsah W, Benvenuti M, Borga M, Comiti F, Lucìa, A, Marchi L, Nardi, L, Righini, M, Surian, N (2016) An integrated approach for investigating geomorphic response to extreme events: methodological framework and application to the October 2011 flood in the Magra River catchment, Italy. Earth Surface Processes and Landforms, **41**, 835–846. doi: 10.1002/esp.3902

Righini M (2017) Geomorphic response to extreme floods in alluvial and semi-alluvial rivers, Unpublished PhD Thesis, University of Padua

Sanyal J and Lu XX (2004) Application of Remote Sensing in Flood Management with Special Reference to Monsoon Asia: A Review. Natural Hazards **33**: 283–301

Schumm SA, Lichty RW (1963) Channel widening and floodplain construction along Cimarron River in southwestern Kansas. U.S. Geological Survey Professional Paper 352D: 71–88

Singh A (1989) Review Article Digital change detection techniques using remotely-sensed data. International Journal of Remote Sensing, **10**(6): 989-1003. doi: 101080/01431168908903939

Sloan J, Miller JR, Lancaster N (2001) Response and recovery of the Eel River, California, and its tributaries to floods in 1955, 1964 and 1997. Geomorphology **36**: 129–154

Smith LC (1997) Satellite remote sensing of river inundation area, stage, and discharge: A review. Hydrologic Processes **11**: 1427–1439

Stweart JH, and La Marche VC Jr (1967) Erosion and deposition produced by the flood of December 1964 on Coffee Creek, Trinity County, California. U.S. Geol Survey Prof Paper 422K

Surian N, Rinaldi M, Pellegrini L, Audisio C, Maraga F, Teruggi L, Turitto O, Ziliani L (2009) Channel adjustments in northern and central Italy over the last 200 years In: James LA, Rathburn SL, Whittecar GR (ed) Management and Restoration of Fluvial Systems with Broad Historical Changes and Human Impacts. Special Paper, 451 Geological Society of America, Boulder, USA, p 83–95

Surian N, Righini M, Lucìa A, Nardi L, Amponsah M, Benvenuti M, Borga M, Cavalli M, Comiti F, Marchi L, Rinaldi M, Viero A (2016) Channel response to extreme floods: insights on controlling factors from six mountain rivers in northern Apennines, Italy. Geomorphology, **272**, 78–91. doi:10.1016/j.geomorph.2016.02.002

Tamminga AD, Eaton BC and Hugenholtz CH (2015) UAS-based remote sensing of fluvial change following an extreme flood event. Earth Surface Process Landforms **40**: 1464–1476. DOI: 101002/esp3728

Tholey N, Clandillon S and De Fraipont P (1997) The contribution of spaceborne SAR and optical data in monitoring flood events: examples in northern and Southern France. Hydrological Processes, vol **11**, 1409-1413

Thompson C, Croke J (2013) Geomorphic effects, flood power, and channel competence of a catastrophic flood in confined and unconfined reaches of the upper Lockyer valley, southeast Queensland, Australia. Geomorphology **197**: 156–169

Walsh SJ, Butler DR, Malanson GP (1998) An overview of scale, pattern, process relationships in geomorphology: a remote sensing and GIS perspective. Geomorphology **21**: 183-205

Wohl E (2014) Time and the rivers flowing: Fluvial geomorphology since 1960. Geomorphology **216**: 263–282

Wolman MG, Gerson R (1978) Relative scales of time 854 and effectiveness of climate in watershed geomorphology. Earth Surface Processes Landforms **3**: 189–208

Wolman MG, Miller JP(1960) Magnitude and frequency of forces in geomorphic processes. Journal of Geology **68**: 54–74

Woodget A, Carbonneau P, Visser F, and Maddock I (2015) Quantifying submerged fluvial topography using hyperspatial resolution UAS imagery and structure from motion photogrammetry," Earth Surf. Process. Landforms, vol. **40**, no. 1, pp. 47–64

Yang X, Damen MCJ and Van Zuidam RA (1999) Satellite remote sensing and GIS for the analysis of channel migration changes in the active Yellow River Delta, China. JAG I vol 1(2): 146-57

PART II – CHANNEL RESPONSE TO EXTREME FLOODS: CASE STUDIES

3. CHANNEL RESPONSE TO EXTREME FLOODS: INSIGHTS ON CONTROLLING FACTORS FROM SIX MOUNTAIN RIVERS IN NORTHERN APENNINES, ITALY.

Nicola Surian [a,*], Margherita Righini [a], Ana Lucía [b], Laura Nardi [c], William Amponsah [d,e], Marco Benvenuti [c], Marco Borga [e], Marco Cavalli [d], Francesco Comiti [b], Lorenzo Marchi [d], Massimo Rinaldi [c], Alessia Viero [d]

[a] Department of Geosciences, University of Padova, Italy; [b] Faculty of Science and Technology, Free University of Bozen-Bolzano, Italy; [c] Department of Earth Sciences, University of Florence, Italy; [d] CNR IRPI, Padova, Italy; [e] Department of Land, Environment, Agriculture and Forestry, University of Padova, Italy.

Geomorphology, 272, 78–91, 2016

Abstract

This work addresses the geomorphic response of mountain rivers to extreme floods, exploring the relationships between morphological changes and controlling factors. The research was conducted on six tributaries of the Magra River (northern Apennines, Italy) whose catchments were affected by an extreme flood (estimated recurrence interval >100 years in most of the basins) on 25 October 2011. An integrated approach was deployed to study this flood, including (i) analysis of channel width changes by comparing aerial photographs taken before and after the flood, (ii) estimate of peak discharges in ungauged streams, (iii) detailed mapping of landslides and analysis of their connectivity with the channel network.

Channel widening occurred in 35 reaches out of 39. In reaches with channel slope <4% (here defined as *nonsteep* reaches), average and maximum ratio of post-flood and pre-flood channel width were 5.2 and 19.7 (i.e., channel widened from 4 to 82 m), respectively. In steep reaches (slope ≥4%), widening was slightly less intense (i.e., average width ratio = 3.4, maximum width ratio = 9.6). The relationships between the degree of channel widening and seven controlling factors were explored at subreach scale by using multiple regression models. In the steep subreaches characterized by higher confinement, the degree of channel widening (i.e., width ratio) showed relatively strong relationships with cross-sectional stream power, unit stream power (calculated based on pre-flood channel width), and lateral confinement, with coefficients of multiple determination (R^2) ranging between 0.43 and 0.67. The

models for the nonsteep subreaches provided a lower explanation of widening variability, with R^2 ranging from 0.30 to 0.38; in these reaches a significant although weak relation was found between the degree of channel widening and the hillslope area supplying sediment to the channels.

Results indicate that hydraulic variables alone are not sufficient to satisfactorily explain the channel response to extreme floods, and inclusion of other factors such as lateral confinement is needed to increase explanatory capability of regression models. Concerning hydraulic variables, this study showed that the degree of channel widening is more strongly related to unit stream power calculated based on pre-flood channel width than to cross-sectional stream power and to unit stream power calculated with post-flood channel width. This could suggest that most width changes occurred after the flood peak. Finally, in terms of hazard, it is crucial to document the type and magnitude of channel changes, to identify controlling factors, and most importantly, to develop tools enabling us to predict where major geomorphic changes occur during an extreme flood.

1. Introduction

Geomorphic effectiveness of large floods has been long studied and debated (e.g., Wolman and Miller, 1960; Gupta and Fox, 1974; Wolman and Gerson, 1978; Magilligan, 1992; Costa and O'Connor, 1995; Phillips, 2002; Kale and Hire, 2004; Thompson and Croke, 2013; Magilligan et al., 2015). A major issue has been the role of large floods in comparison to more frequent floods with lower magnitude. Several studies have contributed to developing the concept of effective and formative discharge proposed originally by Wolman and Miller (1960), pointing out that (i) it may be more appropriate to consider a range of discharges rather than a single formative discharge (Pickup and Rieger, 1979; Surian et al., 2009) and (ii) large floods may play a major role in certain fluvial systems such as steep channels (Johnson and Warburton, 2002; Lenzi et al., 2006), in ephemeral streams in arid and semiarid areas (Harvey, 1984; Reid et al., 1998; Hooke and Mant, 2000), and in bedrock channels (Jansen, 2006).

Another major research question concerns the factors controlling channel response to a large flood event. Most works have focused mainly on hydraulic

variables (e.g., unit stream power, flow duration above a critical threshold; see Magilligan, 1992; Cenderelli and Wohl, 2003; Kale, 2007; Krapesch et al., 2011; Magilligan et al., 2015) but, as suggested by Costa and O'Connor (1995), understanding and prediction of channel and floodplain response to a large flood should incorporate additional factors. Some works have confirmed that hydraulic forces may not be sufficient to explain geomorphic effects (e.g., Heritage et al., 2004; Nardi and Rinaldi, 2015), and consequently, attempts have been made to include other factors. For instance, human interventions and structures have been considered by Langhammer (2010); bedload supply and pre-flood channel planform by Dean and Schmidt (2013); lateral confinement by Thompson and Croke (2013); a bend stress parameter by Buraas et al. (2014).

This work deals with an extreme flood that occurred in the Magra River catchment (northern Apennines, Italy) on 25 October 2011. Channel widening, the dominant geomorphic effect of this event along the channel network, was analyzed in six subcatchments by comparing aerial photographs taken before and after the flood. The working hypothesis was that explanation of geomorphic effects requires models that include other variables (e.g., lateral confinement, sediment supply) besides hydraulic-related variables (cross-sectional or unit stream power). The main aim was thus to explore the relationship between channel widening and a range of controlling factors. Other specific questions addressed were (i) which channel width (i.e., pre- or post-flood width) should be considered to calculate unit stream power in order to have a better explanation of channel response?; and (ii) is sediment supply from hillslopes (i.e., landslides) a key factor driving channel changes in mountain environments?

We were able to address such questions in relatively small catchments (drainage areas between 8.5 and 38.8 km^2) because an integrated approach was deployed to study this flood event (Rinaldi et al., 2015). Besides the analysis of morphological changes, the approach includes field measurements coupled to a rainfall-runoff model to estimate peak discharges in the ungauged streams, detailed mapping of landslides and analysis of sediment connectivity, as well as information concerning other fundamental aspects of the event (e.g., sedimentological characterization of flood deposits, dynamics of large wood transport; Lucía et al., 2015).

2. Study area

2.1. General setting of the area

The Magra River catchment is located in the northern Apennines (northwestern Italy) and covers an area of 1717 km^2, ranging from a maximum elevation of 1901 m asl to sea level (Ligurian Sea) (Fig. 1). The catchment is characterized by ridges with a NW-SE direction, associated to thrust faults, which define two main subcatchments: the Magra (1146 km^2) and the Vara (571 km^2) subcatchments. The catchment is mainly composed of sedimentary rocks (predominantly sandstones and mudstones), with some outcrops of magmatic (ophiolites) and metamorphic rocks. The climate is temperate, with dry summers and most precipitation occurring in autumn. The mean annual precipitation is 1707 mm, reaching maximum values of about 3000 mm in the upper part of the catchment. The Magra catchment is predominantly forested (about 66% of the whole catchment), while urban areas are relatively small and mostly located at low elevations.

2.2. The extreme event on 25 October 2011: rainfall distribution and intensity

Rainfall maps for the study event were obtained based on data collected by the Monte Settepani meteorological radar placed at 1386 m asl on the Apennines, at the border between the Piemonte and Liguria regions. The radar data were processed for a number of error sources (Marra et al., 2014) and were merged with rain-gauge data by using the procedure described by Martens et al. (2013). Because of the large differences in sampling area, the merging was carried out at the event temporal scale and then was scaled down to the temporal resolution used for the flood event analysis and the hydrological modelling.

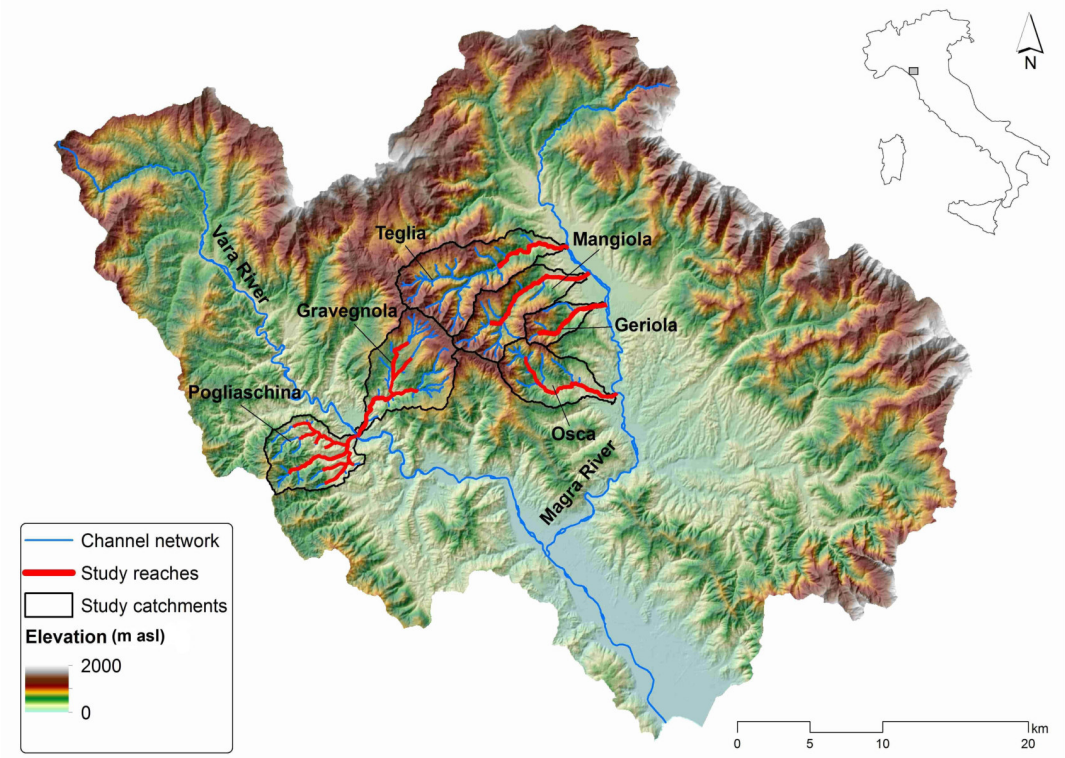

Figure 1. Location map of the Magra River catchment, the six study catchments, and the study reaches.

The obtained rainfall estimates show that maximum hourly rates were up to 149 mm/h, whereas 3-hours maximum and event-accumulation maxima were up to 326 mm and 500 mm, respectively. Recurrence intervals up to 300 years were estimated for this event based on precipitation records. Figure 2 reports the spatial distribution of rainfall maxima corresponding to 3-hours rainfall duration over the Magra River catchment. We selected the 3-hours duration because this is the duration that best corresponds to the response time of the catchments selected for the analysis, which are characterized by sizes ranging between 8.5 and 38.8 km^2 (Table 1). Basin average event-accumulation rainfall amounts over the study basins are also reported in Table 1, showing that all the basins were impacted by high rainfall totals ranging from 267 (Geriola) to 380 mm (Gravegnola). However, the spatial pattern of the 3-hours rain maxima shows huge differences among the basins, with a maximum over the Pogliaschina and a decreasing gradient toward the other basins (Fig. 2). This is reflected in the higher value of the unit peak discharge over the Pogliaschina (Table 1) with respect to the other basins.

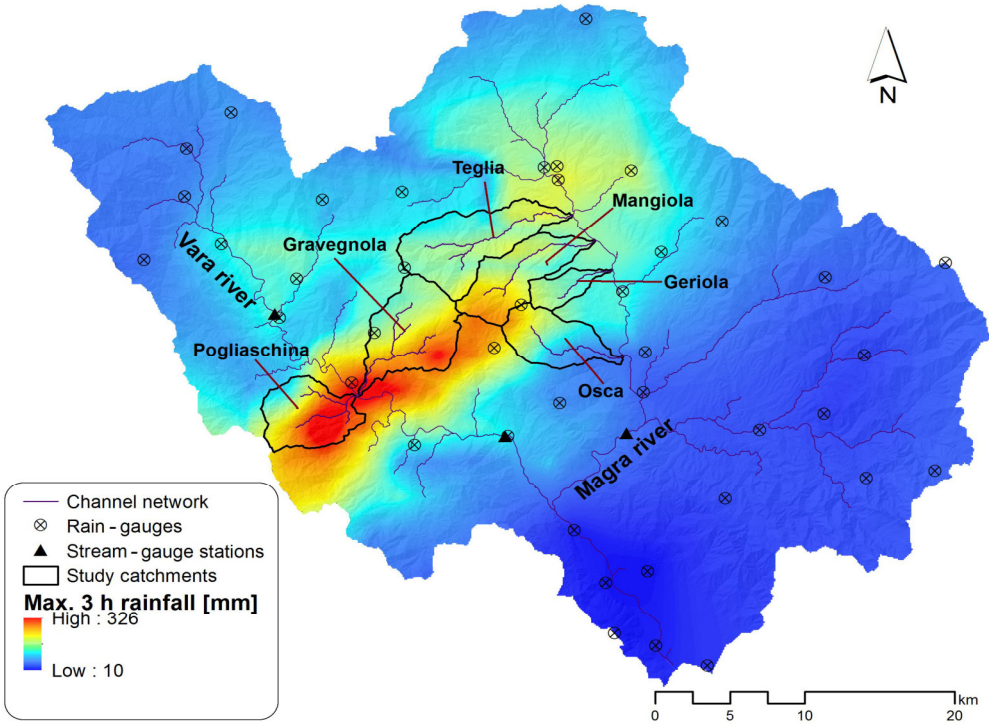

Figure 2. The 25 October 2011 event in the Magra River catchment: spatial distribution of rainfall maxima corresponding to three-hour rainfall duration.

2.3. General characteristics of the six study streams

Six catchments where rainfall was very intense were selected to analyze channel response (Table 1). Teglia, Mangiola, Geriola, and Osca rivers are tributaries of the Magra River, while Gravegnola and Pogliaschina rivers of the Vara River (Fig. 1). Unit peak discharge in these rivers was estimated between 12.8 (Osca) and 23.7 m^3 s^{-1} km^{-2} (Pogliaschina) (Table 1). The recurrence interval of the peak discharge has been estimated by comparing the values of peak discharge (Table 1) with the results of regional equations relating peak discharges to catchment area (Autorità di Bacino interregionale del Fiume Magra, 2006). In the Teglia and Mangiola rivers the peak discharge is associated to a recurrence interval slightly lower than 200 years. The highest recurrence intervals have been obtained for the Gravegnola (between 200 and 500 years) and Pogliaschina (>500 years). The relatively low recurrence interval of the peak discharge in Geriola and Osca (between 30 and 100 years) is consistent with lower rainfall amounts in these catchments (Table 1).

Stream	Drainage area (km^2)	Basin relief (m)	Stream length (km)	Channel slope (%)	D_{50} (mm)	Total rainfall (mm)	3-hour maximum rainfall (mm)	Runoff ratio	Q_{pk} ($m^3 s^{-1}$)	Unit Q_{pk} ($m^3 s^{-1} km^{-2}$)
Teglia	38.8	1035	14.8	4.9	47-69	335	116	0.53	538	13.9
Mangiola	26.2	1012	12.9	6.6	41-95	376	148	0.57	406	15.5
Geriola	8.5	884	7.2	8.8	n.a.	267	116	0.51	121	14.2
Osca	21.8	962	9.9	4.1	44-65	243	125	0.52	279	12.8
Gravegnola	34.6	1106	12.8	7.0	33-79	380	176	0.62	523	15.1
Pogliaschina	25.1	625	9.1	5.6	24-36	350	209	0.61	595	23.7

Table 1. General characteristics of the six study streams and rainfall and discharge characteristics of the 25 October 2011 flood event (D_{50} - Median diameter of bed sediment; Q_{pk} - estimated peak discharge; n.a. - not available)

Streams within the six catchments are characterized by average channel slope ranging from 4.1% (Osca) to 8.8% (Geriola), coarse sediments (mainly gravels and cobbles), and a wide range of conditions in terms of lateral confinement, i.e., from highly to poorly confined reaches. The study reaches correspond to the middle and lower portions of these rivers, which are characterized by partly confined or unconfined conditions (Fig. 1). In addition to the main stems, some tributaries of the Gravegnola and Pogliaschina rivers were also analyzed. According to field observations, intense bedload was widespread in the study streams during the 25 October 2011 flood, and sediment transport also occurred as debris flood (Hungr et al., 2001) in some reaches.

3. Methods

An integrated approach was adopted to investigate the geomorphic effects of the 25 October 2011 flood in the Magra catchment. Analyses of rainfall, peak discharge, channel changes, depositional features and sediment structures, wood dynamics (Lucía et al., 2015), and sediment sources were carried out by field surveys, remote sensing, and numerical modelling at different spatial scales (i.e., from catchment to cross section scale). The whole methodological framework is

described in detail by Rinaldi et al. (2015), while in this work we focus on delineation of spatial units, channel width changes, and potential controlling factors of channel changes. The estimation of peak discharges — used to calculate cross-sectional stream power and unit stream power — and analysis of sediment sources and of their connectivity with study reaches are also described. The last part of the methodological section deals with statistical analysis carried out to explain channel response to the flood event, by exploring the relationships between changes in channel width and controlling factors.

3.1. Morphological characteristics and delineation of spatial units

The first step of this study included (i) analysis of morphological characteristics and (ii) delineation of spatial units. This step is crucial for the subsequent analyses, specifically for a sound interpretation of channel changes. The material used in this step included orthophotos with a spatial resolution of 50 cm, topographic maps at 1:5000 scale, and a digital elevation model (DEM) with a spatial resolution of 10 m. The analysis was carried out by geographic information system (GIS) software (ArcGIS 10.2).

The analyzed morphological characteristics were pre-flood channel areas, alluvial plain areas, lateral confinement, and channel slope. Identification of the pre-flood channel area was straightforward (where channel width was >5-6 m) while more difficult for smaller channels or at locations with dense riparian vegetation. In the latter cases, photo interpretation was supported by use of the topographic maps to reduce the degree of uncertainty. Similarly, definition of the alluvial plain, which includes present floodplain and low terraces (i.e., surfaces that can be some meters higher than the floodplain and can be infrequently flooded), was not always straightforward (e.g., in narrow valley bottoms with dense vegetation cover). Alluvial plain was mainly identified using the DEM and topographic maps, while aerial photographs turned out to be useful where sharp changes in land cover could be clearly associated to elevation changes (e.g., a change from agricultural land to forest). As for lateral confinement, three valley settings were differentiated (Brierley and Fryirs, 2005): confined, partly confined, and laterally unconfined reaches. Lateral confinement was defined by combining two aspects: the degree of confinement,

which is the percentage of channel banks directly in contact with hillslopes or ancient terraces (Brierley and Fryirs, 2005), and the confinement index, which is defined by the ratio between the alluvial plain width and the channel width (Rinaldi et al., 2013). The DEM was employed to estimate channel slope, as the difference in elevation divided by the planimetric distance relative to each reach.

Delineation of spatial units was carried out according to the approach proposed by Rinaldi et al. (2013), which is a modification of the approach by Brierley and Fryirs (2005). According to that approach, stream sectors were defined as macroreaches having similar characteristics in terms of lateral confinement, while reaches are homogeneous also in terms of channel morphology (channel pattern, width, slope) and hydrology. We used the reach scale (reach length was commonly from 1 to 3 km) for an overall assessment of magnitude of channel changes and for a preliminary investigation of controlling factors. For a more accurate analysis of the relation between channel changes and controlling factors, reaches were divided into subreaches having a constant slope. To identify the proper length of the subreaches (i.e., the minimum distance with constant slope), the method proposed by Vocal Ferencevic and Ashmore (2012) was applied. Because DEM resolution was rather low (10 m), the length of subreaches turned out to be on the order of 300-500 m.

3.2. Morphological changes: analysis of channel widening

Morphological changes induced by the 2011 flood were assessed by field surveys and interpretation of aerial photographs. The dominant process observed in the study reaches was channel widening, which was analyzed in detail by comparing aerial photographs taken before and after the flood. Pre-flood orthophotos have a spatial resolution of 50 cm and were taken in 2006 (Gravegnola and Pogliaschina) and 2010 (Teglia, Mangiola, Osca, and Geriola). Because the photos for Gravegnola and Pogliaschina catchments were taken 5 years before the flood, we verified them to be representative of the pre-event situation by the inspection of images taken in July 2011 and available through Google Earth©. Four sets of orthophotos were used to analyze the post-flood situation. The Gravegnola and Pogliaschina channels were analyzed with photos taken on 28 October 2011 by the Liguria region (resolution 10 cm) and 28 November 2011 by the Civil Protection of the Friuli Venezia Giulia

(resolution 15 cm). For the other four catchments, we used photos taken on November 2011 by the Toscana region (resolution 20 cm) and on December 2012 (resolution 30 cm). The latter photos were taken by an *ad hoc* flight contracted to have full coverage of the study catchments.

To assess changes in channel width, channel banks, and islands (i.e., in-channel surfaces covered by woody vegetation), these features were digitized on pre- and post-flood orthophotos. In this work, the term *channel* refers to an active channel, which includes low-flow channels and unvegetated or sparsely vegetated bars (i.e., exposed sediments). Channel width was calculated dividing channel area by the length of the reach or subreach, and changes in channel width were expressed as a width ratio, i.e., channel width after/channel width before the flood (Krapesch et al., 2011). Estimate of channel width, and consequently of width ratio, is affected by errors, in particular related to photo interpretation and digitization. Although rigorous error assessment was not carried out, we judged that, overall, errors are relatively small in this analysis because (i) images with high spatial resolution were used and (ii) the magnitude of changes (i.e., width ratio) was very high in most of the reaches. As mentioned above, larger errors in channel width estimate could concern the smallest channels or some reaches where there was a dense vegetation cover.

3.3. Hydraulic analysis: estimates of peak discharge

The flash flood of 25 October 2011 in the Magra River and its tributaries was studied following an approach that encompasses analysis of rain-gauge data and weather radar observations, post-event surveys aimed at estimating peak discharge and time evolution of the flood in ungauged catchments, and model-based consistency check of rainfall and discharge (Borga et al., 2008). Post-flood assessment of peak discharge was based on the survey of high water marks and cross-sectional geometry and computation of flow velocity using the Manning-Strickler equation under the assumption of uniform flow; for each cross-section a central (more probable) discharge value was assessed, and upper and lower bounds of the estimate were computed. More details on the procedures applied in post-flood surveys and their assumptions can be found in Gaume and Borga (2008) and Marchi

et al. (2009). The consistency of rainfall and discharge data was verified by applying a distributed rainfall-runoff model (Borga et al., 2007). The hydrological model applied in this study uses a mixed Curve Number – Green Ampt method (Grimaldi et al., 2013) for rainfall excess modelling. The procedure consists of applying the SCS-CN approach (Ponce and Hawkins, 1996) to quantify the storm net rainfall total amount and using this value to estimate the effective saturated hydraulic conductivity of the Green-Ampt method. The model simulates the runoff propagation by considering distinct hillslope and channel pathways. A full de Saint Venant model is used to reconstruct the propagation of the flood wave along the main channels of the Magra and Vara rivers. The rainfall-runoff model was first calibrated at three stream-gauge stations located on the Vara and Magra rivers; calibration parameters were then transposed to the ungauged catchments where peak discharges had been estimated by means of post-flood field observations. This enabled a check of the consistency of rainfall and discharge data at the scale of subcatchments and provided the basis for peak discharge computation at channel reach and subreach scale, as required for the analysis of morphological changes of the study streams.

3.4. Sediment sources, delivery, and connectivity

Sediment supplied from hillslopes to channel network during the 2011 flood derived essentially from landslides. The analysis of sediment sources was thus carried out by analyzing GIS-based landslide inventories that were prepared through visual interpretation of digital aerial photographs taken in different periods: 3 days, 33 days, and 14 months (December 2012) after the event, and of a high-resolution image (0.5 m) taken by the WorldView II satellite four days after the event. The satellite image and the post-event aerial photographs cover almost the entire surface of the Pogliaschina and the Gravegnola basins, while the complete coverage of the remaining four basins was guaranteed by the aerial photographs collected 14 months after the event. We visually compared the pre-event orthophotos acquired in 2006 with a satellite image acquired on 20 July 2011, 3 months before the event, available through Google Earth©. The visual comparison of the two pre-event images allowed verification that no significant landslide had occurred in the area between 2006 and the date of the satellite image (20 July 2011). Anecdotal information confirmed that

landslides did not occur between 20 July 2011 and the October 2011 event. The orthophotos flown in December 2012 were taken with less favorable lighting conditions with respect to the other images, making the detection and mapping of the landslides more difficult and locally less accurate. Furthermore, snow cover, natural soil erosion from landslide scars, and artificial sediment removal occurred between the rainfall event and the date of the orthophotos, obliterating partially or completely some of the soil slips and the landslide deposits. Because of the different quality of images, the photointerpretation was focused on three types of shallow landslides recognizable in all available images: (i) translational slides, (ii) earth flows (including also some debris flow phenomena), and (iii) rotational slides (Mondini et al., 2014). Field surveys on landslide sites allowed us to validate the obtained inventories.

In order to evaluate which sediment source areas were effectively coupled to the studied reaches of the channel network (i.e., areas responsible for sediment supply), a geomorphometric analysis of sediment connectivity was carried out. In each catchment, a map of sediment connectivity was derived by calculating the sediment connectivity index (IC, Cavalli et al., 2013) using the SedInConnect tool (Crema et al., 2015). The IC, originally developed by Borselli et al. (2008), is a distributed GIS-based index mainly focused on the influence of topography on sediment connectivity and aiming at representing the linkage between different parts of the catchment (i.e., hillslopes and features of interest such as catchment outlet, main channel network or a given cross section along the channel). The IC is defined by the logarithm of the ratio between an upslope and a downslope component expressing, respectively, the potential for downward routing of the sediment produced upslope and the sediment flux path length to the nearest target or sink. A weighting factor appears in both components of IC to model the impedance to runoff and sediment fluxes. More details can be found in Cavalli et al. (2013). In this study, IC was applied to evaluate the potential connection between hillslopes and the studied reaches. In the IC calculation, Manning's n roughness coefficient, assigned according to different land use types, was used as a weighting factor. The resulting IC maps were used as a support for the removal of decoupled sediment source areas from the total inventory. This operation was then checked by visually inspecting post-event orthophotos. Finally, the variable expressing the sediment supply from the hillslopes to the studied subreaches was computed by summing all the areas of the sediment sources connected to each subreach in the six basins.

3.5. Analysis of controlling factors

Analysis of controlling factors was carried out at the subreach scale, taking into account four geomorphic and three hydraulic factors. The geomorphic factors were channel slope as a proxy of stream morphology (see e.g., Montgomery and Buffington, 1997); confinement index, which represents the width of the alluvial plain and a natural constraint to channel widening; artificial structures that may hinder channel lateral mobility; sediment-supply area, in terms of landslide areas effectively coupled to the main channel network. Stream energy was analyzed taking into account three hydraulic variables closely related to flood power: cross-sectional stream power (W m^{-1}) defined as $\Omega = \gamma QS$, where γ is the specific weight of water (N m^{-3}), Q is the discharge (m^3 s^{-1}), and S is channel slope; unit stream power (W m^{-2}) obtained by dividing cross-sectional stream power by channel width measured before and after the flood ($\omega = \Omega/W_{before}$ and $\omega = \Omega/W_{after}$). Hence statistical analysis was performed considering seven geomorphic and hydraulic variables but taking into account separately independent variables related to stream energy (i.e., channel slope, cross-sectional stream power, unit stream power). Least squares multiple regression analysis was used to investigate which set of variables gave the best explanation of channel response (i.e., channel widening). Software STATGRAPHICS centurion XVI (version 16.2.4) was used for all statistical analyses.

4. Results

4.1. Morphological changes at the reach scale

In this section the morphological characteristics of the study streams and channel changes that took place during the 25 October 2011 flood are illustrated at the reach scale. The aim of this section is to show the magnitude of changes and analyze some of the possible factors that could play a role in the geomorphic response of stream channels. A more accurate analysis of controlling factors was carried out at subreach scale, as described further in the paper.

Following the delineation procedure described above, stream sectors and reaches were defined in the six catchments. Then, only the partly confined and

unconfined reaches were considered for the following morphological analysis (i.e., analysis of changes in channel width) (see study reaches in Fig. 1). The minimum, average, and maximum length of the 39 study reaches is 264, 1573, and 3616 m, respectively (Table 2). All these reaches display typical characteristics of mountain streams and cover relatively wide ranges in terms of channel slope, channel width, and lateral confinement. Channel slope varies between 0.4% and 17.2%, with 5.3% being the average of the 39 reaches; channel width ranges from 3 to 36 m, being 9 m on average; confinement index ranges from 2.3 to 26.6 (Table 2).

Code	L (m)	S (m m^{-1})	Reach typology	W_{pl} (m)	C_i	W_{before} (m)	W_{after} (m)	W_{ratio}	AS (%)	Q_{pk} (m^3 s^{-1})	Ω (W m^{-1})	ω_{before} (W m^{-2})	ω_{after} (W m^{-2})	SS (m^2)
Teglia														
T2.3	2816	0.031	nonsteep	43	4.9	8.9	35.2	4.0	0	457	136895	15364	3887	2884
T3.1	1380	0.024	nonsteep	97	8.2	11.9	60.1	5.1	0	495	116478	9788	1937	2630
T3.2	1975	0.020	nonsteep	132	11.2	11.8	42.7	3.6	20	529	102567	8691	2402	0
T4.1	374	0.021	nonsteep	-	u.c.	17.7	48.3	2.7	50	538	110833	6267	2294	0
Mangiola														
M2.2	1994	0.037	nonsteep	72	6.5	11.1	39.1	3.5	10	255	92888	8353	2375	10768
M2.3	3616	0.049	steep	55	8.4	6.5	34.6	5.3	0	360	173897	26590	5030	76650
M3.1	3600	0.025	nonsteep	215	9.7	22.2	77.3	3.5	0	402	98493	4447	1274	4958
Geriola														
GE1.2	1804	0.140	steep	28	5.5	6.7	18.7	4.0	0	47	62952	9356	3371	1681
GE1.3	1582	0.077	steep	65	7.8	8.2	35.7	4.3	0	79	59213	7180	1658	1363
GE2.1	1555	0.048	steep	107	10.6	10.1	49.4	4.9	0	106	49405	4901	1001	0
GE3.1	968	0.035	nonsteep	-	u.c.	18.5	51.1	2.8	0	114	39425	2128	772	0
Osca														
O1.2	2227	0.064	steep	39	13.0	3.0	28.8	9.6	0	106	67084	22361	2328	7055
O1.3	3296	0.033	nonsteep	52	16.5	3.1	24.8	7.9	0	217	70989	22570	2858	4226
O2.1	2543	0.025	nonsteep	143	20.6	6.9	25.8	3.7	4	268	66526	9629	2582	312
O2.2	891	0.016	nonsteep	135	4.2	32.4	54.4	1.7	0	278	42924	1324	789	0
Gravegnola														
CR1.1	1486	0.121	steep	20	2.4	8.6	21.2	2.5	0	56	66855	7784	3147	7496
CR1.2	1685	0.069	steep	30	3.6	8.3	27.4	3.3	0	84	58850	7051	2150	17906
CR1.3	1338	0.045	steep	208	21.1	9.5	88.0	9.2	0	159	70762	7429	804	764
SU1.1	1168	0.172	steep	24	2.5	9.4	19.6	2.1	0	53	89299	9494	4565	21828
SU1.2	646	0.134	steep	62	5.8	10.7	59.2	5.5	0	72	92029	8578	1553	4477
V1.1	1772	0.034	nonsteep	42	6.3	6.6	29.5	4.5	0	293	95275	14541	3230	27226
GR1.1	2817	0.023	nonsteep	96	7.2	13.4	60.0	4.5	10	449	106600	7946	1776	13718
GR2.1	1917	0.019	nonsteep	177	5.0	35.5	105.4	3.0	30	519	90636	2550	860	232
Pogliaschina														
P1.1	2008	0.026	nonsteep	35	11.1	3.1	6.9	2.2	10	31	7712	2465	1120	5085
P1.2	2686	0.015	nonsteep	58	15.8	3.7	28.5	7.7	30	146	21732	5881	763	40685
P1.3	461	0.020	nonsteep	90	21.8	4.1	81.7	19.7	70	188	8952	2158	110	1628
P2.1	499	0.004	nonsteep	137	26.6	5.1	32.3	6.3	40	581	25569	4965	793	0
PO1.1	492	0.041	steep	20	6.0	3.3	4.1	1.2	0	54	29056	8705	7112	113
PO1.2	844	0.034	nonsteep	48	12.5	3.8	7.2	1.9	0	61	15675	4106	2180	8661
RG1.1	557	0.068	steep	18	3.6	5.0	5.0	1.0	0	6	3752	757	750	1419
SO1.1	742	0.166	steep	16	2.3	6.8	9.1	1.3	0	4	5538	817	607	25354
CN1.1	2567	0.053	steep	19	3.2	6.0	14.8	2.5	0	118	61378	10306	4134	24664
CN1.2	1188	0.026	nonsteep	39	10.0	3.9	39.0	10.0	0	170	43919	11241	1125	18239
CN1.4	503	0.029	nonsteep	62	20.3	3.0	26.4	8.7	0	206	68978	22617	2611	4824
RN1.1	700	0.088	steep	27	4.0	6.6	7.1	1.1	0	34	29901	4501	4200	3200
RN1.2	1207	0.044	steep	26	4.1	6.4	6.4	1.0	0	54	25843	4027	4027	22449
RN1.3	1450	0.025	nonsteep	42	5.7	7.3	13.3	1.8	0	126	26126	3574	1959	8827
B1.1	264	0.089	steep	17	3.0	5.8	5.8	1.0	0	11	9837	1686	1686	3843
GI1.1	1722	0.068	steep	29	5.7	7.3	7.3	1.0	0	34	21048	2903	2883	18675

Table 2. Morphological characteristics, channel width changes, and controlling factors at reach scale.
Code - reach identification code (T - Teglia; M - Mangiola; GE - Geriola; O - Osca; CR - Casserola; SU - Suvero; V - Veppo; GR - Gravegnola; P - Pogliaschina; PO - Pogliasca; RG - Redovego; SO - Sottano; CN - Cassana; RN - Redarena; B - Benoia; GI - Ginepro); L - reach length; S - channel slope; Reach typology - steep, reach with slope ≥4%; nonsteep, reach with slope <4%;W_{pl} - width of the alluvial plain; C_i - confinement index (W_{pl}/W_{before}); W_{before} - channel width before the flood; W_{after} - channel width after the flood; W_{ratio} - channel width after the flood/channel width before the flood; AS - percentage of reach length with artificial structures (e.g., walls, ripraps) preventing lateral mobility; Q_{pk} - peak discharge; Ω - cross-sectional stream power at the peak discharge; ω_{before} - unit stream power calculated based on channel width before the flood (Ω/W_{before}); ω_{after} - unit stream power calculated based on channel width after the flood (Ω/W_{after}); SS – sediment supply area expressed in terms of landslide area connected with the stream reach.
Note. u.c.: unconfined

Considering such a range of morphological characteristics, and specifically the variability in channel slope, the whole data set was analyzed considering two subsets: the first including reaches with a slope <4% (hereafter called *nonsteep reaches*), and the second with reaches having slope ≥4% (*steep reaches*). The two subsets consist of 21 and 18 reaches, respectively. The selection of such threshold stems from a widely accepted definition of steep channels, characterized as sediment supply-limited and with stepped morphology, as those having slopes higher than ~3-5% (Montgomery and Buffington, 1997; Comiti and Mao, 2012).

Channel widening occurred in 35 reaches, while no significant change in channel width was detected only in 4 reaches (see width ratios in Table 2). In the subset of nonsteep reaches, the minimum, average, and maximum width ratio was 1.7, 5.2, and 19.7 respectively. Most intense changes occurred along the Pogliaschina River (reach P1.3) where the channel widened from 4.1 up to 81.7 m (Table 2, Fig. 3). Although there were several artificial structures along this reach (i.e., along 70% of the reach), in several sites the channel took up the whole alluvial plain, and locally, widening of the alluvial plain occurred by the erosion of valley slopes (Fig. 3D). Figure 3 shows two reaches of the Teglia River (the downstream part of reach T3.2 and the short, unconfined reach T4.1) where widening was less intense (width ratio was 3.6 and 2.7 in T3.2 and T4.1, respectively). Artificial structures (along 20% and 50% of T3.2 and T4.1, respectively) had some effect in these cases as shown by sharp changes in the degree of widening along the two reaches.

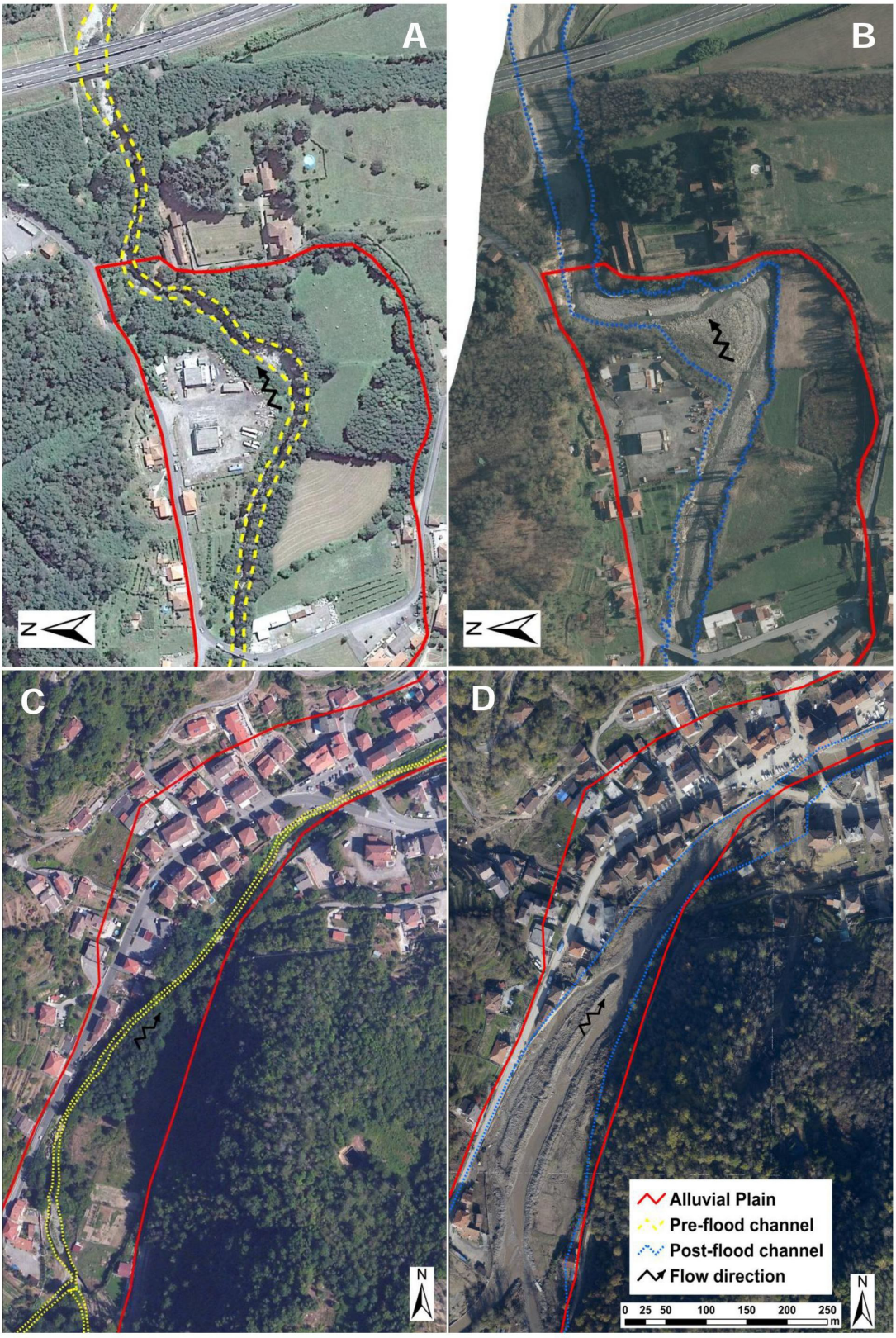

Figure 3. Pre- and post-flood aerial photographs showing morphological changes along nonsteep reaches of the Teglia River (A and B), reaches T3.2 and T4.1, and Pogliaschina River (C and D), reach P1.3. Refer to Table 2 for more information about morphological characteristics and channel width changes in these reaches.

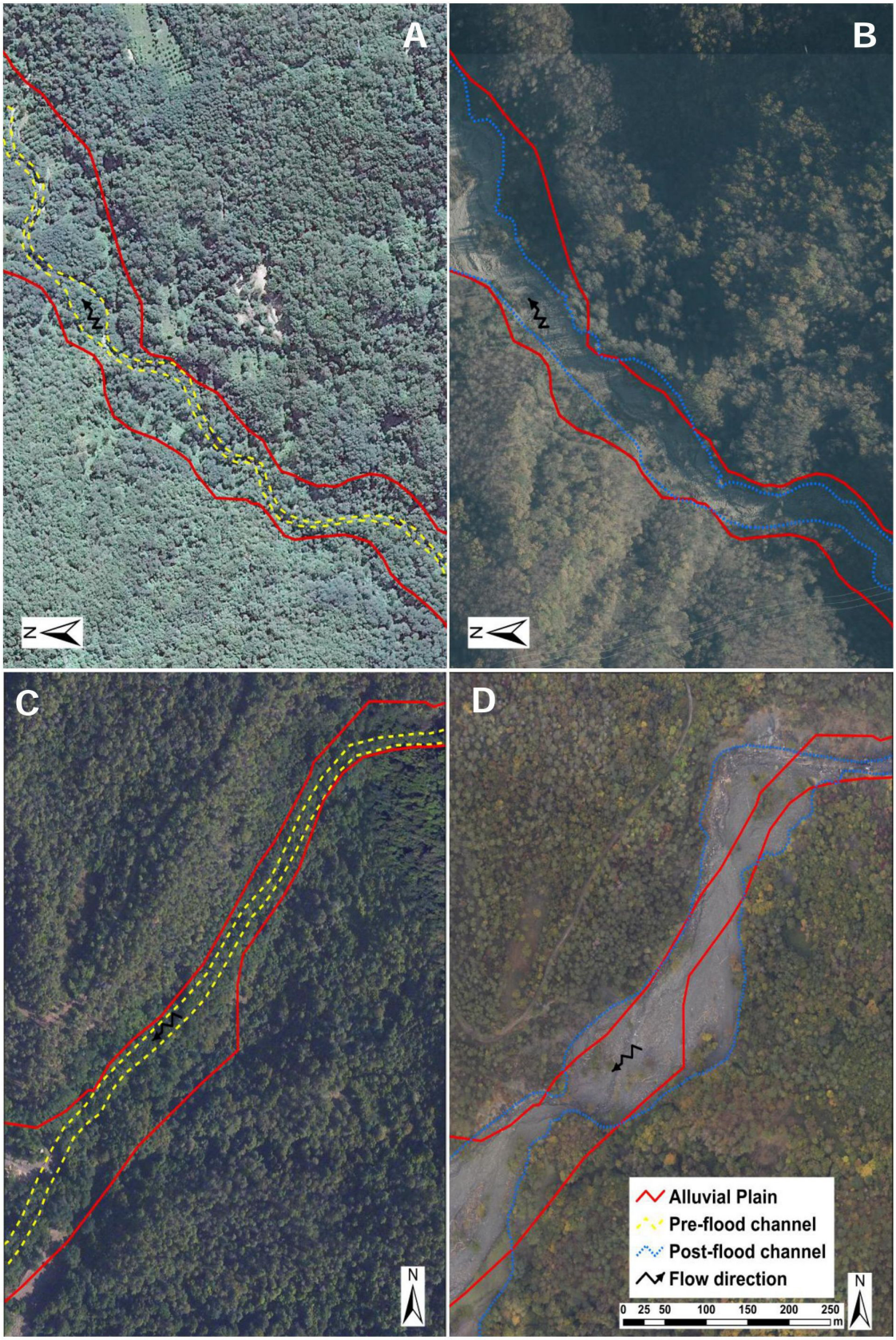

Figure 4. Pre- and post-flood aerial photographs showing morphological changes along steep reaches of the Geriola River (A and B), reach GE1.3, and Suvero River (C and D), reach SU1.2. Refer to Table 2 for more information about morphological characteristics and channel width changes in these reaches.

In the 18 reaches characterized by steep slopes, the minimum, average, and maximum width ratio was 1.0, 3.4, and 9.6, respectively. There are no artificial structures along these reaches, but the presence of narrow alluvial plains was likely a limiting factor for channel widening. Some reaches, e.g., GE1.2, CR1.2, SU1.1, were characterized by relatively moderate or low width ratios, 4.0, 3.3, and 2.1, respectively; but such ratios approximate their confinement index values, meaning that channel widening took up most of the alluvial plain (Table 2). Two examples of widening along steep channels are shown in Fig. 4. The first example refers to the Suvero River (tributary of the Gravegnola River): in reach SU1.2 (slope = 13%) the channel widened from 10.7 up to 59.2 m (width ratio = 5.5), took up almost completely the alluvial plain and, locally, eroded significant portions of the valley slopes (Fig. 4D). The other example refers to the Geriola River where in reach GE1.3 (slope = 7.7%) widening was slightly less intense than in the Suvero (i.e., from 8.2 to 35.7 m; width ratio = 4.3) but still with local erosion of valley slopes (Fig. 4B).

4.2. Estimate of peak discharge

Post-flood field estimates of peak discharge were carried out in five out of the six studied catchments: one cross section was surveyed in the Mangiola and Teglia rivers (in both catchments close to basin outlet), two in the Osca and Gravegnola, and six in the Pogliaschina. Only in Geriola were no cross sections found suitable for recognition of high water marks and topographic survey because of major channel changes caused by the flood. The agreement of model-computed peak discharges with post-flood estimates can be deemed rather satisfactory, with 7 out of 12 cross sections lying within the range of discharges resulting from the computation based on field surveys. Model-computed discharges were then used in the analysis of the factors controlling morphological changes in the studied channels. This was done by applying the rainfall runoff model at multiple cross sections located at the end of each investigated channel reach and subreach (Table 2). In the Teglia River, ~75% of the basin area lies upstream of a dam for hydroelectric power production; peak discharge in the investigated reaches, which are located downstream of the dam, was assessed by summing the outflow from the dam to the model-computed discharge of the interbasin downstream of the dam.

Estimates of peak discharge, cross-sectional stream power, and unit stream power at the reach scale are reported in Table 2. Peak discharge ranged from 4 $m^3 s^{-1}$ (Sottano River, a small tributary of Pogliaschina River) to 595 $m^3 s^{-1}$ (Pogliaschina River). Cross-sectional stream power varied between 7712 and 136,895 W m^{-1} in the nonsteep reaches and between 3752 and 173,897 W m^{-1} in the steep reaches. Unit stream power calculated using channel width before the flood ranged between 757 and 26,590 W m^{-2}, while that calculated using post-flood channel width ranged between 110 and 7112 W m^{-2}. Notably, in most of the reaches unit stream power largely exceeded the threshold value of 300 W m^{-2} that Magilligan (1992) and later other researchers referred to for differentiating reaches where major geomorphic changes occurred from those reaches where changes were more limited.

4.3. Sediment sources, delivery, and connectivity

The sediment-source inventory compiled through photointerpretation in the six catchments featured 1196 landslides for a total surface of about 917,000 m^2, which represents 0.6% of the study area (Table 3). Pogliaschina and Gravegnola catchments show the highest number of mapped landslides. This result is attributable mainly to the extreme intensity of the rainfall (Fig. 2) and the resultant flood (Table 1) in these two basins, but also to the higher quality of the available orthophotos in terms of spatial resolution and date of acquisition than to data sets available for the other four catchments. Among the analyzed landslide types, earth flow is the most represented class, with percentages ranging from 66% to 86% of the individual landslide inventories. The remaining sediment sources are mainly translational landslides, while the rotational landslide class represents <2% of the cases.

Catchment	All landslides[a]		Coupled landslides		Percentage of coupled landslides
	n°	Surface (m^2)	n°	Surface (m^2)	
Teglia	186	133070	10	7345	5.5
Mangiola	157	151322	42	92377	61
Geriola	33	16054	7	5508	34.3
Osca	125	67589	21	12593	18.6
Gravegnola	257	206232	100	99189	48.1
Pogliaschina	438	342585	189	213384	62.3

Table 3 Summary results of the inventory of all landslides in catchments and landslides coupled to the study reaches according to sediment-connectivity analysis

The total sediment-source inventory was filtered to limit the inventory to the landslides effectively contributing to sediment supply in the study reaches (Table 3) by assessing the sediment-connectivity pattern using the index of connectivity (Cavalli et al., 2013). Figure 5 illustrates the adopted criteria for selecting the landslides coupled to the study reaches. Notably, even if all the mapped slope instabilities (red polygons in Fig. 5A) are located very close to the analyzed channel network, most of these features in Fig. 5B are characterized by low values of IC (i.e., low connectivity) due to the gentle local slope and to the land use type that favor sediment storage. Conversely, the two landslides classified as coupled are well-linked to the stream network as can be observed on the orthophoto (Fig. 5A) and are characterized by medium values of IC, very close to high values of IC (hot colors in Fig. 5B). The connectivity analysis allowed us to reduce the initial inventory by about 62%, with the highest reduction (by around 94.5%) for the Teglia basin where the presence of a dam in the catchment significantly reduced the former mapped landslides (Table 3). Excluding all the sediment sources upstream of the dam, only 10 landslides with a total area of about 7345 m^2 were coupled to the stream reaches.

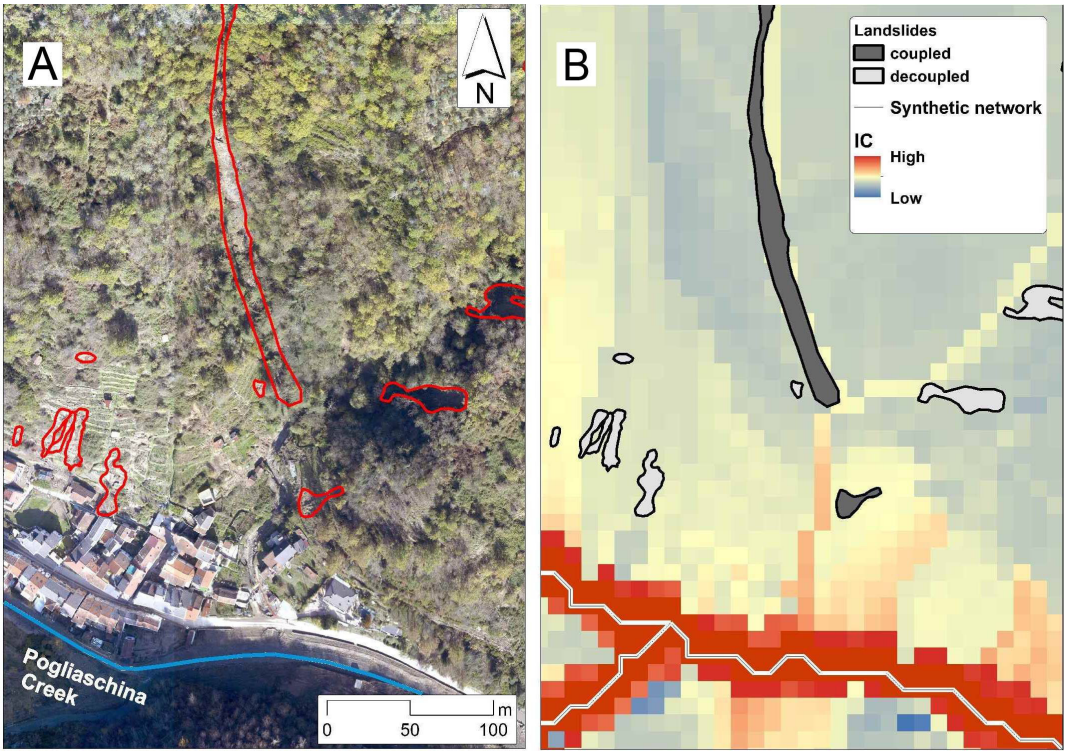

Figure. 5. Example of the sediment connectivity analysis carried out to limit the initial sediment-sources inventory to landslides effectively coupled to the study reaches. (A) The initial inventory superimposed on an orthophoto. (B) Coupled and decoupled landslides according to the analysis of the sediment connectivity map. The IC is the sediment connectivity index (see the text for more details).

Among all the analyzed stream reaches, SO1.1, RN1.2 in the Pogliaschina, M2.3 in the Mangiola, and SU 1.1 in the Gravegnola (Table 2) feature the highest value of sediment supply per unit channel length (34.2, 18.6, 21.2, and 18.7 m^2 m^{-1}, respectively), and several reaches in the Pogliaschina and in the Gravegnola exceed the value of 10 m^2 m^{-1}. We also note that about 60% of the total sediment sources appear to be connected to the studied reaches in the Mangiola and Pogliaschina catchments (Table 3).

4.4. Analysis of controlling factors

The relationships between the degree of channel widening and possible controlling factors were explored using multiple regression analysis. The analysis was carried out for the widening (i.e., width ratio) at subreach scale. The whole data set includes 157 subreaches, with a minimum, average, and maximum length of 157, 392, and 630 m, respectively. Seven controlling variables were considered (i.e., confinement index, percentage of reach length with artificial structures, sediment-supply area, channel slope, cross-sectional stream power, and unit stream power calculated using pre-flood and post-flood channel width), but each regression model incorporated only three to four variables. Each model included only one of the variables expressing potential or flood flow energy (i.e., channel slope, cross-sectional stream power, unit stream power).

The first analysis was carried out on the whole data set. All four multiple regression models turned out to be significant ($p < 0.001$) and gave moderate coefficients of multiple determination (R^2 and adjusted R^2 ranged between 0.36 and 0.51 and between 0.35 and 0.50, respectively) (Table 4).

	Model 1		Model 2		Model 3		Model 4	
	R^2 = 0.30 R^2_{adj} = 0.27 *p*-value<0.001		R^2 = 0.34 R^2_{adj} = 0.30 *p*-value<0.001		R^2 = 0.38 R^2_{adj} = 0.36 *p*-value<0.001		R^2 = 0.37 R^2_{adj} = 0.33 *p*-value<0.001	
	R^2	*p*-value	R^2	*p*-value	R^2	*p*-value	R^2	*p*-value
C_i	0.23	<0.001	0.23	<0.001	0.23	<0.001	0.23	<0.001
Percentage of reach length with artificial structures	0.05	0.481	0.05	0.203	0.05	0.085	0.05	0.997
Sediment supply area	0.07	0.006	0.07	0.001	0.07	0.013	0.07	0.006
Channel slope	0.01	0.756	-	-	-	-	-	-
Ω (Wm^{-1})	-	-	1.33E-06	0.042	-	-	-	-
ω_{before} (Wm^{-2})	-	-	-	-	0.14	0.001	-	-
ω_{after} (Wm^{-2})	-	-	-	-	-	-	0.12	0.005

Table 4. Multiple regression models between width ratio and controlling factors for the whole data set (157 subreaches).

The best model was the one including unit stream power calculated based on pre-flood channel width and confinement index as explanatory variables (model 3 in Table 4).

To achieve a better understanding of controlling factors, the data set was split into two subsets using the same criteria as adopted for the analysis at reach scale (i.e., nonsteep and steep subreaches, based on the 4% threshold). Therefore, multiple regressions were carried out on one subset including 89 nonsteep subreaches and a second one including 68 subreaches with steep slope. Percentage of reach length with artificial structures was not taken into account for the steep subreaches because only 1 subreach out of 68 has some structures.

All four multiple regression models for the nonsteep subreaches turned out to be significant ($p < 0.001$) and gave moderate coefficients of multiple determination (R^2 and adjusted R^2 ranged between 0.30 and 0.38 and between 0.27 and 0.36, respectively) (Table 5). The best model including unit stream power calculated based on pre-flood channel width (R^2 = 0.38 and adjusted R^2 = 0.36) has the following equation:

$$W_{ratio} = -0.719 + 0.174*\omega_{before} + 0.292*C_i + 0.275*AS + 0.026*SS \quad (1)$$

where W_{ratio} is the ratio of channel width after the flood/channel width before the flood, ω_{before} is the unit stream power calculated based on pre-flood channel width (W m^{-2}), C_i is the confinement index, AS is the percentage of reach length with artificial structures, SS is the sediment supply area (m^2).

	Model 1		Model 2		Model 3		Model 4	
	R^2 = 0.30 R^2_{adj} = 0.27 *p*-value<0.001		R^2 = 0.34 R^2_{adj} = 0.30 *p*-value<0.001		R^2 = 0.38 R^2_{adj} = 0.36 *p*-value<0.001		R^2 = 0.37 R^2_{adj} = 0.33 *p*-value<0.001	
	R^2	*p*-value	R^2	*p*-value	R^2	*p*-value	R^2	*p*-value
C_i	0.23	<0.001	0.23	<0.001	0.23	<0.001	0.23	<0.001
Percentage of reach length with artificial structures	0.05	0.481	0.05	0.203	0.05	0.085	0.05	0.997
Sediment supply area	0.07	0.006	0.07	0.001	0.07	0.013	0.07	0.006
Channel slope	0.01	0.756	-	-	-	-	-	-
Ω (Wm^{-1})	-	-	1.33E-06	0.042	-	-	-	-
ω_{before} (Wm^{-2})	-	-	-	-	0.14	0.001	-	-
ω_{after} (Wm^{-2})	-	-	-	-	-	-	0.12	0.005

Table 5. Multiple regression models for the relationships between width ratio and controlling factors for the nonsteep subreaches

The variable being the best predictor of width ratio was confinement index (R^2 = 0.23; significant in all four regression models). Significant relationships, although with very low R^2 values, were also found for the rate of sediment supply (R^2 = 0.07) and for unit stream power calculated in the two ways (R^2 = 0.14 and R^2 = 0.12, using pre-flood and post-flood channel width, respectively). The relationships with percentage of reach length with artificial structures, channel slope, and cross-sectional stream power were weak or very weak and were statistically not significant ($p > 0.05$).

The four multiple regression models for the subset of steep subreaches were significant ($p < 0.001$) and gave higher coefficients of multiple determination than those obtained for the nonsteep subreaches (R^2 and adjusted R^2 ranged between 0.43 and 0.67 and between 0.41 and 0.65, respectively) (Table 6). The best model including unit stream power calculated based on pre-flood channel width (R^2 = 0.67 and adjusted R^2 = 0.65) has the following equation:

$$W_{ratio} = -2.118 + 0.317*\omega_{before} + 0.366*C_i + 0.004*SS \quad (2)$$

where W_{ratio} is the ratio of channel width after the flood/channel width before the flood, ω_{before} is the unit stream power calculated based on pre-flood channel width (W m^{-2}), C_i is the confinement index, SS is the sediment supply area (m^2).

	Model 1		Model 2		Model 3		Model 4	
	R^2 = 0.44 R^2_{adj} = 0.42 *p*-value<0.001		R^2 = 0.65 R^2_{adj} = 0.64 *p*-value<0.001		R^2 = 0.67 R^2_{adj} = 0.65 *p*-value<0.001		R^2 = 0.43 R^2_{adj} = 0.41 *p*-value<0.001	
	R^2	*p*-value	R^2	*p*-value	R^2	*p*-value	R^2	*p*-value
C_i	0.43	<0.001	0.43	<0.001	0.43	<0.001	0.43	<0.001
Sediment supply area	0.06	0.925	0.06	0.65	0.06	0.751	0.06	0.813
Channel slope	0.02	0.295	-	-	-	-	-	-
Ω (Wm^{-1})	-	-	0.44	<0.001	-	-	-	-
ω_{before} (Wm^{-2})	-	-	-	-	0.50	<0.001	-	-
ω_{after} (Wm^{-2})	-	-	-	-	-	-	0.02	0.704

Table 6. Multiple regression models for the relationships between width ratio and controlling factors for the steep subreaches.

The width ratio showed clear relationships with three variables: confinement index (R^2 = 0.43), cross-sectional stream power (R^2 = 0.44), and unit stream power calculated based on pre-flood channel width (R^2 = 0.50). In turn, the relationships with the three other variables (sediment-supply area, channel slope, and unit stream power calculated based on post-flood channel width) were weak and statistically not significant ($p > 0.05$).

To explore further results of the multiple regression models, we examined the controlling factors of the two best models (i.e., model 3 for the nonsteep and steep subreaches, see Tables 5 and 6) by estimating simple regression models (Fig. 6). Simple regression analyses confirmed that confinement index and unit stream power (using pre-flood channel width) are the best explanatory variables, for the nonsteep and steep channels. Width ratio was more clearly related to confinement index in steep subreaches (R^2 = 0.53) (Fig. 6D) than in nonsteep subreaches (R^2 = 0.32) (Fig.

6A). In steep subreaches, unit stream power — being the most important predictor among hydraulic variables — explained 52% of the degree of channel widening, which increased following a non-linear function (Fig. 6E). In nonsteep subreaches, unit stream power also was the most important predictor among hydraulic variables, but its relation with the degree of channel widening was much weaker (R^2 = 0.23) (Fig. 6B). Notably, the most intense channel widening (width ratio up to 20) that occurred in the Pogliaschina and Gravegnola catchments is not associated to the highest values of unit stream power (Fig. 6B). Hence, most interesting, the plots of Fig. 6 showed that the relationships between width ratio and controlling factors are not linear. This helps to explain why multiple regression models, which rely on linear relations, did not have very high coefficients of multiple determination (adjusted R^2 were 0.36 and 0.65, respectively).

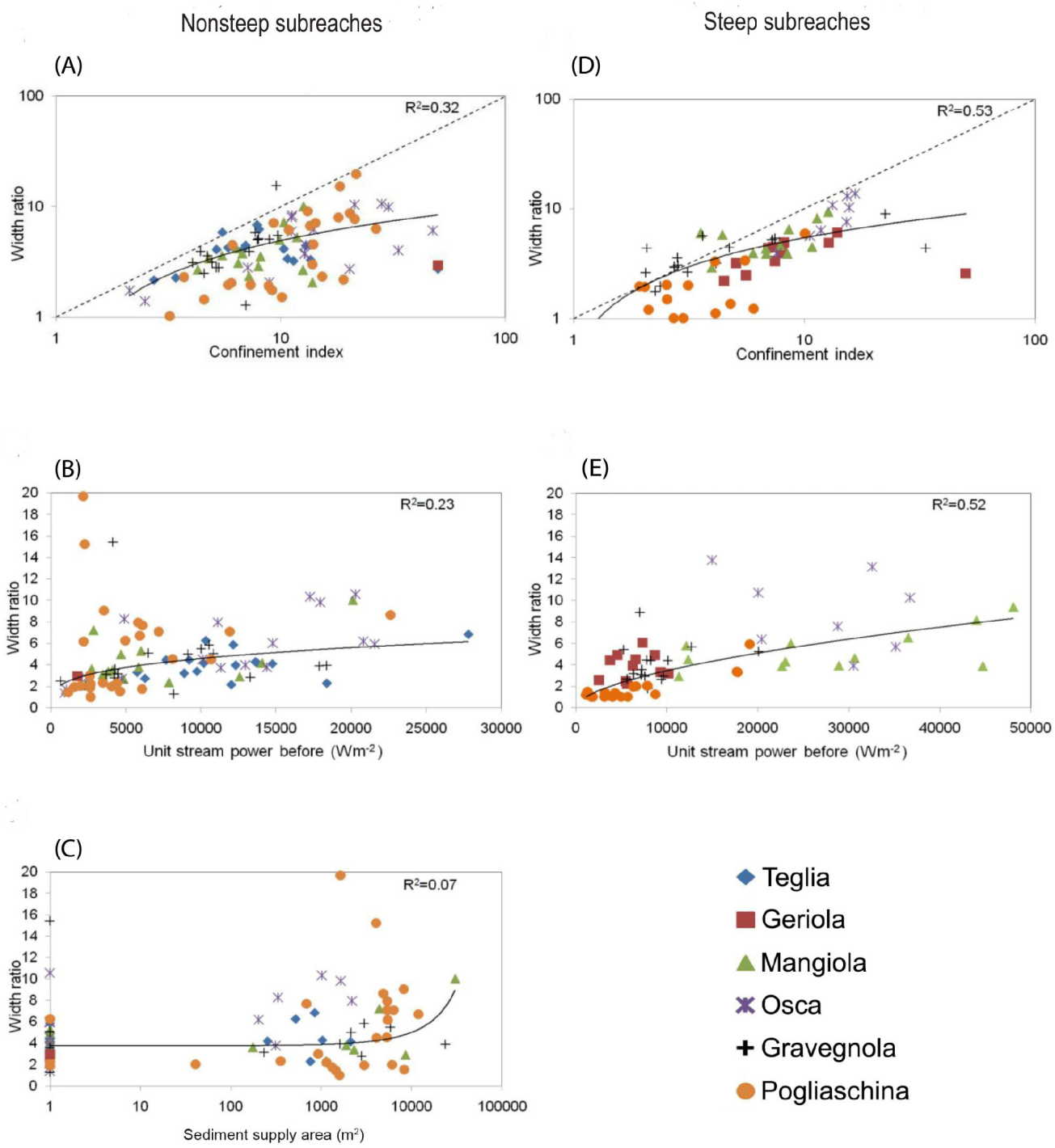

Figure 6. Simple regression models between width ratio and controlling factors. Only significant factors of the two best models obtained by multiple regression analysis (see Tables 5 and 6) are shown: (A), (B), and (C) refer to nonsteep subreaches; (D) and (E) to steep subreaches. In (A) and (D) the dashed lines represent the 1:1 relationship.

5. Discussion and conclusions

5.1. Regression models and controlling factors

Results confirmed the main hypothesis of this work that hydraulic variables alone are not sufficient to explain channel response to an extreme flood event. The inclusion of other factors, specifically lateral confinement, channel slope, hillslope sediment supply, and percentage of reach length with artificial structures, led to satisfactory models explaining the observed variability in the degree of channel widening. Differences between the two sets of subreaches (with nonsteep and steep slopes) appeared in terms of overall explanatory capability of the models and most significant explanatory variables.

In the steep (≥4%) subreaches, which were characterized also by higher confinement, channel widening occurred mainly through lateral erosion and, as confirmed also by field observations, depositional processes were less significant. In these subreaches, cross-sectional stream power, unit stream power (calculated based on pre-flood channel width), and lateral confinement showed good relationships with the degree of channel widening (i.e., width ratio) and significant statistical models were obtained (Table 6, Fig. 6). These results suggest that the widening process is essentially controlled by two factors: flood power and valley confinement. Notably, flood duration above a critical threshold (e.g., related to bedload transport) was not included in our analysis, but it is a variable that very likely would increase the robustness of regression models in these sub-reaches (Costa and O'Connor, 1995; Magilligan et al., 2015). Unfortunately, data on thresholds for bedload transport are not available for the study streams, neither are grain size distributions for all the analyzed reaches.

The models obtained for the nonsteep subreaches, compared to the steep subreaches, are less satisfactory as they provide a lower explanation of widening variability. Besides, the degree of channel widening showed relatively weak relationships with all the significant explanatory variables (i.e., lateral confinement, sediment supply area, unit stream power; Table 5, Fig. 6). These results suggest that widening at the lower slopes and with less confined channels is a more complex process and that additional factors should be considered to better understand

geomorphic response in these reaches. Likely, widening in these cases results from a combination of bar formation and lateral erosion, with sediment (volumes and size) supplied from landslides and upstream reaches becoming significant. Notable bar formation and channel aggradation were observed in several of these reaches (Rinaldi et al., 2015), and repeated avulsion processes might have occurred during the event in these aggrading subreaches. As to additional factors, large riparian trees coupled to wood jams could have played a role by occasionally reinforcing banks and, therefore, hampering channel widening.

5.2. Unit stream power and geomorphic response

The analysis carried out in the six subcatchments of the Magra River basin showed that unit stream power calculated based on pre-flood channel width has stronger relations with channel widening in comparison to unit stream power calculated based on post-flood channel width and to cross-sectional stream power. Because peak discharge was used for stream power calculation, we are aware that neither pre-flood nor post-flood channel width is actually appropriate for the estimation of unit stream power, as the most appropriate would be the (unknown) width at the flood-peak time. The fact that using the pre-flood width gives better relations with the degree of channel widening (i.e., width ratio) could suggest that most width changes occurred after the flood peak. This hypothesis is supported by a video that allowed flood reconstruction along one reach of the Mangiola River (the video documents channel changes during the whole flood event; see Rinaldi et al., 2015, for more details). Statistical analyses and the video on the Mangiola River are not sufficient to validate the hypothesis that most channel widening took place after the flood peak, but the results of this work show clearly that using unit stream power based on post-flood width is not effective to explain geomorphic response, at least in streams that underwent intense widening in terms of width ratio.

5.3. The role of sediment supply in channel response

Some previous works (e.g., Harvey, 2001; Sloan et al., 2001) pointed out that sediment supply from hillslopes was a major driving factor of channel response

during extreme flood events. On the other hand, examples also show that landslides, although coupled with channel network, may have minor effects on channel processes (e.g., Milan, 2012). The detailed landslide inventory and the analysis of sediment connectivity allowed us to assess the extent to which sediment supply from hillslopes influenced channel response in the six study catchments. It is worth clarifying that we only assessed sediment-source areas, without an estimation of the involved volume that would require a rather uncertain estimation of landslide thickness. Moreover, once a landslide was considered to be coupled to the study reaches, its entire area was assumed to contribute to sediment supply without taking into account that part of the landslide material, especially in channelized earth flows, could be blocked by large wood (Lucía et al., 2015). In the steep reaches, although notable sediment sources were coupled with some reaches (see Table 2), no significant relation was found between the degree of channel widening and the hillslope area supplying sediment to the channels. Likely, freshly-eroded colluvium was transferred to downstream reaches given the typical supply-limited conditions of high-energy channels, or remained stored in the smallest tributaries before entering the main channels.

In the nonsteep reaches, a significant although weak relation was found (Table 5 and Fig. 6C). This would suggest that during the flood a redistribution of the material stored in the alluvial plains was likely the dominant process, whereas the contribution of material from hillslopes was relevant only at specific sites and was thus not reflected in the analysis of the whole data set, which included 89 nonsteep subreaches. Notably, remarkable channel widening (i.e., width ratio up to 6) also took place along several subreaches that received no sediment input from landslides (Fig. 6C).

5.4. Practical implication for river management and risk mitigation

Although the six study catchments are not densely populated, the 25 October 2011 flood caused severe damages to infrastructures, specifically to roads and bridges, and loss of lives. Such catastrophic effects of the flood mainly reflected channel dynamics (i.e., bank erosion, bed aggradation, channel avulsion, intense transport of large wood) or inundation processes caused or enhanced by bridge

clogging due to large wood. Therefore, in terms of hazard, documenting the type and magnitude of channel response is crucial in identifying controlling factors of such response and in developing tools to enable channel dynamic predictions. Recently, Buraas et al. (2014) stated that there is still a general lack in the capability to predict where major geomorphic changes take place during an extreme flood event. In this respect, the regression models and other outcomes of this study can be used to predict the degree of channel widening and to support planning along river corridors through hazard mapping. For instance, the 2011 flood showed that in steep, relatively confined mountain reaches the whole, relatively narrow, alluvial plain may undergo major geomorphic changes, which are effectively explained by regression models that include lateral confinement and unit stream power. This study pointed out that in nonsteep reaches predicting the degree of channel widening is more uncertain and that risk mitigation may not rely only on protection structures that can be partly effective during extreme floods in mountain environments.

References

Autorità di Bacino interregionale del Fiume Magra, 2006. Piano stralcio "Assetto Idrogeologico" del bacino del Fiume Magra e del Torrente Parmignola – Relazione Generale. Unpublished report, 209 p. (http://www.adbmagra.it/), Sarzana (Italy) (in Italian).

Borga, M., Boscolo, P., Zanon, F., Sangati, M., 2007. Hydrometeorological analysis of the August 29, 2003 flash flood in the eastern Italian Alps. Journal of Hydrometeorology **8** (5): 1049–1067.

Borga, M., Gaume, E., Creutin, J.D., Marchi, L., 2008. Surveying flash floods: gauging the ungauged extremes. Hydrological Processes **22**(18): 3883-3885.

Borselli, L., Cassi, P., Torri, D., 2008. Prolegomena to sediment and flow connectivity in the landscape: a GIS and field numerical assessment. Catena, **75**(3): 268-277.

Brierley, G.J., Fryirs K.A., 2005. Geomorphology and River Management: Applications of the River Style Framework. Blackwell, Oxford, pp. 398.

Buraas, E.M., Renshaw, C.E., Magilligan, F.J., Dade, W.B., 2014. Impact of reach geometry on stream channel sensitivity to extreme floods. Earth Surface Processes and Landforms **39**: 1778–1789.

Cavalli, M., Trevisani, S., Comiti, F., Marchi, L., 2013. Geomorphometric assessment of spatial sediment connectivity in small Alpine catchments. Geomorphology **188**: 31–41.

Cenderelli, D.A., Wohl, E.E., 2003. Flow hydraulics and geomorphic effects of glacial-lake outburst floods in the Mount Everest region, Nepal. Earth Surface Processes and Landforms **28**: 385–407.

Comiti F., Mao L. 2012. Recent advances in the dynamics of steep channels. In: Church, M., Biron, P.M., Roy, A.G. (Eds.), Gravel-bed Rivers: Processes, Tools, Environments. Chichester, Wiley, pp. 353-377.

Costa, J.E., O'Connor, J.E., 1995. Geomorphically effective floods. In: Costa, J.E., Miller, A.J., Potter, K.W., Wilcock, P. (Eds.), Natural and Anthropogenic Influences in Fluvial Geomorphology. Monograph, vol. **89**. American Geophysical Union, Washington, D.C., pp. 45–56.

Crema, S., Schenato, L., Goldin, B., Marchi, L., Cavalli, M., 2015. Toward the development of a stand-alone application for the assessment of sediment connectivity. Rendiconti Online della Soc. Geol. Ital. **34**: 58–61.

Dean, D.J., Schmidt, J.C., 2013. The geomorphic effectiveness of a large flood on the Rio Grande in the Big Bend region: Insights on geomorphic controls and post-flood geomorphic response. Geomorphology **201**, 183–198.

Gaume, E., Borga, M., 2008. Post-flood field investigations in upland catchments after major flash floods: proposal of a methodology and illustrations. Journal of Flood Risk Management **1**(4): 175–189.

Grimaldi, S., Petroselli, A., Romano, N., 2013. Green-Ampt Curve-Number mixed procedure as an empirical tool for rainfall-runoff modelling in small and ungauged basins. Hydrological Processes **27** (8): 253-264.

Gupta, A., Fox, H., 1974. Effects of high magnitude floods on channel form: a case study in the Maryland Piedmont. Water Resour. Res. **10**: 499–509.

Harvey, A.M. 1984. Geomorphological response to an extreme flood: a case from Southern Spain. Earth Surface Processes and Landforms **9**: 267–279.

Harvey, A.M., 2001. Coupling between hillslopes and channels in upland fluvial systems: implications for landscape sensitivity, illustrated from the Howgill Fells, northwest England. Catena **42**: 225-250.

Heritage, G.L., Large, A.R.G., Moon, B.P., Jewitt, G., 2004. Channel hydraulics and geomorphic effects of an extreme flood event on the Sabie River, South Africa. Catena **58**: 151–181.

Hooke, J.M., Mant, J.M., 2000. Geomorphological impacts of a flood event on ephemeral channels in SE Spain. Geomorphology **34**(3-4): 163–180.

Hungr, O., Evans, S.G., Bovis, M.J., Hutchinson, J.N., 2001. A review of the classification of landslides of the flow type. Environmental and Engineering Geoscience **7**: 221-238.

Jansen, J.D., 2006. Flood magnitude–frequency and lithologic control on bedrock river incision in post-orogenic terrain. Geomorphology **82**: 39–57.

Johnson, R.M., Warburton, J., 2002. Flooding and geomorphic impacts in a mountain torrent: Raise Beck, central Lake District, England. Earth Surface Processes and Landforms **27**: 945–969.

Kale, V.S., 2007. Geomorphic effectiveness of extraordinary floods on three large rivers of the Indian Peninsula. Geomorphology **85**: 306–316.

Kale, V.S., Hire, P.S., 2004. Effectiveness of monsoon floods on the Tapi River, India: role of channel geometry and hydrologic regime. Geomorphology **57**: 275–291.

Krapesch, G., Hauer, C., Habersack, H., 2011. Scale orientated analysis of river width changes due to extreme flood hazard. Natural Hazards and Earth System Sciences **11**: 2137–2147.

Langhammer, L., 2010. Analysis of the relationship between the stream regulations and the geomorphologic effects of floods. Natural Hazards **54**, 121–139.

Lenzi, M.A., Mao, L., Comiti, F., 2006. Effective discharge for sediment transport in a mountain river: computational approaches and geomorphic effectiveness. Journal of Hydrology **326**: 257-276.

Lucía, A., Comiti, F., Borga, M., Cavalli, M., Marchi, L., 2015. Dynamics of large wood during a flash flood in two mountain catchments. Natural Hazards and Earth System Sciences, **15**(8): 1741-1755.

Magilligan, F.J., 1992. Thresholds and the spatial variability of flood power during extreme floods. Geomorphology **5**: 373–390.

Magilligan, F.J., Buraas, E.M., Renshaw, C.E., 2015. The efficacy of stream power and flow duration on geomorphic responses to catastrophic flooding. Geomorphology **228**: 175-188.

Marchi, L., Borga, M., Preciso, E., Sangati, M., Gaume, E., Bain, V., Delrieu, G., Bonnifait, L., Pogačnik, N., 2009. Comprehensive post-event survey of a flash flood in Western Slovenia: observation strategy and lessons learned. Hydrological Processes **23**(26): 3761-3770.

Marra, F., Nikolopoulos, E.I., Creutin, J.D., Borga, M., 2014. Radar rainfall estimation for the identification of debris-flow occurrence thresholds. Journal of Hydrology **519**: 1607-1619.

Martens, B., Cabus, P., De Jongh, I., Verhoest, N.E.C., 2013. Merging weather radar observations with ground-based measurements of rainfall using an adaptive multiquadric surface fitting algorithm. Journal of Hydrology **500**: 84-96.

Milan, D.J., 2012. Geomorphic impact and system recovery following an extreme flood in an upland stream: Thinhope Burn, northern England, UK. Geomorphology **13:**, 319-328.

Mondini, A.C., Viero, A., Cavalli, M., Marchi, L., Herrera, G., Guzzetti, F., 2014. Comparison of event landslide inventories: the Pogliaschina catchment test case, Italy. Natural Hazards Earth System Sciences **14**: 1749–1759.

Montgomery, R.D., Buffington, J.M., 1997. Channel-reach morphology in mountain drainage basin. Geol. Soc. Am. Bull. **109** (5): 596-611.

Nardi, L., Rinaldi, M., 2015. Spatio-temporal patterns of channel changes in response to a major flood event: the case of the Magra River (central-northern Italy). Earth Surface Processes and Landforms **40**: 326-339.

Phillips, J.D., 2002. Geomorphic impacts of flash flooding in a forested headwater basin. Journal of Hydrology **269**: 236–250.

Pickup, G., Rieger W.A., 1979. A conceptual model of the relationship between channel characteristics and discharge. Earth Surface Processes **4**: 37-42.

Ponce, V.M., Hawkins, E.R.H., 1996. Runoff curve number: has it reached maturity? Journal of Hydrologic Engineering **1**(1): 11–19.

Reid, I., Laronne, J.B., Powell, D.M., 1998. Flash-flood and bedload dynamics of desert gravel-bed streams. Hydrological Processes **12**: 543-557.

Rinaldi, M., Surian, N., Comiti, F., Bussettini, M., 2013. A method for the assessment and analysis of the hydromorphological condition of Italian streams: the Morphological Quality Index (MQI). Geomorphology **180-181**: 96–108.

Rinaldi, M., Amponsah, W., Benvenuti, M., Borga, M., Comiti, F., Lucìa, A., Marchi, L., Nardi, L., Righini, M., Surian, N., 2015. An integrated approach for investigating geomorphic response to extreme

events: methodological framework and application to the October 2011 flood in the Magra River catchment, Italy. Earth Surface Processes and Landforms **41**: 835–846. doi: 10.1002/esp.3902.

Sloan, J., Miller, J.R., Lancaster, N., 2001. Response and recovery of the Eel River, California, and its tributaries to floods in 1955, 1964, and 1997. Geomorphology **36**: 129-154.

Surian, N., Mao, L., Giacomin M., Ziliani, L., 2009. Morphological effects of different channel forming discharges in a gravel-bed river. Earth Surface Processes and Landforms **34**: 1093–1107.

Thompson, C., Croke, J., 2013. Geomorphic effects, flood power, and channel competence of a catastrophic flood in confined and unconfined reaches of the upper Lockyer valley, southeast Queensland, Australia. Geomorphology **197**: 156–169.

Vocal Ferencevic, M.V., Ashmore, P., 2012. Creating and evaluating digital elevation model-based stream-power map as a stream assessment tool. River Research and Applications **28**: 1394–1416.

Wolman, M.G., Gerson, R.,1978. Relative scales of time and effectiveness of climate in watershed geomorphology. Earth Surface Processes **3**: 189–208.

Wolman, M.G, Miller, J.P., 1960. Magnitude and frequency of forces in geomorphic processes. Journal of Geology **68**: 54–74.

4. CHANNEL WIDENING DURING EXTREME FLOODS: HOW TO INTEGRATE IT WITHIN RIVER CORRIDOR PLANNING ?

Francesco Comiti[a]; Margherita Righini[b]; Laura Nardi[c]; Ana Lucía[a]; William Amponsah[d,e]; Marco Cavalli[d]; Nicola Surian[b]; Lorenzo Marchi[d]; Massimo Rinaldi [c]; Marco Borga[e]

[a]Faculty of Science and Technology, Free University of Bozen-Bolzano, Italy; [b]Department of Geosciences, University of Padova, Italy; [c]Department of Earth Sciences, University of Florence, Italy; [d]CNR IRPI, Padova, Italy; [e]Department of Land, Environment, Agriculture and Forestry, University of Padova, Italy.

Proceedings of the 13th Congress Interpraevent 2016, Lucerne, Switzerland, 477-486

Abstract

Channel widening taking place during large flood events can be substantial in mountain rivers, with consequent great potential damages to infrastructures and buildings. The purpose of this work is twofold: i) to provide a quantitative assessment of geomorphic effects of an extreme flood event (recurrence interval > 100 years); ii) to test on this study case a new hydromorphological methodological framework (IDRAIM) developed to guide river corridor planning and management. As to the first objective, field surveys were integrated with remote sensing, GIS and statistical analyses for a flood event occurred in 2011 in Northwestern Italy. Channel widening ratios (width after / width before the flood) were calculated and then correlated with different controlling factors, and envelope relationships were then obtained. The tool of the IDRAIM framework used for the second objective was the Event Dynamics Classification (EDC) applied to selected study reaches, whose widening ratios turned out to correspond well with the EDC classes. Based on the results obtained, a practical procedure for predicting the expected widening is finally proposed.

Introduction

Infrequent, high-magnitude floods can lead to sudden, dramatic channel changes in alluvial and semi-alluvial channels. Indeed, the geomorphic role of large floods has long been debated (e.g. Wolman and Miller, 1960; Costa and O'Connor, 1995; Phillips, 2002; Magilligan et al., 2015). Nonetheless, rather few are the studies which have analyzed in detail the magnitude of channel widening determined by extreme floods in Alpine rivers (Krapesch et al., 2011), despite the paramount

relevance of such process on flood hazard. In fact, a sound river corridor planning should include – beside flood inundation depth and velocities – the expected channel dynamics (bank erosion and bed incision/aggradation) occurring during flood events, as these can both substantially modify the flooding pattern and cause direct damage to buildings and infrastructures.

Unfortunately, the expected sudden and notable changes in channel width during floods are typically not included in flood hazard mapping. Indeed, our current understanding of the factors controlling channel widening is very limited. In fact, hydrodynamic forces were found to be not sufficient to explain geomorphic effects (e.g. Heritage et al., 2004; Nardi and Rinaldi, 2015), and thus other factors, such as bedload supply and pre-flood channel planform (Dean and Schmidt, 2013), lateral confinement (Thompson and Croke, 2013), and channel curvature (Buraas et al., 2014) should be also accounted for in the prediction of widening. However, field data available to build reliable statistical models or to validate numerical morphodynamic models are very limited. On the other hand, easy-to-use tools applicable by practitioners of river management agencies are much needed to predict the reach-scale morphological response of the channel network to extreme (recurrence intervals RI>100 yr) flood events.

The purpose of this work is twofold: i) to provide a quantitative assessment of the channel widening associated to an extreme flood event which occurred in 2011 in Northwestern Italy (Magra River basin); and ii) to test on this study case a new methodological framework (IDRAIM) developed to guide river corridor planning and management which focuses on channel adjustments occurring both in the long-term and during extreme events.

Methods

Study case: the 2011 flood event in the Magra River basin

The Magra River basin is located in the northern Apennines (Italy) and covers an area of 1717 km^2, ranging from sea level to a maximum elevation of 1901 m a.s.l. (Fig. 1). Sedimentary rocks (mostly sandstones and mudstones) prevail in the basin, but some outcrops of magmatic (ophiolites) and metamorphic rocks are also present.

The climate is Mediterranean, with dry summers and the most abundant precipitation occurring in autumn. The mean annual precipitation is about 1700 mm, and maximum values (up to about 3000 mm) are observed in the upper part of the catchment. Forests cover 66% of total basin area and occupy most of catchments slopes. Agricultural areas, urban areas and transportation structures mostly lie in the valley floors and on the lower sectors of the slopes.

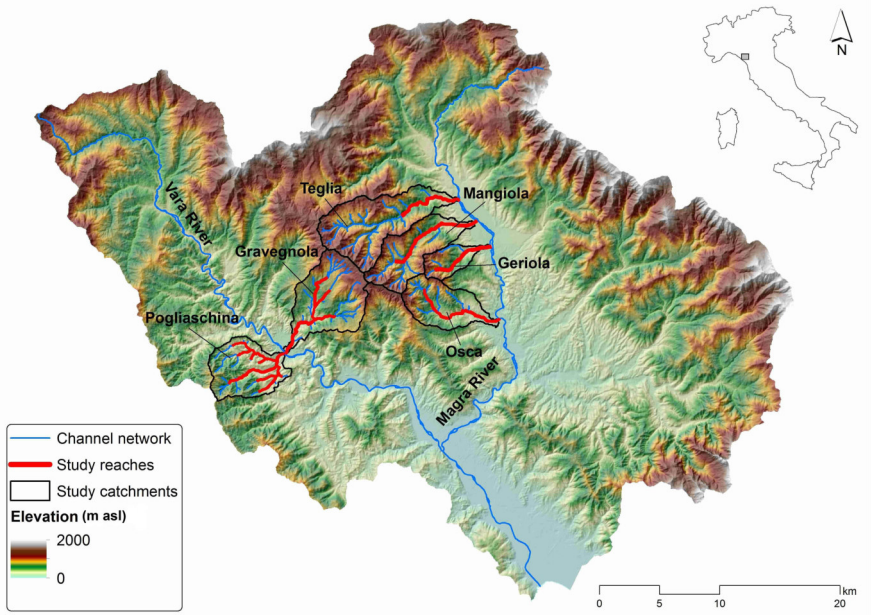

Figure 1. Location map of the Magra River basin and of the analyzed tributaries (from Surian et al., 2016).

An intense precipitation event took place within the river basin on October 25th, 2011, and originated a flash flood both in the Magra River (with a peak discharge having a RI of about 100 yr, Nardi and Rinaldi, 2015) and along several tributaries, there with extremely high peak flows (up to RI>300 yr, based on historical rainfall data), where enormous volumes of large wood were eroded from the floodplains (Lucìa et al., 2015) causing extensive bridge clogging. Rainfall maps for the study event were obtained based on data from a rain gauges network and the Monte Settepani radar, and the estimates show that maximum hourly rates were up to 149 mm/hr, whereas three-hours maximum and event-accumulation maxima were up to 326 mm and 500 mm, respectively. Antecedent moisture conditions in the basins were intermediate. An integrated approach was adopted to investigate the geomorphic effects of the 2011 flood in the Magra catchment, and the whole approach is described in detail by Rinaldi et al. (2016).

Six catchments chosen among those where rainfall was most intense were selected to analyze channel response: Pogliaschina, Gravegnola, Osca, Teglia, Geriola and Mangiola (Fig. 1). In these rivers, unit peak discharge estimates range from 12.8 $m^3s^{-1}km^{-2}$ (Osca) to 23.7 $m^3s^{-1}km^{-2}$ (Pogliaschina). Streams within the six catchments are characterized by average channel slope ranging from 4.1% (Osca) to 8.8% (Geriola), coarse sediments (mainly gravels and cobbles), and a wide range of conditions in terms of lateral confinement, but only partly- and unconfined reaches were analyzed for channel widening. Importantly, artificial structures (bed and bank protections) were very limited before the flood.

The morphological changes induced by the 2011 flood were assessed by field surveys and interpretation of aerial photographs. To assess changes in channel width, channel banks and islands (i.e. in-channel surfaces covered by woody vegetation) were digitized on pre- and post-flood orthophotos (Fig. 2). The term "channel" refers to the active channel, which includes low-flow channels and unvegetated or sparsely vegetated bars (i.e. exposed sediments). Then, channel width was calculated dividing channel area by the length of the reach, and changes in channel width were expressed as width ratio W_r, i.e. channel width after / channel width before the flood, as in Krapesch et al. (2011).

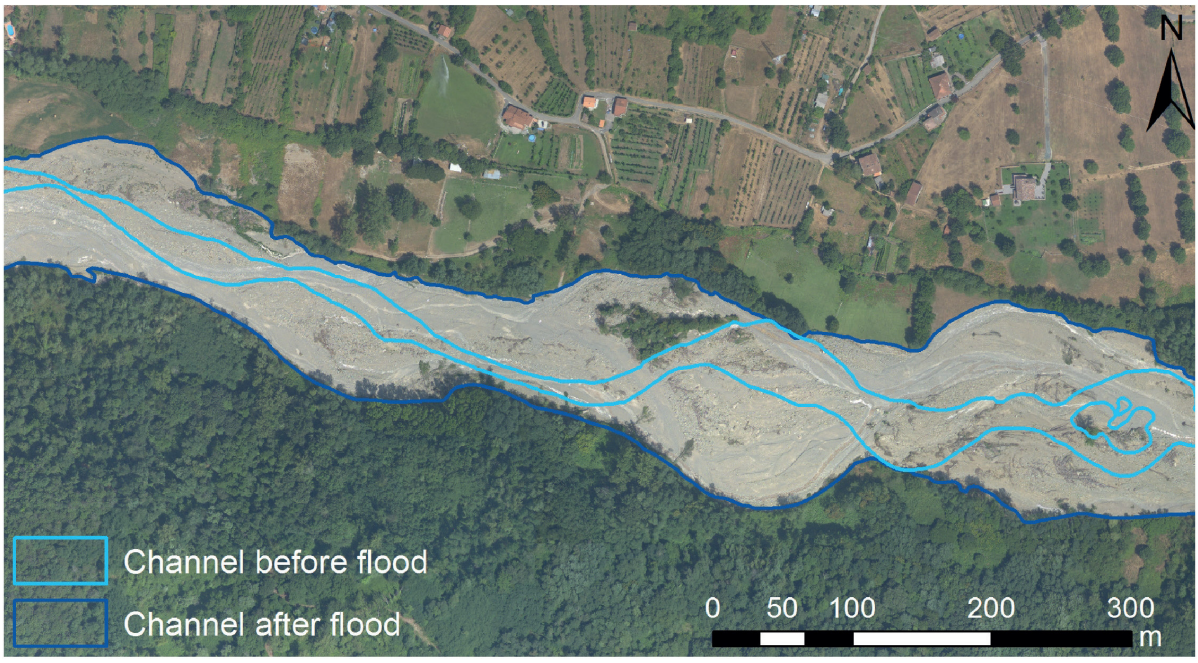

Figure 2. Example of the channel widening observed in the Mangiola River.

The IDRAIM methodological framework

The IDRAIM methodological framework (Rinaldi et al., 2014, 2015) includes the following four phases: (1) catchment-wide characterization of the fluvial system; (2) evolutionary trajectory reconstruction and assessment of current river conditions; (3) description of future trends of channel evolution; (4) identification of management options. A series of specific tools have been developed for the assessment of river conditions, in terms of morphological quality and channel dynamics. These latter include the "Morphological Dynamics Index", the "Event Dynamics Classification", and the "River Morphodynamic Corridors".

The present work focuses specifically on the "Event Dynamics Classification" (EDC), applying it to selected study reaches and comparing them with observed geomorphic changes. In particular, EDC leads to classify each reach into one of four classes of expected event dynamics (very high, high, medium, low), adopting a guided logical procedure based on flow charts. The assessment is carried out by combining two aspects (Table 1): i) the expected magnitude of morphological changes (4 classes) and ii) the clogging conditions (2 classes, i.e. likely or not likely occurrence of clogging, mostly by wood elements) at critical cross-sections (bridges and culverts) during an extreme event.

		Clogging probability	
		High (H)	Low (L)
Expected morphological changes	Very relevant (I)	Very high	Very high
	Relevant (II)	Very high	High
	Intermediate (III)	High	Medium
	Small (IV)	Medium	Low

Table1. Classification of EDC (Event Dynamics Classification, from low to very high) based on the expected morphological changes (from small to very relevant) coupled to the clogging probability (high or low) (From Rinaldi et al., 2015).

EDC provide information on the expected magnitude of channel dynamics in a given reach on a one-dimensional scale. This information has to be integrated with a 2-D analysis to define the areas of the fluvial corridor that will be affected by such dynamics ("Event Morphodynamic Corridor", EMC). The procedure suggested in IDRAIM for the delineation of the event river morphodynamic corridor (EMC) includes

(i) reconstruction of historical channel changes; (ii) determining the expected flood spatial dynamics based on EDC class; iii) identification of natural elements of confinement (e.g., hillslopes, old terraces); and (iv) identification of reliable protection works preventing lateral channel mobility. All the details of the methodology for both EDC and EMC can be found in Rinaldi et al. (2014 and 2015).

Results

Channel widening in the Magra River basin

The "Width Ratio" (W_r) measured in all the analyzed reaches (n=157) of the six basins described above are plotted in Figure 4 against the estimated unit stream power of the flood peak, calculated using the pre-event channel width (as in Krapesch et al., 2011) as $\omega = \gamma QS/W$, where γ is the specific weight of water, Q is the flood peak discharge, S is channel slope, and W is the channel width measured before the flood. The unit stream power estimated using the pre-event width was found to lead to better statistical results compared to its calculation through the post-event width (Surian et al., 2016).

The widening data (n=35) measured in the main channel of the Magra River (Nardi and Rinaldi, 2015) are reported as well. The large variability (log-log scale graph) of the channel response to similar flow energy is clearly apparent, especially at intermediate unit stream power (1000-10000 Wm^{-2}). The best fit (R^2 = 0.44) power equation including all data is the following:

$$W_r = 0.07\omega^{0.44} \quad \text{(Eq. 1)}$$

Based on this regression, the minimum unit stream power required to cause some widening turns out to be about 400 Wm^{-2}. However, one reach of the Magra River exhibited a width ratio of 1.08 for a unit stream power as low as 173 Wm^{-2}. On the other side, very limited widening (W_r<1.1) was observed in some reaches for ω up to about 5000 Wm^{-2}. Very intense channel widening (W_r>10) was instead observed for ω>2000 Wm^{-2} in other reaches (Gravegnola, Pogliaschina, Osca channels). As a consequence of the enormous scatter in the relationship, indications on the maximum expected width ratios are sounder to plan on the safety side. To this aim, the following equation (dashed line in Fig. 3) represents the upper envelope of

the plot, fitted to a linear trend excluding the seemingly outliers (9 out of 192 reaches, i.e. about 5%):

$W_r \approx 0.002\omega$ (Eq. 2).

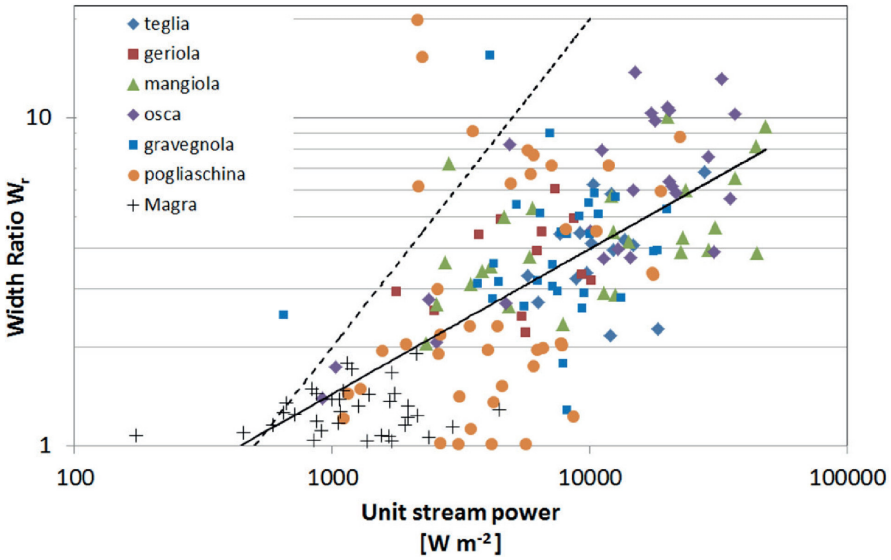

Figure 3. Scatterplot of width ratio vs unit stream power (calculated based on the pre-event channel width) for the study reaches. Data from Nardi and Rinaldi (2015) are also included. The solid line represents the best fit equation (Eq. 1), the dashed line the upper envelope curve (Eq. 2).

Nonetheless, the lateral confinement (expressed by the confined index calculated as alluvial plain width divided by pre-event channel width) plays a relevant role on the maximum width ratios, as shown in Figure 4, where most of the data plot below – in some cases considerably – the equality line. However, 10 reaches feature widening ratios exceeding the confinement index, an indication that part of the hillslopes was also eroded during the flood (this was verified in the field). Therefore, in most of cases the widening was not limited by the lateral extent of the erodible corridor, although a positive correlation exists between the two variables.

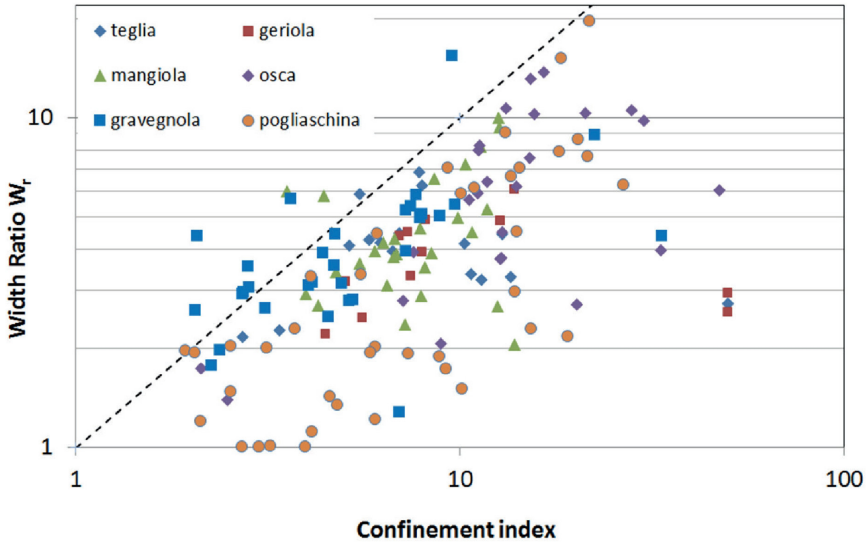

Figure 4. Scatterplot of width ratio vs confinement index (i.e. alluvial plain width / pre-event channel width) for the study reaches. Data from Nardi and Rinaldi (2015) are not available. The dashed line represents the 1:1 relationship.

When plotting the widening magnitude against the pre-flood channel width, an inverse relationship is shown (Fig. 5). The plot shows how large is the variability in the width ratios observed in the narrower (1-10 m) reaches, and that for large channels (>100 m) width ratios > 1.5-2 should not be expected.

The envelope curve (fitted by eye to a simple power form, excluding 5% of the dataset) is given by following equation:

$$W_r \approx 25 W_b^{-1/2} \quad \text{(Eq. 3)}$$

A more complete, in-depth statistical analysis – entailing multiple factors – for the understanding of the variability in the observed width ratios is presented in Surian et al. (2016), whereas the practical prediction of the widening extent is discussed in the next section.

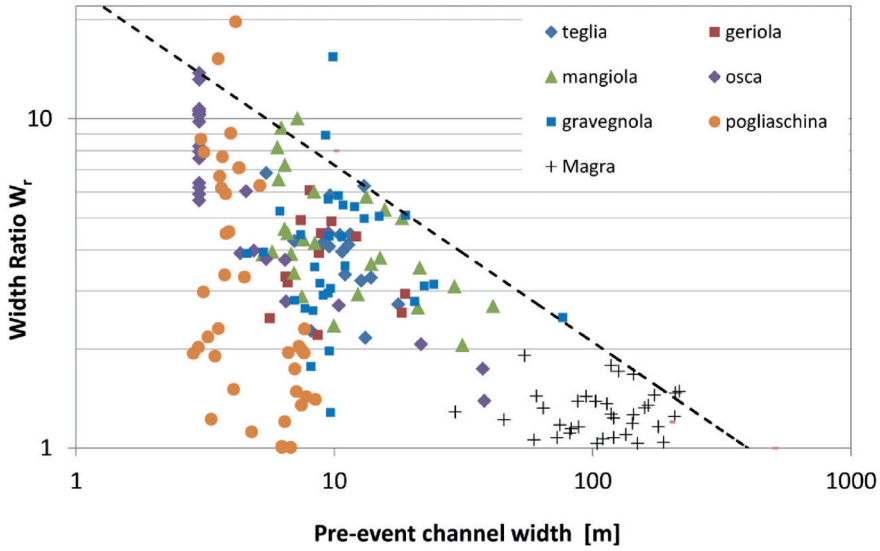

Figure 5. Scatterplot of width ratio vs pre-event channel width for the study reaches. Data from Nardi and Rinaldi (2015) are also included. The dashed line represents equation 3 (envelope curve).

River reach	Confinement class	Slope	Expected morphological changes	Clogging probability	EDC class	Width ratio
Magra 3_1	Partly confined	0.016	Intermediate	Low	High	1.3
Magra 3_8	Unconfined	0.006	Relevant	High	Very high	1.6
Magra 6_3	Unconfined	<0.001	Intermediate	Low	Medium	1.0
Mangiola 2_2	Partly confined	0.037	Very relevant	High	Very high	3.5
Mangiola 2_3	Unconfined	0.049	Very relevant	High	Very high	5.3

Table 2. EDC (Event Dynamics Classification), width ratio and basic characteristics of some reaches of the Magra and Mangiola rivers.

Predicting channel widening based on morphological analysis

The "Event Dynamics Classification" (EDC) was applied to some reaches of the Magra and Mangiola rivers, as a preliminary test. Table 2 presents the EDC classification along with the width ratio measured after the 2011 flood event. The partly confined reach classified as "Very high" event dynamics (the highest, indicating that flood waters and bedload transport are expected to abandon the existing channel as a result of avulsion processes related to relevant aggradation, landslide damming or bridge clogging) featured a widening of 3.5, much higher than the one falling into "High" class (W_r=1.3). For the unconfined reaches, the lowest slope Magra reach (close to the river outlet) classified with "Medium" dynamics (a class indicating that avulsions are not expected, and only local bank erosions and limited aggradation

or incision are expected) showed no widening during the 2011 event, whereas a "Very high" dynamics was attributed to the steeper reach in the Mangiola which was characterized by W_r=5.3.

Discussion and conclusions

The magnitude of the channel widening occurred during the 2011 flood in the Magra River basin is hugely variable, and the relevance and significance of the different factors (including unit stream power, confinement index and sediment supply as well) are mediated by channel slope, as statistically demonstrated in Surian et al. (2016). A simplified approach to a first order estimation of the average extent of the widening expected during a large (RI>100 yr) flood in mountain basins could be based on the upper envelope curves for the observed width ratios, with the caution that our database is limited to one river basin (although large and diverse) and to one event. The procedure should entail: i) application of eqs. 2-3 and averaging of their results, in order to derive the maximum potential width ratio based on flow energy/channel size; ii) assessment of the confinement index; iii) evaluation of EDC class.

In case the W_r estimated by the integrated application of eqs. 2-3 is larger than the confinement index, and the EDC class is "high" or "very high" (meaning that artificial bank protections are not present, not reliable or not relevant for the event dynamics), the W_r should be assumed equal to the confinement index, or even slightly higher in case of poorly resistant hillslope substrates. In case EDC is high or very high, but the confinement index is larger than what predicted by Eqs. 2-3, then the latter values should be adopted. Finally, if EDC classes are low to medium (due to either stable bank protections, or cohesive banks/very low slopes), the potential for widening is limited, and the width ratios predicted by eqs. 2-3 should be considered unrealistic, and a very limited widening (even null) could be assumed. Further post-event analysis will be obviously of great importance to broaden the dataset and to test the suggested simplified approach.

References

Buraas, E.M., Renshaw, C.E., Magilligan, F.J., Dade, W.B., 2014. Impact of reach geometry on stream channel sensitivity to extreme floods. Earth Surface Processes and Landforms **39**: 1778–1789.

Dean, D.J., Schmidt, J.C. 2013. The geomorphic effectiveness 693 of a large flood on the Rio Grande in the Big Bend region: Insights on geomorphic controls and post-flood geomorphic response. Geomorphology **201**: 183–198.

Costa, J.E., O'Connor, J.E., 1995. Geomorphically effective floods. In: Costa, J.E., Miller, A.J., Potter, K.W., Wilcock, P. (Eds.), Natural and Anthropogenic Influences in Fluvial Geomorphology. Monograph, vol. **89**. American Geophysical Union, Washington, D.C.: 45–56.

Heritage, G.L., Large, A.R.G., Moon, B.P., Jewitt, G., 2004. Channel hydraulics and geomorphic effects of an extreme flood event on the Sabie River, South Africa. Catena **58**: 151–181.

Krapesch, G., Hauer, C., Habersack, H., 2011. Scale orientated analysis of river width changes due to extreme flood hazard. Natural Hazards and Earth System Sciences **11**: 2137–2147.

Lucìa, A., Comiti, F., Borga, M., Cavalli, M., Marchi, L., 2015. Dynamics of large wood during a flash flood in two mountain catchments. Nat. Hazards Earth Syst. Sci., **15**: 1741–1755.

Magilligan, F.J., Buraas, E.M., Renshaw, C.E., 2015. The efficacy of stream power and flow duration on geomorphic responses to catastrophic flooding. Geomorphology **228**: 175-188.

Nardi, L., Rinaldi, M., 2015. Spatio-temporal patterns of channel changes in response to a major flood event: the case of the Magra River (central-northern Italy). Earth Surface Processes and Landforms **40**: 326-339.

Phillips, J. D., 2002. Geomorphic impacts of flash flooding in a forested headwater basin. Journal of Hydrology **269**: 236–250.

Rinaldi M., Surian N., Comiti F., Bussettini M., 2014. IDRAIM – Sistema di valutazione idromorfologica, analisi e monitoraggio dei corsi d'acqua. Istituto Superiore per la Protezione e la Ricerca Ambientale, Roma, 113/2014, ISBN 978-88-448-0661-3

Rinaldi M., Surian N., Comiti F., Bussettini M., 2015. A methodological framework for hydromorphological assessment, analysis and monitoring (IDRAIM) aimed at promoting integrated river management. Geomorphology **251**: 122-136.

Rinaldi M., Amponsah W., Benvenuti M., Borga M., Comiti F., Lucìa, A., Marchi L., Nardi, L., Righini, M., Surian, N., 2016. An integrated approach for investigating geomorphic response to an extreme flood event: methodological framework and application to the October 2011 flood in the Magra River catchment, Italy . Earth Surface Processes and Landforms **41**, 835–846. doi: 10.1002/esp.3902.

Surian N., Righini M., Lucìa A., Nardi L., Amponsah M., Benvenuti M., Borga M., Cavalli M., Comiti F., Marchi L., Rinaldi M., Viero A., 2016. Channel response to extreme floods: insights on controlling factors from six mountain rivers in northern Apennines, Italy. Geomorphology **272**, 78–91. doi:10.1016/j.geomorph.2016.02.002.

Thompson, C., Croke, J., 2013. Geomorphic effects, flood power, and channel competence of a catastrophic flood in confined and unconfined reaches of the upper Lockyer valley, southeast Queensland, Australia. Geomorphology **197**: 156–169.

Wolman, M.G, Miller, J.P., 1960. Magnitude and frequency of forces in geomorphic processes. Journal of Geology **68**: 54–74.

5. GEOMORPHIC RESPONSE TO AN EXTREME FLOOD IN TWO MEDITERRANEAN RIVERS (NORTHEASTERN SARDINIA, ITALY): ANALYSIS OF CONTROLLING FACTORS

Margherita Righini[a], Nicola Surian[a], Ellen Wohl[b], Lorenzo Marchi[c], Francesco Comiti[d], William Amponsah[c,e], Marco Borga[e]

[a]Department of Geosciences, University of Padova, Italy; [b]Department of Geosciences, Colorado State University, Fort Collins, Colorado, USA; [c]CNR IRPI, Padova, Italy; [d]Faculty of Science and Technology, Free University of Bozen-Bolzano, Italy; [e]Department of Land, Environment, Agriculture and Forestry, University of Padova, Italy

Geomorphology, in revision

Abstract

A high-magnitude, low frequency flood affected two Mediterranean rivers (northeastern Sardinia, Italy) on 18 November 2013. This study investigates the response of channel reaches with minimal human impacts that have different morphological settings (i.e., alluvial, semi-alluvial and bedrock boundaries) with the aims of i) detecting the morphological effects of this large flood and ii) analyzing a range of morphological and hydraulic variables as potential controlling factors of channel response. Channel widening was the dominant geomorphic response observed and occurred with different magnitude among the study sub-reaches. Within individual sub-reaches, channel width increased from 1.1 to 6.2 times the pre-flood width. A significant trend in channel widening is observed, especially in alluvial sub-reaches where the narrowest channels were prone to enlarge more compared to the widest channels. Considerable erosion of hillslopes also occurred in confined and partly confined semi-alluvial and bedrock sub-reaches. Statistical analyses of the observed changes in channel width and a series of selected morphological and hydraulic controlling factors showed robust correlations, although stronger in alluvial sub-reaches, between lateral confinement and unit stream power, calculated based on channel width before the flood. Analysis and documentation of channel response and its variability through different morphological settings is crucial to provide a basis from which to forecast future river sensitivity to geomorphic adjustment to high-magnitude floods.

Introduction

The geomorphic effectiveness of a large flood can be defined as the amount of morphological change caused by the flood and the subsequent time required for the channel to recover (Wolman and Gerson, 1978). River response to infrequent, high-magnitude floods can vary significantly and a range of controlling factors might influence this variation, with important impacts on the surrounding environment and population (Baker, 1988). Impacts of extreme floods have long been studied and different aspects have been investigated. Previous works have focused on diverse aspects of geomorphic change during floods, including change in channel bed elevation (i.e., amount of erosion and deposition) (Hooke and Mant, 2000; Krapesh, 2011; Thompson and Croke, 2013; Hooke, 2016b), erosive and depositional features (Ortega, 2009), riverbank erosion processes and channel widening (Bowen, 2010; Krapesh, 2011; Grove, 2013; Buraas et al., 2014; Magilligan et al., 2015; Nardi and Rinaldi, 2015; Surian et al. 2016), stripping of floodplain surfaces (Nanson, 1986), channel straightening (Baker,1988; Knighton, 1998), destruction of controlling structures (Langhammer, 2010), and vegetation response (Hooke and Mant, 2000; Renofalt, 2007). The documented variability of extreme flood effects reveals that floods of similar magnitude can result in varying impacts at a site over time and between sites (Hooke, 2015), highlighting the fact that not all extreme floods generate major geomorphic effects (Wolman and Gerson, 1978; Costa and O'Connor, 1995).

In fact, Wolman and Gerson (1978) argued that the relative importance of individual events in changing landscape cannot be measured exclusively in terms of recurrence interval or magnitude because geomorphic effectiveness is driven by complex sets of interrelated factors (e.g., climate, topography, lithology). To better understand channel dynamics and to develop predictive tools for assessing the temporal and spatial variations of geomorphic effects of extreme floods, much research focused on investigation of possible driving forces to evaluate the ability of a flood to be geomorphically effective and its capacity to modify the channel morphology and forms over its duration (Wolman and Miller, 1960; Baker, 1977; Wolman and Gerson, 1978; Miller, 1990; Costa and O'Connor, 1995; Phillips, 2002; Magilligan et al., 2015). Several works focused mostly on hydraulic forces (e.g., discharge, velocity, shear stress, stream power, unit stream power, energy

expenditure) as main driving factors. However, Costa and O'Connor (1995) pointed out the limitations of considering only hydraulic forces as predictors of geomorphic response, and Buraas et al. (2014) argued that variations in the magnitude and spatial distribution of geomorphic responses to large floods reflect complex and interrelated factors. Some recent works confirmed that understanding and prediction of channel and floodplain response to a large flood should incorporate additional factors (Langhammer, 2010; Thompson and Crooke, 2013; Dean and Schmidt, 2013; Nardi and Rinaldi, 2015; Rinaldi et al., 2016; Surian et al., 2016). The inability to easily predict channel changes and to characterize the high spatial and magnitude variability in channel response to extreme floods as a result of the interplay of multiple hydraulic and geomorphic factors makes the investigation of potential controlling factors influencing flood geomorphic effectiveness particularly challenging.

This work deals with geomorphic response of two Mediterranean rivers in the Posada catchment (northeastern Sardinia, Italy) to an extreme flash flood that occurred in November 2013, considering a range of morphological and hydraulic variables as potential controlling factors. The main goals of the study are i) detecting the morphological effects of a large flood and ii) analyzing a range of morphological and hydraulic variables as potential controlling factors of channel response. The study was carried out on reaches with minimal human impact in terms of urbanization and infrastructure, allowing us to investigate as much as possible the river's natural behavior in response to the 2013 flood. Therefore, the wide variability in terms of channel morphology, specifically the downstream alternation of bedrock, semi-alluvial and alluvial channels, provides insight into different stream responses to the flood and a better understanding of the main driving variables in a range of morphological settings.

2. Study area

2.1 General setting of the area

The study area lies in the northeastern part of Sardinia, the second largest Italian island located in western Mediterranean Sea. The study reaches belong to the Posada River catchment (Fig.1), which covers a total area of 685 km^2 and ranges in

elevation from 1120 m to 0.8 m above sea level. The analyzed channel reaches were selected on the Posada River and on its main tributary (Mannu di Bitti River, 302 km^2 in terms of drainage area).

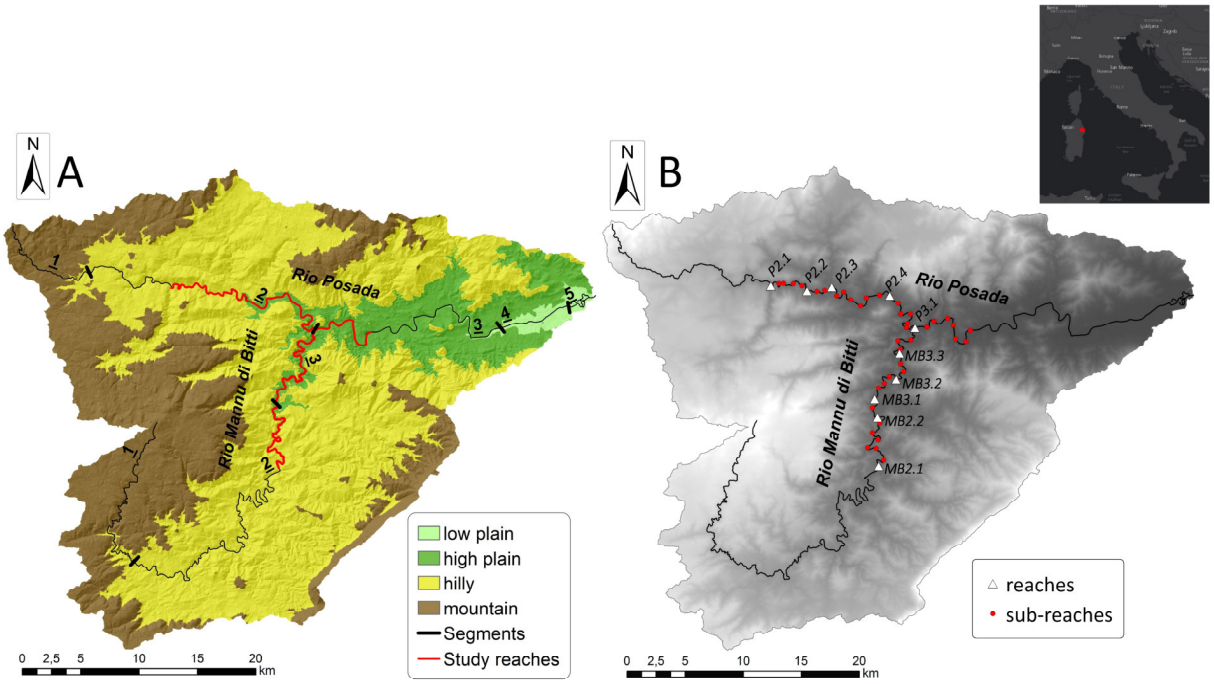

Figure 1. Location map of the Posada River catchment and the study reaches. Posada catchment: delineation of landscape units and segments (A); delineation of study reaches and sub-reaches (B).

The geology of the study area is characterized by the Paleozoic basement complex, which mainly consists of a complex of schists and Hercynian granite outcropping in the eastern part and south-western part of the island (Carmignani et al., 2001). These rocks were polydeformed and metamorphosed during the Variscan (Hercynian) Orogeny (Di Pisa and Oggiano, 2001). The folded Paleozoic basement is manly covered by Mesozoic dolostones and limestones and Quaternary deposits, consisting of sediments of continental origin, represented by alluvial pebbly deposits and mostly located in the Posada plain. The area is characterized by the Posada-Asinara Line (E-W direction), a crustal scale discontinuity that divides migmatites from the metasedimentary sequences affected by greenschist- to amphibolite-facies metamorphism (Carmignani et al., 2001; Frassi, 2014).

The morphology of the study area is particularly influenced by lithology. Rugged and steep mountain and hilly areas predominate in the southwestern portion, mostly characterized by Paleozoic metamorphic and magmatic rocks (granite,

ortogniess and shist), while the northeastern part of the basin is mostly gentle hilly and sub-plain areas characterized by limestone-dolomitic complex and alluvial Pleistocene formation composed of sands and well cemented pebbles. At the base of the carbonate complex, the plain is also made up of a formation of buried fans and recent alluvium deposited by the actual fluvial system (Ardau et al., 1999). The Posada catchment presents a dense drainage network characterized by minor streams that erode the Paleozoic basement, creating typical V-shaped valleys. The study rivers are predominantly single-threaded and flow through narrow canyons upstream and moderately wide alluvial valleys downstream.

The climate is Mediterranean, characterized by dry (May–September) and wet periods (October–April) (Delitala et al., 2000). Mean annual precipitation is highly variable, with a mean annual rainfall of 700–1000 mm (De Waele et al., 2010). Accordingly with analyses of the extreme rainfall regime in Sardinia (Bodini et al., 2010), the study area is comprised in the region characterized by the highest frequency of heavy rainfall events. The occurrence of daily and sub-daily intense rainfall in the area is due to the interaction between high and steep mountains near the sea on the central and South-east coast and warm and moist atmospheric currents from Africa (Bodini et al., 2010). Not surprisingly, the Posada basin was affected in the past by several extreme flood and flash flood events, like the 1951 flood and the more recent 2004 and 2008 floods (Bodini and Cossu, 2010; De Waele 2008). These floods caused several fatalities and heavy damages to buildings, infrastructures, economic activities and ecosystems.

2.2 The extreme flood of 18 November 2013

On 18th November, 2013, an extra tropical cyclone passed over Northern Africa and crossed the western Mediterranean Sea, developing slow-moving embedded thunderstorm complexes, increasing its potential instability because of the relatively high sea surface temperature (Chessa et al., 1999; Niedda et al., 2015). Rainstorms caused by this mesoscale convective system in eastern Sardinia lasted approximately 12 hours. A noticeable characteristic defined of the precipitation event was its organization into well-defined banded structures (Amponsah et al., 2016). The steadiness of these rainbands led to highly variable precipitation accumulations,

with point maximum rainfall accumulations exceeding 500 mm, corresponding to recurrence period exceeding 400 years. In the Posada catchment, maximum point rainfall amounts were about 420 mm, corresponding to recurrence periods exceeding 300 years. The rainstorm temporal structure features two main cloudbursts: from 7am to 1pm CET (with maximum intensity at 10-12am) and from 1pm to 7pm CET (with maxima between 2-4 pm). The highest rainfall intensities, with point hourly peaks exceeding 100 mm/hr, were observed during the second period. The rainstorm caused widespread flooding, severe damages to urban areas and road network, and caused 16 fatalities in the whole island (Niedda et al., 2015).

3. Methods

The analysis focused on 22-km-long and 18-km-long reaches of the Posada and Mannu di Bitti Rivers, respectively, where major channel response occurred. The study was carried out applying an integrated approach (Rinaldi et al., 2016) to analyze i) geomorphic response magnitude and patterns, ii) the impact of the flood on riparian vegetation and the role of vegetation in enhancing or inhibiting channel adjustment, iii) the hydrological parameters (i.e., the estimation of rainfall and the assessment of peak discharge), and iv) a series of selected morphological and hydraulic controlling factors.

3.1 Geomorphic analysis

Post-flood field surveys were performed in six channel reaches with length ranging from 1.7 to 6 km and a channel gradient varying from 0.3% to 2.6%. The observations included: (i) qualitative assessment of the main morphological channel characteristics, (ii) analysis of geomorphic flood effects (i.e., planimetric and vertical changes, bank and island erosion), (iii) sampling surface sediment and (iv) inventory of artificial structures (e.g., bank protections).

The quantitative analysis of the geomorphic features (i.e., channel width, channel slope, alluvial plain and island extension, lateral confinement and channel sinuosity) and channel changes were performed through the use of a geographic

information system (GIS) software (ArcGIS 10.3). The visual skills-based interpretation procedure applied to a set of high resolution pre- and post-flood satellite images (i.e. pixel size from 0.5 to 1 m); besides, a digital elevation model with a 10 m spatial resolution and topographic maps at 1:10000 scale were used. The analysis of the pre flood satellite images taken in 2011 was carried out using data stored in the Basemap gallery available in ArcGIS Explorer Desktop by the World Imagery Service. The post flood images taken in April 2014 were WorldView-2 pan-sharped 4 band imageries with a spatial resolution of 50 cm and were purchased *ad hoc* for this study. Furthermore, Google Earth satellite imageries were employed in some cases, as a supporting tool for the more difficult visual interpretation features. The analysis aimed at providing data on (i) general setting of the river's morphological conditions and delineation of the channel in different spatial units of decreasing hierarchy, (ii) channel morphological characteristics and features pre and post flood, and occurrence and magnitude of channel changes.

In the first step, a subdivision of the Posada catchment into physiographic units and a segmentation of the river network into homogeneous reaches was carried out, based on a hierarchical spatial framework (Rinaldi et al., 2016). Distinction of homogeneous stream reaches took into account channel lateral confinement, channel morphology, artificial features, and relevant discontinuities in terms of flow and sediment discharges. Reaches were further partitioned in sub-reaches according to the approach of Ferencevic and Ashmore (2012). The sub-reach scale was adopted for the analysis of the variability in channel response within the same stream.

In the second step, the analysis addressed the interpretation and the quantification of the following morphological characteristics, which are crucial to better understand the processes responsible for channel changes: channel area, alluvial plain area, island area, channel centerline, channel slope, lateral confinement, channel sinuosity and channel bed type. The channel area was digitized on pre and post satellite images within ArcGIS 10.3, referring to the active-channel area, defined as the portion of the river corridor relatively free of vegetation (unvegetated or sparsely vegetated bars), that conveys most of the water and sediment during high flow (Czuba et al., 2012). Alluvial plain area included present floodplain and low terraces (i.e., surfaces that can be some meters higher than the

floodplain and can be infrequently flooded) (Surian et al., 2016). Islands were digitized and identified as in-channel surfaces covered by shrub or woody vegetation. The channel centerline was defined by a semi-automated process extracting an equidistant line from channel boundaries calculated every meter. A semi-automated approach was also employed to define channel slope based on DEM analysis by the Hydrology tool available in ArcGIS. Lateral confinement, defined as the natural channel lateral constraint reflecting channel potential lateral mobility, was determined considering two parameters: the confinement degree, which is the percentage of channel banks directly in contact with hillslopes or ancient terraces (Brierley and Fryirs, 2005) and the confinement index (*CI*), defined by the ratio between the alluvial plain width and the channel width (Rinaldi et al., 2013). These parameters allowed us to define three valley settings: confined, partly confined and unconfined reaches and sub-reaches as in Rinaldi et al., 2013. Channel sinuosity – measured as sinuosity index (Si) based on the axis of the overall planimetric river course - was considered as being representative of the planimetric pattern of the bankfull channel, which could have an influence on bank erosion processes and therefore on widening (Nardi and Rinaldi, 2015).

The alternation over short distances of bedrock and alluvial channels (Fig. 2) made it necessary to split the dataset into three subsets based on the percentage of exposed bedrock: bedrock (*B*), semi-alluvial (*SA*) and alluvial (*A*) sub-reaches. We defined bedrock channels as the reaches in which exposed bedrock ranged from 50 to 100%, including streams covered by an alluvial veneer typically largely mobilized during high flow (Tinkler and Wohl, 1998). The definition of Tinkler and Wohl (1998) was integrated with that put forward by Meshkova et al. (2012) as well as by a classification specifically developed for this case of study. In fact, we classified both bedrock constrained (i.e., channel laterally confined by competent bedrock but having an alluvial bed) and bedrock confined (i.e., channel with a rocky bed but with alluvial sidewalls) with exposed bedrock ranging from 50 to 100% (i.e., spatial continuity of exposed bedrock within the sub-reach) as “bedrock sub-reaches”. Based on the statistical distribution of the percentage of exposed bedrock within the dataset, we considered the mixed alluvial–bedrock sub-reaches ranging from 10 to 49% of exposed bedrock as “semi-alluvial sub-reaches” (i.e., spatial discontinuity of exposed rock confined or constrained or presence of rock outcrops). Finally, we

considered “alluvial sub-reaches” those channel portions without any evidence of bedrock or with very sparsely exposed (< 10% in length) and mainly related to the presence of isolated bedrock outcrops. The non-parametric Kruskal-Wallis test of variance was used to determine the morphological characteristics of each channel bed type subset.

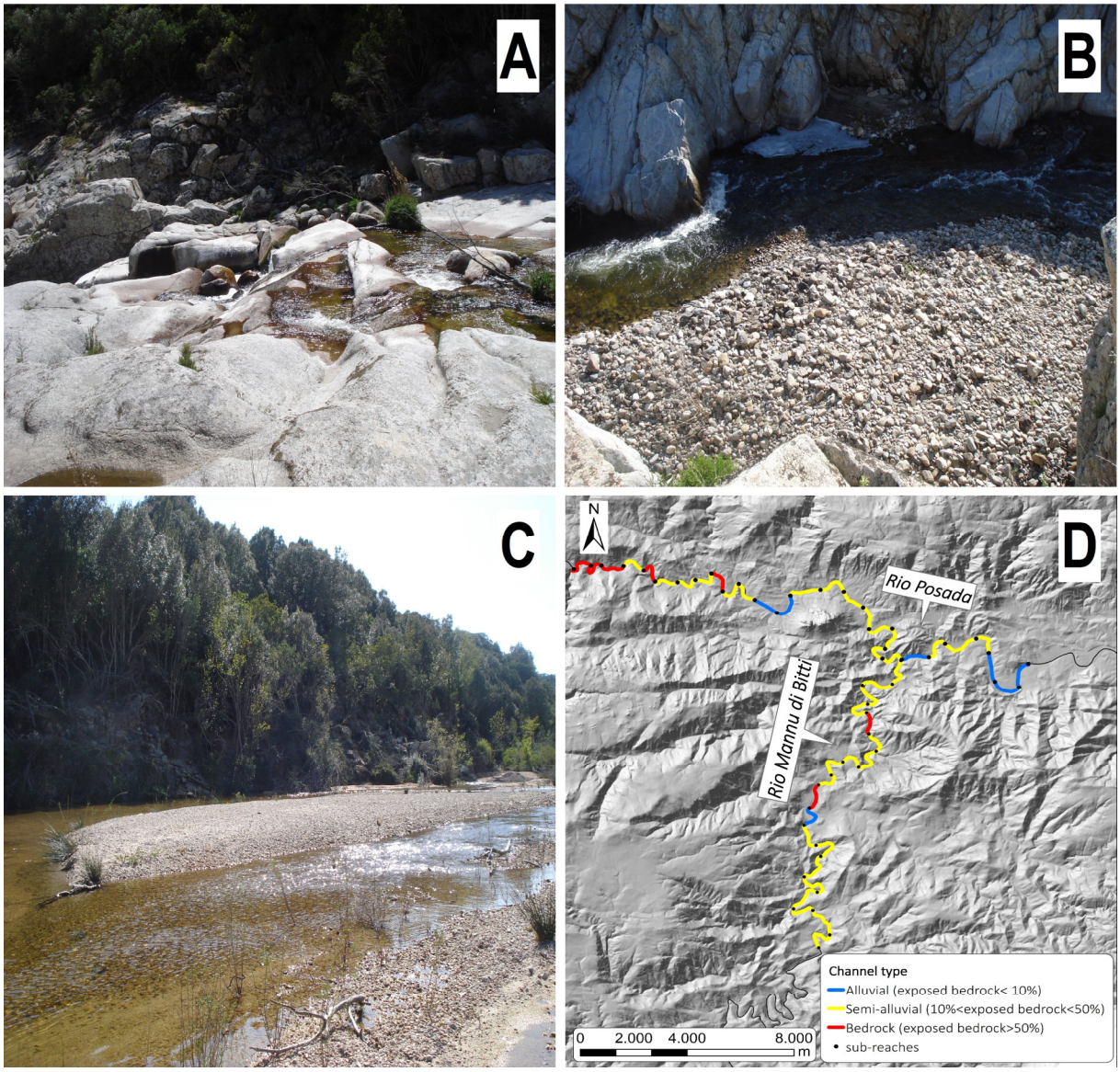

Figure 2. Examples of bedrock (A), semi-alluvial (B) and alluvial (C) sub-reaches. (D) Channel bed type distribution within the Posada and Mannu di Bitti Rivers.

In the third step, the study aimed at the analysis and quantification of morphological channel changes in response to the November 2013 flood. The analysis mainly focused on planimetric changes within the channel, the riparian zone and across the whole floodplain. Channel changes were dominated by channel widening of the overall channel corridor and the reactivation of parts of the pre-event

floodplain. Channel widening was not simply considered as channel lateral expansion, but it might be interpreted as different processes including i) bank erosion and retreat; ii) overbank deposition of bedload material on the floodplain; iii) in-channel island stripping and erosion; iv) widening of floodplain surfaces (i.e., of valley bottom); and v) erosion of top soil and riparian vegetation, specifically in bedrock channels. Field evidences of channel bed aggradation/incision are limited, and no reliable measurements of bed-level changes are available. Channel width changes were quantified through the comparison of pre and post-flood satellite images. The channel width was calculated dividing channel area by the length of the sub-reach, and the quantification of channel widening was expressed in terms of width ratio (Wr); i.e., channel width after/channel width before the flood (Krapesch et al., 2011). However, this kind of analysis was affected by errors due principally to visual skills-based interpretation procedure and digitization. Nonetheless, errors were negligible compared to the rate of changes that were measured.

3.2 Vegetation analysis

Existing research demonstrates that vegetation can be an important control on river form and activity and previous works have pointed out the significant role of the valley-bottom vegetation during a flood (Hickin, 1984; Baker, 1988; Thorne, 1990; Hickey and Salas, 1995; Abernethy and Rutherfurd, 2000; Simon and Collison, 2002; Renofalt, 2007; Gurnell et al., 2012).

The main aim of this analysis was to determine the flood impact on woody vegetation (i.e., vegetation removal) and, conversely, the role of woody vegetation on geomorphic adjustment. The analysis addressed the areal quantification and the assessment of i) the pre and post flood spatial distribution of the riparian woody vegetation (i.e., areas of prevailing woody/shrub vegetation adjacent to the active channel within the floodplain), ii) woody/shrub islands and iii) areas covered by herbaceous or unvegetated areas (i.e., areas of prevailing grassland, crops, pastures and artificial surfaces within the floodplain). A supervised classification was performed in ENVI 5.0 on post flood satellite images to quantify location and extent of woody vegetation. Training data were collected to classify the image into three cover types: water, sediment/rock, shrub/woody vegetation. To ensure the optimal

accuracy of the classification result, the confusion matrix error was calculated at the reach scale to assess the accuracy of the classification by comparing results with ground truth information and reporting the overall accuracy, producer and user accuracies. The analysis of pre-flood woody vegetation was carried out in GIS applying a backwards semi-automated approach using as a starting point the output of post-flood supervised classification because of the lack of pre-flood images suitable for ENVI application. Water and sediment/rock vector features obtained from post-flood image classification were subtracted from the floodplain vector feature obtained by user interpretation on pre-flood image. The latter output was intersected with the post-flood woody land cover feature and the pre flood riparian and island in-channel woody vegetation were obtained. The quantification of the obtained woody vegetation cover was carried out finally at the sub-reach scale and expressed in terms of woody vegetation cover percentage. Therefore, the estimation of the effect of the flood on the woody vegetation was expressed in terms of loss of woody vegetation employing the vegetation change index (I_v); i.e., the ratio between the post-flood and the pre-flood woody vegetation cover percentage. Assessment of land cover classes as possible controlling channel response was performed by simple regression analysis.

3.3 Hydrologic analysis

The hydrological analysis performed to support the assessment of the geomorphic changes caused by the flash flood on November 2013 in the Posada River basin was based on a threefold approach (Borga et al., 2008): i) radar-based estimation of rainfall fields; ii) spatially-detailed assessment of peak discharge in ungauged streams across the river network, by means of post-flood field surveys and application of the Manning-Strickler equation under assumption of uniform flow; and iii) application of a rainfall-runoff model to check the consistency of rainfall and discharge data.

The hydrological analysis involved, in addition to the Posada River basin, the neighbouring Cedrino River basin (Amponsah et al., 2016), located south of the Posada River basin. Considering these two basins allowed us to extend the hydrological analysis to the two largest basins hit by the flood of 18th November 2013

and to exploit the flood hydrograph recorded in a downstream cross section of Cedrino River for the calibration of the hydrological model. Calibration parameters were used for the application of the hydrological model to the ungauged catchments where peak discharges had been estimated by means of post-flood field observations. Such a transposition of calibration parameters enabled us to verify the consistency of model calibration at the scale of tributaries of the main rivers. The rainfall-runoff model was then applied to assess peak discharge in representative cross section of the channel sub-reaches where the geomorphic changes caused by the flood were studied, permitting us to compute stream power, similarly to what presented in Surian et al., (2016).

3.4 Controlling factors

We investigated the influence and the role of a range of controlling factors on the channel responses and morphological adjustment variability within the channel and the floodplain. Both morphological and hydraulic factors were considered as possible driving forces generating changes at the sub-reach scale. Channel slope (S), confinement index (*CI*), sinuosity index (Si), and exposed bedrock percentage were investigated as possible morphological controlling factors. Also, three hydraulic controlling variables were considered, representing factors related to the flood energy available to perform geomorphic work: cross sectional stream power (Wm^{-1}), expressed as $\Omega = \gamma QS$, where γ (kg m^3) is the specific weight of water, Q (m^3 s^{-1}) is the peak discharge and S (mm^{-1}) is channel slope; and unit stream power (Wm^{-2}), obtained by dividing the cross sectional stream power by channel width W_b (m) measured before the flood ($\omega=\Omega/W_b$) and after W_a (m) the flood ($\omega=\Omega/W_a$). A first step of the analysis consisted of performing simple regressions between channel planimetric response (i.e., channel widening expressed as width ratio and floodplain widening or hillslope erosion) and individual morphological and hydraulic variables on the entire dataset at the sub-reach scale. In the second step, simple regression was performed considering the same variables on different sub-reaches grouped as a function of channel bed type (i.e., bedrock, semi-alluvial and alluvial channel). Results of simple regressions on the whole dataset and on the study reaches were

expressed in terms of values of R squared and *p-value*. We used the Software R (version 3.2.3) for all the statistical analyses.

4. Results

4.1 Spatial units delineation and morphological sub-reaches characterization

The entire catchment has been divided into four different physiographic units mainly based on the topographic, geologic and geomorphologic characteristics (Fig. 1A). Landscape unit 1 consists of the mountain areas (mountain areas up to 1200 m a.s.l.); landscape unit 2 consists of hilly areas (mountain areas <600 m a.s.l. and characterized by dolostones and limestones); landscape unit 3 corresponds to a high plain characterized by Pleistocene and recent alluvial deposits; and landscape unit 4 consisted of low plain area characterized by actual fluvial and marine deposits confined to the most downstream portion of the catchment near the river mouth. Based on the intersection of the main streams with the landscape units, five and three segments have been distinguished for the Posada and the Mannu di Bitti Rivers, respectively. A total of 10 preliminary reaches have been identified by analyzing the valley setting confinement in more detail.

In order to define sub-reaches, water surface slope and the presence of hydrologic discontinuities (i.e., main river tributaries) were used as key parameters. Water surface slope was calculated for several longitudinal distances (100, 500, 700, 1000, 1500 m) along the main streamflow identified on the DEM. Finally, a total of 48 sub-reaches have been identified, 28 for the Posada River and 20 for the Mannu di Bitti River, with a length ranging from 750 to 1200 m (Fig. 1B). An alphanumeric code has been used to identify segments and reaches and sub-reaches where the letter identifies the study river, the first number (increasing in the downstream direction) indicates the segment, the second number the reach, and the third the sub-reach (Nardi and Rinaldi, 2014). The study sub-reaches reflect a representative range in terms of channel width, channel slope, lateral confinement, channel sinuosity and percentage of exposed bedrock (Table1). The minimum, maximum and average pre-flood channel widths of the 48 study sub-reaches are 9.3, 142 and 22 m, respectively. Channel slope ranges from a minimum of 0.1% to a maximum of 3.5%,

with an average of 0.9%. The 48 sub-reaches displays a wide variability in lateral confinement including unconfined, partly confined and confined sub-reaches, with values of confinement index (*CI*) ranging between 1 and 6.7, with an average of 2.9. The average of the sinuosity index (Si) is 1.6, varying from a minimum of 1 to a maximum of 3.6. The wide variability in channel and valley morphological characteristics, especially in the alternation of bedrock, semi-alluvial and alluvial channels, and the consequently different channel dynamics, led us to investigate these three classes separately (Fig. 2) (Table 1).

Sub-reaches *(n=48)*	**Alluvial** *(n=7)*				**Semi-alluvial** *(n=34)*				**Bedrock** *(n=7)*			
	min	*max*	*mean*	*SD*	*min*	*max*	*mean*	*SD*	*min*	*max*	*mean*	*SD*
Morphological characteristics												
W_b(m)	14.8	141.0	47.3	47.8	9.3	30.6	18.3	5.1	12.2	17.6	14.9	1.7
W_pb(m)	75.7	274.5	136	71.1	15.6	157.9	52.1	33.4	16.60	58.2	28.4	14.8
Confinement index (*CI*)	1.9	6.7	4.2	2	1	6.7	2.8	1.5	1.1	4.8	2	1.3
Slope (mm^{-1})	0.001	0.006	0.01	0.004	0.001	0.02	0.007	0.005	0.003	0.04	0.02	0.01
% exposed bedrock	0	7.4	2.7	3.1	13.3	42.1	27.5	9.4	51.6	100	76.7	23.8
Sinuosity index (Si)	1	2	1.3	0.4	1.1	3.6	1.4	0.7	1.1	2.4	1.5	0.5
pre-flood island area (m^2)	0	4501	1238.3	1715	0	26395	1703.6	4579.4	560.5	2828	1253	779.6
Pre-flood woody area (%)	40	100	70	20	40	100	70	20	50	100	70	20
Hydraulic parameters												
Q_{peak}(m^3s)	1454	3724	2812	1110.4	1296	3680	1980	606.6	620	2187	1438	537.4
Ω (Wm^{-1})	53485	306623	156301	94061.6	55679	420476	129472	66066.8	14912	279733	224456	130825.3
ω_{before} (Wm^{-2})	379	13997	6490	5214.9	3598	28784	7924	4799.4	509	18435	15593	28783.5
ω_{after} (Wm^{-2})	342	30301	1678	1096.8	943	8889	4538	1291.4	162	5073	2349	2655.5
Morphological changes												
W_r	1.1	6.2	3.7	2	1.8	5.6	3.4	1.1	2.1	6.2	3.5	1.3
W_a(m)	70.9	156.5	104.7	27.2	28.5	132.9	60	21	37.7	76.1	51.3	12.8
W_pa(m)	89	277.3	156.7	64.9	47.8	195.5	77.4	32	-	-	-	-
right bank retreat (m)	0.2	11.5	4.7	4.5	0.3	37.5	9.6	7.8	-	-	-	-
left bank retreat (m)	0	36.7	9.0	12.7	0	31	12.9	7.9	-	-	-	-
post-flood island area (m^2)	0	16097	5274	600.8	0	20605	5582	5150.8	0	4857	1760	1908.5
Island area changes (m^2)	-2024.5	16097	4035.9	6450.4	-13845	19.840	38.53	6269	-1113	2145.1	505.9	1352.5
I_v	0.1	0.5	0.3	0.2	0.03	0.5	0.3	0.1	0.02	0.3	0.1	0.1

Table 1. Summary of main morphological characteristics and principal parameters to evaluate channel changes in terms of minimum, maximum, mean and standard deviation (*SD*) for the channel type sub-sets at the sub-reach scale. Code: W_b: pre-flood width; W_a: post-flood width; W*r*: width ratio; W_pb: pre-flood alluvial plain width; W_{pa}: post-flood alluvial plain width; island area changes (negative values indicate island erosion, while positive values indicate island formation); Q_{peak}: peak discharge; Ω: cross-sectional stream power; ω_{before}: unit stream power using pre-flood channel width; ω_{after}:unit stream power using post-flood channel width; I_v: vegetation change index.
Note: W_{pa} and right/left bank retreat were not assessed in bedrock channels since vegetation removal was the dominant process with no significant change in channel and floodplain morphology.

Bedrock sub-reaches (B)

Bedrock sub-reaches are defined as those bedrock constrained or confined channels with exposed bedrock ranging from 50 to 100% (Tinkler and Wohl, 1998; Meshkova et al., 2012). Within the 48 study sub-reaches, 5 and 2 bedrock sub-reaches were identified in the Posada and Mannu di Bitti Rivers, respectively, with an average value of exposed bedrock percentage of 76.7% (Fig. 3A). They are mainly distributed in the upstream reaches (P2.1 and P2.2) in the Posada, and in the middle portion of the Mannu di Bitti (MB3.1 and MB3.2) (Fig. 2D). Bedrock sub-reaches are characterized by a single flow path and sinuous and meandering planform with similar value of pre-flood channel width, with an average value of 14.9 m (Fig. 3B). The Posada River featured a bedrock step-pool system (bedrock confined and constrained) sub-reach upstream (P2.1.1), whereas the other classified as 'bedrock channel' exhibit bedrock confined (P2.1.3, MB3.1.1, MB3.2.3) or constrained (P2.1.2, P1.1.5, P2.3.1). The results of the Kruskal-Wallis test show significant differences (*p-value*<0.05) in the channel confinement distribution among the three subsets. As reported in Figure 3C, and as expected, most of the bedrock sub-reaches are confined and a few of them are partly confined, with an average value of confinement index equal to 2. It is evident that bedrock sub-reaches correspond to the steepest ones, with an average channel slope of 2%, with the progressive lower slope sub-reaches having less exposed bedrock and variable degrees of alluviation. The channel pattern varies from sinuous to meandering showing a sinuosity index of 2.1 (Fig. 3D and Fig. 3E) (Table 1).

Semi-alluvial sub-reaches (SA)

Semi-alluvial sub-reaches were identified by analyzing the frequency of exposed bedrock distribution within the sub-reach population, and observing whether there were any significant breaks in the distribution. The frequency histogram showed two evident breaks at 10% and 50% of exposed bedrock, selected as valid thresholds to distinguish semi-alluvial sub-reaches. They are characterized by a more discontinuous spatial distribution of confined or constrained exposed bedrock or presence of bedrock outcrops. A total of 34 sub-reaches were classified as semi-alluvial; 18 and 16 for the Posada and Mannu di Bitti Rivers, respectively (Fig. 2D), with an average value of exposed bedrock of 27.5% (Fig. 3A). The semi-alluvial

channels show a fair variability in the pre-flood channel width, with an average value of 18.3 m (Fig. 3B). As shown in Figure 3C, semi-alluvial sub-reaches present a wider variability in lateral confinement, including most of the partly confined channels, with 2.8 as an average value of confinement index. The semi-alluvial sub-reaches also display an average channel slope of 0.7% and a sinuosity index of 1.7, varying the channel pattern from sinuous to meandering (Fig. 3D and Fig. 3E) (Table 1).

Alluvial sub-reaches (A)

Alluvial sub-reaches are characterized by recent alluvial sediments (from coarse gravel to large cobble), without any evidence of bedrock or with very sparsely exposed bedrock covering less than 10% and mainly related to the presence of isolated bedrock outcrops. A total of seven alluvial sub-reaches were identified, mainly distributed within the middle and the downstream portion of the Posada River and principally in the high plain landscape unit (P2.3 and P3.1 reaches). In the Mannu di Bitti River only one sub-reach located in the upstream part of the stream close to the confluence with an important tributary was classified as “alluvial” (Fig. 2D). The value of exposed bedrock for this channel bed type is very low, averaging 2.7%. Figure 3B shows a wider variability of pre-flood channel width for the alluvial sub-reaches, with an average value of 47.3 m (Table 1). Alluvial sub-reaches are characterized by partly confined and unconfined conditions, with all confinement index values greater than 2 and an average value equal to 4.2 (Fig. 3C). The alluvial sub-reaches also exhibit a lower value of channel gradient, with an average channel slope of 0.6% and a sinuosity index of 1.3, varying the channel pattern from straight to meandering (Fig. 3D and Fig. 3E) (Table 1).

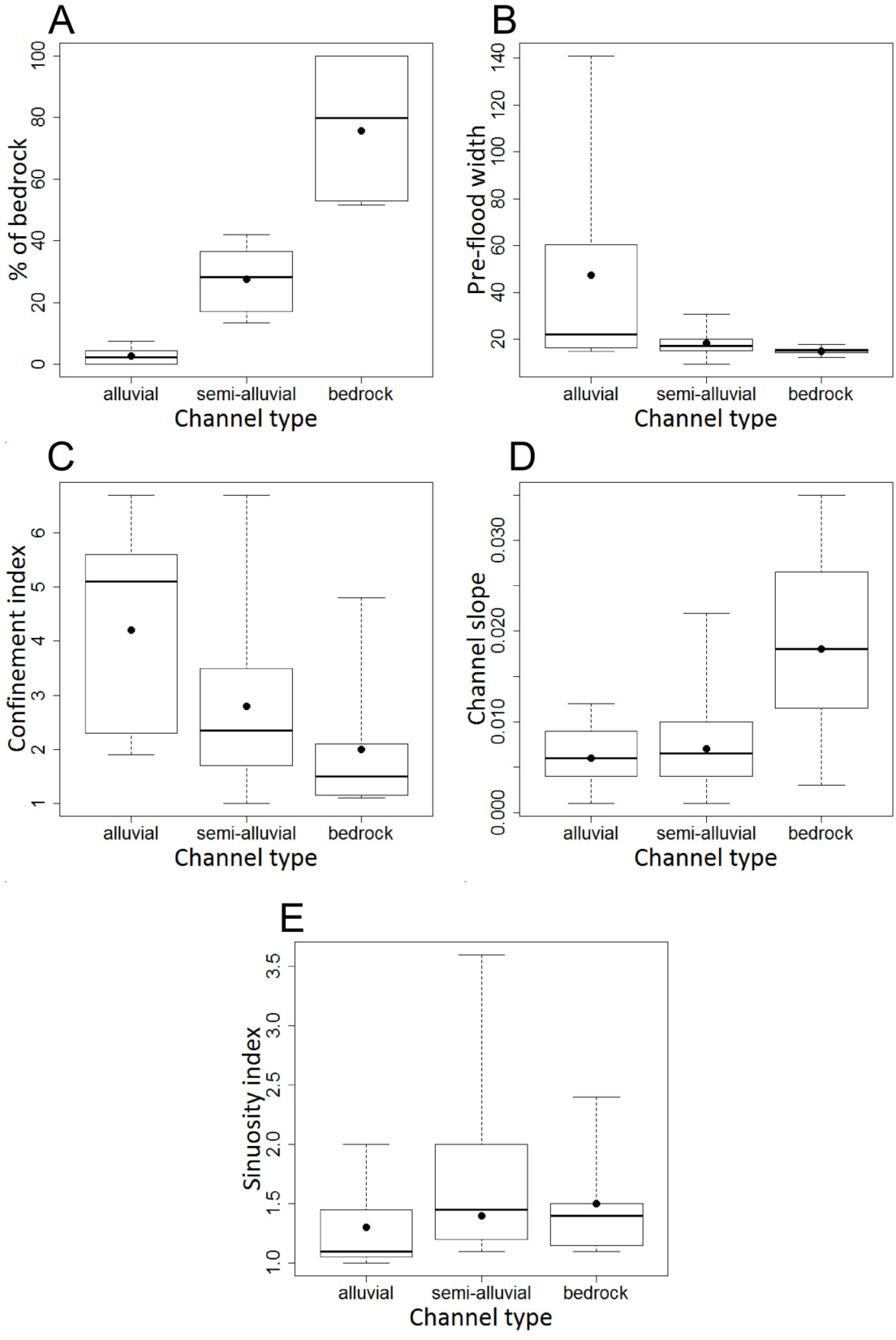

Figure 3. Boxplot of percentage of exposed bedrock (A); pre-flood channel width (B); confinement index (C); channel slope (D); and sinuosity index (E) for channel bed type subsets. IQR is the interquartile range represented by the box, upper and lower whiskers represent maximum and minimum values, respectively; dots represent the mean values; the horizontal line represents median values

4.2 Channel and floodplain changes

Overall, 19 % and 11 % of the length of the Posada and Mannu di Bitti Rivers have been affected by geomorphic changes, respectively. Flood effects were observed within the channel and across the floodplain by erosion of banks and of valley slopes. Channel widening occurred through lateral erosion (Fig. 4) and, as confirmed also by field observations, depositional processes were negligible.

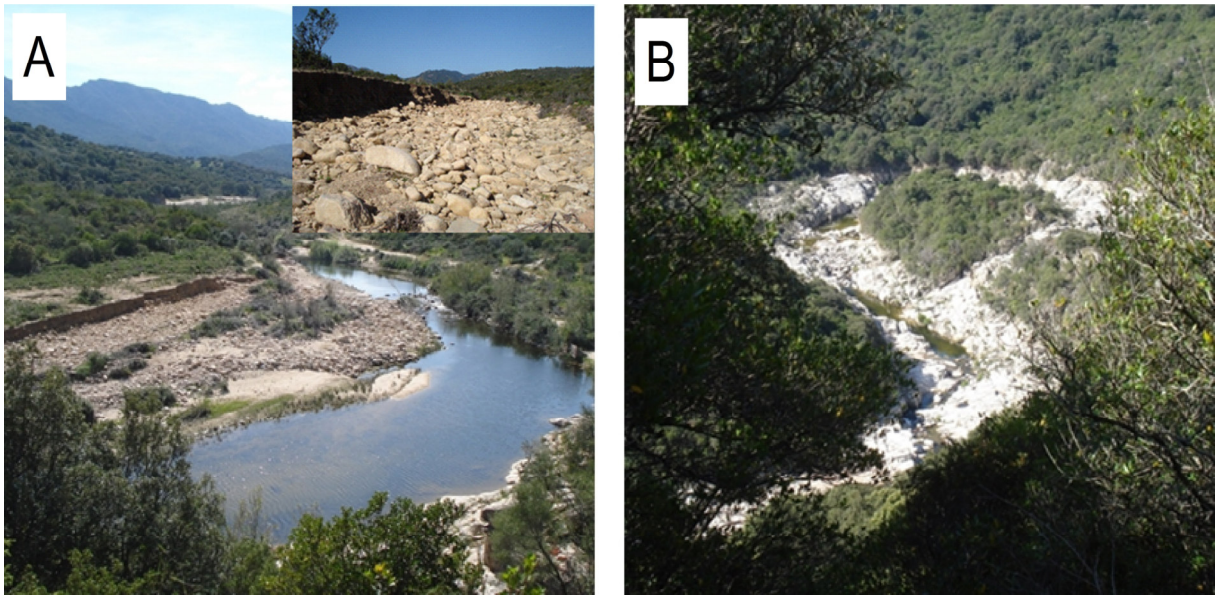

Figure. 4. Alluvial channel where widening was dominated by lateral erosion of fine-grained floodplain surfaces down to basal gravels and cobbles (A). Bedrock channels where floodwaters followed the most direct path downstream, removing topsoil and woody vegetation (B).

The channel widening affected all the 48 study sub-reaches (Table 1) and the values of width ratio ranged between 1.1, observed in sub-reach P3.1.7, and 6.2, observed in sub-reaches P3.1.1 and MB3.1.1. Changes in channel width were more pronounced in the middle portion of the study reaches, and at the confluence between the Mannu di Bitti and the Posada rivers. A decreasing variability in channel widening was recorded from the alluvial, to the semi-alluvial and bedrock sub-reaches (Fig. 5A). In bedrock sub-reaches the width ratio ranges from 2.1 (from a pre-flood channel width of 17.6 to 37.7 m) to 6.2 (from a pre-flood channel width of 12.2 to 76 m) (Fig. 5A) (Table 1). Bedrock confined channels featured lower values of average width ratio, i.e. 3 compared to the average value of bedrock constrained

channels, i.e., 4.5. Whereas bedrock confined and constrained sub-reach feature the lower value in width ratio, i.e. 2.1.

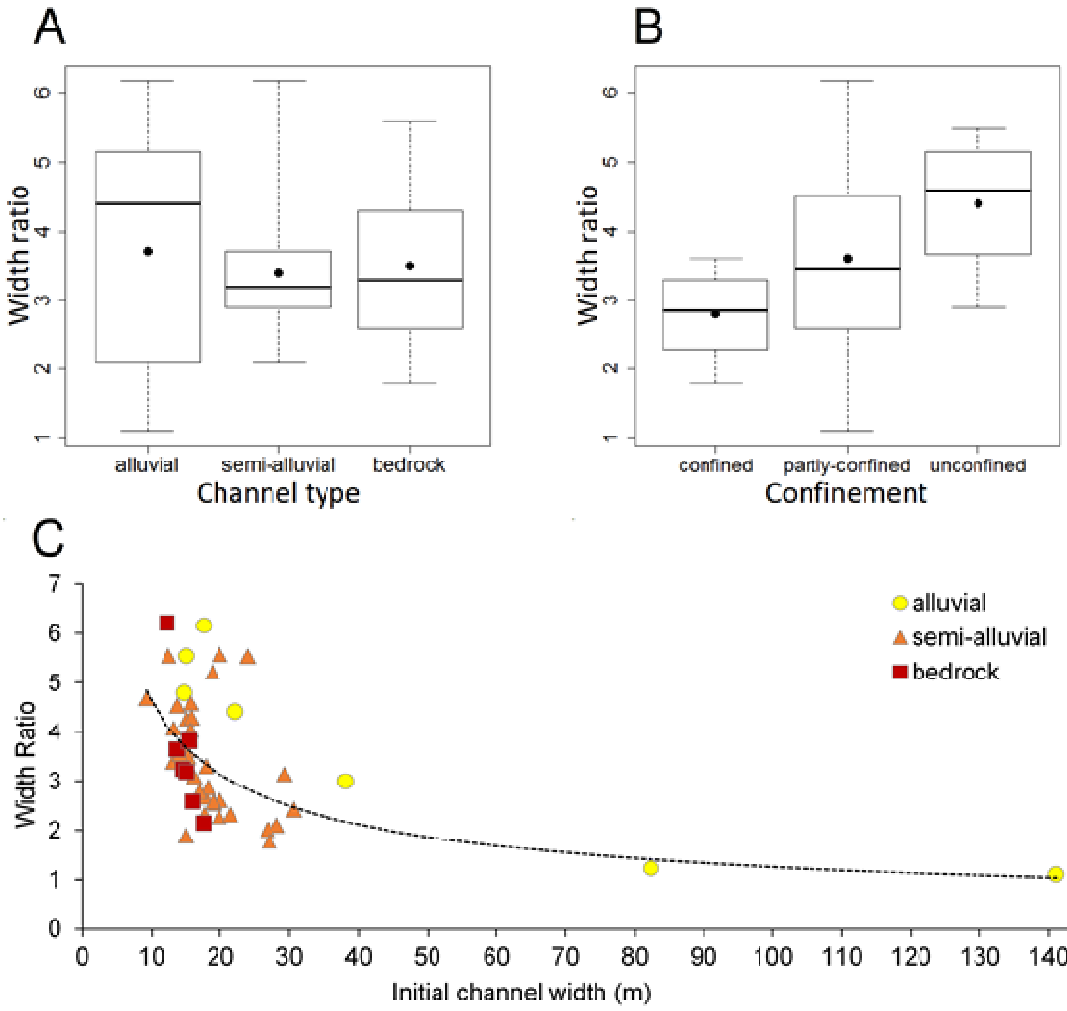

Figure 5. Boxplot of width ratio within channel type sub-set (A) and confinement class (B). IQR is the interquartile range represented by the box, upper and lower whiskers represent maximum and minimum values, respectively; dots represent the mean values; the horizontal line represent median values. Width ratio magnitude against pre-channel width (W_b) for channel type sub-sets (C).

As expected, the higher values of width ratio within the bedrock class occurred in the partly confined sub-reaches rather than in the confined ones (Figs.5B and 6A). In semi-alluvial sub-reaches, the width ratio varies from 1.8 (from a pre-flood channel width of 27.1 to 48.2 m) to 5.6 m (from a pre-flood channel width of 19.9 to 111.1 m) (Fig. 5A) (Table 1). The higher values of width ratio within the semi-alluvial class occurred in unconfined and partly confined sub-reaches (Figs. 5B and 6B) (Table 1). In alluvial sub-reaches, the width ratio varies from 1.1 (from a pre-flood channel width

of 141 to 156.5 m) to 6 (from a pre-flood channel width of 17.6 to 108.3 m) (Figs. 5A and Fig. 6C) (Table 1).

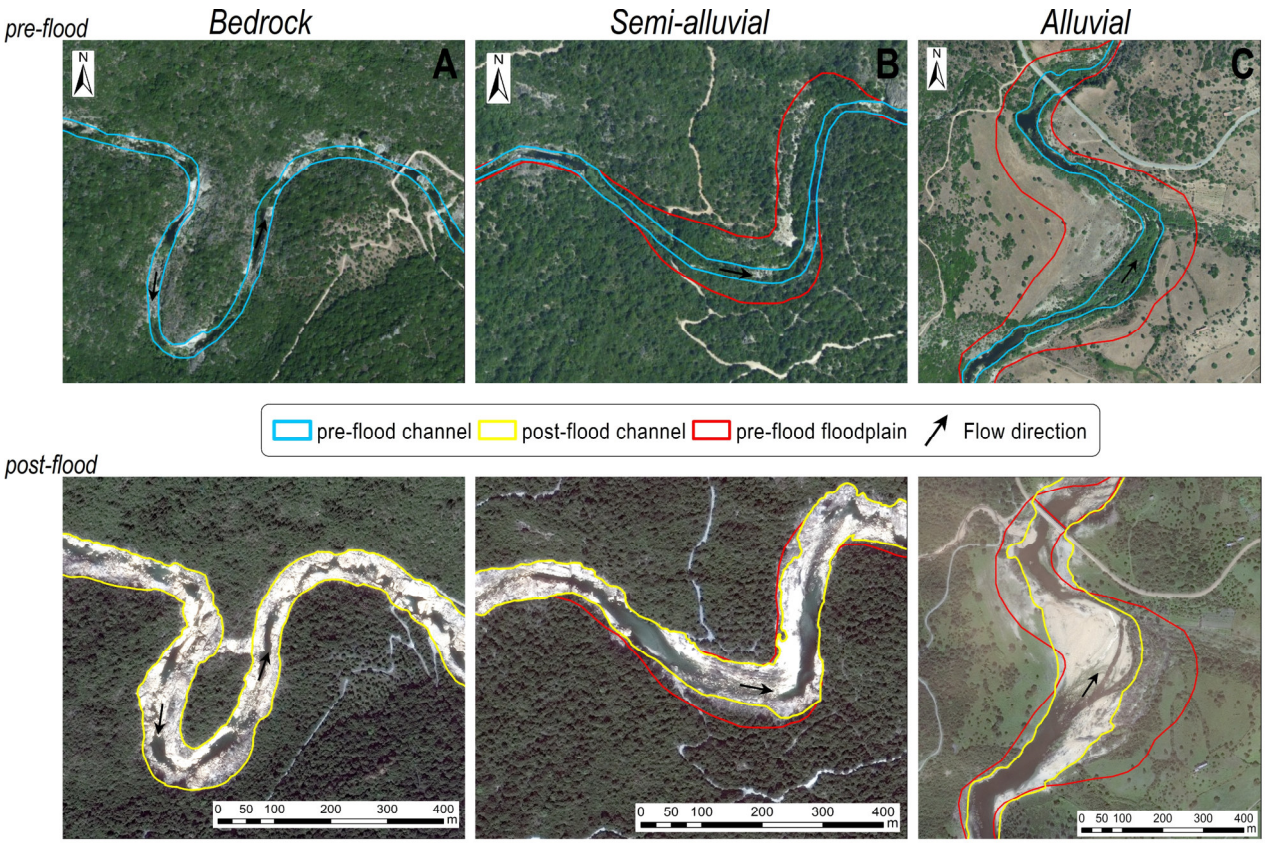

Figure 6. Pre and post flood satellite images for channel type subset: bedrock (A), semi-alluvial (B) and alluvial (C).

Riverbank retreat in the Posada and Mannu di Bitti ranges from no erosion up to 36 and 37 m, respectively (Table 1). An overview of the initial channel width and the corresponding channel response in terms of channel widening was carried out by plotting the widening magnitude against the pre-flood channel width, resulting in an inverse relationship (Fig. 5C). The findings revealed two different behaviors of channels affected by the flood, depending on the initial width. The plot shows large variability in the width ratios in the narrower sub-reaches (i.e. pre-flood width 10-20 m), while in wider sub-reaches (pre-flood width up to 30 m), width ratios were < 3. This trend is particularly evident in the alluvial sub-reaches where the higher width ratios were found in the narrower pre-flood channels (10-20 m), while the lower width ratio occurred in the larger pre-flood channels (up to 30 m). The same trend was slightly observed in the semi-alluvial sub-reaches, while in the bedrock channels a

large variability in width ratio is shown, although the initial channel width is quite uniform (ranging from 12.2 to 17.6) (Fig. 5C).

In most of cases the widening was not limited by the lateral extent of the erodible corridor. The floodplain widened at the expenses of hillslope toes, in particular in confined and partly confined sub-reaches, which implies that widening ratios exceed the confinement index. Floodplain widening ranged from a minimum of 10 m (i.e., from 102 to 112 m) to a maximum of 35 m (i.e., from 16 to 51 m), and from a minimum of 3 m (i.e., from 274 to 277 m) to a maximum of 38 m (i.e., from 92 to 130 m), in semi-alluvial and alluvial channels respectively (Table 1).

4.3 Vegetation analysis

Woody vegetation, mostly consisting of dense stands of *Quercus pubescens, Quercus suber* and *Quercus Ilex*, was mapped by means of supervised image classification in ENVI 5.0, as described in section 3.2. The maximum likelihood classification provided good results, discriminating well between areas of woody land cover, sediment/rock, water and unclassified (Fig. 7B and Fig. 7D), with an overall accuracy ranging from 90% to 99% at reach scale.

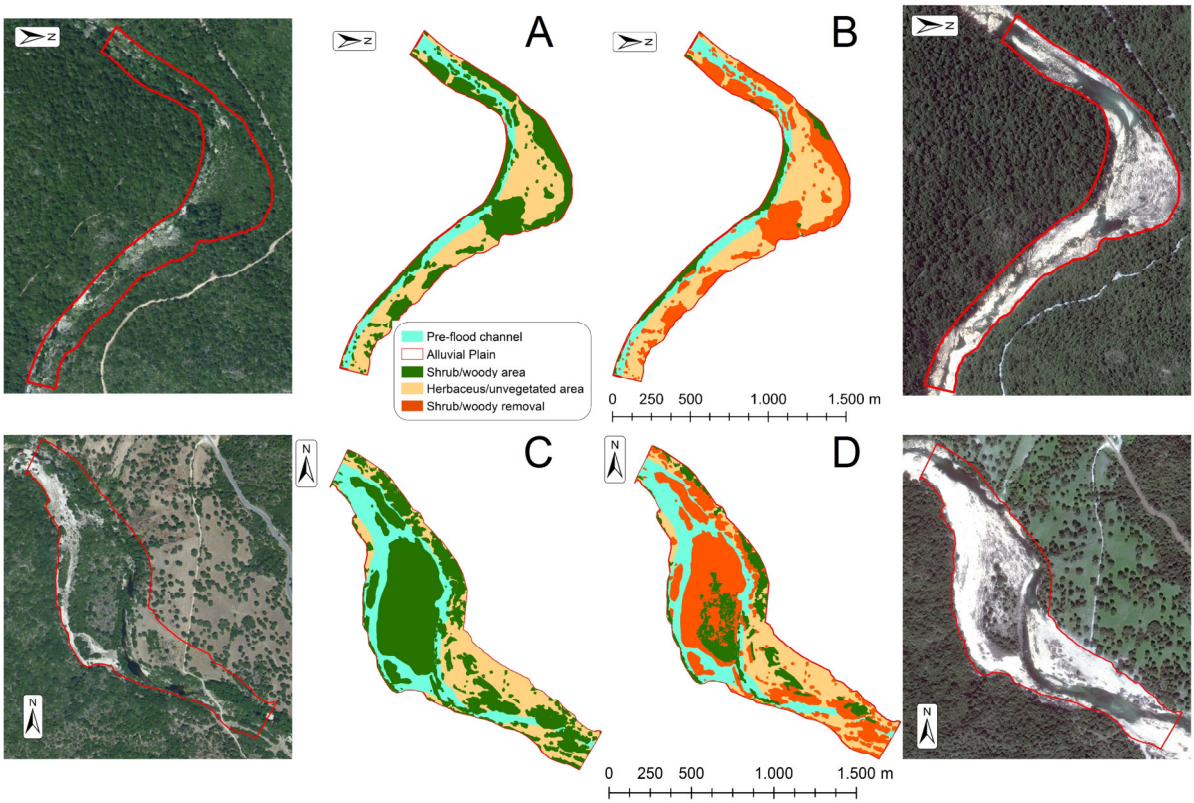

Figure 7. Pre-flood (A, C) and post-flood (B, D) satellite images of sub-reach P2.1.4 (I_v=0.9) and P2.3.3 (I_v=0.98) Pre-flood classification (A, C) showing land cover prior to the flood. Post classification change image (B, D) showing areas of vegetation loss in orange and areas that remained vegetated after the flood in green.

A Kruskal-Wallis test shows that the amount of woody vegetation available prior to the flood was more extensive than the amount of herbaceous/unvegetated land cover, considering all the study sub-reaches (n=48), occupying on average more than the 60% of the channel and the floodplain areas in all three channel subsets. In general, most of the mapped woody vegetation was removed by the flood (i.e., more than the 50% on average). In bedrock sub-reaches, I_v index showed the lower average value 0.1, indicating that in these channels most of the pre-flood woody vegetation was removed (Fig. 8). Both alluvial and semi-alluvial sub-reaches exhibited average values of I_v equal to 0.3 (Fig. 8). However, channel widening and vegetation removal processes (i.e., I_v) did not turn out to be significantly related. Therefore, the assessment of woody vegetation as a possible controlling factor in enhancing or obstructing changes in channel width was performed by bivariate regression between width ratio and pre-flood woody vegetation area. The overall analysis results showed a non-statistically significant correlation between the amount of woody vegetation prior to the 2013 flood and width ratio (*p-value*>0.05). However, in the Posada River sub-reaches (n=28), pre-flood woody vegetation displayed a small but significant correlation with width ratio (R^2=0.34), without any significant and evident differences among the three channel types.

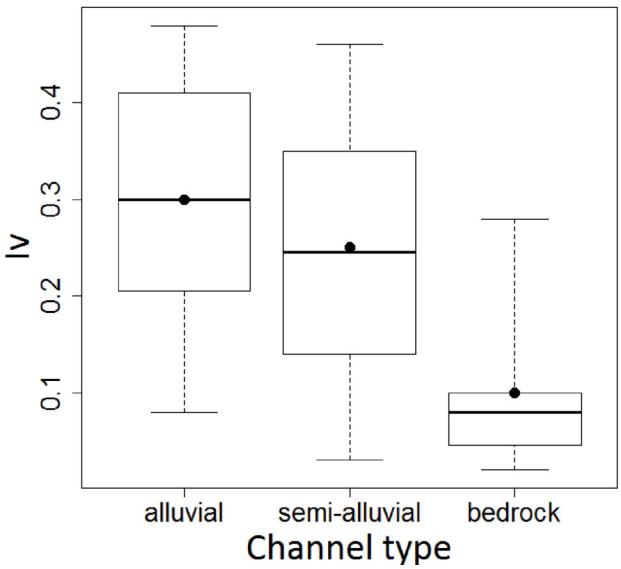

Figure 8. Boxplot of vegetation change index I_v for the channel type sub-sets. IQR is the interquartile range represented by the box, upper and lower whiskers represent maximum

and minimum values, respectively; dots represent the mean values; the horizontal line represents median values.

4.4 Channel and floodplain widening and morphological controlling factors

Simple regression analyses were used to interpret relationships between controlling factors and observed channel changes (Table 2). Confinement index (*CI*), sinuosity index (Si), channel slope (S), and exposed bedrock percentage were investigated as possible morphological controlling factors for the two most relevant changes, i.e., channel and floodplain widening. The first step consisted of analyzing the whole dataset, while in the second step the dataset was split according to the different channel bed types (Table 2).

Controlling factor	***Channel type sub-set***							
	Dataset(n=48)		*Alluvial(n=7)*		*Semi-alluvial(n=34)*		*Bedrock(n=7)*	
	R^2	*p-value*	R^2	*p-value*	R^2	*p-value*	R^2	*p-value*
Confinment index *(CI)*	0.44	***0.001***	0.86	***0.002***	0.33	***0.001***	0.89	***0.001***
% of exposed bedrock	0.01	*0.48*	0.57	***0.047***	0.03	*0.369*	0.24	*0.259*
Sinuosity index (Si)	0.03	*0.37*	0.16	*0.443*	0.01	*0.799*	0.21	*0.381*
Slope(mm^{-1})	0.01	*0.77*	0.17	*0.357*	0.02	*0.403*	0.1	*0.498*
I_v	0.04	*0.*18	0.05	*0.62*	0.01	*0.520*	0.75	***0.001***
Ω (Wm^{-1})	0.04	*0.16*	0.02	*0.78*	0.06	*0.17*	0.03	*0.71*
ω_{before}(Wm^{-2})	0.21	***0.004***	0.57	***0.06***	0.13	***0.05***	0.09	*0.53*
ω_{after} (Wm^{-2})	0.004	*0.93*	0.10	*0.56*	0.002	*0.84*	0.03	*0.79*

Table 2. Summary of results from statistical analyses using simple regressions between width ratio and morphological and hydraulic controlling factors. Statistically significant correlations (*p-value*<0.05) highlighted in bold.

Lateral confinement, expressed as confinement index, affected channel widening and banks retreat. Differences in the values of width ratio between confinement classes were assessed by Kruskal-Wallis test. Results showed statistically significant differences between values of lateral confinement: the more relevant widening occurred in unconfined sub-reaches (average width ratio of 4.4), while the lower occurred in the confined sub-reaches (average width ratio of 2.8) (Fig. 4B), as it could be expected. Indeed, the trend of bivariate regression has showed a positive correlation between changes in channel width and decreasing lateral confinement. Figure 9A shows the regression analysis on the whole dataset, which produced a statistically significant result (*p-value*<0.05; R^2=0.44). In alluvial and bedrock sub-reaches, the confinement index provided a very good explanation of

channel widening, with R squared values of 0.86 and 0.89, respectively (Fig. 9B). In the semi-alluvial sub-reaches, lateral confinement showed relatively low relationships with widening (R^2=0.33) (Fig. 9B).

As for sinuosity, higher average values in width ratio were detected in sinuous alluvial sub-reaches (average Wr=4.3) and straight alluvial sub-reaches (average Wr=3.9), although the analysis gave a statistically non-significant relationship for the whole dataset and for the channel bed type subsets (*p-value*>0.05).

Channel widening was more intense in bedrock and semi-alluvial sub-reaches with slope exceeding 1%. In alluvial sub-reaches, a larger value in channel width change was measured in sub-reaches with 0.6% channel gradient. Nevertheless, no significant relationship was found between channel gradient and channel widening in the whole dataset and within the channel bed type subsets (*p-value*>0.05).

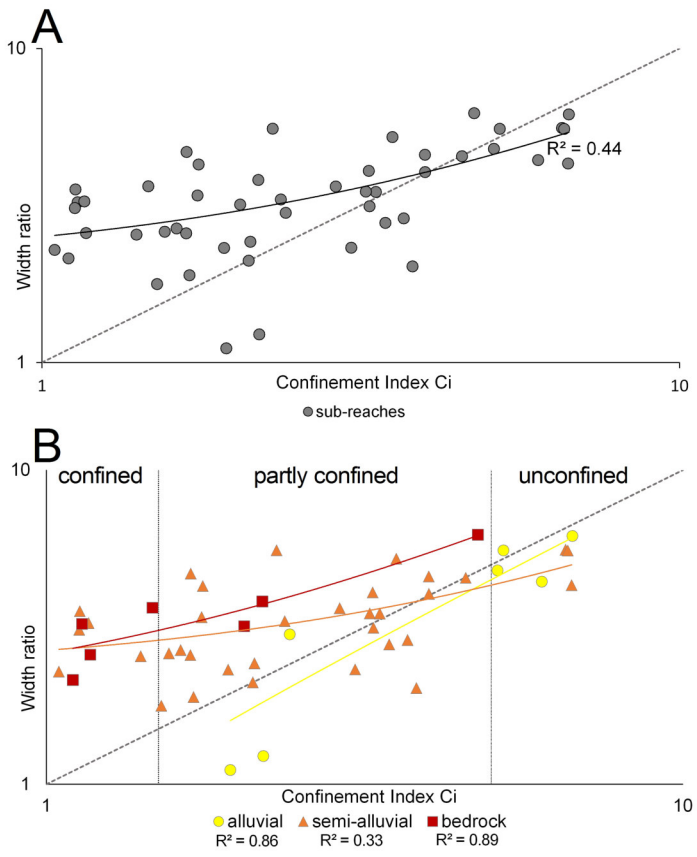

Figure 9. Simple regression models (log-log scale graph) between width ratio and confinement index (*CI*) for the whole dataset (A) and the channel type sub-set (B).The dashed line represents the 1:1 relationship; all values above this line indicate hillslope erosion and floodplain widening (except for bedrock channels where no significant changes in channel and floodplain morphology occurred).

The low amount of exposed bedrock in alluvial sub-reaches influenced channel response in terms of channel widening, resulting in a statistically significant correlation (*p-value*<0.05; R^2=0.57). In the bedrock sub-reaches, channel widening tended to decrease for high values of exposed bedrock (R^2=0.24). Higher values of widening magnitude were detected in those partly confined sub-reaches with exposed bedrock percentage closer to 50%, even if the simple regression gave a non-significant correlation (*p-value*>0.05). In semi-alluvial sub-reaches, the analysis did not provide a clear trend for channel widening and exposed bedrock as a control variable, giving a statistically insignificant correlation (*p-value*>0.05; R^2=0.03).

As mentioned above, width ratio exceeded the confinement index in all the bedrock and most of the semi-alluvial sub-reaches, thereby indicating that hillslope erosion (i.e., floodplain widening). Confinement setting highly influenced floodplain widening and in partly confined and confined sub-reaches (i.e., *CI* < 5), where the floodplain is limited and not wide enough to accommodate the largest available discharge. Indeed, as showed in Figure 9B, hillslope erosion was dominant in all confined sub-reaches.

4.5 Channel widening and hydraulic controlling factors

Field-estimated of peak discharges at some cross-sections exceed previous envelope curves for the northwestern Mediterranean (Marchi et al., 2010). Catchment areas upstream of the studied channel reaches (from 200 to 300 km^2 in Mannu di Bitti and from 45 to 560 km^2 in Posada) encompass the range where the flood occurred with the highest intensity. Model-computed peak discharge shows a good agreement with post-flood field estimates; model application to the studied sub-reaches results in unit peak discharges varying from 7 to 9.7 $m^3s^{-1}km^{-2}$ in the Mannu di Bitti and from 6.6 to 14 $m^3s^{-1}km^{-2}$ in the Posada. These values correspond to recurrence period exceeding 100 years and for some sections exceeding 300 years.

The stream power shows the highest peak in the upstream portion of the Posada study reach (P2.1.2), achieving values of cross sectional stream power Ω and unit stream power ω using channel width before and after the flood of 420476 Wm^{-1}, 28784 Wm^{-2} and 8889 Wm^{-2}, respectively (Table 1). Within the Mannu di Bitti

River, the highest values of stream power were observed in the middle portion of the study reach (MB3.1.1), achieving values of cross sectional stream power Ω and unit stream powers ω using channel width before and after the flood of 337809 Wm^{-1}, 27634 $Wm^{-2}$and 4442 Wm^{-2}, respectively.

Statistical analysis results of simple regression on the whole dataset between the response variables (width ratio) and the three selected hydraulic variables showed that hydraulic controlling factors in general did not have strong correlations with channel response to the flood. Statistically non-significant correlations were found between width ratio and cross sectional stream power (*p-value*=0.16) and unit stream power using channel width after the flood (*p-value*=0.93), while unit stream power using channel width before the flood exhibited a significant positive relationship with channel widening (*p-value*=0.004; R^2=0.21). A Kruskall-Wallis test provided statistically significant differences in unit stream power using pre-flood channel width among bedrock, alluvial (*p-value*=0.02) and semi-alluvial (*p-value*=0.02) sub-reaches, with average values of 15593 Wm^{-2}, 6490 Wm^2 and 7924 Wm^2, respectively (Fig. 10B). The test revealed statistically significant differences in unit stream power using post-flood channel width among bedrock sub-reaches and alluvial (*p-value*=0.02) and semi-alluvial (*p-value*=0.02) reaches, with average values of 4538 Wm^{-2}, 1678 Wm^{-2} and 2349 Wm^{-2}, respectively (Fig. 10C).

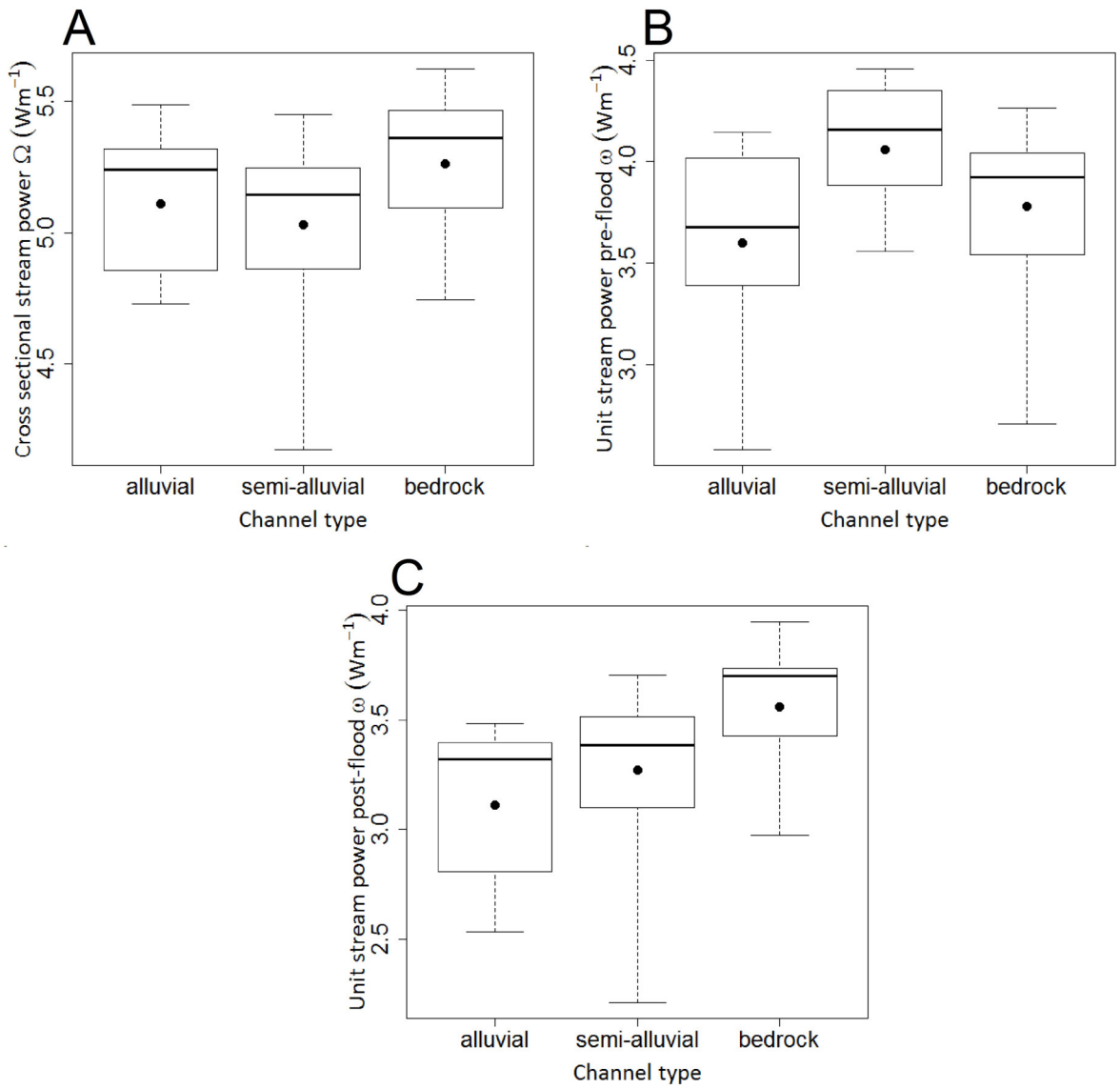

Figure 10. Boxplots of cross-sectional stream power (A); unit stream power pre-flood width (B); and unit stream power post-flood width (C). All data are log transformed.

Observed changes in channel width within bedrock sub-reaches turned out in statistically insignificant relationships with cross sectional stream power (*p-value*=0.71), unit stream power using channel width after (*p-value*=0.79) and before (*p-value*=0.53) the flood (Fig. 11B, 11D and 11F). In contrast, the analysis within semi-alluvial and alluvial sub-reaches gave a positive, statistically significant correlation with unit stream power using pre-flood channel width, especially in alluvial channels (*p-value*=0.06 and R^2=0.57, *p-value*=0.05 and R^2=0.13 in alluvial and semi-alluvial sub-reaches, respectively) (Fig. 11D).

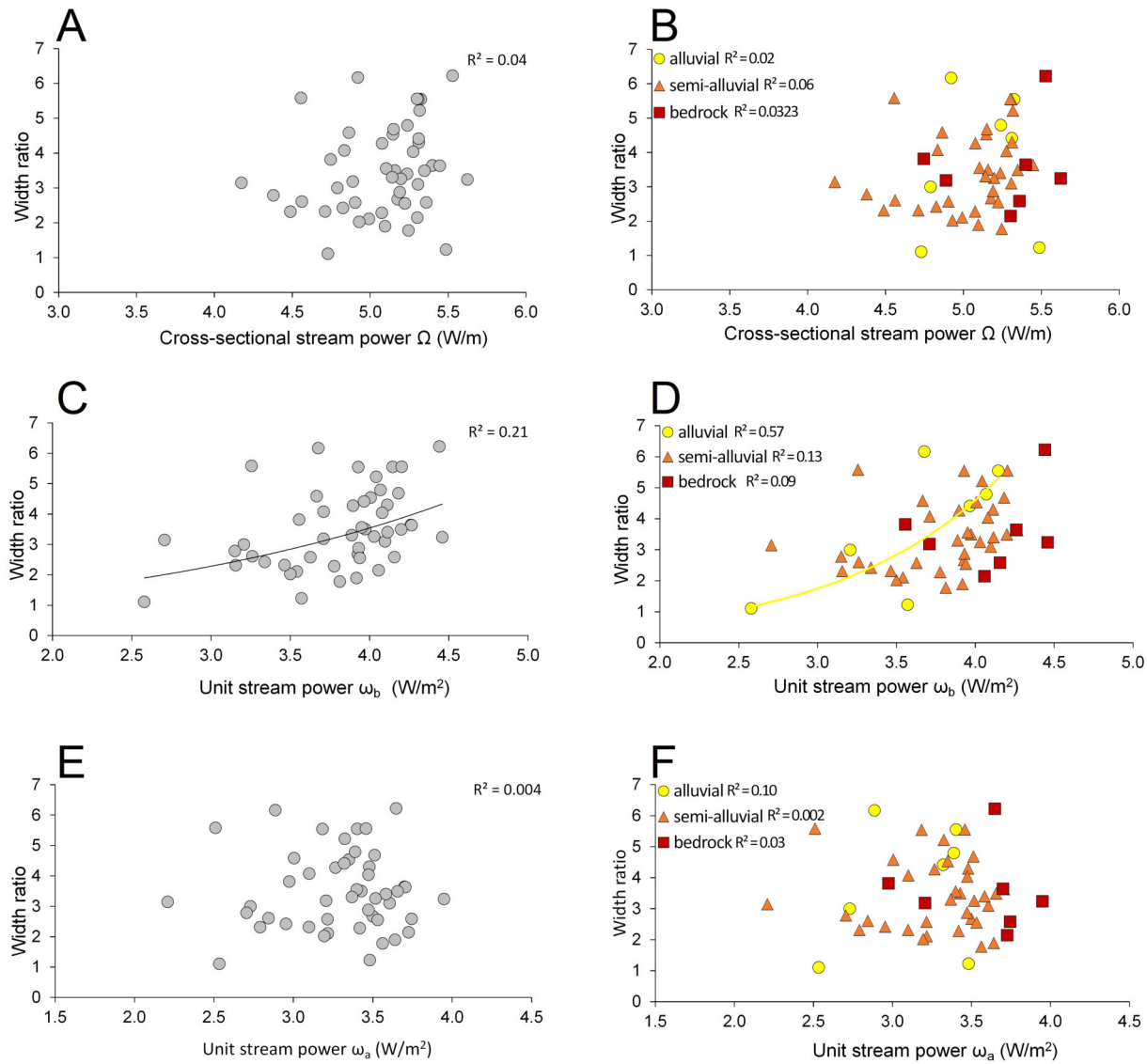

Figure 11. Simple regression models between hydrographic variables and width ratio for the whole dataset and the channel type sub-sets: cross sectional stream power (A, B); unit stream power using pre-flood width (C, D). In D the yellow line represents the correlation between width ratio and unit stream power using pre-flood width for the alluvial sub-reaches (R^2=0.57); unit stream power using post-flood width (E, F). All data are log transformed.

5. Discussion

The 2013 flood in the Posada River catchment featured an extreme magnitude, as testified by the very large unit peak discharges estimated in the channel network. Results indicated the evident geomorphic effectiveness of the 2013 flood as a channel and even valley-shaping event. Major morphological changes were mainly localized in the middle portion of the catchment, where individual large floods are likely to be most geomorphically powerful (Wohl, 2010). However,

differences in channel response among sub-reaches demonstrate a high variability in channel sensitivity to the flood. These were largely related to channel and valley pre-flood conditions, confirming the key role of intrinsic morphological aspects of channels, as well as hydraulic forces, to explain channel response. The magnitude and the dominant processes of channel adjustment varied within the study reaches and included channel widening, vegetation stripping, and floodplain and hillslope erosion (Fig. 4). Channel widening was the dominant observed channel response and was interpreted to reflect different processes characterizing the three channel type sub-sets. Overall, two general trends can be seen depending on pre-flood channel width, especially in alluvial sub-reaches. Smaller channels showed higher variability and tended to widen more, whereas wider channels underwent smaller adjustment (Krapesh et al. 2011; Surian et al., 2016). Indeed, channels are likely to be widened by extreme flows until they are wide enough to accommodate the largest available discharge (Wolman and Gerson, 1978).

In alluvial channels, widening was dominated by lateral erosion, in-channel island erosion and stripping. The flow dissipated over the floodplain in lower gradient sub-reaches, eroding fine-grained floodplain surfaces down to basal gravels and cobbles (Fig. 4A). The boundary of semi-alluvial channels is partly composed of alluvium and partly of bare rock constricting the flow and the presence of rock outcrops plays a crucial role in the morphodynamics of those channels. Channel-boundary resistance as a function of bedrock characteristics and exposure might sharpen the thresholds between driving and resisting forces in controlling geomorphic adjustment and promoting preferential bank erosion. Hence, in semi-alluvial sub-reaches, geomorphic response was controlled by a number of factors that result in longitudinally highly variable patterns of change and reflect the physical complexity of those channels. Bedrock sub-reaches behaved quite differently from alluvial channels because a bedrock channel cannot substantially widen, incise or shift its bed without eroding bedrock (Meshkova et al., 2010). It cannot adjust laterally, nor incise without eroding bedrock. However, during the large flood, preferential bank erosion was promoted in bedrock channels with at least partial alluvial cover or alluvial sidewalls (Meshkova et al., 2010), and erosion focused on in-channel vegetation and on the channel walls, eroding the topsoil and riparian vegetation and resulting in an increase in the geomorphic effectiveness of floods.

Fairly differences in channel widening were observed between bedrock constrained and confined channels, where lateral erosion is much more limited by confining competent bedrock walls.

Basin-scale factors (e.g., basin morphometry, climate, lithology, sediment connectivity) and channel factors (e.g., lateral confinement, bedrock exposure, sinuosity, channel gradient) might control channel and floodplain response to large-magnitude floods. Findings of morphological controlling factor analysis showed that the degree of channel width change increased with decreasing lateral channel confinement (Fig. 12).

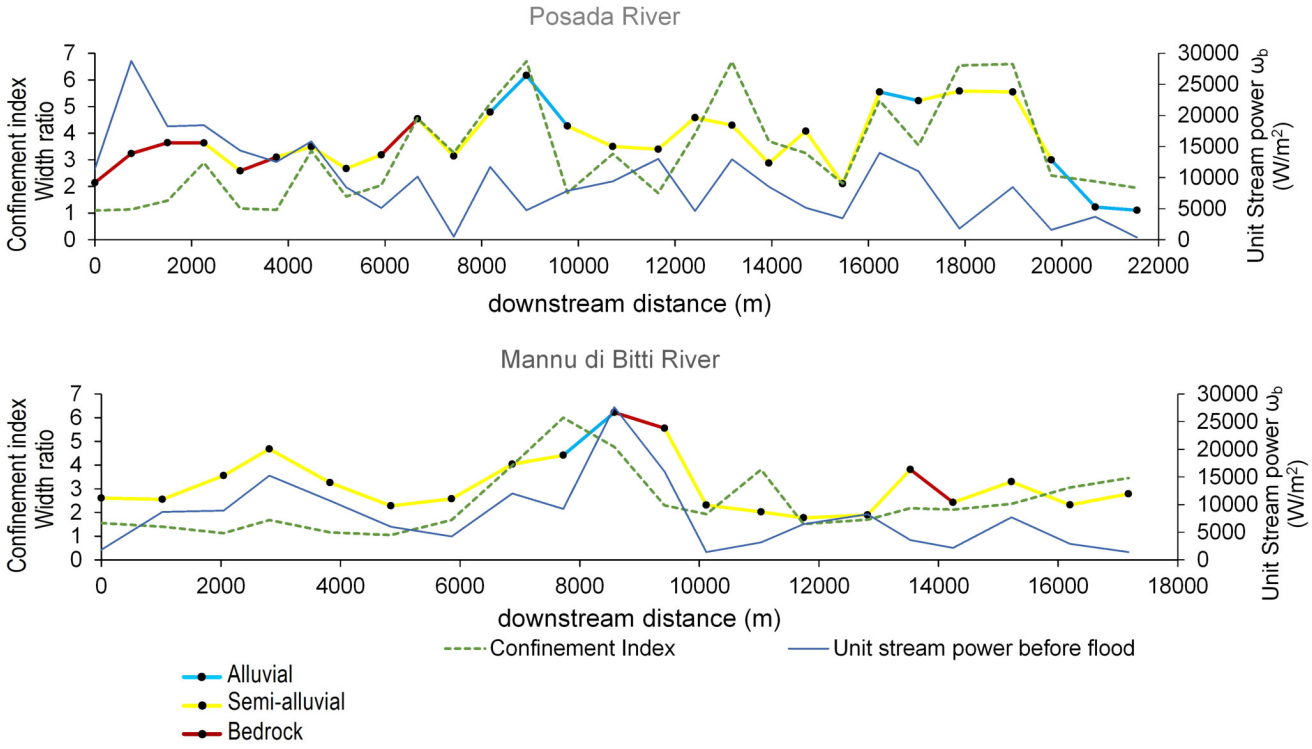

Figure 12. Downstream trend of width ratio and the most significant explanatory variables: confinement index and unit stream power using pre-flood width in Posada (A) and Mannu di Bitti (B) Rivers.

In our study, major changes occurred along unconfined and partly confined sub-reaches, in valley portions that allowed greater capacity for adjustment, while minor widening occurred in the steeper confined sub-reaches. In alluvial and semi-alluvial lower gradient unconfined and partly confined settings, flood flows dissipated over the floodplain surfaces, which were stripped and reactivated to greater extents.

Furthermore, lateral confinement is strictly related to the percentage of confining bedrock walls, which create natural constrictions and limit lateral channel mobility in bedrock and semi-alluvial channels. Observing downstream pattern of percentage of exposed bedrock and width ratio, channel adjustments seems to occur downstream of the largest bedrock constrictions. However, in upstream reaches, bedrock and semi-alluvial reaches dominated confined and partly confined valleys and concentrated flow exceeded valley natural constraints, eroding the hillslopes. Locally, channel adjustment was controlled by channel sinuosity. In sub-reach P2.1.2, floodwaters followed the most direct path downstream, cutting off the meander bend in a bedrock channel, removing topsoil and woody vegetation (Fig. 4B). Furthermore, in some high sinuosity semi-alluvial channels where bedrock constrictions were limited, lateral channel mobility increased, exceeding the width ratio value of 3.

During the 2013 flood, sediment load was not substantial relative to the flood magnitude and there is no evidence of landslides connected to the channel network during the flood, mostly due to the geological and geomorphological setting of the study area. In this study we lack the quantification of sediment supply and channel-bed incision or aggradation. However, field observations evidenced negligible depositional processes. The hypothesis that sediments might be supplied from the 35 tributaries flowing into the two main streams, considering tributary junctions as ‘sedimentary links’ where longitudinal trends in channel slope and grain size may be interrupted by abrupt increases in sediment supply (Rice, 1998; Dean and Schmidt, 2013; Nardi and Rinaldi, 2015), was generally not supported by planimetric changes downstream from tributaries. However, there was evidence of the role played by few tributaries. For instance in the Mannu di Bitti reach MB3.1.1, most intense widening occurred downstream from a tributary where remarkable fan deposition may indicate the likelihood of coarse bedload yield and its influence over channel response.

Several studies have argued that riverside vegetation is an important factor influencing the occurrence and progress of stream-bed and river-bank erosion (Thorne, 1990; Abernethy and Rutherfurd, 2000) and that channel and floodplain vegetation, as part of the boundary roughness elements, may exert a significant influence on the resistance to flow (Hickin, 1984; Thorne, 1990), as well as influencing the rate of lateral migration of channels (Hickin, 1984). However, a major flood such as the 2013 flood may overcome the resistance threshold that the

vegetation provides and vegetation may be damaged to the extent that it does not completely prevent erosion (Hickey, 1995; Renofalt, 2007). In the case of the 2013 flood, marginal vegetation as well as floodplain vegetation were considerably modified and the presence of vegetation did not play a significant role in channel widening, similar to what observed in other high-magnitude events in mountain rivers (Lucìa et al., 2015; Comiti et al., 2016).

Analysis of hydraulic controlling factors pointed out that unit stream power calculated using pre-flood channel width is the most important predictor of channel widening among the hydraulic parameters that we evaluated. The statistically relevant relation between unit stream power calculated using pre-flood channel width and channel widening may suggest that most morphological changes likely occurred after the flood peak (Surian et al., 2016). Unit stream power along the entire studied reaches exceeded 300 Wm^{-2}, i.e., well above the empirical threshold for major morphological changes suggested by Magilligan (1992). On the other hand, the highest values in unit stream power were observed in confined bedrock and semi-alluvial sub-reaches, which did not match with higher values in channel widening (Fig. 12), possibly because they represent a zone of resistant constriction and high stream power causing higher morphological adjustment in immediately downstream sub-reaches (Dean and Schmidt, 2013). These results confirm the dominant role of lateral confinement in controlling geomorphic response in bedrock and semi-alluvial channels. In alluvial sub-reaches unit stream power computed with pre-flood width showed high positive relationship with channel widening: in these cases channel enlargement occurred through lateral and island erosion with loss of vegetation (Fig. 12).

6. Conclusions

Our results show that flood-driven geomorphic change is controlled by several factors, both morphological and hydraulic, that result in variable patterns of change and reflect the physical complexity of the river system and the complex nature of high-magnitude events (Costa and O'Connor, 1995; Thompson and Crooke, 2013; Buraas et al., 2014; Nardi and Rinaldi, 2015; Surian et al., 2016). During the extreme

flood analyzed in this study, rivers significantly widened, especially in the sub-reaches with smaller pre-flood width, and depending mostly on i) lateral confinement, especially in alluvial and bedrock channels, ii) percentage of exposed bedrock, and iii) and unit stream power calculated using the pre-flood width. Other controlling factors such as channel sinuosity, woody vegetation cover, and input of sediments do not have such explanatory power at the sub-reach scale, but were relevant at some specific sites. In alluvial channels, lateral confinement and unit stream power calculated using pre-flood width explained 86% and 57% of channel widening, respectively, although the presence of patchy bedrock outcrops (i.e., <10%) seems to locally limit lateral channel expansions. In semi-alluvial channels, higher morphological variability shows less clear behavior depending on site specific conditions, and lateral confinement and unit stream power calculated using pre-flood width explain 33% and 13%, respectively. However, local analysis and observation better explains geomorphic response in these channel type subsets. Bedrock channel behavior during high-magnitude floods depended mostly on channel confinement which limited channel lateral erosion, and experienced high unit stream power resulting in considerable loss of vegetation and topsoil erosion.

Width ratios at the sub-reach scale can be used as the lower limit for the minimum morphological spatial demand for rivers during extreme floods (Krapesch et al., 2011), particularly in unconfined alluvial channels. Besides, in confined and partly confined bedrock and semi-alluvial sub-reaches where lateral mobility is limited, a considerable erosion of hillslopes occurred. Hence, in terms of fluvial risk and hazard assessment in the presence of the latter pre-flood conditions, it is important to remember that the lateral boundaries of the fluvial corridor are not fixed and may undergo remarkable morphological change. It is crucial to document the behavior, the range of variability of channel response and to detect controlling factors in order to provide a basis from which to forecast future river sensitivity to geomorphic adjustment to high-magnitude floods and to develop new predictive and explanatory tools (Rinaldi et al., 2016; Surian et al., 2016).

References

Abernethy, B., and Rutherfurd, I.D., 2000. The effect of riparian tree roots on the mass-stability of riverbanks. Earth Surface Processes and Landforms **25**(9): 921-937.

Amponsah, W., Zoccatelli, D., Marra, F., Marchi, L., Crema, S., Niedda, M., and, Borga, M., 2016. Observational and hydrological modelling uncertainty in flash flood analysis. Submitted to J. Hydrol.

Ardau, F., Barbieri, G., Vernier, A., Vernier E., 1999. Salinisation phenomena in the Posada costal aquifer (North-East Sardinia). in: De Breuck, W. et al. (Ed.) Proceedings of the 15th Salt-Water Intrusion Meeting Ghent (Belgium), 25-29 May 1998. Natuurwetenschappelijk Tijdschrift, **79**(1-4): 125-131.

Baker, V.R., 1988. Flood erosion. In: Flood Geomorphology. John Wiley & Sons New York. pp 81-95.

Baker, V.R., 1977. "Stream-channel response to floods, with examples from central Texas". Geological Society of America Bulletin **88** (8).

Bodini, A., Cossu, Q.A., 2010. Vulnerability assessment of Central-East Sardinia (Italy) to extreme rainfall events. Nat. Hazards Earth Syst. Sci., **10**: 61–72.

Bowen, M.W., Juracek, K.E., 2011. Assessment of the geomorphic effects of large floods using streamgage data: the 1951 floods in eastern Kansas, USA Phys. Geography, **32** (1): 52–77.

Borga, M., Gaume, E., Creutin, J.D., Marchi, L., 2008. Surveying flash floods: gauging the ungauged extremes. Hydrological Processes, **22**(18): 3883-3885. doi: 10.1002/hyp.7111.

Brierley, G.J, Fryirs, K.A., 2005. Geomorphology and River Management: Applications of the River Style Framework. Blackwell: Oxford.Buraas, E.M., Renshaw, C.E., Magilligan, F.J., Dade, W.B., 2014. Impact of reach geometry on stream channel sensitivity to extreme floods. Earth Surface Processes and Landforms **39**: 1778–1789.

Carmignani, L., Oggiano, G., Barca, S., Conti, P., Salvadori, I., Eltrudis, A., Funedda, A., Pasci, S., 2001. Geologia della Sardegna. Note illustrative della Carta Geologica della Sardegna a scala 1:200.000, Memorie Descrittive della Carta Geologica d'Italia. Istituto Poligrafico e Zecca dello Stato, Roma, pp 1–283.

Comiti, F., Lucía, A., Rickenmann D., 2016. Large wood recruitment and transport during large floods: A review. Geomorphology **269**: 23-39.

Costa, J.E., O'Connor, J.E., 1995. Geomorphically effective floods. In: Costa, J.E., Miller, A.J., Potter, K.W., Wilcock, P. (Eds.), Natural and Anthropogenic Influences in Fluvial Geomorphology. Monograph, vol. **89**. American Geophysical Union, Washington, D.C., pp. 45–56.

Czuba, J.A., Magirl C.S., Czuba, C.R., Curran, C.A., Johnson, K.H., Olsen, T.D., Kimball, H.K., Gish, C.C., 2012. Geomorphic Analysis of the River Response to Sedimentation Downstream of Mount Rainier, Washington. Open-File Report 2012–1242, U.S. Department of the Interior U.S. Geological Survey.

Dean, D.J., Schmidt, J.C., 2013. The geomorphic effectiveness of a large flood on the Rio Grande in the Big Bend region: Insights on geomorphic controls and post-flood geomorphic response. Geomorphology **201**: 183–198.

Delitala, A.M.S., Cesari, D., Chessa, P.A., Ward, M.N., 2000. Precipitation over Sardinia (Italy) during the 1946-1993 rainy seasons and associated large-scale climate variations. Int. J. Climatol., **20**: 519–541.

De Waele, J.L.V., Martina, M., Sanna, L., Cabras, S., Cossu, Q.A., 2010. Flash flood hydrology in karstic terrain: Flumineddu Canyon, central-east Sardinia. Geomorphology **120**: 162–173.DOI: 10.1016/j.geomorph.2010.03.021.

Di Pisa, A., Oggiano, G., 2001. Introduction to the Sardinia geologic evolution. Rendiconti Seminario Facoltà Scienze Università Cagliari Supplemento Vol. **71** Fasc. 2.

Frassi, C., 2015. Structure of the Variscan metamorphic complexes in the central transect of the Posada-Asinara Line (SW Gallura region, Northern Sardinia, Italy), Journal of Maps, **11**:1, 136-145, DOI: 10.1080/17445647.2014.944945.

Gurnell, A.M., Bertoldi, W., Corenblit, D., 2012. Changing river channels: the roles of hydrological processes, plants and pioneer fluvial landforms in humid temperate, mixed load, gravel bed rivers. Earth-Science Reviews **111**: 129–141.

Heritage, G.L., Large, A.R.G., Moon, B.P., Jewitt, G., 2004. Channel hydraulics and geomorphic effects of an extreme flood event on the Sabie River, South Africa. Catena **58**: 151–181.

Hickey, J.T., Salas J.D., 1995. Environmental effects of extreme floods. Paper presented at the US–Italy workshop on the hydrometeorology, impacts, and management of extreme floods, Perugia, Italy, 13–17. November 1995.

Hickin, E.J., 1984. "Vegetation and river channel dynamics." Canadian Geographer / Le Géographecanadien **28**(2): 111-126.

Hooke, J.M., Mant, J.M., 2000. Geomorphological impacts of a flood event on ephemeral channels in SE Spain. Geomorphology **34** (3-4): 163–180.

Hooke, J.M., 2015. Variations in flood magnitude–effect relations and the implications for flood risk assessment and river management. Geomorphology **263**:19–38.

Hooke, J.M., 2016a. Morphological impacts of flow events of varying magnitude on ephemeral channels in a semiarid region. Geomorphology **252**: 128–143.

Hooke, J.M., 2016b. Geomorphological impacts of an extreme flood in SE Spain. Geomorphology **263**: 19–38.

Kale, V.S., Hire, P.S., 2004. Effectiveness of monsoon floods 751 on the Tapi River, India: role of channel geometry and hydrologic regime. Geomorphology **57**: 275–291.

Kale, V. S., 2007. Geomorphic effectiveness of extraordinary floods on three large rivers of the Indian Peninsula. Geomorphology **85**: 306–316.

Knighton, D., 1998. Fluvial forms and processes: a new perspective. London, Hodder Education.

Krapesch, G., Hauer, C., Habersack, H., 2011. Scale orientated analysis of river width changes due to extreme flood hazard. Natural Hazards and Earth System Sciences **11:** 2137–2147.

Marchi, L., Borga, M., Preciso, E., Gaume, E., 2010. Characterisation of selected extreme flash floods in Europe and implications for flood risk management, Journal of Hydrology, **394**(1-2): 118-133. doi: 10.1016/j.jhydrol.2010.07.017

Langhammer, L., 2010. Analysis of the relationship between the stream regulations and the geomorphologic effects of floods. Natural Hazards **54**: 121–139.

Lucía, A., Comiti, F., Borga, M., Cavalli, M., Marchi, L, 2015. Dynamics of large wood during a flash flood in two mountain catchments. Natural Hazards and Earth System Sciences, **15** (8): 1741-1755.

Magilligan, F.J., 1992. Thresholds and the spatial variability of flood power during extreme floods. Geomorphology **5**: 373–390.

Magilligan, F.J., Buraas, E.M., Renshaw, C.E., 2015. The efficacy of stream power and flow duration on geomorphic responses to catastrophic flooding. Geomorphology **228**: 175-188.

Meshkova, L.V., Carling, P.A. and Buffin-Bélanger, T. (2012) Nomenclature, Complexity, Semi-Alluvial Channels and Sediment-Flux-Driven Bedrock Erosion, in Gravel-Bed Rivers: Processes, Tools, Environments (eds M. Church, P. M. Biron and A. G. Roy), John Wiley & Sons, Ltd, Chichester, UK. doi:10.1002/9781119952497.ch31

Miller, A.J., 1990. Flood hydrology and geomorphic effectiveness in the central Appalachians. Earth Surface Processes and Landforms **15**: 119–13.

Nardi, L., Rinaldi, M., 2015. Spatio-temporal patterns of channel changes in response to a major flood event: the case of the Magra River (central-northern Italy). Earth Surface Processes and Landforms **40**: 326-339.

Niedda, M., Amponsah, W., Marchi, L., Zoccatelli, D., Marra, F., Crema, S., Pirastru, M., Marrosu, R., Borga, M., 2015. Il ciclone Cleopatra del 18 novembre 2013 in Sardegna:analisi e modellazione dell'evento di piena. Quaderni di Idronomia Montana **32**/1: 47–58 (in Italian).

Nanson, GC., 1986. Episodes of vertical accretion and catastrophic stripping: a model of disequilibrium flood-plain development. Bulletin of the Geological Society of America **97**: 1467–1475.

Ortega, J.A., Garzón Heydt Guillermina, 2009. Geomorphological and sedimentological analysis of flash-flood deposits. The case of the 1997 Rivillas flood (Spain). Geomorphology **112:** 1–14.

Phillips, J.D., 2002. Geomorphic impacts of flash flooding in a forested headwater basin. Journal of Hydrology **269**: 236–250.

Renofalt, B., Merritt, D.M., Nilsson, C., 2007. Connecting variation in vegetation and stream flow: the role of geomorphic context in vegetation response to large floods along boreal rivers. Journal of Applied Ecology **44**: 147–157.

Rice, S.P., Church, M., 1998. Grain size along two gravel-bed rivers: statistical variation, spatial pattern and sedimentary links. Earth Surf. Process. Landforms **23**: 345–363.

Rice, S.P., 1998. Which tributaries disrupt downstream fining along gravel-bed rivers? Geomorphology **22**: 39-56.

Rinaldi, M., Surian, N., Comiti, F., Bussettini, M., 2013. A method for the assessment and analysis of the hydromorphological condition of Italian streams: the Morphological Quality Index (MQI). Geomorphology **180-181**: 96–108.

Rinaldi M., Amponsah W., Benvenuti M., Borga M., Comiti F., Lucìa, A., Marchi L., Nardi, L., Righini, M., Surian, N., 2016. An integrated approach for investigating geomorphic response to extreme events: methodological framework and application to the October 2011 flood in the Magra River catchment, Italy. Earth Surface Processes and Landforms **41**: 835–846. doi: 10.1002/esp.3902.

Rutherfurd, I., 2000. Some human impacts on australian stream channel morphology. River Management: The Australasian Experience, Wiley, Chichester, UK:11-49.

Simon, A., Collison, A.J.C., 2002. Quantifying the mechanical and hydrologic effects of riparian vegetation on streambank stability. Earth Surface Processes and Landforms **27**(5): 527-546.

Surian, N., Righini, M., Lucìa, A., Nardi, L., Amponsah, M., Benvenuti, M., Borga, M., Cavalli, M., Comiti, F., Marchi, L., Rinaldi, M., Viero, A., 2016. Channel response to extreme floods: insights on controlling factors from six mountain rivers in northern Apennines Italy. Geomorphology, **272**: 78–91. doi:10.1016/j.geomorph.2016.02.002

Thompson, C., Croke, J., 2013. Geomorphic effects, flood power, and channel competence of a catastrophic flood in confined and unconfined reaches of the upper Lockyer valley, southeast Queensland, Australia. Geomorphology **197**: 156–169.

Thorne, C.R., 1990. Effects of vegetation on riverbank erosion and stability. In: Thornes, J.B. ed. Vegetation and Erosion: Processes and Environments. Wiley, Chichester.

Tinkler, K.J., and Wohl, E.E., 1998. Rivers over rock: Fluvial processes in bedrock channels: American Geophysical Union Geophysical Monograph **107**.

Vocal Ferencevic, M.V., Ashmore, P., 2012. Creating and evaluating digital elevation model-based stream-power map as a stream assessment tool. River Research and Applications **28**: 1394–1416.

Wohl, E., 2010. Mountain rivers revisited. AGU, Water Resources Monograph **19**.

Wolman, M.G., Gerson, R., 1978. Relative scales of time and effectiveness of climate in watershed geomorphology. Earth Surface Processes and Landforms **3**: 189–208.

Wolman, M.G, Miller, J.P., 1960. Magnitude and frequency of forces in geomorphic processes. Journal of Geology **68**: 54–74.

6. THE FLASH-FLOOD OF THE LIERZA CREEK (NORTHEASTERN ITALY): ANALYSIS AND INTERPRETATION OF ITS LIMITED GEOMORPHIC EFFECTS

Margherita Righini[a], Nicola Surian[a], Lorenzo Marchi[b], William Amponsah[b,c], Marco Borga[c]

[a]Department of Geosciences, University of Padova, Italy; [b]CNR IRPI, Padova, Italy; [c]Department of Land, Environment, Agriculture and Forestry, University of Padova, Italy

Abstract

On the August 2nd 2014 the Lierza Creek, a small stream in northeastern Italy (basin area 7.5 km^2), was hit by an extreme rainstorm that triggered severe flash flooding causing four casualties and major damages to infrastructures. The flood-generating rainstorm produced maximum accumulations up to 200 mm within 1.5 hour. Despite the rainstorm caused widespread shallow landslides, limited and localized lateral erosion and channel widening were observed after the event. To explain the relatively small geomorphic effectiveness of the flood, the analysis was focused on the role of flow duration examining combined influence of flow duration and cumulate energy expenditure. Besides, a basin with similar flood magnitude (i.e., peak discharge, unit stream power), topographic and geomorphic characteristics (i.e., drainage area, channel gradient, valley setting, channel width), but different flow duration and available amount of cumulate energy expenditure for geomorphic changes was compared with the Lierza Creek.

Introduction

The geomorphic effectiveness of a flood can be defined in a variety of ways (Dean and Smith, 2013). Geomorphic effectiveness of extreme or catastrophic events can be explain as the amount of work done (Wolman et al., 1960) or by the degree of landscape modifications during a flood (Miller at al., 1987). High magnitude low-frequency floods might be effective geomorphic events in many mountains rivers context because of their attitude in generating large hydraulic driving forces necessary to exceed channel boundary resistant (Wohl, 2010).

Wolman and Gerson (1978) argued that geomorphic effectiveness of a given event could not be defined in absolute terms of frequency or rarity and magnitude of forces, but also by considering the rate of recovery. Subsequent studies emphasized

that extreme floods have rare occurrence, although not all extreme floods generate pervasive and extraordinary geomorphic impacts, showing in some cases negligible correspondence between a flood's recurrence interval and its immediate geomorphic impacts (Costa and O'Connor, 1995; Magilligan et al., 2015). Particularly, the role of flow duration as a measure of the distribution of stream power integrating the energy expenditure over the course of the flood for determining the geomorphic effectiveness of floods was supported by Costa and O'Connor and more recently by Magilligan et al., (2015). Furthermore, Hooke (2016) argued that the same size flow could have differing effects depending on the state of the system. Morphological changes of comparable flows occurred at different duration may be compared, showing similar or dissimilar order magnitude changes and having pervasive long-last widening or only locally limited changes (Wohl, 2010).

On August 2nd 2014 the Lierza Creek (northeastern Italy) was hit by an extreme rainstorm with a recurrence interval of point hourly intensity exceeding 500 years. However, limited channel changes were observed, despite major flood occurred in terms of absolute magnitude (Marchi et al., 2016). The objectives of this study are i) to quantify the amount, locations, and nature of morphological changes as channel response to 2014 flood and ii) to analyze the geomorphic effectiveness of the flood by comparing with a catchment roughly similar in terms of drainage area, magnitude (i.e., peak discharge, cross sectional stream power and unit stream power) and geomorphological characteristics (i.e., lateral confinement, channel gradient and channel width), and assessing the overall geomorphic effectiveness of two floods with different duration and total energy expenditure.

1. General setting and the flash flood of 2nd August 2014 in the Lierza Creek

The Lierza catchment belongs to the Piave River basin (northeastern Italy). It is located in a hilly area of the Venetian Prealps, and at the chosen outlet (Molinetto della Croda waterfall) it covers a 7.5-km^2 drainage area, ranging from a maximum elevation of 475 m a.s.l. to 169 m a.s.l. (Figure 1A). The local climate is classified as humid subtropical (*Cfa*) according to the Köppen–Geiger classification (Peel et al., 2007; Marchi et al., 2016). The study area has an average annual precipitation of 1134 mm and the average temperature is 13.8°C. The catchment is mainly

composed of marls, claystone and conglomerates. Land use is mainly woodland (64.8%), grassland and pasture (8.8%), and vineyards (17.6%). In the study reach the Lierza displays a plane bed morphology, it is composed of gravel and cobble and has an average gradient of 2.5 %. Sinuosity is quite low and the channel is generally straight and partly confined by alluvial terraces, hillslope or bedrock walls.

On 2nd to 3rd of August 2014 a wide cyclonic circulation from the British Island drove moist and unstable currents on the Venetian Plain towards E-SE. High intensity rainfalls of convective origin affected the Veneto and Friuli-Venezia Giulia Plain, causing the formation of intense cloudburst through the Treviso foothills, favored by the orographic influence of the Venetian Prealps. Short bursts of high intensity rainfall washed through the Treviso foothills producing a largest flow after a prolonged wet period in the Lierza Creek basin, causing four causalities. Event rainfall persisted for 100 minutes with a point intensity which exceeded 150 mm hourly and the post-flood survived average unit peak discharge turned out to be around 18 $m^3s^{-1}km^2$ (Destro et al., 2016; Marchi et al., 2016).

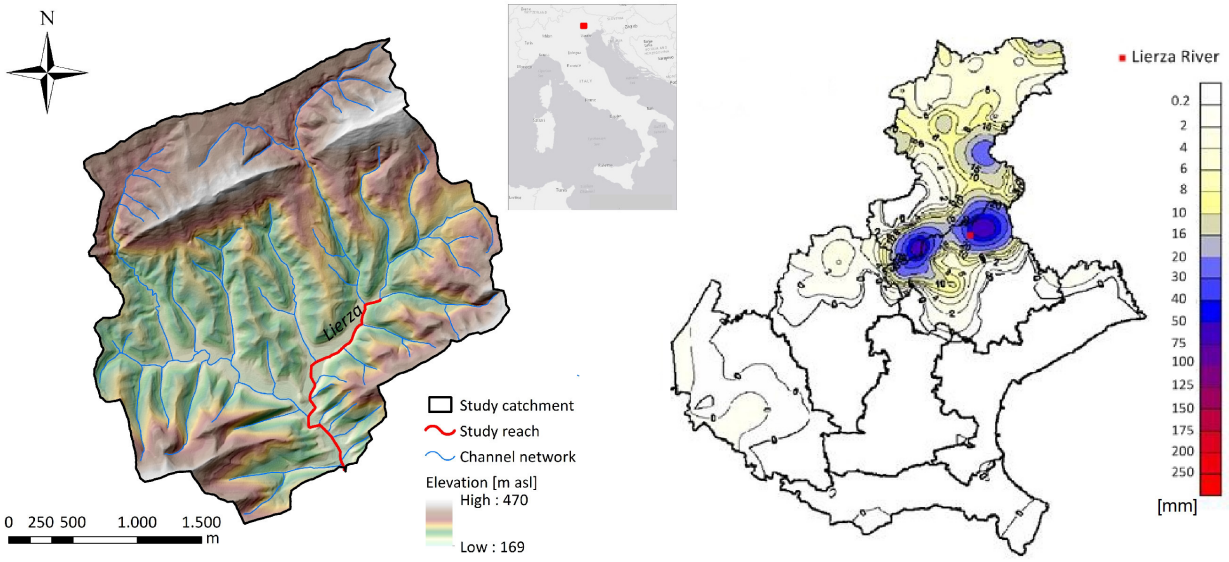

Figure 1. Location map of the Lierza Creek catchment and the study reach (A) and spatial distribution of rainfall across Veneto Region (B), red dot indicates Lierza Creek location.

2. Methods

We combined detailed field analyses and GIS-based analysis to characterize the geomorphic impacts of 2 August 2014 flood. This paper is mainly based on data

acquired during post-flood field surveys carried out to evaluate i) morphological and artificial characteristics of the stream (e.g., bank type, valley confinement, channel gradient, bank protections), ii) geomorphic effects (e.g., lateral erosion, sediment deposition), iii) sediment input and characteristics, and iv) hydrological and hydraulics event characteristics (e.g., peak discharge and unit stream power).

2.1. Geomorphological survey

Topographic and morphological surveys of the Lierza Creek consisted in detecting channel gradient, characterizing and assessing sediment size, banks type, valley setting, channel width, and identifying the presence of artificiality. Topography of channel thalweg was measured by dGPS surveys, to an accuracy of 2-3 cm in order to get a detail channel gradient measurement surveying each 10-m spaced site.

Sediments size was determined by sampling 10 sites mainly located on main channel, bars and overbank gravels deposited across floodplains during the flood. We sampled at least 100 clasts per each site by random sampling, measuring the intermediate b-axis (Bunt and Abt, 2001).

Channel banks were classified into three classes: composite banks, with an upper layer of cohesive material (silt and clay) and a lower layer of non-cohesive material (gravels and cobbles), cohesive banks and non-cohesive banks.

Detection of geomorphic changes (i.e., lateral erosion, overbank pebble deposits and landslide coupled to the main stream), their pattern and location consisted in sampling 2-km longitudinal profile upstream of the Molinetto della Croda waterfall, where channel/floodplain adjustments and shallow landslides directly connected to the main channel were observed. The length and height of each lateral erosion scar, and the area and thickness of overbank deposits were measured and located by GPS.

Field records were collected by means of Trimble Nomad hand-held GPS surveys to an accuracy of ± 1-3 m, and subsequently have been exported and mapped for GIS analysis. Whereas, alluvial plain extension was mainly identified using remote sensing approach (i.e., DEM and topographic maps).

2.2. Hydrological analysis

Hydrological analysis focused on the analysis of high spatial and temporal resolution rainfall data obtained by radar observations and rain gauges data, and the evaluation of post event discharge surveys. The consistency of rainfall and discharge observations was verified by applying a distributed rainfall-runoff model (Borga et al., 2008). Post-event surveys were conducted in three cross sections along the Lierza Creek in order to estimate peak discharges. Peak discharge was assessed from high water marks and cross sectional geometry through the Manning-Strickler hydraulic equation under assumption of uniform flow (Gaume and Borga, 2008; Marchi et al., 2009).

2.3. Stream power hydrograph comparison

Time series of discharge data from hydrological modelling are combined with estimate energy slope and channel width to compute stream power hydrographs (equation 1):

$$\varepsilon_t = \int_{t_0}^{T} \{\gamma \,.\, S \,.\, Q\,(t)\,/W\}\, dt \qquad (1)$$

Where ε_t is the cumulated energy expenditure (MJm^{-2}); γ is the specific weight of water (Nm^{-3}); Q is the discharge (m^3s^{-1}); S is the energy slope (mm^{-1}); W is the channel width (m); t is the flood flow duration, t_0-T (hours).

Total energy expenditure represents the distribution of stream power per unit cross-sectional area throughout the flood hydrograph (Costa and O'Connor, 1995; Magilligan et al., 2015) obtained by integrating unit stream power over the duration of the flood event. Observing stream power hydrographs, the event energy expenditure was derived computing the area between the inflation points. The value of the starting point of the energy expenditure on the rising limb corresponds to the unit stream power value at the first rise of event hydrograph, whereas the end point, identified on the recession limb, corresponds to the end of event direct runoff.

In order to evaluate the role of flow duration and total energy expenditure in geomorphic effectiveness of 2014 flood we compared the resulted stream power

hydrographs with those from a previous investigated river affected by a large flood and notable morphological changes (Cassana Creek, northern Apennines) for selected sections with comparable channel gradient.

3. Results

3.1. Geomorphic effects of the Agust 2014 flood in the Lierza Creek

The investigated reach has an average channel width of 7 m and an average channel gradient of 2.5 %. The floodplain width maximum extension resulted 137.8 m and the measure of confinement index (i.e., the ratio between the alluvial plain width including the channel, and the channel width) and the confinement degree (i.e., the percentage of banks directly not in contact with the alluvial plain but with hillslopes or ancient terraces, over the total length of the two banks) turned out to be 14.9 and 10.3, respectively. According to these values the investigated reach can be defined partly confined.

Some examples of the morphological effects caused by the flood are illustrated in Figure 2, while Figure 3 shows the distribution and location of such effects. The surveys exhibited the alternation between affected and unaffected channel portions. The geomorphic effects observed are: lateral bank erosion, floodplain stripping, shallow landslide coupled with the main stream channel, bar formation and cobbles strewn on floodplain.

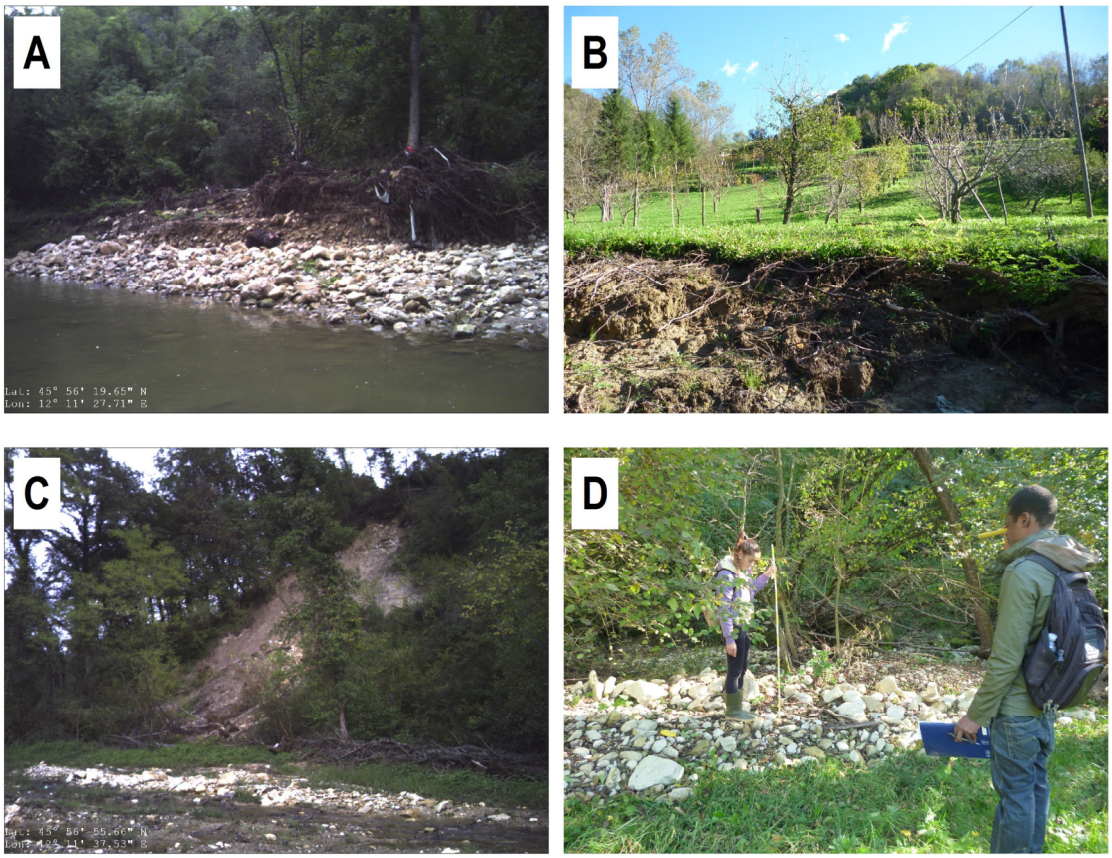

Figure 2. Geomorphic effects: bank lateral erosion and proximal channel bar formation (A); floodplain stripping (B); shallow landslide coupled with the main stream (C); cobbles strewn on floodplain (D).

Lateral erosion occurred mainly in correspondence of non-cohesive and composite banks, and where the floodplain extension was suitable for channel lateral adjustment (i.e., lower lateral confinement), causing bank erosion and floodplain stripping (Figure 2A and 2B) (Table 1).

Stream banks type	*Confinment Index*	*Bank erosion length (m)*	*Bank height (m)*	*Average bank retreat (m)*
cohesive	5.9	11.8	1.6	0.5
composite	8.7	7.2	2.2	3.4
non-cohesive	9.8	25.6	1.8	4.6
composite	17.8	18.5	4.5	1.5
non-cohesive	19.7	7	1	3
non-cohesive	17.8	12	1.5	2.3
cohesive	16.3	11.6	1.7	0.4
non-cohesive	11.7	8	1.6	5
non-cohesive	15.7	4.4	2.3	1.5
non-cohesive	17.9	7.4	1.5	1.4

Table 1. Eroded stream bank types, confinement index, linear length, height and average retreat of stream banks erosion,

However, overall channel width remained quite stable, except for limited locally channel widening. Considering the ratio between post and pre-flood channel width (i.e., width ratio), channel widened maximum to 1.7 times the initial channel width (i.e., from 7 to 11.8 m). Commonly, lateral erosion was associated with variation in channel gradient and took place at local increase in channel slope downstream of the main tributaries (Figure 3).

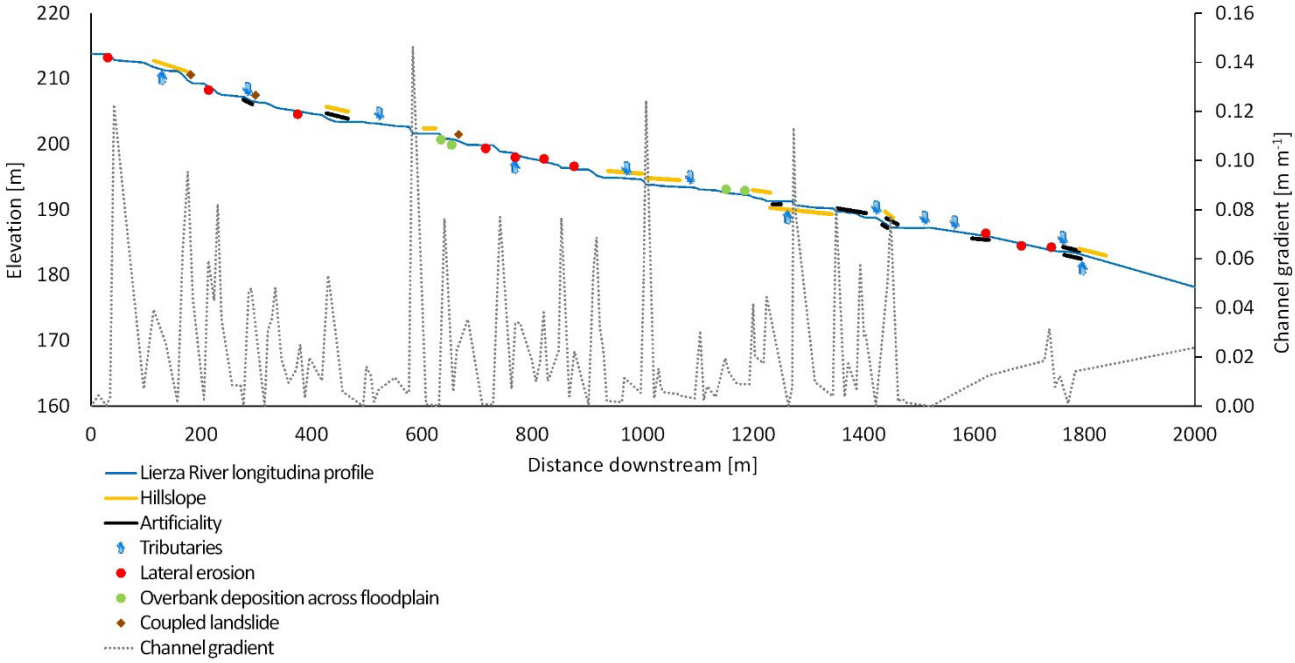

Figure 3. Morphological characteristics and flood effects along the study reach: hillslope and artificial structures confinement, erosion and deposition features location, mass failure location.

Starting from the characterization of banks, 46.6% of the banks are cohesive, while the 8.8% and 3.2% are composite and non-cohesive respectively (Figure 4). The estimation of percentage of minimum potential erodible banks length, excluding longitudinal bank protections and the direct contact with valley slopes representing the 6.8% and the 10.8% respectively, turned out to be the 58.4% of the total surveyed banks. However, the eroded banks represent only the 5.4% (i.e., 114 m) (Figure 4) (Table 1).

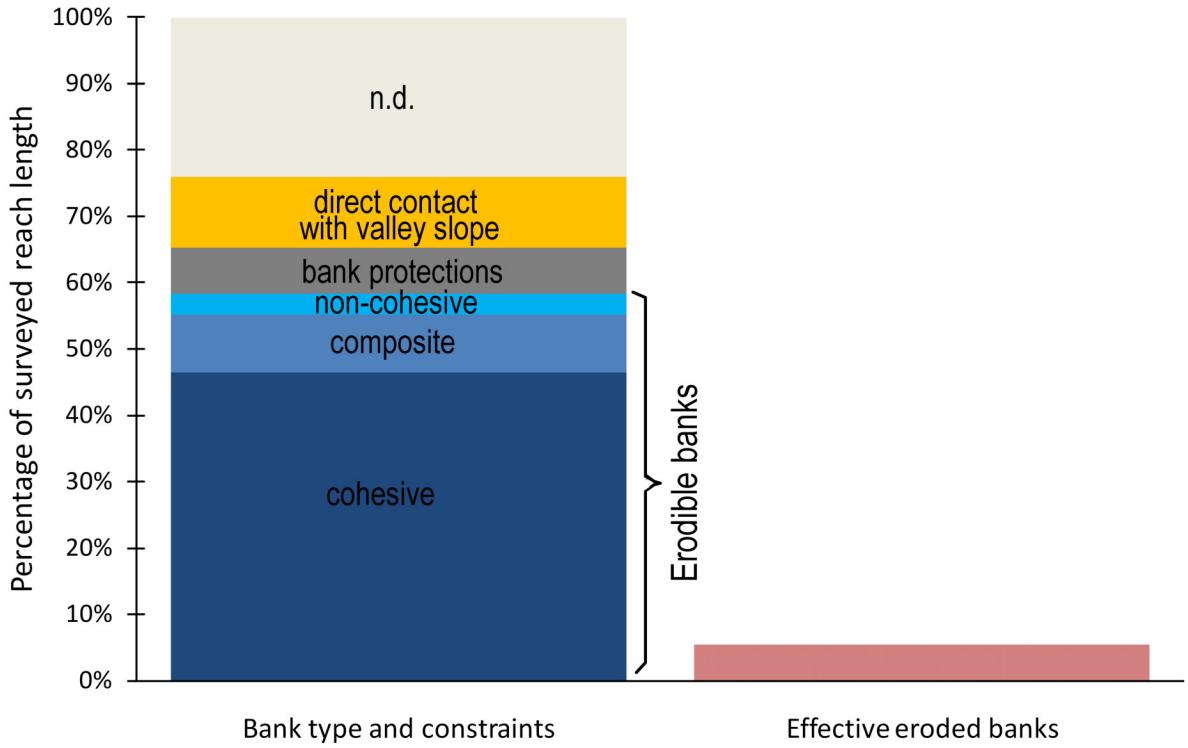

Figure 4. Lateral erosion in relation with bank composition and constraints (natural and artificial). Note. n.d.: no data available.

Particles entrained by the flood were deposited not only in channel proximal settings, where mass failures formed bars in proximity of bank erosion (Figure 2A), but slightly across grass-covered floodplains distal from the channel without any evidences of stripping (Figure 2D).

For the bed-derived particles, clasts subsurface sediment size D_{50} ranged from 78.8 to 113.4 mm in channel up to 143.1 mm for channel bars proximal to lateral erosions. Rather, material deposited proximal to landslides is finer than the material in adjacent channel-proximal bars (i.e., D_{50}=93.3 mm) (Table 2).

Site	D_{50}	D_{16}	D_{84}
Channel	78.8	43.0	128.7
Channel bar proximal lateral erosion	105.3	55.2	240.1
Channel confluence	113.4	64.4	305.4
Channel proximal landslide	93.3	61.0	153.4
Right bank gravel bar proximal lateral erosion	106.8	56.1	297.3
Cobbles strewn on floodplain	99.8	53.2	212.0
Channel	97.2	49.3	229.1
Cobbles strewn on floodplain	107.6	57.0	279.2
Channel	111.2	49.9	227.1
Left bank gravel bar proximal lateral erosion	143.1	68.4	330.0

Table 2. Grain size characteristics D_{50} -median diameter of bed sediment; D_{16} and D_{84} – percentile.

The estimated volumes of overbank coarse material across the floodplain, generally showing lenticular shape, was limited to 20.3 m^3. However, abundant deposition was observed both upstream and immediately downstream to the Molinetto della Croda waterfall (i.e., total volume of 216 m^3, representing the event sediment yield, without considering the amount of suspended sediments) (Veneto Region, 2014). Figure 3 shows that deposition observed along the study reach is mainly associated with local decrease in channel gradient occurring downstream of input of sediment deriving both from few shallow landslides coupled with the main stream or confluences with tributaries.

Destro et al. (2016) have conducted a detail landslide inventory between February and March 2015 in the Lierza basin, obtaining a total of 400 landslides. Landslides density and source area extent seem to be closely correlated to the land use (i.e., 100 landslides/km^2 with source areas less than 50 m^2 in the vineyards; and 42 landslides/km^2 with source areas greater than 50 m^2 in the woodland). However, the authors observed that the majority of those landslides are not effectively coupled with the channel network. Indeed, along the study reach only three shallow landslides affecting the woody slope were observed directly coupled to the stream and contributing to the sediment supply, without obstructing the flow that only in one site diverted across the floodplain (Destro et. al., 2016).

Concerning hydraulic analysis the event was characterized by an extreme flow response. Indirect estimates of peak discharge from flood marks were checked against the results of rainfall-runoff modelling: the two estimates provided consistent results (Destro et al., 2016). The extreme peak discharge observed in this small stream balanced low channel slope not favorable to the formation of high-energy flows (Marchi et al., 2016). Model application to the studied reach resulted in high values of peak discharges varying from 40.3 to 131.6 m^3s^{-1}, and minimum and maximum values in unit peak discharge from 12.2 to 27.6 $m^3s^{-1}km^{-2}$, respectively. The unit stream power was determined using channel cross-sectional geometry considering pre-flood channel width and slope data measured after the flood, nonetheless not notable changes in channel geometry occurred. The unit stream power ω shows the highest peak in the downstream portion of the study reach, achieving values of 40,486 Wm^{-2}.

3.2. Comparison between extreme floods in similar streams

In order to document and clarify the limited geomorphic effectiveness of the August 2014 flood, we investigated the role of both total energy expenditure and peak unit stream power on geomorphic response. To achieve this, a comparison between hydraulic parameters and geomorphic response of the Lierza Creek with the Cassana Creek was carried out.

The Cassana is a small tributary of Pogliaschina River (Liguria Region, Italy) hit by an extreme flood in October 2011, recording 3-hour maximum and event accumulation maxima up to 326 mm and 500 mm, respectively and an estimated unit peak discharge ranging from 11.8 to 20.6 $m^3s^{-1}km^{-2}$ (Marchi et al., 2016). The flood triggered intense geomorphic impacts analyzed in Surian et al. (2016). The Cassana catchment covers a drainage area of 7.9 km^2 and it is mainly composed of sedimentary rocks (predominantly sandstones and mudstones). The channel is a partly confined alluvial reach, characterized by an average channel gradient of 3% and an average initial channel width of 5 m. In this case high values in unit stream power matched intense channel widening during the 2011 flood. The channel featured width ratios from 2 (i.e., from 7.5 to 15 m) up to 8 (i.e., from 3 to 26.4 m) (Surian et al., 2016).

Unit stream power hydrographs comparison (Figure 5A and 5B) shows representing reaches with similar channel gradient, i.e. 5% in hydrograph A, and 5% and 7% in hydrograph B for the Lierza and for the Cassana creeks respectively.

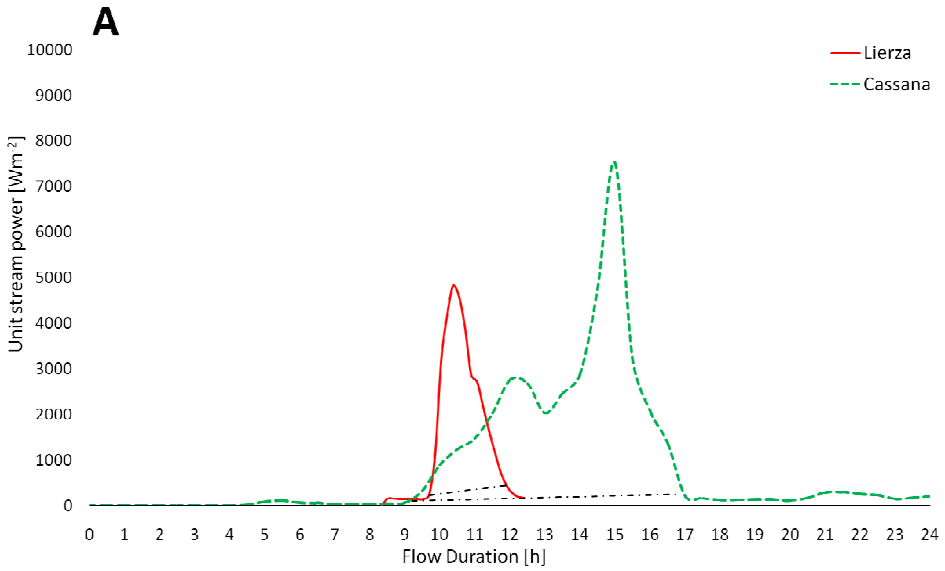

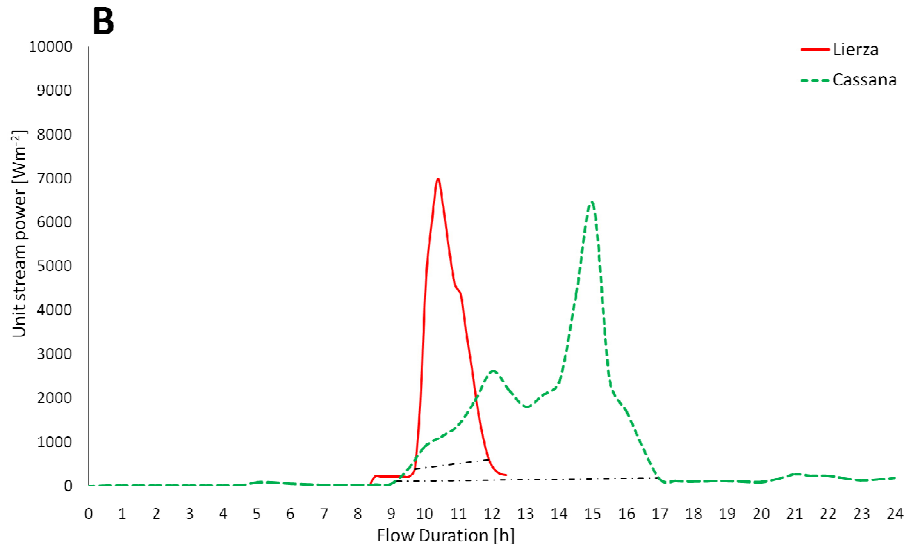

Figure 5. Unit stream power hydrographs: comparison between Lierza (red line) and Cassana (dashed green line). Black dash lines represent inflection points on the stream power hydrograph.

Starting from the observation of hydrograph shape both creeks showed rapidly rising hydrographs, typically associated with flash floods, and usually diverse in processes than those connected to more gradual rising limb hydrographs (Magilligan et al., 2015). Based on this analysis the comparison shows considerable differences in cumulative energy expenditure available for geomorphic adjustment for the Lierza and Cassana respectively. Figure 5A shows the portion of the flood between inflection points resulted in a total energy expenditure of 372 MJm^{-2} along the Lierza, and 1448 MJm^{-2} along the Cassana, corresponding to width ratios of 1.3 and 2 respectively. Figure 5B presents a cross section of the Lierza Creek without changes in channel width and with a total energy expenditure of 555 MJm^{-2}, compared to a cross section of the Cassana Creek featuring a total energy expenditure of 1186 MJm^{-2} and a width ratio of 2. However, the comparison of unit stream power hydrographs for selected cross sections was not sufficient to interpret clearly the role of short duration flood in determining limited geomorphic effects during the 2014 flood.

Analysis of both peak unit stream power and total energy expenditure from all surveyed cross sections show no significant differences in peak flow hydraulics distribution (i.e., 11,178 and 11,849 Wm^{-2} are the mean peak unit stream power values estimated for the Cassana and Lierza respectively), albeit Lierza exhibits maximum values considerably higher (i.e., 40,486 Wm^{-2}) as for Cassana (i.e., 22,617 Wm^{-2}) (Figure 6A). Conversely significant differences characterize total energy

expenditure distribution, showing notable higher values in the Cassana, being 2,043 and 770 MJm^{-2} the mean total energy expenditure, respectively in the Cassana and Lierza (Figure 6B).

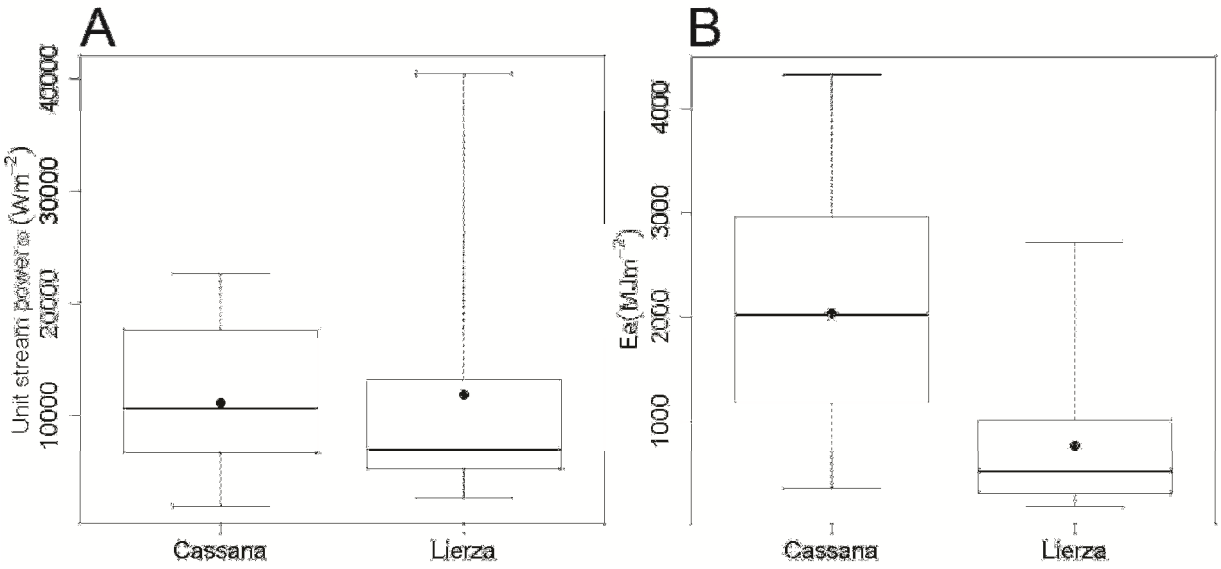

Fig. 6 Peak unit stream power (A) and total energy expenditure (B) distributions for Cassana and Lierza. Plot boxes report lower quartile, median and upper quartile values of unit stream power and total energy expenditure. Whiskers from each end of the box show the data range and black dots the mean values.

Therefore, deeper analysis of hydraulic variables shows a strong linear relations and significant correlations (*p-value*<0.05) between discrete peaks and cumulate energy expenditure values for both Lierza (R^2=0.93) and Cassana creeks (R^2=0.99) (Figure 7). Although the strong correlations between the two hydraulic variables within the same catchment, the 2014 event in the Lierza Creek produces a remarkable different and much lower gradient trend line compared with that for the Cassana Creek during 2011 flood (Figure 7).

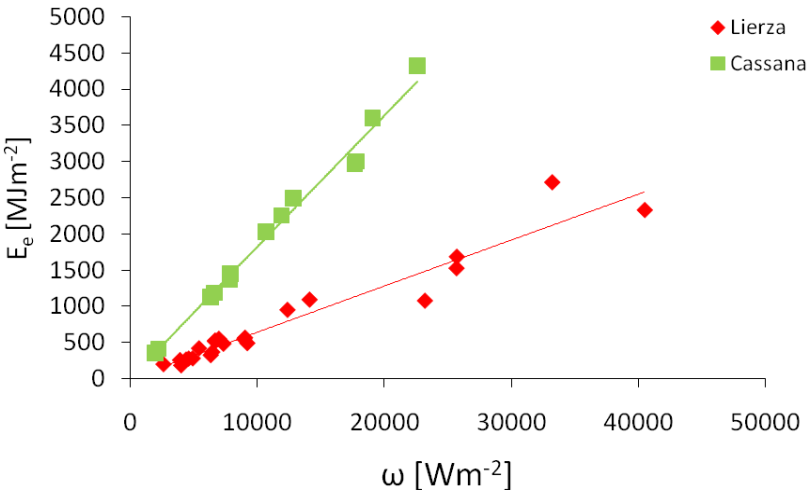

Fig. 7 Total energy expenditure in relation to peak flow hydraulic values (i.e.,unit peak stream power) at surveyed cross sections for Lierza and Cassana creeks.

To demonstrate the potential explanatory roles of both discrete and cumulate energy expenditure in determining channel widening the data on changes in channel width (i.e., width ratio) from all cross sections have been analyzed in relation to the computed peak flow hydraulics (i.e., peak unit stream power) and total energy expenditure derived from the surveyed profiles. Changes in channel width show little consistent relationships to any hydraulic variables at either floods (Figure 8A and 8B). However, higher but weak relations of width ratio to total energy expenditure is observed for both rivers, slightly higher for the Cassana (Figure 8A).

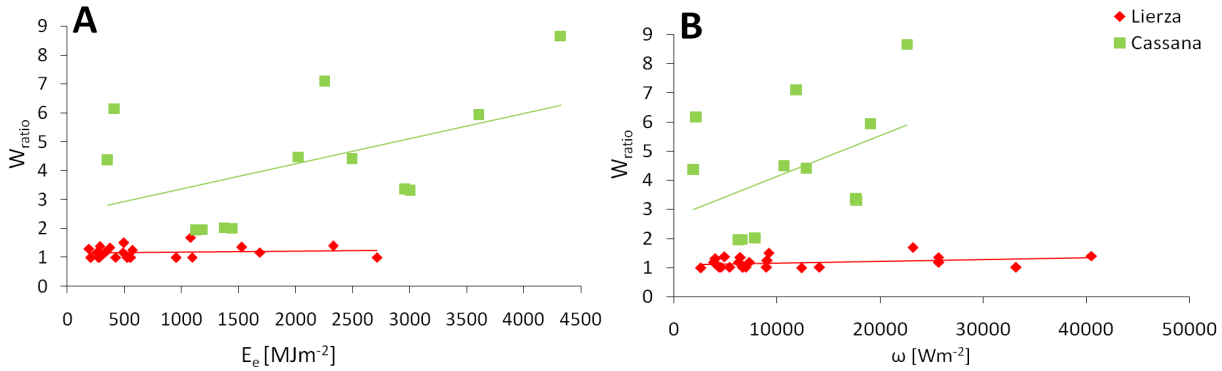

Fig. 8 Width ratio in relation with total energy expenditure (A) and peak unit stream power (B) at surveyed cross sections for Lierza and Cassana creeks.

Lack of consistency in relationships between hydrodynamic forces and channel widening lead to analyze the distribution of available total energy expenditure for channel adjustment during the 2014 flood across three different type of banks characterized by artificial constraints, composite or non cohesive banks, and cohesive banks respectively (Figure 9A). Findings demonstrate significant differences among the three classes. Cross sections with banks characterized by artificial constraints feature highest values (2713 MJm^{-2}) of available total energy expenditure, and a mean value (1499 MJm^{-2}) similar to cohesive banks class energy expenditure mean value (913 MJm^{-2}). Significantly much lower mean value in available energy expenditure was observed in highly erodible banks (356 MJm^{-2}) featuring maximum value below 500 MJm^{-2}. In terms of mean values of width ratio no significant differences were obtained among the three classes (mean width ratio= 1.2) (Figure 9B). However, cohesive banks class shows a lower median value in width ratio tending effectively to no adjustments (median width ratio=1).

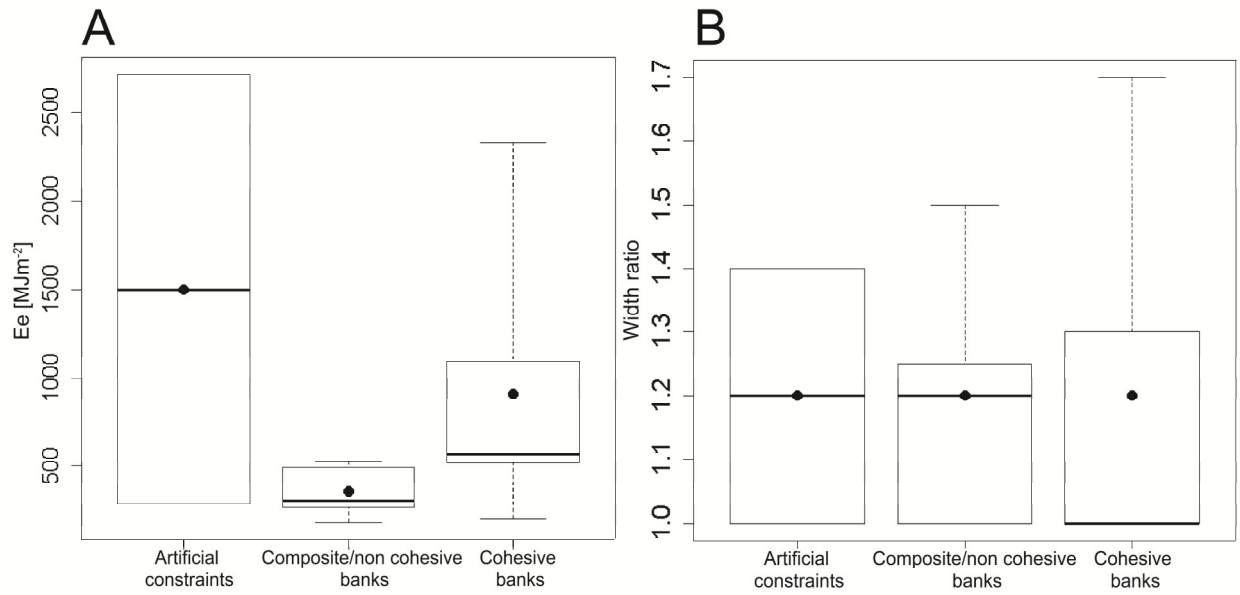

Fig. 9 Total energy expenditure distributions (A) and width ratio (B) for Lierza banks type. Plot boxes report lower quartile, median and upper quartile values of total energy expenditure and width ratio for banks with artificial constraints, composite or non cohesive, and cohesive banks. Whiskers from each end of the box show the data range and black dots the mean values.

4. Discussion and final remarks

Discontinuous occurrence and small magnitude of geomorphic effects along the Lierza Creek contrasts with the flood high intensity and observed high unit peak discharge during the 2014 flood (Marchi et al., 2016). Channel bank erosion and widening are perhaps the most common geomorphic effects associated with flooding (Nardi and Rinaldi, 2015; Magiligan et al., 2015; Surian et al., 2016) commonly producing significant changes in the pre-flood channel morphology.

The changes observed after the 2014 flood are quite small compared with those occurring in the Cassana Creek, albeit comparable values of the peak hydraulic parameters, and grater maximum values were observed for the Lierza Creek. Although high energy flows might have high sediment transport capacity, the Lierza maintained a fairly uniform width and minor local variations occurred (eroded banks represent only the 5.4% of the erodible fluvial corridor). Intense geomorphic effects did not occur even in portions allowing greater capacity for adjustment, as downstream of the largest constrictions (i.e., resistant cohesive banks and bedrock walls, hillslopes, bank protections), and where there are significant portions of floodplain or higher erodible banks.

Findings have confirmed that using stream power independently of duration does not describe the entirety of the event, and total energy, representing both the magnitude and duration of an event (not just discrete peaks in energy expenditure), is more suitable to quantify event magnitudes and to determine the geomorphic effectiveness of a single event. As it was expected, strong correlations between peak stream power and cumulate energy within the same catchment were observed, but noteworthy difference of the trend lines between the compared rivers. Comparable values of peak unit stream power correspond to different values of available total energy expenditure, always higher in the Cassana Creek. In the two studied streams, however, even energy expenditure has shown limited capability in determining the amount of channel adjustment in terms of channel widening.

Beside hydrodynamic forces express in terms of peak unit stream power, the coupled influence of total energy over the flow duration and channel boundary resistance related to the geomorphic and geologic characteristics of the system (e.g., lateral confinement, bank type, lithology) gave only locally limited changes, confirming that geomorphic response is not always proportional to event magnitude. Bank composition (i.e., occurrence of cohesive, composite or non-cohesive banks) and lateral constraints (bank protections) are likely significant controlling factors of geomorphic response in the Lierza Creek.

The same size flows can have different effects depending on the state and initial conditions of the system (i.e., intrinsic thresholds) interrelated to the available energy expenditure over the course of the flood. Likewise, in the domain of flash floods (i.e., floods with rapid rise rates and short flow duration) a high magnitude flood can generate pervasive or negligible geomorphic effects, depending on the flood duration and energy expenditure combined with the complexity of the pre-flood system conditions.

References

Borga, M., Gaume, E., Creutin, J.D., Marchi, L., 2008. Surveying flash floods: gauging the ungauged extremes. Hydrol. Process. **22**: 3883–3885.

Costa, J.E., O'Connor, J.E., 1995. Geomorphically effective floods. In: Costa, J.E., Miller, A.J., Potter, K.W., Wilcock, P. (Eds.), Natural and Anthropogenic Influences in Fluvial Geomorphology. Monograph, vol. **89**. American Geophysical Union, Washington, D.C., pp. 45–56.

Dean, D.J., Schmidt, J.C., 2013. The geomorphic effectiveness of a large flood on the Rio Grande in the Big Bend region: Insights on geomorphic controls and post-flood geomorphic response. Geomorphology **201**: 183–198.

Destro, E., Marchi, L., Amponsah, W., Tarolli, P., Crema, S., Zoccatelli, D., Marra, F., Borga M., 2016. Hydrological analysis of the flash flood event of August 2, 2014 in a small basin of the Venetian Prealps. Quaderni di Idronomia Montana **34** (in Italian).

Gaume, E., Borga, M., 2008. Post-flood field investigations in upland catchments after major flash floods: proposal of a methodology and illustrations. J. Flood Risk Manage **1**: 175–189.

Hooke, J.M., 2016. Morphological impacts of flow events of varying magnitude on ephemeral channels in a semiarid region. Geomorphology **252**: 128–143.

Magilligan, F.J., Buraas, E.M., Renshaw, C.E., 2015. The efficacy of stream power and flow duration on geomorphic responses to catastrophic flooding. Geomorphology **228**: 175-188.

Marchi, L., Borga, M., Preciso, E., Sangati, M., Gaume, E., Bain, V., Delrieu, G., Bonnifait, L., Pogačnik, N., 2009. Comprehensive post-event survey of a flash flood in Western Slovenia: observation strategy and lessons learned. Hydrol. Process. **23** (26): 3761–3770.

Marchi, L., Cavalli, M., Amponsah, W., Borga, M., Crema,S., 2016. Upper limits of flash flood stream power in Europe, Geomorphology **272**: 68-77. doi.org/10.1016/j.geomorph.2015.11.005.

Miller, A.J., 1987. What does it take to make a geomorphically effective flood? Some lessons from the November 1985 flood in West Virginia. In: Kite, J.S. (Ed.), Research on the Late Cenezoic of the Potomac Highlands, West Virginia. Open File Rep. OF8801.West Virginia Geol. and Econ. Survey, Morgantown,WV, 3–30.

Nardi, L., Rinaldi, M., 2015. Spatio–temporal patterns of channel changes in response to a major flood event: the case of the Magra River (central–northern Italy). Earth Surface Processes and Landforms **40**: 326 – 339.

Regione del Veneto-Sezione Bacino idrografico Piave Livenza - Sezione di Treviso (2014). Stima della portata massima transitata sul fiume Lierza in occasione dell'evento di piena del 2 Agosto 2014, in località "Molinetto della Croda" (Comune di Refrontolo). Integrazione alla relazione idrologica e idraulica del 14 Agosto 2014. (in italian)

Surian, N., Righini, M., Lucìa, A., Nardi, L., Amponsah, M., Benvenuti, M., Borga, M., Cavalli, M., Comiti, F., Marchi, L., Rinaldi, M., Viero, A., 2016. Channel response to extreme floods: insights on controlling factors from six mountain rivers in northern Apennines Italy. Geomorphology: **272**, 78–91. doi:10.1016/j.geomorph.2016.02.002.

Wohl, E., 2010. Mountain rivers revisited. AGU, Water Resources Monograph **19**.

Wolman, M.G., Gerson, R., 1978. Relative scales of time and effectiveness of climate in watershed geomorphology. Earth Surface Processes and Landforms **3**: 189–208.

PART III – CONCLUSIONS

7. FINAL REMARKS

The results of this thesis emphasise the importance of documentation of extreme floods for interpreting geomorphic processes responsible for channel changes, the complexity and the wide variability in channel sensitivity to change, and the importance of a synergic use of different methods to provide a fundamental knowledge for understanding the geomorphic effects (Appendix 1). Furthermore, the present availability of high spatial resolution data offers great opportunities and new challenges in the analysis of flood geomorphic response allowing a synoptic view of channel dynamics of individual flood events across different spatial scales, as well as measurements of the whole river corridor over long distances (Chapter 2).

The three studied events featured typical characteristics of catastrophic floods including low frequency occurrence and magnitude great enough to exceed thresholds needed for notable geomorphic changes.

Findings of this work permitted to develop a conceptual model describing the expected channel behavior in response to a large flood starting from specific initial morphological conditions, built on the most significant controlling factors resulted from the statistical analysis of observed changes (Figure 1). The model provides basis to improve our capability of predicting channel dynamics and, therefore, geomorphic hazard.

Planimetric changes were the main focus of the study because channel widening and the reactivation of wide portions of the floodplain turned out to be the most remarkable morphological responses to the floods. In alluvial channels, distinctly different processes responsible for channel widening were observed during the post-flood analysis (i.e., field reconnaissance and interpretation of post-flood images): i) bank erosion and retreat; ii) overbank deposition of bedload material on the floodplain; iii) island erosion; iv) erosion of valley slopes. In semi-alluvial channels the main process causing channel widening is also related to topsoil and valley bottom vegetation erosion, especially in bedrock constrained (i.e., channel laterally confined by competent bedrock but having an alluvial bed) and bedrock confined (i.e., channel with a rocky bed but with alluvial sidewalls) channel portions, without an effective adjustment of channel cross-sectional geometry (Figure 1). Channel widening was very relevant (i.e., width ratio

ranging from 2 to 10) in most cases, and it varied from very high (i.e., width ratio ranging from 10 to 20) to moderate (i.e., width ratio up to 2) in unconfined alluvial channels were the largest changes in channel width were observed. In confined, semi-alluvial rivers lower adjustments occurred, especially in combination with short duration floods (i.e., width ratio very close to 1). Fluvial valley side erosion was observed in several reaches. This process mostly occurred in the upstream part of the study catchments, generally characterized by confined valley with limited floodplain and high channel gradient. Fluvial valley side erosion was particularly pronounced in confined and partly confined semi-alluvial and steeper partly confined alluvial channels, showing in most of cases that the widening was not limited by the lateral extent of the erodible corridor (Figure 1).

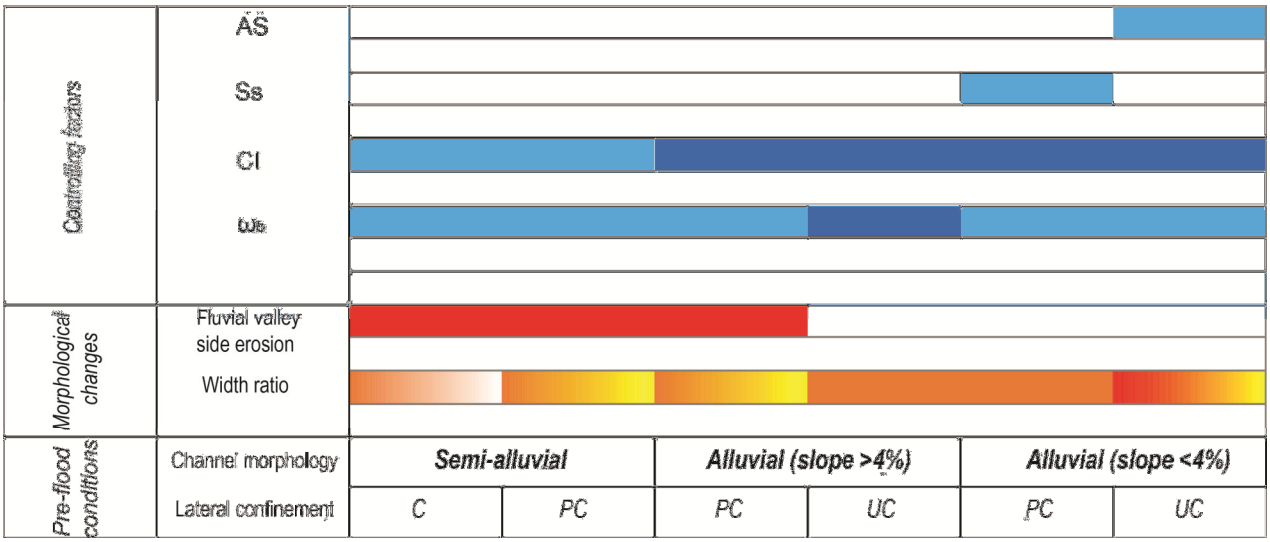

Figure 1. Conceptual model describing morphological response to extreme floods and most influential controlling factors in alluvial and semi-alluvial rivers. Lateral confinement - C: confined; PC: partly confined; UC: unconfined. Morphological changes - Width ratio: very high, i.e. up to 20 (red); high, i.e. from 2 to 10 (orange); moderate, i.e. up to 2 (yellow); very low or negligible (white) - Fluvial valley side erosion: high probability of occurrence (red); low probability of occurrence (white). The role of controlling factors in determining morphological changes - major (blue): minor or moderate (light blue); negligible (white); - ω_b: peak unit stream power calculated using pre-flood channel width; CI: confinement index; Ss: sediment supply; AS: artificial structures.

A deeper analysis of channel width changes underlined two different behaviours depending on the initial channel width. Notable channel width changes were observed in the lower gradient, alluvial channels analyzed. Larger variability in width ratios as well as the largest widening occurred in the narrower reaches, while less intense channel widening occurred in larger alluvial reaches (Krapesch et al., 2011) (Chapters 3, 4 and 5) (Figure 2). Results also point out that the greater geomorphic effects occurred in the smaller basins (Figure 2), with the exception of the Lierza Creek, where these effects were negligible, and in the middle portions of larger drainage basins (Wohl, 2008).

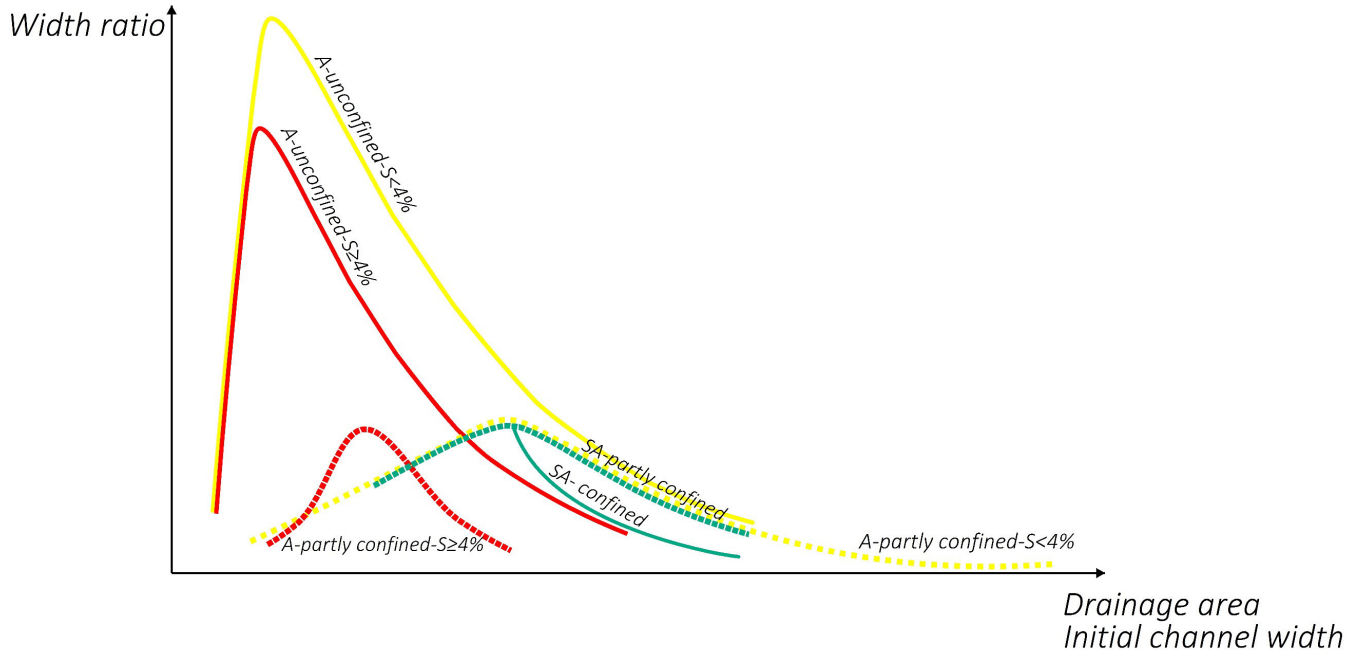

Figure 2. Relationships between channel widening (i.e., width ratio) and drainage area and initial channel width for different morphological settings.

Findings show that flood-driven geomorphic changes are controlled by several factors, both morphological and hydraulic ones, that result in variable patterns of change thereby reflecting the physical complexity of the river system and the complex nature of high-magnitude events (Costa and O'Connor, 1995; Krapesch et al., 2011; Thompson and Crooke, 2013; Buraas et al., 2014; Nardi and Rinaldi, 2015) (Chapter 3, 4 and 5). Results point out that hydraulic forces are often not sufficient to explain satisfactorily the channel response to extreme floods and the inclusion of other factors is needed to increase the explanatory capability of channel response model.

Valley morphology provides the template in which channel form and process adjust to change, and variations in valley-bottom width and gradient can constrain channel adjustment to perturbations (Wohl, 2010). Indeed, and not surprisingly, the channel confinement – expressed in terms of confinement index - resulted the most relevant explanatory variable for planimetric changes. Low lateral confinement controlled channel widening in alluvial reaches with mobile bed in valley portions that allowed greater capacity for adjustment far from the hillslopes and with extended floodplains. Nonetheless, not always lateral confinement limits planimetric changes in partly confined and confined semi-alluvial channels, as very high flood power can erode hillslopes toes and thus determine channel widening (Chapter 3, 4 and 5) (Figure 1).

Other controlling factors such as woody vegetation cover, channel sinuosity, input of sediments, and artificial structures do not have such explanatory power at the sub-reach scale, but were relevant at some specific sites. Marginal vegetation as well as floodplain vegetation were considerably modified by the floods that occurred in the Magra and Posada catchments. However, the presence of vegetation did not play a significant role in channel widening, similar to what observed in other high-magnitude events in mountain rivers (Lucìa et al., 2015; Comiti et al., 2016). Clearly, major floods in mountain rivers overcome the resistance threshold that vegetation can provide (Dunkerley, 2014).

Different sources of sediment were observed within the investigated rivers, i.e. coupled landslides, bank erosion and tributaries. Despite sediment supply might be one of the factors controlling channel changes during extreme floods, no statistically significant role was found, except for the lower gradient, alluvial reaches. High-energy flows can have profound sedimentological effects, and sediment supply could be likely more significant in determining channel-bed incision or aggradation. However, due to the lack of data, it was not possible to assess whether major bed-level changes occurred in conjunction with planform variations.

The analyzed rivers were characterized by a diverse degree of human pressures in terms of bank protections (i.e., ranging from 0% up to 70% of reach length), which may have hindered lateral channel mobility. Although there were several artificial structures, in many reaches they did not prevent channel widening, especially in lower gradient unconfined alluvial channels, where the channel took up the whole alluvial plain after destroying the existing bank protections. However, locally bank protections may have some effects in limiting channel lateral mobility in unconfined alluvial channels (Chapter 3) (Figure 1).

Concerning hydraulic variables, the delineation of peak unit stream power faced with a great difference between initial and post-flood channel width. Neither pre-flood nor post-flood channel width is proper for the estimation of peak unit stream power, as the most appropriate would be the width at the flood-peak time. The present findings point out that peak unit stream power calculated using pre-flood channel width is the most significant predictor of channel widening among the hydraulic parameters that were evaluated, at least in streams that underwent intense widening. However, it has major role in determining channel width changes in alluvial reaches, suggesting that most of

width changes occurred after the flood peak, especially in alluvial sub-reaches (Chapter 3, 4 and 5). In semi-alluvial channels characterized by more resistant boundaries (e.g., confined and partly confined or cohesive river banks), the peak unit stream power has a smaller explanatory capability for channel widening comparing to alluvial channels (Chapter 5 and 6). Although the higher values in peak unit stream power were observed in confined and partly confined semi-alluvial reaches, here channel widening did not reach large magnitudes possibly because they represent a zone of resistant constriction causing negligible or moderate morphological effects, leading to higher morphological adjustments occurring immediately downstream (Dean and Schmidt, 2013)

However, a large variability in geomorphic response was observed within semi-alluvial channels. Therefore, the presence of resistant boundaries (i.e., cohesive banks and/or bedrock walls) sharpening the thresholds between driving and resisting forces in controlling geomorphic adjustment and promoting preferential bank erosion, combined with the influence of flow duration and cumulated energy expenditure may explain the wide variability of geomorphic effectiveness from significant to negligible effects (Chapter 6).

Recently, Buraas et al. (2014) stated that there is still a general lack in the capability to predict where major geomorphic changes take place during an extreme flood event. Therefore, in terms of hazard, documenting the type and magnitude of channel response is crucial to identify controlling factors of such response, to develop tools (e.g., Event Dynamics Classification, Chapter 4) for channel dynamic predictions, and thus to support a sound planning of river corridors.

The proposed conceptual model (Figure 1) provides a preliminary basis for i) describing magnitude and patterns of channel planimetric changes for mountain streams located in the Mediterranean areas and ii) defining the most influential controlling factors. Additional post-flood datasets would enhance the current study and could provide a validation of the proposed model. In conclusion, the results of this thesis have provided i) a quantification and detailing analysis of magnitude and patterns of planimetric changes during extreme events, ii) the identification of several potential controlling factors among geomorphic and hydraulic driving forces and the analysis of their mutual role in determining morphological changes, iii) the development of empirical and conceptual models suitable for specific physiographic and hydrologic characteristic areas.

Implication for flood management

Knowledge of channel evolution and channel short-term adjustment and its causes might be used as basis for defining flood management strategies and sustainable interventions. This study puts forward new basis for tools enabling to define appropriate strategies for assessing the amount of channel effects to mitigate flood risk in ungauged mountain streams. Strategies need to allow for the channel changes, and this is beginning to be sighted in such ideas as 'minimum morphological spatial demand of rivers' (Krapesch et al., 2011) or 'freedom space' of rivers (Biron et al., 2014).

Generally identification of the trajectories of channel evolution according to potential management strategies does not include the morphological adjustment of very large flood events because of i) the great uncertainty in assessing such effects (Rinaldi et al., 2011; Surian et al., 2011), ii) the lower magnitude of widening compared to long term channel changes magnitude (but very high intensity concentrated in a very short time), iii) the consideration that a short-term fluctuation of channel width does not counteract the long-term river evolution (Rinaldi et al., 2011).

The illustrated geomorphic approach is a structured procedure for a detail analysis at adequate investigation spatial scale reflecting local conditions (i.e., sub-reach scale), suitable for supporting the design of flood hazard maps, interventions and mitigation measures through the identification of hydrologic and geomorphic thresholds depending on the capacity of the river to react to high magnitude adjustment. Therefore, the identification of the most significant variables and indicators related to geomorphic changes is a key to define interventions type and setting, not restricted to the erodible corridor, and to develop specific land-use policies and associated tools for planning, from local to catchment scale.

The results of the thesis will allow river managers to define reaches with natural tendency to lateral mobility and changes in channel width, thus enhancing geomorphic approaches to river management, by assuming present boundary conditions as starting point to understand channel variability and to provide a short term vision of river functioning.

For these reasons understanding how a river channel adjusts to large flood events may have important implications for a series of management issues, including i) increasing effort to mitigate high-magnitude floods consequences; ii) understanding how

different management strategies and land use scenarios could affect channel dynamics; iii) understanding of their role in the long-term geomorphic trajectory; iv) predicting more complex evolutionary trajectories, likely future trends and recovery potential; v) promoting design actions requiring knowledge from different disciplines; vi) supporting sustainable regional actions aimed at flood risk mitigation.

References

Buraas, E.M., Renshaw, C.E., Magilligan, F.J., Dade,W.·.B., 2014. Impact of reach geometry on stream channel sensitivity to extreme floods. Earth Surf. Process. Landf. **39**: 1778 – 1789.

Biron, P.M., Buffin-Bélanger, T., Larocque, M., Choné, G., Cloutier, C.A., Ouellet, M.A., Demers, S., Olsen, T., Desjarlais, C., Eyquem, J., 2014. Freedom space for rivers: a sustainable management approach to enhance river resilience. Environ. Manag. **54**, 1056–1073.

Costa, J.E, O'Connor, J.E., 1995. Geomorphically effective floods. In Natural and Anthropogenic Influences in Fluvial Geomorphology, Costa JE, Miller AJ, Potter KW, Wilcock PR (eds). Geophysical Monograph **89**, The Wolman Volume, American Geophysical Union: Washington, DC. 45 – 56.

Croke, J., Fryirs, K.,Thompson, C., 2013. Channel–floodplain connectivity during an extreme flood event: implications for sediment erosion, deposition, and delivery. Earth Surf. Process. Landforms **38**: 1444 – 1456. DOI: 10.1002/esp.3430

Dean, D.J., Schmidt, J.C., 2013. The geomorphic effectiveness of a large flood on the Rio Grande in the Big Bend region: Insights on geomorphic controls and post–flood geomorphic response. Geomorphology **201**: 183 – 198.

Krapesch, G., Hauer, C., Habersack, H., 2011. Scale orientated analysis of river width changes due to extreme flood hazard. Natural Hazards and Earth System Sciences **11**: 2137 – 2147.

Lucía, A., Comiti, F., Borga, M., Cavalli, M., Marchi, L, 2015. Dynamics of large wood during a flash flood in two mountain catchments. Natural Hazards and Earth System Sciences, **15** (8): 1741–1755.

Magilligan, F.J., Buraas, E.M., Renshaw, C.E., 2015. The efficacy of stream power and flow duration on geomorphic responses to catastrophic flooding. Geomorphology **228**: 175 – 188.

Nardi, L., Rinaldi, M., 2015. Spatio–temporal patterns of channel changes in response to a major flood event: the case of the Magra River (central–northern Italy). Earth Surface Processes and Landforms **40**: 326 – 339.

Rinaldi, M.; Piégay, H.; Surian, N., 2011. Geomorphological approaches for river management and restoration in Italian and French rivers. In: A.Simon, S.E.Bennett, J.M.Castro. Stream restoration in dynamic fluvial systems: scientific approaches, analyses and tools, pp. 95-113, Washington DC, USA: American Geophysical Union, Geophysical Monograph Series **194**.

Rinaldi, M,. Surian, N., Comiti, F., Bussettini, M., 2013. A methodological framework for hydromorphological assessment, analysis and monitoring (IDRAIM) aimed at promoting integrated river management. Geomorphology **251**: 122 – 136.

Surian, N.; Rinaldi, M.; Pellegrini, L., 2011. Channel adjustments of alluvial channels and implications for river management and restoration. Geogr. Fis. Dinam. Quat., **34**: 145-152, ISSN:0391-9838

Thompson, C., Croke, J., 2013. Geomorphic effects, flood power, and channel competence of a catastrophic flood in confined and unconfined reaches of the upper Lockyer valley, southeast Queensland, Australia. Geomorphology **197**: 156 – 169.

Wohl, E., 2008. Review of effects of large floods in resistant–boundary channels, in Gravel–Bed Rivers VI: From process Uderstanding to River Restoration, edited by H., Habersack, H., Piégay, and M., Rinaldi, pp. 181 – 212, Elselvier, Amsterdam.

Wohl, E., 2010. Mountain rivers revisited. AGU, Water Resources Monograph **19**.

APPENDIX

APPENDIX 1. AN INTEGRATED APPROACH FOR INVESTIGATING GEOMORPHIC RESPONSE TO EXTREME EVENTS: METHODOLOGICAL FRAMEWORK AND APPLICATION TO THE OCTOBER 2011 FLOOD IN THE MAGRA RIVER CATCHMENT, ITALY

Massimo Rinaldi[1*], William Amponsah[2], Marco Benvenuti[1], Marco Borga[3], Francesco Comiti[4], Ana Lucía[4], Lorenzo Marchi[2], Laura Nardi[1], Margherita Righini[5], Nicola Surian[5]

[1]Department of Earth Sciences, University of Florence, Italy; [2]CNR IRPI, Padova, Italy; [3]Department of Land, Environment, Agriculture and Forestry, University of Padova, Italy; [4]Faculty of Science and Technology, Free University of Bozen-Bolzano, Italy; [5]Department of Geosciences, University of Padova, Italy

Earth Surf. Process. Landforms 41, 835–846, 2016

Abstract

A high-magnitude flash flood, which took place on 25th October 2011 in the Magra river catchment (1717 km^2), central-northern Italy, is used to illustrate some aspects of the geomorphic response to the flood. An overall methodological framework is described for using interlinked observations and analyses of the geomorphic impacts of an extreme event.

The following methods and analyses were carried out: (i) hydrological and hydraulic analysis of the event; (ii) sediment delivery by event landslide mapping; (iii) identification and estimation of wood recruitment, deposition, and budgeting; (iv) interpretation of morphological processes by analysing fluvial deposits; (v) remote sensing and GIS analysis of channel width changes.

In response to the high-magnitude hydrological event, a large number of landslides occurred, consisting of earth flows, soil slips, and translational slides, and a large quantity of wood was recruited, in most part deriving from floodplain erosion caused by bank retreat and channel widening. The most important impact of the flood event within the valley floor was an impressive widening of the overall channel bed and the reactivation of wide portions of the pre-event floodplain. Along the investigated (unconfined or partly confined) streams (total investigated length of 93.5

km), the channel width after the flood was up to about 20 times the channel width before the event.

The study has shown that a synergic use of different methods and types of evidence provides fundamental information for characterising and understanding the geomorphic effects of intense flood events. The prediction of geomorphic response to a flood event is still challenging and many limitations exist; however a robust geomorphological analysis can contribute to the identification of the most critical reaches.

Introduction

Over the last years, the Mediterranean region has been affected by an increasing number of heavy precipitation events causing flash floods, debris flows and other types of landslides, as well as severe morphological channel changes (Llasat et al., 2010; Boudevillain et al., 2011; Tarolli et al., 2012; Flaounas et al., 2013). The peninsular part of Italy is particularly prone to this type of phenomenon, due to a combination of distinctive topographic and meteorological characteristics (Salvati et al., 2010). Precipitation events with rainfall greater than 100 mm in less than one day are not unusual, and are likely to increase in the near future as a consequence of climate change, causing notable management concerns (Giorgi, 2006).

High intensity flood events can significantly affect channel morphology, inducing drastic bed level adjustments and/or dramatic planform adjustments in unconfined settings. Several studies have documented morphological changes occurring in response to flood events, and a wide range of responses has been reported (e.g., Harvey, 1984; Miller, 1990; Lapointe et al., 1998; Magilligan et al., 1998; Heritage et al., 2004; Fuller, 2008; Arnaud-Fassetta, 2013; Thompson and Croke, 2013). However, few studies provide high quality and quantitative morphological change data related to very infrequent extreme floods.

Forecasting the occurrence of flash floods and predicting their impacts on the fluvial system are challenging. The accuracy of forecasting is still insufficient to allow reliable prediction of the amount, timing, and basin-specific locations of the meteorological event and of the morphological responses in the river system. With

this in mind, advances in the identification of the predominant mechanisms, and particularly of their interactions across different spatial scales, are required.

The complex pattern of an extreme meteorological event and the high spatial variability of the morphological responses require the use of a wide range of measurements and 'observational' methods. Integrated and interlinked approaches can be the key for a better understanding and prediction of such events and their morphological responses.

A range of methods has been used to analyse the geomorphic responses to large floods. These mainly include: (i) reconstruction of the hydrological event by various sources of data and intensive post-event campaigns (e.g., Gaume et al., 2004); (ii) analysis of flood hydraulic variables (e.g., Howard and Dolan, 1981; Miller, 1990; Wohl et al., 1994; Benito, 1997; Heritage et al., 2004; Thompson and Croke, 2013); (iii) event landslide mapping and sediment connectivity (e.g., Wells and Harvey, 1987; Guzzetti et al., 2012); (iv) dynamics of large wood (e.g., Lucìa et al., 2015); (v) geomorphic and sedimentological analysis of flood deposits (e.g., Wells and Harvey, 1987; Macklin et al., 1992); (vi) quantification of channel changes by field or remotely-sensed data (e.g., Arnaud-Fassetta et al., 2005; Krapesch et al., 2011; Thompson and Croke, 2013) and morphological sediment budgeting (e.g., Fuller, 2008; Milan, 2012; Thompson and Croke, 2013). Notwithstanding this variety of methods and approaches, few studies have attempted to integrate various data sources and methods to analyse the geomorphic impacts of extreme events.

In this paper, a major flash flood event which took place on 25th October 2011 in the Magra river catchment, central-northern Italy, is used as a study case, aiming to: (i) describe and discuss an overall methodological framework for analysing the geomorphic impacts of an extreme event; (ii) illustrate some general aspects of the geomorphic response to the flood. More detailed analyses and discussion of specific aspects of the 25th October 2011 flood event in the Magra catchment are reported in a series of other papers (Mondini et al., 2014; Nardi and Rinaldi, 2015; Lucìa et al., 2015; Surian et al., 2015). The main novelty of this paper consists in the presentation of an integrated approach combining various data sources, observations and analyses to support an understanding of the geomorphic impacts of extreme events.

Study area

The Magra catchment (Fig. 1) covers an area of 1717 km2 and extends over the inner portion of the Northern Apennines. The middle and upper portion of the catchment is dominated by hilly and mountain areas, with a basin relief of 1901 m, whereas the lower part, downstream from the confluence with the Vara River, is occupied by a large (up to 3 km wide) alluvial and coastal plain (Fig. 1A). The catchment is composed of rocks arranged into distinct units (Fig. 1B) delimited by regional NW-SE trending thrust faults piled up since the early Cenozoic.

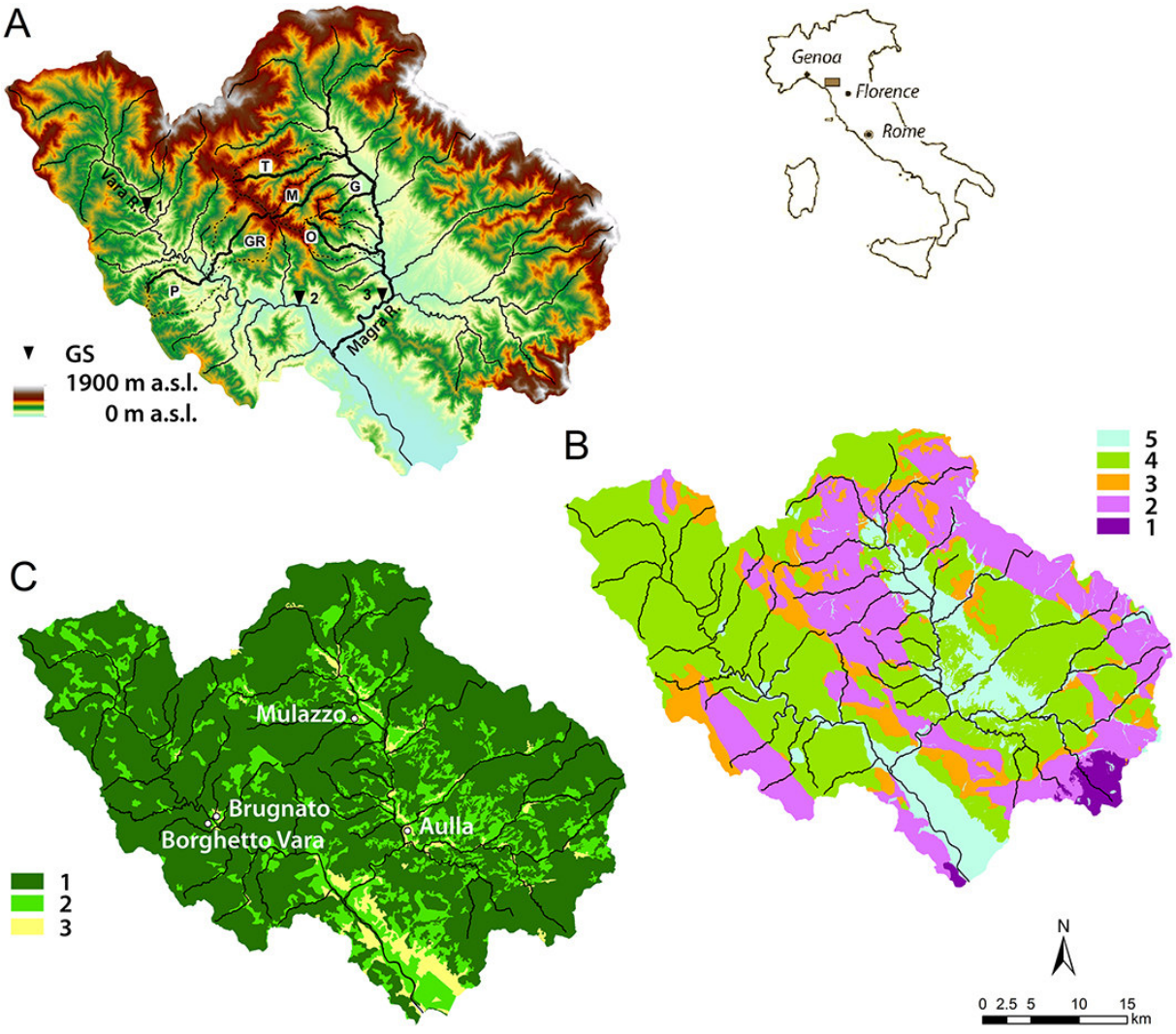

Figure 1. Main characteristics of the Magra catchment. A: representation by DEM and investigated sub-catchments. T: Teglia; M: Mangiola; G: Geriola; O: Osca; GR: Gravegnola; P: Pogliaschina. Streams investigated in this study are indicated with a thick line. GS: gauging stations used for the rainfall-runoff model calibration. 1: Nasceto; 2: Piana Battolla; 3: Calamazza. B: Geological setting. 1: Metamorphic Tuscan Units (Triassic-Lower Neogene); 2: Non Metamorphic Tuscan Units (Triassic-Lower Neogene); 3: Sub-Ligurid Units (Eocene-Oligocene); 4: Ligurid Units (Jurassic-Eocene); 5: Fluvio-lacustrine deposits (Neogene-Quaternary). C: Land use. 1: Forests and semi-natural areas; 2: agricultural lands; 3: urbanised and artificial areas.

The lithological nature of the catchment in large part made of easily erodible arenaceous and muddy bedrock results in high sediment delivery. Land cover is mainly forest and semi-natural areas (79% total cover), followed by agriculture (18%) which dominates, together with artificial and urban areas (3% of the total cover), in the downstream part of the catchment (Fig. 1C). About 158.000 people live within the Magra river basin, mainly concentrated in the lower part of the catchment.

The precipitation event took place on October 25th 2011, with hourly rainfall intensities of up to 130 mm h-1 and a peak in rain accumulation exceeding 500 mm in eight hours. The storm triggered a flash flood with very intense specific peak floods, in some cases exceeding 20 m3 s-1 km-2, corresponding to return periods exceeding 200-300 years.

In this study, we analysed a series of streams and related sub-catchments (Teglia, Mangiola, Osca, Geriola, middle portion of the Magra, Gravegnola, Pogliaschina) located in the Magra basin area with the most rainfall (Fig.1). They have been selected because they represent the areas affected by the most impressive morphological changes and associated damages. In fact, the event originated severe flood damage and loss of lives in some of the towns located in the valley floor of these sub-catchments (e.g., Borghetto Vara, Brugnato, Aulla), and/or damage associated to landslides and intense mass transport along small tributaries (e.g., Mulazzo) (Fig. 1). The main characteristics of the investigated sub-catchments are summarised in Table 1. Mean annual discharge along the middle portion of the Magra River recorded at the Calamazza gauging station (drainage area 932 km2, Fig. 1) is 40 m3 s-1 (corresponding to a unit mean annual discharge of about 0.04 m3 s-1 km-2).

Other major flood events have occurred in the Magra catchment during about the last 100 years (e.g., 1940, 1954, 1959, 1966, 1999, 2000), although reliable information on flood peak discharge and return period of these past events is scarce.

Stream	Drainage area (km²)	Basin relief (m)	Stream length (km)	Bed slope (%)	D_{50} (mm)	Q_{pk} (m³/s)	*Unit* Q_{pk} (m³ s⁻¹ km⁻²)
Teglia	38.8	1035	14.8	4.9	47 – 69	538	13.9
Mangiola	26.2	1012	12.9	6.6	41 – 95	406	15.5
Geriola	8.5	884	7.2	8.8	n.a.	121	14.2
Osca	21.8	962	9.9	4.1	44 – 65	279	12.8
middle Magra	956	1825	32.2	0.6	25 – 52	4200	4.4
Gravegnola	34.6	1106	12.8	7.0	33 – 79	523	15.1
Pogliaschina	25.1	625	9.1	5.6	24 – 36	595	23.7

Table 1. General characteristics of the investigated rivers. Middle Magra refers to the portion upstream from the confluence of the Vara River (see Fig. 1). D_{50}: median diameter of bed sediment (n.a.: not available); Q_{pk}: estimated peak discharge of the 25th October 2011. Unit Q_{pk}: estimated unit peak discharge.

Methods and data collection

A range of different approaches and methods can be used for the analysis of geomorphic responses to a flood event. A summary of the spatial scales and methods related to the various components of an overall analysis of the geomorphic response to a flood event is reported in Figure 2, while additional information is also provided in the following sections.

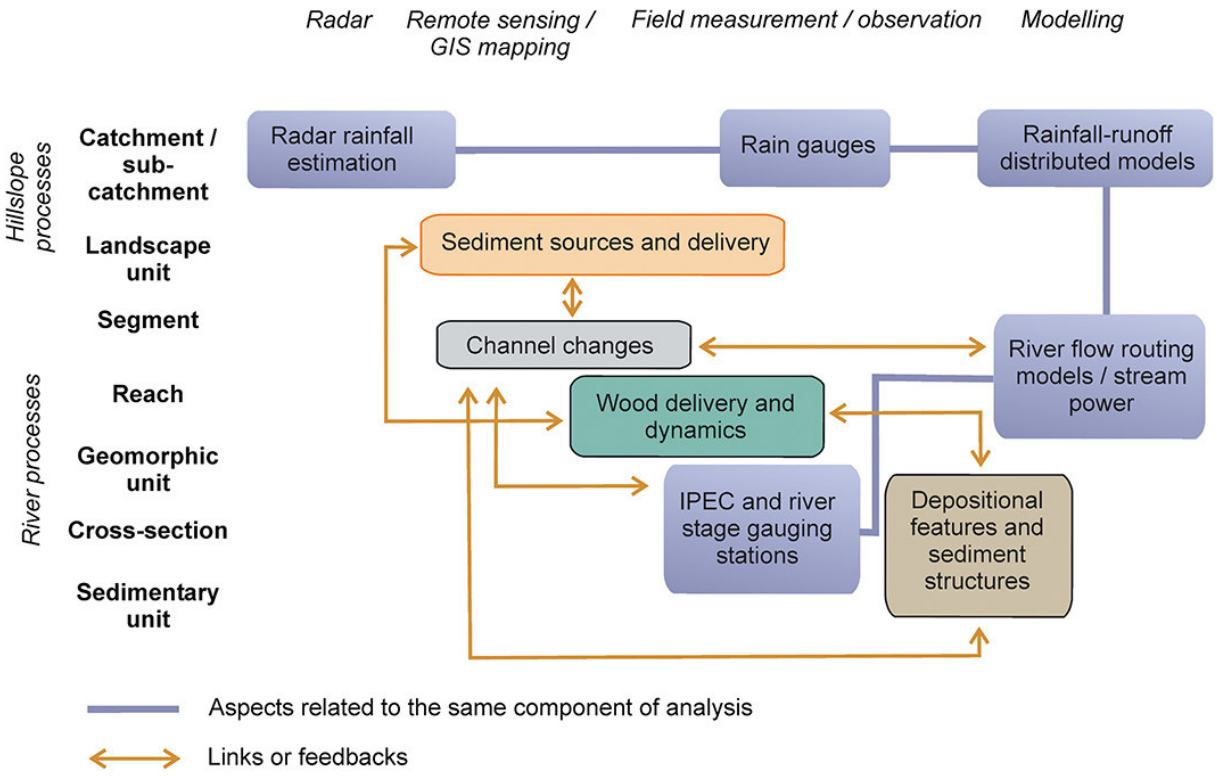

Figure 2. Schematic diagram of spatial scales, approaches, and coupling of process controls on the flood time scale.

Hydrological analysis

As a consequence of the limited spatial and temporal scales, which characterise the flash-flood events, the conventional monitoring networks for rainfall and river discharge are often too sparse for collecting data suitable for the analysis of these events. This has prompted the development of a monitoring strategy that integrates data from hydrometeorological networks with data specifically collected by means of Intensive Post-Event Campaigns (termed IPEC, hereafter) (Gaume et al., 2004; Borga et al., 2008; Braud et al., 2014). The methodology applied in this study for flood documentation and analysis has been detailed in previous papers (Gaume and Borga, 2008; Marchi et al., 2009). We briefly recall here the main components: (i) post-flood assessment of peak discharge in ungauged channels through the survey of high water marks in specific river cross sections, and the application of hydraulic equations and models; (ii) reconstruction of the time evolution of the flood by means of interviewing eyewitnesses and by the collection of documentation (newspapers, reports, videos); (iii) use of carefully corrected radar rainfall estimates to represent the space-time variability of the triggering rainfall; (iv) use of a distributed hydrological model to evaluate the consistency of rainfall and discharge data.

In order to depict the spatial variability of flood response within the Magra catchment, the peak discharge was reconstructed by means of the IPEC methodology at multiple river sections corresponding to catchments impacted by different rainfall depths and intensities and are representative of different geological and land use conditions. The slope-conveyance method was used for discharge estimation (Marchi et al., 2009), based on one-dimensional Manning–Strickler equation. Geomorphological observations, e.g., channel widening, incision and aggradation, recognition of landslides coupled to the river system, are also carried out during the survey, and adopted to check consistency of peak discharge reconstruction. A distributed rainfall-runoff model was then applied for checking the consistency of the rainfall and discharge (Gaume and Borga, 2008; Marchi et al., 2009) and for computing peak discharge at ungauged cross-sections, including the outlets of the catchments reported in Table 1 and the cross-sections where stream power was assessed.

In order to explain the spatial pattern of observed changes, which occurred during the flood, cross-sectional stream power and unit stream power (Ω and ω,

respectively) were analysed, being considered as hydraulic variables that potentially control channel responses (e.g., Vocal Ferencevic and Ashmore, 2012).

Sediment sources and delivery

Landslide inventory maps (Guzzetti et al., 2012) are the core element in the analysis of sediment entrainment and delivery. The comparison and analysis of pre- and post-event aerial photographs, complemented by field checks, is a valuable approach for the preparation of inventory maps of landslides triggered by the rainstorm, their classification into main typologies, and visual recognition of the linkage with stream channels.

In this study, landslide inventory maps were implemented in two of the sub-catchments most heavily affected by mass wasting. A test of the feasibility of semi-automated landslide mapping using panchromatic and multispectral aerial photographs was successfully performed (Mondini et al., 2014). The coupling/decoupling of sediment sources with the channels is of utmost importance for understanding sediment dynamics and can be visually recognised in the field and on aerial images (e.g., Harvey, 2001; Milan, 2012).

Wood transport and deposition

The role of large wood (LW) during this event was studied in two tributaries of the Vara River, i.e. the Gravegnola and the Pogliaschina catchments. These two basins were selected because large volumes of wood were recruited there and transported during the event, causing clogging at several bridges (Lucìa et al., 2015). Field surveys were carried out along a channel length of 11.5 km and 19.4 km in the Gravegnola and Pogliaschina, respectively. The two channels were divided into relatively homogeneous reaches in terms of their width, slope and LW presence. Subsequently, orthophotos taken before (0.5 m pixel resolution) and after (0.1 m resolution) the flood were analysed by a GIS software. This enabled an estimation of the eroded floodplain areas required to quantify the LW input from the valley bottom.

Deposited LW elements and jams were digitized on the post-event orthophotos, and the volume of single wood elements was estimated. Based on

estimated volumes of recruited and deposited LW along each reach, a LW budget was computed at both the reach and the basin scale.

Morphological and sedimentological processes and features

Observation and interpretation of geomorphic and sedimentary features and processes conducted after and possibly during the flood event are fundamental to developing a better understanding of the mechanisms responsible for channel changes. To this purpose, a video shot by a witness along the right bank of the Mangiola River (Movie S1) was extremely useful in reconstructing the intra-event succession of erosional and depositional processes and in the development of in-channel geomorphic units.

A post-flood field reconnaissance allowed for the collection of qualitative information on the processes (e.g., sediment transport, bank erosion) responsible for the morphological changes. Sedimentological analysis of flood deposits was performed through the qualitative field characterisation of the texture and structure of flood deposits. It was thus possible to interpret the depositional mechanisms and hydraulic conditions responsible for the bed structure, bedforms, and geomorphic units created during the event (e.g., Wells and Harvey, 1987; Komar, 1989; Macklin et al., 1992).

Morphological channel response

For the analysis of channel changes, the investigated streams were divided into a series of relatively homogeneous reaches in terms of channel morphology, lateral confinement, hydrology and other characteristics, along which boundary conditions are sufficiently uniform and the river maintains a near consistent set of process-form interactions (Brierley and Fryirs, 2005; Rinaldi et al., 2013, 2015).

A quantitative and systematic analysis of channel width was carried out along the unconfined or partly confined reaches. Changes in channel width were quantified using a GIS and aerial photographs captured before and after the flood, respectively in 2006 (Gravegnola and Pogliaschina rivers) or 2010 (Teglia, Mangiola, Osca, Geriola, and Magra rivers), and 2011/2012. They were expressed as width ratio, i.e.

channel width after/channel width before the flood (Krapesch et al., 2011). Estimates of changes in channel width were clearly affected by several errors, in particular due to photo interpretation and digitization. Although rigorous error assessment was not carried out, we judged that, overall, errors were relative small in this analysis because (i) images with high spatial resolution (i.e. resolution between 0.1 and 0.5 m) were used, and (ii) magnitude of changes (i.e. width ratio) was very high in most of the reaches. For the partly confined and unconfined reaches, an investigation on historical channel morphology was also carried out (with specific reference to the end of the 19th century and the 1950s) in order to assess whether and to what extent the post-flood changes involved portions of the alluvial plain occupied by the channel bed in historical times.

Results

Rainstorm characterisation and flood response analysis

The spatial rainfall distribution was estimated based on merging data from a weather radar and a set of 40 raingauge stations located over the Magra catchment. This resulted in a merged rainfall field at 2 km grid spacing and 30 min temporal resolution. A characteristic of the rainfall event was its organization in a well-defined banded structure, which persisted in the same locations for the duration of the event (Fig. 3), impacting some of the basins considered in this study. The maximum hourly rainfall intensity was up to 130 mm h-1, whereas cumulated values up to 540 mm in eight hours were locally registered within the basin, in areas corresponding to the Pogliaschina and Gravegnola basins. The corresponding estimated return period exceeds 500 years for both durations.

Post-event surveys (February and March 2012) permitted a reconstruction of peak discharge at 35 cross-sections; the drainage area of the considered catchments varies from 0.5 to 77 km2. The values of unit peak discharge range from 1 to 30 m3 s-1 km-2 in tributaries with drainage areas in the 5-10 km2 range, thus confirm the large variability in the intensity of flood response, in agreement with the great differences in rainfall input between different sectors of the Magra catchment (Fig. 3). In the application of the Manning-Strickler equation we used a range of values of the roughness coefficient to account for the relevant uncertainty. This resulted in an

uncertainty range around 20% of the central, most probable, value. Larger uncertainties, indicatively up to 50% of the central value, can be presumed for a few cross-sections in which the flood had caused relevant morphological changes (mostly widening). Since part of these changes may have occurred after the flood peak, in some cases the surveyed river section geometry could be wider than the cross section at the flood peak. The values of peak discharge estimated through post-flood surveys have been successfully validated by means of the comparison with the application of a rainfall-runoff model that had been previously calibrated on three gauging stations located on the Magra (Calamazza) and Vara (Piana Battolla and Nasceto) rivers (Fig.1).

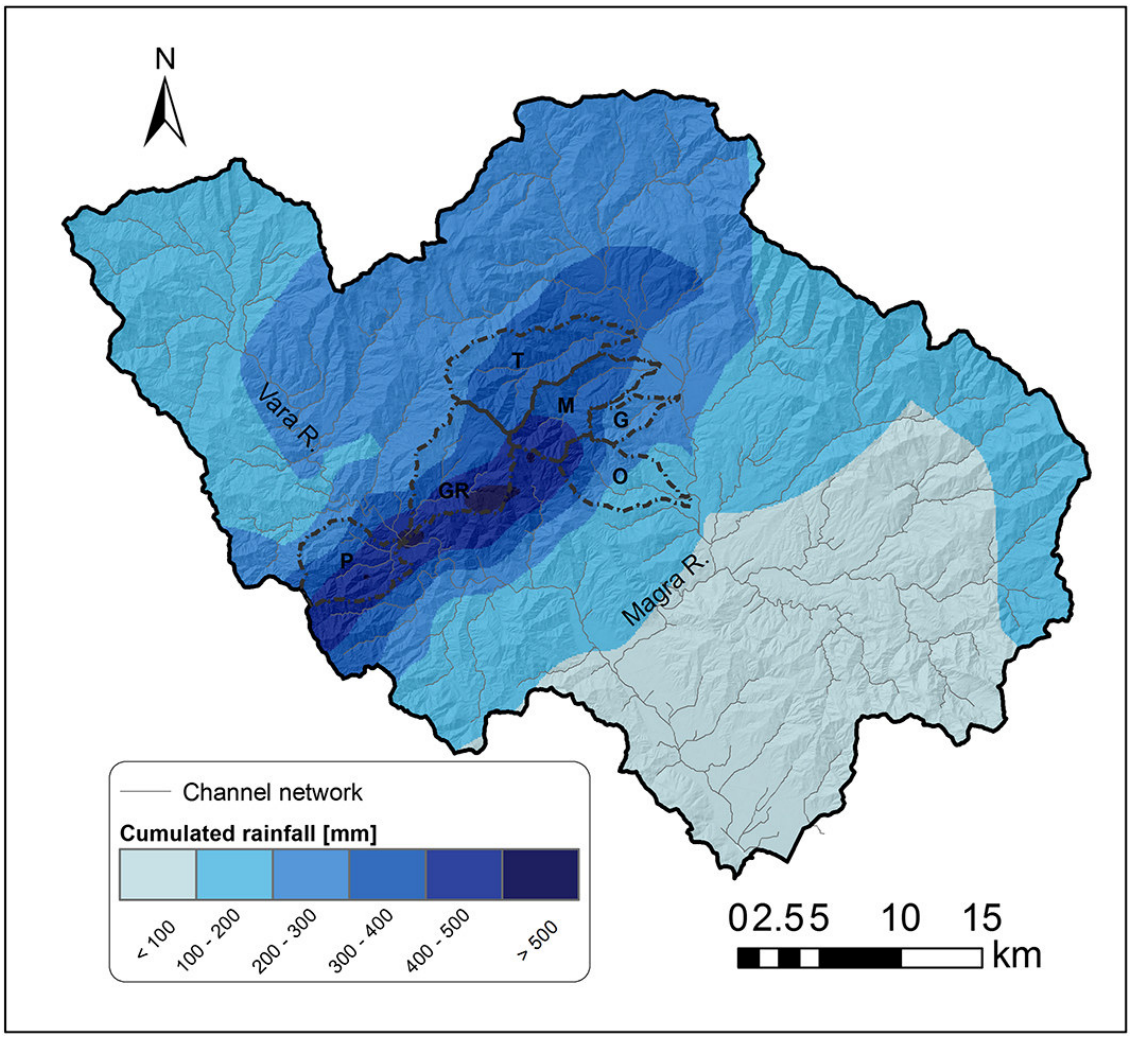

Figure 3. Map of cumulative rainfall for the rainsorm of 25 October 2011. T: Teglia; M: Mangiola; G: Geriola; O: Osca; GR: Gravegnola; P: Pogliaschina.

Sediment sources and wood dynamics

Figure 4A presents the inventory map of the landslides triggered by the rainstorm of 25 October 2011 in the Pogliaschina and Gravegnola catchments, which lie in one of the areas that were most severely affected by the rainstorm. In the Pogliaschina catchment, landslides occupy approximately 0.44 km2, i.e. 1.8% of the catchment area, and mostly took place in the central and lower parts of this sub-catchment, whereas landslide density was markedly lower in the upper (western) part. Differences in the distribution of landslides cannot be ascribed to the spatial variability of rainfall, nor to topographic factors. In fact, the south-western sector of the Pogliaschina sub-catchment, where few landslides occurred, was affected by large rainfall amounts and is characterised by steep slopes. Instead, the geological conditions were most likely significantly relevant for landslide distribution. Notwithstanding the broad presence of the Macigno Flysch Formation in the Pogliaschina (55% of catchment area), only 16% of the landslide area corresponds to soils that mantle this formation. About 65% of the landslides originated from the sandy soils that cover the Monte Gottero Formation, although this lithotype outcrops only in 35% of the catchment area. The higher susceptibility to the mass wasting of soils originated from the Monte Gottero Flysch was confirmed by geotechnical laboratory tests (Mondini et al., 2014). In the Gravegnola sub-catchment (Fig. 4A), the landslides triggered by the rainstorm of 25th October 2011 cover 0.3 km2, i.e. approximately 0.9% of the catchment area. The slopes most susceptible to landslides in the Gravegnola correspond to paleo-landslide deposits, which cover 21% of the catchment area and account for 35% of the landslide areas. In both sub-catchments, the majority of landslides were earth flows, followed by soil slips and translational slides. A GIS-based analysis of sediment connectivity led to discard from the inventories several landslides that were poorly connected with the channel network, but did not alter the general portrait that shows a larger landslide area in Pogliaschina catchment than in Gravegnola. However, if we consider only the landslides adjacent to the main channels and directly coupled with them, around one third of the landslides mapped in the Gravegnola basin lies in this class. Therefore, notwithstanding their limited extent, landslides in this sub-catchment were an effective provider of sediment for the channel network. In the Pogliaschina only 3.2% of the landslide area is directly coupled with the main channels.

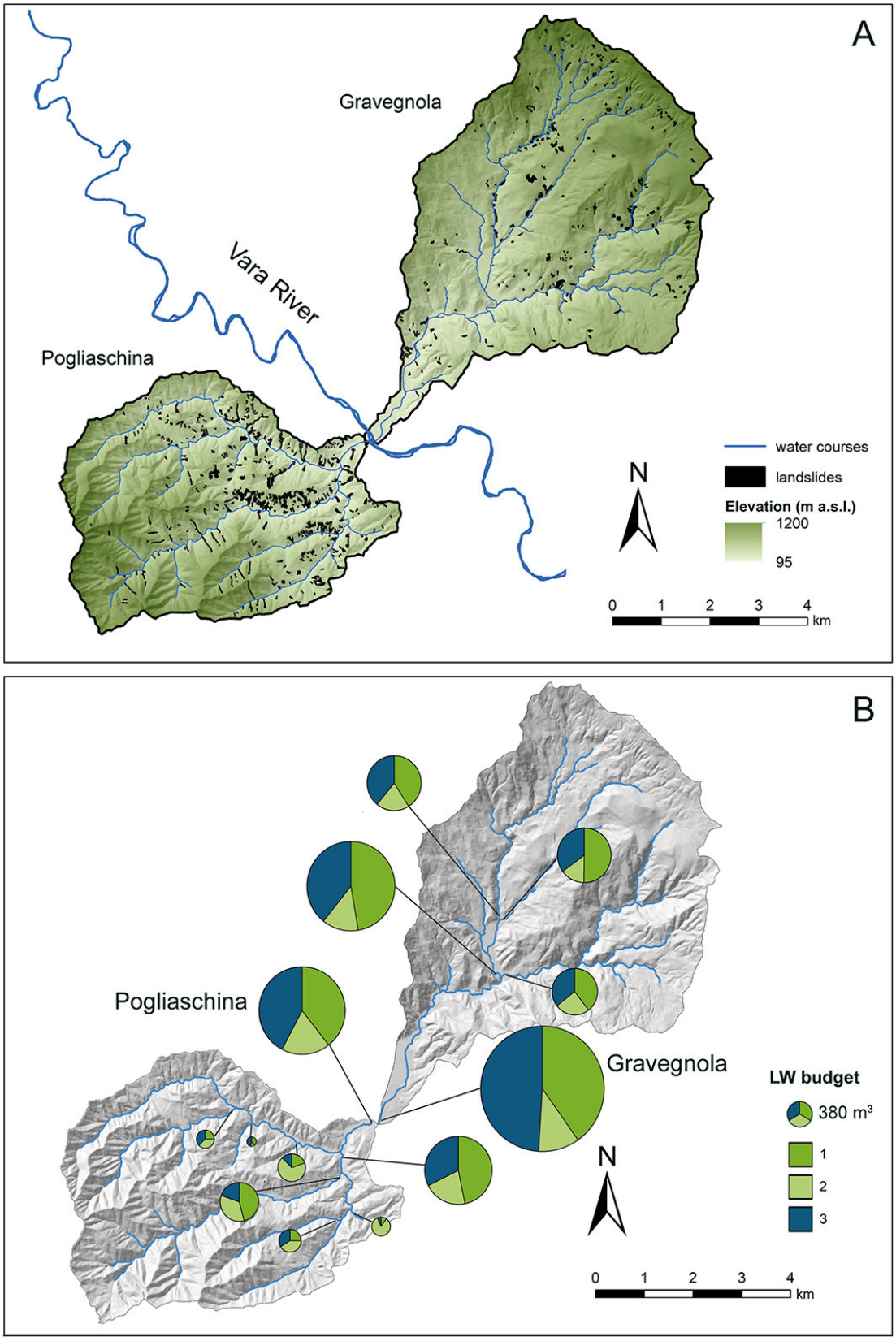

Figure 4. Landslide distribution and wood budget in the Gravegnola and Pogliaschina catchments. A: Map of event landslides. B: Large Wood (LW) budget summarized at the sub basin scale. 1: LW recruitment from floodplain; 2: LW recruitment from hillslopes; 3: LW deposited. The size of the circles depends on LW recruited in each sub-catchment.

The LW budget for the Pogliaschina River is compared with that of the Gravegnola River to show contrasting results related to various controlling factors (Fig. 4B). In fact, the total LW recruited in the Gravegnola basin (9400 m3) turns out to be much greater than that in the Pogliaschina catchment (4800 m3), despite the comparable basin size (about 276 m3 per km2 of catchment area compared to 191 m3 km-2, respectively). Most of the recruited LW in both sub-catchments derived from floodplain erosion (79% in Gravegnola and 68% in Pogliaschina), whereas the remainder was originated from hillslope processes, predominantly landslides as the contribution of debris flows was almost negligible.

Out of the total LW recruited, 96% and 74% remained deposited (mostly trapped at bridges) in the channels of the Gravegnola and Pogliaschina, respectively. Therefore, the Gravegnola River exported 360 m3 to the Vara River, whereas the LW output of the Pogliaschina amounted to 1270 m3. The large alluvial fan of the Gravegnola River acted as a sink for LW transport, in contrast to the effect of the Pogliaschina's fan, being almost absent. The LW budget varied greatly within the catchments: the amounts of LW recruited and deposited is more balanced near the outlet of these catchments, while there is more recruitment than deposition in the headwaters (Lucìa et al., 2015).

Channel processes and geomorphic features

The flood event was characterised by intense bedload transport along the investigated streams. Observations conducted during the post-flood field reconnaissance indicate that, in some portions of the Gravegnola, Mangiola and Teglia, sediment transport occurred as debris flood, i.e. a very rapid, surging flow of water, heavily charged with debris, occurring in steep channels (Hungr et al., 2001).

The most impressive effect of flood-related erosion within the valley floor is represented by the widening of the overall channel bed (see Morphological channel response) and the reactivation of wide portions of the pre-event floodplain (Fig. 5). Channel widening occurred as the result of two distinctly different processes observed during post-flood field surveys in many sites along the tributaries and the Magra River (Nardi and Rinaldi, 2015), i.e. bank erosion and overbank deposition of bedload material. Field evidence of aggradation was also impressive and widespread

(e.g., development of large depositional units, overbank deposition on the floodplain), often combined with LW deposition, but no reliable measurements of bed-level changes are available.

Among the plethora of erosional and depositional features generated by the 25th October 2011 flood event, we focused on the evidence observed along the Teglia and Mangiola rivers. Data have been collected along some reaches of flow expansion, i.e. where the valley confined in the bedrock suddenly widens downstream (Fig. 5).

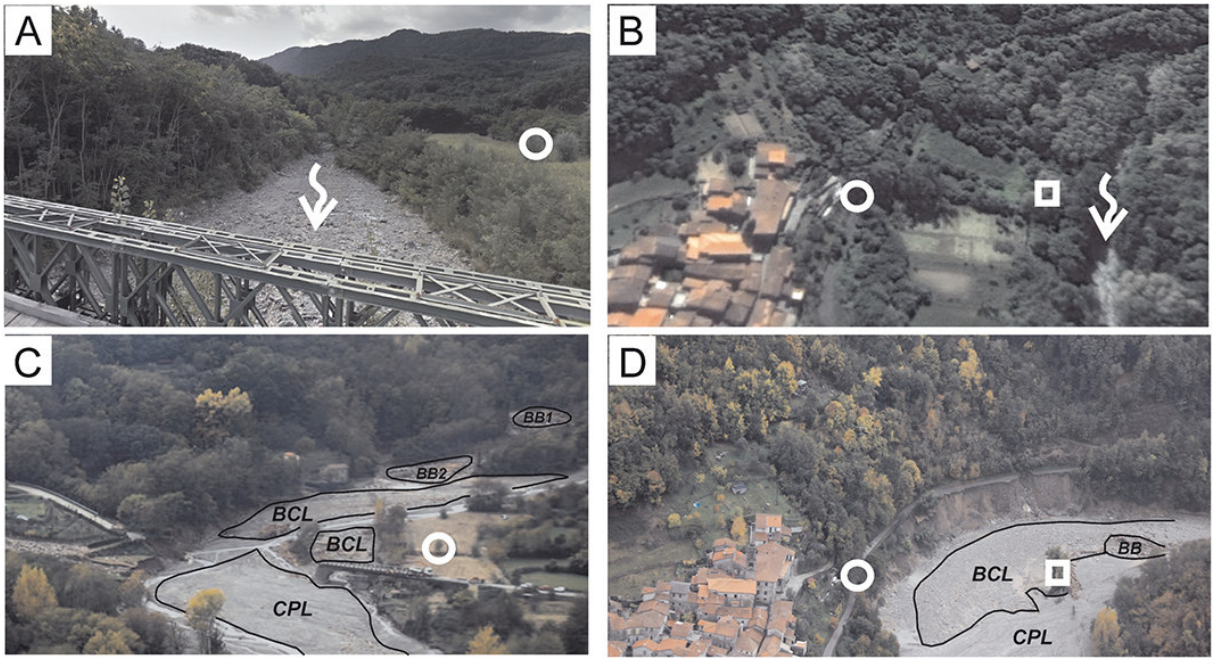

Figure 5. Channel widening and depositional features along some reaches of the Mangiola and Teglia. A: Mangiola Creek in its final reach before the flood (October 2011). B: Teglia Creek nearby the village of Castagnetoli before the flood (October 2011). C, D: Mangiola and Teglia immediately after the flood, respectively, with indications of the main depositional features created by the flood event. BB1 and BB2: boulder bars; BCL: boulder-cobble lobe; CPL: cobble-pebble lobe. The white squares and/or circles indicate common points between pre- and post-flood photos. The white arrows indicate the flow direction.

A common feature observed in the two investigated reaches is the distribution of various depositional features at different elevations over the active channel, displaying a discrete gradient of bed roughness. From the upstream confined reaches to the expansion areas, we observed a post-flood morphology made of elongated or arcuate bouldery macroforms (boulder bars or berms: BB) representing the highest deposits within the channels. These are followed by fan-shaped bouldery-cobbly deposits (boulder-cobble lobes: BCL) dissected by low-flow channels, related

to a further fan-shaped cobbly-pebbly planform (cobble-pebble lobes: CPL) downstream. The latter are in turn dissected by the lowermost low-flow channels. The boulder bar morphology resembles that of boulder berms described in the literature as typical deposits which form during high flood stages in condition of flow expansion and separation (Carling, 1989).

Sediment textures and structures of the different post-flood features were observed (Fig. 6). BB deposits consist of a frame of large arenaceous boulders (average diameter >1 m) which are dominantly sub-angular in the Teglia River, and mostly rounded to well-rounded in shape in the Mangiola (Fig. 6A).

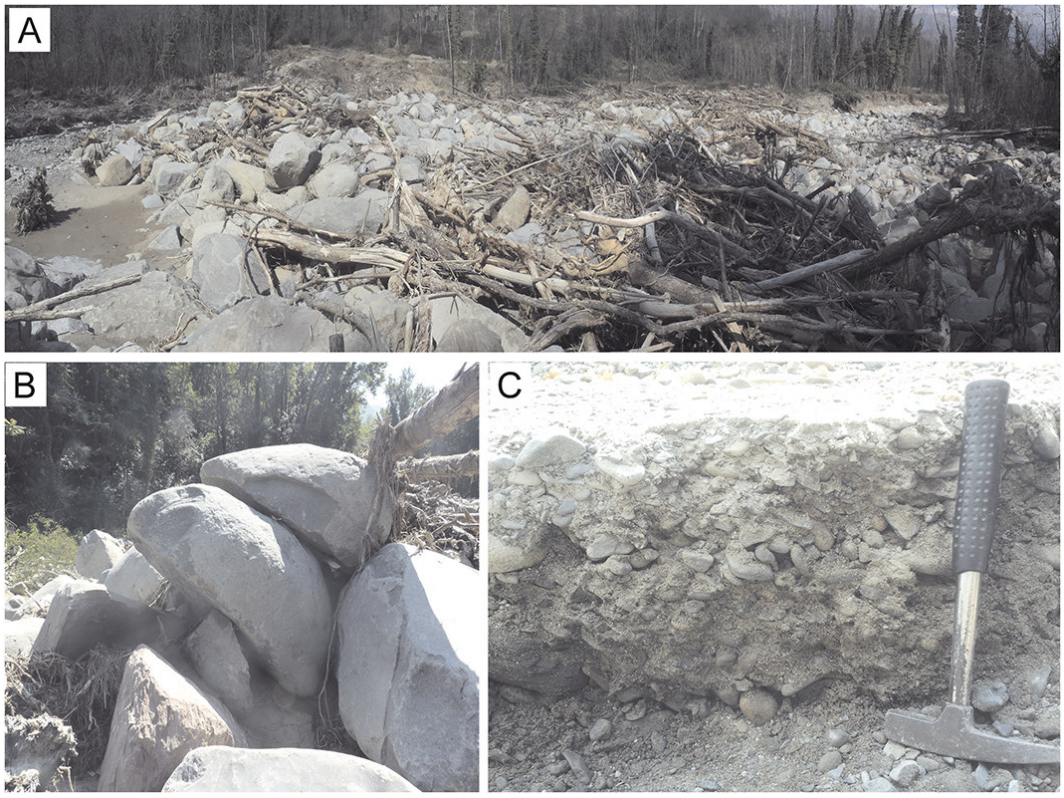

Figure 6. Sediment textures and structures of different fluvial deposits. A: panoramic view of the boulder bar (BB2 in Fig. 5C) formed in the Mangiola Creek (taken on March 2012). In the foreground tree log jam representing the waning stage of the flood peak. B: imbricated boulders in the boulder bar (BB2 in Fig. 5C) of the Mangiola Creek; C: section of the CPL deposits in the Mangiola Creek. The gravelly deposit is characterised by an alternation of sand matrix-rich and openwork framework, hammer for scale (see text for details).

Impact pits and grooves are commonly observed on the clast surfaces (Fig. 6B). The frame is typically openwork with clusters of imbricated clasts. The BCL displays a surface texture hinting to a polymodal grain-size distribution reflecting a poorly sorted sediment. This is made of a frame of clast-supported smaller boulders (diameter <1 m) and cobbles with a space-filling matrix made of pebbly-sandy

sediments. Larger clasts are frequently imbricated and aggregated in distinct clusters. In section, the CPL deposits display a rhythmical alternation of matrix-rich and openwork centimetre-decimetre thick gravelly layers (Fig. 6C).

The video of the flood along the Mangiola River (see Supporting Information Movie S1) offers precious documentation of the intra-event succession of erosional and depositional processes otherwise not achievable from post-flood field evidence.

The following is a summary of the succession of erosional and depositional episodes during the flood event and related morphological changes (Fig. 7): (i) at 3.40 pm, the flow is around the bankfull stage, and no significant changes in the two branches and the thickly vegetated floodplain have yet occurred (Fig. 7C); (ii) about one hour later, the floodplain forest upstream from the point of observation has been partially stripped whereas the riparian forest downstream is still intact; (iii) during the interval when the flood peak occurred (4.48 – 4.53 pm), boulder bars (BB1 and BB2 reported in Fig. 5) are being created in the part where the floodplain was previously eroded; (iv) during the recessional phase (between 5.00 and 6.13 pm), the riparian forest in front of and downstream of the point of observation was largely cleared and most of the channel widening had occurred (Fig. 7D).

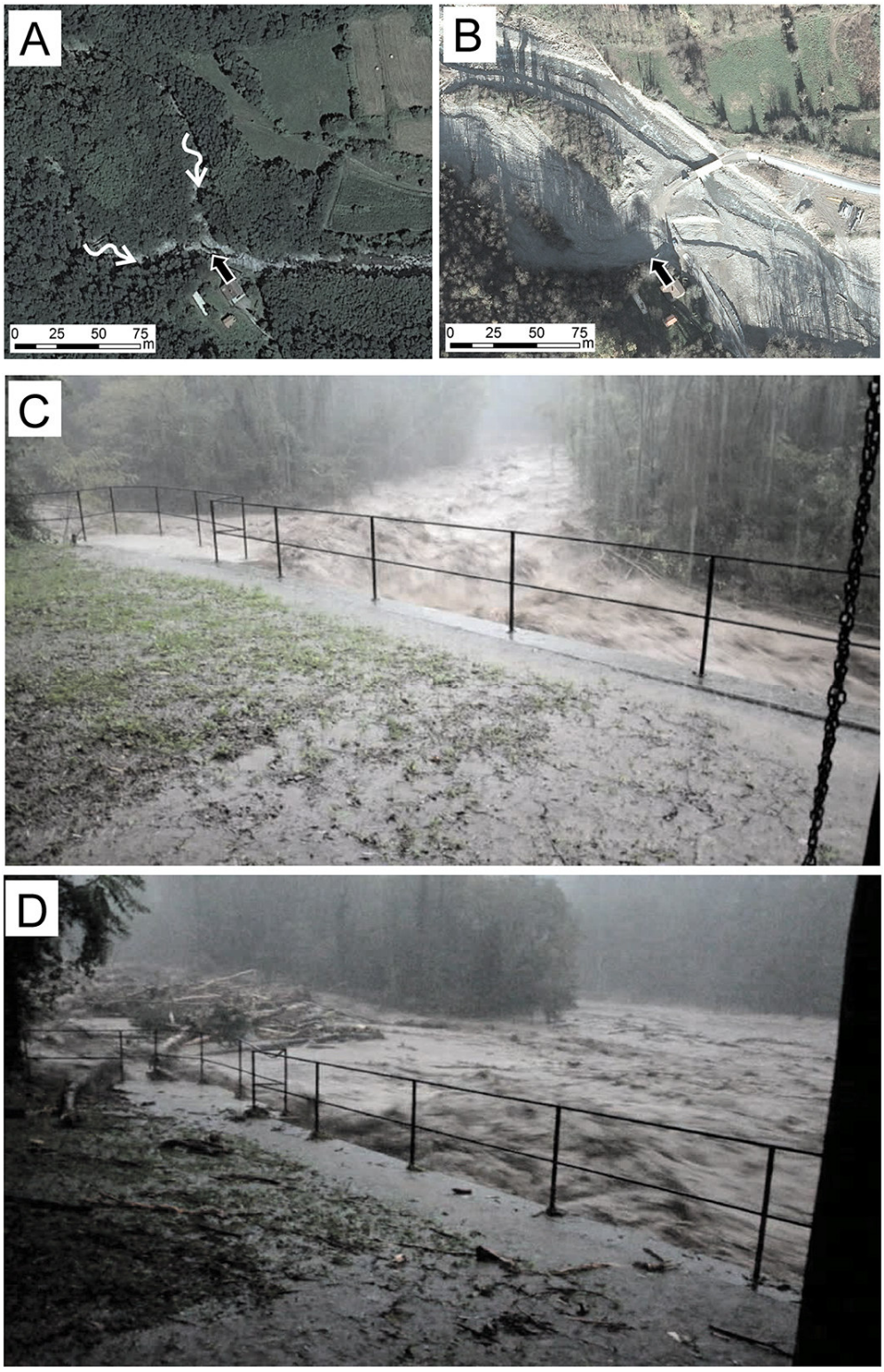

Figure 7. Summary of the video documentation of the flood event along the Mangiola Creek. A: image of the site before the flood (October 2011), showing a partly confined channel with two branches separated by a large island (the white arrows indicate the two branches and flow direction); B: aerial photo after the flood, showing a wide, wandering pattern; C: flood event during the raising phase of the hydrograph at approximately bankfull stage and before the peak; D: flood event during the recessional phase (see text for details). The black arrows on A and B indicate the point and direction of video observation.

Changes in channel width

A summary of the results of changes in channel width for the main partly confined and unconfined reaches within the five sub-catchments is illustrated in Figure 8 and reported in Table 2, the latter including a series of potential controlling factors (confinement, bed slope, stream power), which provide a broader characterisation of the physical conditions of reaches where channel width changes were measured.

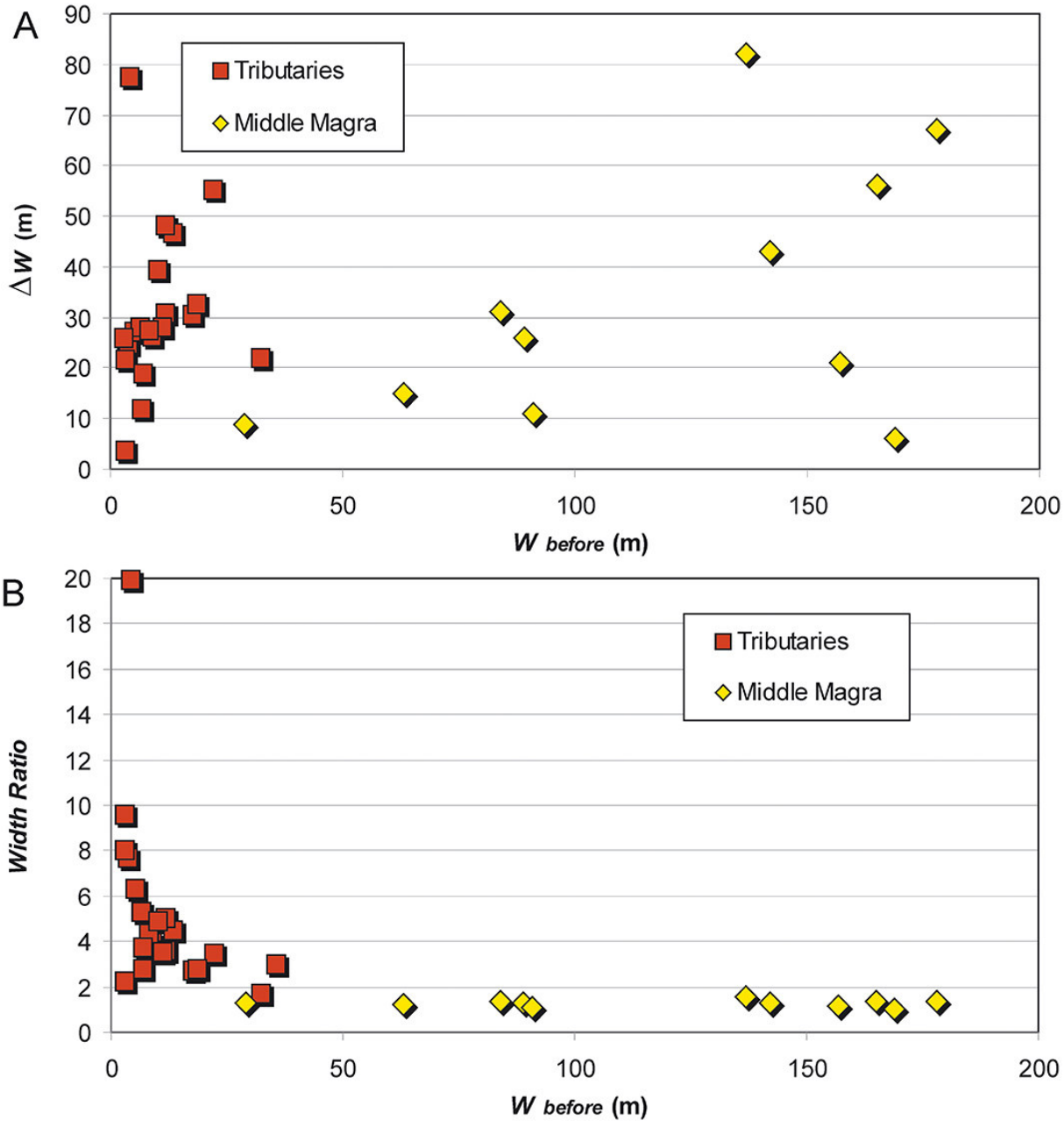

Figure 8. Changes in channel width in response to the flood event. A: changes in channel width vs. width before the flood; B: width ratio vs. width before the flood.

Concerning the investigated reaches in the Gravegnola and Pogliaschina rivers, the width ratio varies from a minimum of 2.2 to a maximum of 19.9 (Table 2). Remarkable planform changes also took place along the other streams, where the width ratio varies from a minimum of 1.7 to a maximum of 9.6 (Table 2). In several sections the channel widened over the whole floodplain, causing a notable erosion of riparian vegetation. Along the medium portion of the Magra River, widening was still significant, but less intense than along the tributaries in relation to the pre-flood channel width (Fig. 8). In fact, the width ratio for the middle Magra River ranges from 1.0 to 1.6.

Stream	***Ci***	***S*** (m m^{-1})	W_{before} (m)	W_{after} (m)	***W Ratio***	Ω (W m^{-1})	ω (W m^{-2})
Teglia	4.9÷11.2	0.020÷0.031	8.9÷17.7	35.2÷60.1	2.7÷5.1	102567÷136895	6267÷15364
Mangiola	6.5÷8.4	0.025÷0.049	6.5÷22.2	34.6÷77.3	3.5÷5.3	92888÷173897	4447÷26590
Geriola	5.5÷10.6	0.035÷0.140	6.7÷18.5	18.7÷51.1	2.8÷4.9	39425÷62952	2128÷9356
Osca	3.5÷20.6	0.016÷0.064	3.0÷32.4	24.8÷54.4	1.7÷9.6	66526 ÷70989	9629÷22570
Middle Magra	2.5÷5.8	0.003÷0.016	29÷178	38÷245	1.0÷1.6	90449÷197078	775÷5350
Gravegnola	5.0÷7.2	0.019÷0.023	13.4÷35.5	60.0÷105.4	3.0÷4.5	90636÷106600	2550÷7946
Pogliaschina	11.1÷26.6	0.004÷0.026	3.1÷5.1	6.9÷81.7	2.2÷19.9	7712÷25569	2158÷5881

Table 2. Ranges of morphological characteristics and changes in channel width along partly confined and unconfined portions of the streams investigated in this study. *Ci*: initial confinement index (=alluvial plain width / channel width before the flood); *S*: bed slope; W_{before}: channel width before the flood; W_{after}: channel width after the flood; *W Ratio*: channel width after / channel width before the flood; Ω: cross-sectional stream power associated to the estimated peak discharge; ω: unit stream power (=Ω/W_{before}).

A statistical analysis (simple and multiple regressions) between the observed changes and a series of morphological and hydraulic potential controlling factors was carried out on the Magra River (Nardi and Rinaldi, 2015) and on the tributaries (Surian et al., 2015). Low correlations were found to explain the spatial pattern and the variability of changes in channel width along the Magra River, while higher correlations were found for the tributaries. Specifically, relatively good regression models were obtained for steeper reaches (i.e., reach slope ≥4%) using confinement index and unit stream power as explanatory variables (Surian et al., 2015).

Historical analysis of the tributaries showed that, most of the reaches where intense channel widening took place, in the 1950s had a wider channel associated to a wandering or braided morphology, whereas the pre-flood morphology was a single-

thread channel. Along the Magra River, analysis of evolutionary trajectories has shown that the post-flood channel width is amply included within the range of variability from the end of the 19th century to the present (Nardi and Rinaldi, 2014).

Discussion

The integration of different approaches and methods at a variety of spatial scales is a key feature for the monitoring and post-flood analysis of flash floods, due to the limited spatial and temporal scales characterising such events.

There are clear links between the various investigated aspects (Fig.2). Observations on channel changes such as widening, incision or aggradation, and identification of landslides connected to the channel are important for various purposes, e.g. for the correct interpretation of field measurements and the computation of peak discharge during IPEC, as well as the identification of cross sections which are not reliable for the latter since they drastically changed the geometry during or after the peak stage (Braud et al., 2014). Flow data measured at gauging stations are used to calibrate a distributed hydrological model, while the latter is important for evaluating the consistency of the discharge computations resulting from IPEC (Borga et al., 2008). Maps representing the spatial and temporal variability of rainfall within the catchment are important for assisting the interpretation of the occurrence and distribution of landslides.

Feedbacks between channel and hillslope processes are also evident and may not be identified well if both aspects are not sufficiently analysed (e.g., Wells and Harvey, 1987). In our study, we could envisage a positive feedback among channel-coupled landslides, channel widening, and large wood erosion. Indeed, sediment supply from coupled landslides most likely caused augmented channel aggradation and instability, promoting channel widening and thus erosion of the riparian forest. Widening causes the channel to occupy the whole valley floor, resulting in the coupling of more landslides – delivering additional large wood – which were not connected to the channel network prior to the event.

The integration of post-flood observations on depositional geomorphic features, their spatial pattern, texture and sedimentary structures is also extremely important to understanding, at sub-reach scale, the mechanisms of transport and

hydrodynamic conditions which determine reach-scale modifications of channel geometry and size (e.g., Wells and Harvey, 1987; Komar, 1989; Macklin et al., 1992). Video documentation of the flood event, when available, is also extremely useful for interpreting the intra-event timing and succession of geomorphic processes responsible for channel changes. In our study, the video of the flood clearly shows that in the Mangiola reach, where boulder bars formed, large boulders were rolling in a downstream direction. Frequent impact marks on the boulder surfaces also testify a jumping mode of boulder transport.

Raised boulder bars form a mutual interlocking of clasts hinting at a sort of inertial freezing. Specifically, such flood deposits reflect transport processes intermediate between debris flows and normal streamflow, indicated as debris flood by Hungr et al. (2001). We refer to these deposits as peaks of turbulent flood-flows which following to sudden flow expansion generated lobes of boulder-size clasts deposited through frictional interlocking (Carling, 1989).

The video (between 3.40 pm and 4.48 pm) captures the creation of the space available for the development of BB1 and BB2. Catastrophic stripping of the former floodplain and subsequent channel widening were evidently followed by the development of the BB deposits. The development of this boulder bar complex may have been related to a surge-like flow causing the floodplain erosion and subsequent deposition. A possible explanation may be represented by the collapse of a landslide of tree-log dams somewhere upstream, giving rise to surging floodwater.

Finally, remotely-sensed data and/or topographic field surveys before and after the flood can be used to quantify channel response related to a flood event. The increasing availability of GPS field surveys, LIDAR, and terrestrial laser scanning provide excellent data to produce high resolution DoDs (DEM of Difference) and use them for calculating sediment budgets (e.g., Wheaton et al., 2010; Milan et al., 2012; Thompson and Croke, 2013).

Another important issue is the need to perform an overall analysis on the whole catchment, although the flood event and responses may be concentrated only in some areas. Because the intensity of controlling variables and response could be extremely variable within the catchment (e.g., Harvey, 1984; Miller, 1990; Fuller, 2008; Thompson and Croke, 2013), the entire range of geomorphic response to the

flood event should be considered, allowing the identification of hydrologic and geomorphic thresholds.

Concerning the application of an integrated approach, we believe that the type of analysis can be replicated in other catchments with similar characteristics. Besides a documentation of the event, understanding how and to what extent it is possible to predict morphological response in similar catchments or in the same catchment for similar hydrometeorological events is a challenging issue. A series of important limitations make it extremely difficult to achieve a prediction of possible geomorphic responses. Although some relationship of geomorphic response at catchment scale to storm localization is usually evident, some issues are particularly critical and need to be addressed in future research. For example, the identification of the most significant variables and indicators related to geomorphic changes is a key issue. Various studies have highlighted some correlations between a number of flood hydraulic variables (e.g., stream power, velocity, slope, flow duration) and geomorphic response (Howard and Dolan, 1981; Wohl et al., 1994; Benito, 1997; Thompson and Croke, 2013; Magilligan et al., 2015). In our study, no robust statistical relationships between hydraulic variables and the response of the Magra River were found (Nardi and Rinaldi, 2015), whereas relatively good regression models were obtained for steeper reaches (i.e., reach slope ≥4%) using confinement index together with unit stream power as explanatory variables (Surian et al., 2015).

Recognising that prediction of possible channel response is a critical issue, setting the river in an appropriate spatial and temporal context and conducting a robust geomorphological analysis are fundamental. A classification of the river network into channel typologies based on some key characteristics and variables (e.g., lateral confinement, channel morphology, sediment calibre, and bed slope) provides a basic knowledge of a given reach's sensitivity to flood events. For example, this study has shown that partly confined or unconfined reaches with a relatively narrow floodplain in a mountain or hilly physiographic setting are extremely sensitive to changes, and during extreme events the channel can completely occupy the available valley floor and aggrade. Historical information on past channel morphology and on its evolutionary trajectory is highly recommended for alluvial, relatively large, dynamic rivers. River reaches showing a braided morphology in the past or experiencing long-term instability may tend to partially recover their previous

morphology (for example, reaches where intense channel narrowing occurred in the past may tend to recover part of their original width). The study of Nardi and Rinaldi (2014) on the Magra River suggests that previous morphological conditions on longer (last 100–150 years) and shorter (last 10–15 years) timescales may have some influence and are useful for a better interpretation of possible channel response to an intense flood event (Rinaldi et al., 2015).

Interpretation of sedimentary structures and facies in the geological record of ancient fluvial deposits may also provide additional clues of potential channel response and processes during extreme events. For example, boulder bar deposits in the alluvial sediment record in zones of flow expansion represent a clear indication that very intense coarse transport and deposition can periodically occur in that site.

Conclusions

A high-magnitude flash flood which took place on 25th October 2011 in the Magra catchment was used to illustrate the application of an overall methodological framework for using interlinked observations, approaches, and analyses. The flood event was characterised by intense bedload transport. Along some steep reaches of the investigated tributaries, sediment transport occurred as debris flood. The most common morphological response to the flood was channel widening and the reactivation of wide portions of the pre-event floodplain. The video documentation clearly shows that most of the widening and deposition of boulder bars occurred during the recessional phase of the flood.

In this paper, we have shown how a synergic use of different methods and types of evidence can provide fundamental knowledge for understanding the geomorphic effects of flood events. The combined use of geomorphological, sedimentological and hydraulic data and evidence can greatly contribute to the identification of the most critical reaches.

References

Arnaud-Fassetta, G., 2013. Dyke breaching and crevasse-splay sedimentary sequences of the Rhône Delta, France, caused by extreme river- flood of December 2003. Geografia Fisica e Dinamica Quaternaria, **36** (1): 7-26.

Benito, G., 1997. Energy expenditure and geomorphic work of the cataclysmic Missoula flooding in the Columbia River Gorge, USA. Earth Surf. Process. Landf. **22**: 457 – 472.

Borga, M., Gaume, E., Creutin, J.D., Marchi, L., 2008. Surveying flash floods: gauging the ungauged extremes. Hydrological Processes, **22**(18): 3883-3885, DOI: 10.1002/hyp.7111.

Boudevillain, B., Delrieu, G., Galabertier, B., Bonnifait, L., Bouilloud, L., Kirstetter, P.E., Mosini, M.L., 2011. The Cévennes-Vivarais Mediterranean Hydrometeorological Observatory database. Water Resources Research, **47**(7), W07701.

Braud, I., Ayral, P.A., Bouvier, C., Branger, F., Delrieu, G., Le Coz, J., Nord, G., Vandervaere, J.P., Anquetin, S., Adamovic, M., Andrieu, J., Batiot, C., Boudevillain, B., Brunet, P., Carreau, J., Confoland, A., Didon-Lescot, J.F., Domergue, J.M., Douvinet, J., Dramais, G., Freydier, R., Gérard, S., Huza, J., Leblois, E., Le Bourgeois, O., Le Boursicaud, R., Marchand, P., Martin, P., Nottale, L., Patris, N., Renard, B., Seidel, J.L., Taupin, J.D., Vannier, O., Vincendon, B., Wijbrans, A., 2014. Multi-scale hydrometeorological observation and modelling for flash flood understanding. Hydrology and Earth System Sciences, **18** (9): 3733-3761.

Brierley, G.J., Fryirs, K.A., 2005. Geomorphology and River Management: Applications of the River Style Framework. Blackwell, Oxford, UK, 398 pp.

Carling, P.A., 1989. Hydrodynamic models of boulder berm deposition. Geomorphology, **2**: 319-340.

Flaounas, E., Drobinski, P., Vrac, M., Bastin, S., Lebeaupin-Brossier, C., Stéfanon, M., Borga, M., Calvet, J.C., 2013. Precipitation and temperature space-time variability and extremes in the Mediterranean region: evaluation of dynamical and statistical downscaling methods. Climate Dynamics, **40** (11-12): 2687-2705.

Fuller, I.C., 2008. Geomorphic impacts of a 100-year flood: Kiwitea Stream, Manawatu catchment, New Zealand. Geomorphology **98**: 84–95.

Gaume E, Borga M. 2008. Post-flood field investigations in upland catchments after major flash floods: proposal of a methodology and illustrations. Journal of Flood Risk Management **1**(4): 175–189.

Gaume, E., Livet, M., Desbordes, M., Villeneuve, J.P., 2004: Hydrological analysis of the river Aude, France, flash flood on 12 and 13 November 1999. Journal of Hydrology, **286** (1-4): 135-154.

Giorgi, F., 2006. Climate change hot-spots, Geophys. Res. Lett., **33**: L08707, doi:10.1029/2006GL025734.

Guzzetti, F., Mondini, A.C., Cardinali, M., Fiorucci, F., Santangelo, M., and Chang, K.T., 2012. Landslide inventory maps: New tools for an old problem. Earth-Sci. Rev., **112**: 42–66.

Harvey, A.M., 1984. Geomorphological response to an extreme flood: a case from Southern Spain. Earth Surface Processes and Landforms, **9**: 267-279.

Harvey, A.M., 2001. Coupling between hillslopes and channels in upland fluvial systems: implications for landscape sensitivity, illustrated from the Howgill Fells, northwest England. Catena, **42**: 225-250.

Heritage, G.L., Large, A.R.G., Moon, B.P., Jewitt, G., 2004. Channel hydraulics and geomorphic effects of an extreme flood event on the Sabie River, South Africa. Catena **58**: 151 – 181.

Howard, A., Dolan, R., 1981. Geomorphology of the Colorado River in the Grand Canyon. J. Geol. **89**: 269 – 298.

Hungr, O., Evans, S.G., Bovis, M.J., Hutchinson, J.N., 2001. A review of the classification of landslides of the flow type. Environmental & Engineering Geoscience, **7**(3): 221-238.

Krapesch, G., Hauer, C., Habersack, H., 2011. Scale orientated analysis of river width changes due to extreme flood hazard. Natural Hazards and Earth System Sciences **11**: 2137–2147.

Komar, P.D., 1989. Flow competence evaluation of the hydraulic parameters of floods: an assessment of the technique. In: Beven K, and Carling P. (eds), Floods: hydrological, sedimentological and geomorphological implications. Wiley, Chichester, UK, 107-134.

Lapointe, M.F., Secretan, Y., Driscoll, S.N., Bergeron, N., Leclerc, M.. 1998. Response of the Ha! Ha! River to the flood of July 1996 in the Saguenay Region of Quebec: large scale avulsion in a glaciated valley. Water Resources Research **34**: 2383–2392.

Llasat, M.C., Llasat-Botija, M., Prat, M.A., Porcu, F., Price, C., Mugnai, A., Lagouvardos, K., Kotroni, V., Katsanos, D., Michaelides, S., Yair, Y., Savvidou, K., Nicolaides, K., 2010: High-impact floods and flash floods in Mediterranean countries: the FLASH preliminary database. Adv. Geosci., **23**: 47–55.

Lucìa, A., Comiti, F., Borga, M., Cavalli, M., Marchi, L., 2015. Dynamics of large wood during a flash flood in two mountain catchments. Nat. Hazards Earth Syst. Sci., **3**: 1643-1680.

Macklin, M.G., Rumsby, B.T., Heap, M.T., 1992. Flood alluviation and entrenchment: Holocene valley-floor development and transformation in the British uplands. Geological Society of America Bulletin, **104:** 631–43.

Magilligan, F.J., Phillips, J.D., James, L.A., Gomez, B., 1998. Geomorphic and sedimentological controls on the effectiveness of an extreme flood. Journal of Geology **106**: 87–95.

Magilligan, F.J., Buraas, E.M., Renshaw, C.E., 2015. The efficacy of stream power and flow duration on geomorphic responses to catastrophic flooding. Geomorphology **228**: 175-188.

Marchi, L., Borga, M., Preciso, E., Sangati, M., Gaume, E., Bain, V., Delrieu, G., Bonnifait, L., Pogačnik, N., 2009. Comprehensive post-event survey of a flash flood in Western Slovenia: observation strategy and lessons learned. Hydrological Processes, **23**(26): 3761-3770, DOI: 10.1002/hyp.7542.

Milan, D.J., 2012. Geomorphic impact and system recovery following an extreme flood in an upland stream: Thinhope Burn, northern England, UK. Geomorphology, **138**(1), 319-328.

Miller, A.J., 1990. Flood hydrology and geomorphic effectiveness in the central Appalachians. Earth Surface Processes and Landforms **15**, 119–134.

Mondini, A.C., Viero, A., Cavalli, M., Marchi, L., Herrera, G., Guzzetti, F., 2014. Comparison of event landslide inventories: the Pogliaschina catchment test case, Italy. Nat. Hazards Earth Syst. Sci., **14**: 1749-1759, doi:10.5194/nhess-14-1749-2014.

Nardi, L., Rinaldi, M. 2015. Spatio-temporal patterns of channel changes in response to a major flood event: the case of the Magra River (central– northern Italy). Earth Surface Processes and Landforms, **40**: 326-339, doi: 10.1002/esp.3636.

Rinaldi, M., Surian, N., Comiti, F., Bussettini, M., 2013. A method for the assessment and analysis of the hydromorphological condition of Italian streams: The Morphological Quality Index (MQI). Geomorphology, **180-181**: 96-108, doi: 10.1016/j.geomorph.2012.09.009.

Rinaldi, M., Surian, N., Comiti, F., Bussettini, M., 2015. A methodological framework for hydromorphological assessment, analysis and monitoring (IDRAIM) aimed at promoting integrated river management. Geomorphology, doi:10.1016/j.geomorph.2015.05.010, Early View.

Salvati, P., Bianchi, C., Rossi, M., Guzzetti, F., 2010. Societal landslide and flood risk in Italy. Nat. Hazards Earth Syst. Sci., **10** (3): 465–483.

Surian, N., Righini, M., Lucìa, A.V., Nardi, L., Amponsah, W., Benvenuti, M., Borga, M., Cavalli, M., Comiti, F., Marchi, L., Rinaldi, M., Viero, A., 2015. Channel response to extreme floods: insights on controlling factors from six mountain rivers in northern Apennines, Italy. Geomorphology, **272**: 78–91. doi:10.1016/j.geomorph.2016.02.002.

Tarolli, P., Borga, M., Morin, E., Delrieu, G., 2012. Analysis of flash flood regimes in the North-Western and South-Eastern Mediterranean regions. Nat. Hazards Earth Syst. Sci., **12**: 1255–1265.

Thompson, C., Croke, J., 2013. Geomorphic effects, flood power, and channel competence of a catastrophic flood in confined and unconfined reaches of the upper Lockyer valley, southeast Queensland, Australia. Geomorphology **197**: 156–169.

Vocal Ferencevic, M.V., Ashmore, P., 2011. Creating and evaluating digital elevation model-based stream-power map as a stream assessment tool. River Res.Applic. **28**:1394-1416.

Wells, S.G., Harvey, A.M., 1987. Sedimentologic and geomorphic variations in storm-generated alluvial fans, Howgill Fells, northwest England. Geological Society of America Bulletin, **98**: 182-198.

Wheaton, J.M., Brasington, J., Darby, S.E., and Sear, D.A., 2010. Accounting for uncertainty in DEMs from repeat topographic surveys: improved sediment budgets. Earth Surface Processes and Landforms **35**: 136-156.

Wohl, E.E., Greenbaum, N., Schick, A.P., Baker, V.R., 1994. Controls on bed- rock channel incision along Nahal Paran, Israel. Earth Surface Pro- cesses and Landforms **19**: 1–13.

ACKNOWLEDGEMENTS

Fondazione CARIPARO is gratefully acknowledged for funding my PhD fellowship.

I would like to thank all the people that contributed to this thesis. Particular gratitude to my supervisor Prof. Nicola Surian for introducing me to fluvial geomorphology, for much support and help. In addition, my co-supervisors Prof. Francesco Comiti, Dr. Lorenzo Marchi and Prof. Ellen Wohl who greatly improved my work with careful and objective criticism.

I would like to thank William Amponsah for sharing his data, a great scientific contribution for hydrological and hydraulic aspects of my PhD project.

My gratitude is extended to Dr. Marco Cavalli for the support on many works and for critical and precious advice and technical assistance, and to Prof. Sara Rathburn for her willingness and useful discussions during my period abroad at Colorado State University (USA). Thanks to Prof. Marco Borga for his scientific contribution concerning hydrological data.

Many thanks also to Dr. Ana Lucìa Vela and Dr. Laura Nardi for their reciprocal help and collaboration regarding remote sensing techniques implementation.

I would like to thank Dr. Bruno Golfieri for his help and support on statistical analysis.

Many thanks to the students who were involved during field work in the Posada and Lierza catchments.

My gratitude is extended to all my colleagues, friends and to my family for continuous personal support and encouragement.

I thank Arnaud Fassetta and Janet Hooke provided very helpful reviews and suggestions.